UNIVERSITY OF SOUTHAMPTON

FACULTY OF MEDICINE

Investigation of members of the human epidermal growth factor receptor family as potential therapeutic targets for bladder cancer

by

Regina Mora Vidal

Thesis for the degree of Doctor of Philosophy

June 2013

UNIVERSITY OF SOUTHAMPTON

ABSTRACT

FACULTY OF MEDICINE

Doctor of Philosophy

INVESTIGATION OF MEMBERS OF THE HUMAN EPIDERMAL GROWTH FACTOR RECEPTOR FAMILY AS POTENTIAL THERAPEUTIC TARGETS FOR BLADDER CANCER

by Regina Mora Vidal

Conventional bladder cancer treatment typically involves surgery and/or chemotherapy or radiotherapy, but outcomes still remain far from optimal. Research is now focused on the identification of molecular targets which could be used for targeted therapy. The epidermal growth factor receptors 1 and 2 (EGFR and HER2) have been found to be overexpressed in some bladder cancers and have been linked to poor prognosis. These cell membrane receptors have tyrosine kinase activity in their cytoplasmic domain and transduce signals controlling cell growth, survival and differentiation through various intracellular pathways. EGFR and HER2 are deregulated in various cancers, but their role in bladder cancer is still undefined. The aim of this project was to investigate whether EGFR and/or HER2 inhibition may be an effective treatment for bladder carcinoma. In order to do this, the effect of three different tyrosine kinase inhibitors (TKIs) that target EGFR and/or HER2 (lapatinib, erlotinib and CP654577) was evaluated in a panel of well-characterized bladder cancer-derived cell lines.

EGFR and HER2 expression was determined in the six bladder cancer cell lines. Dose-response curves were generated to determine sensitivity to lapatinib, erlotinib or CP654577. Cell cycle analysis and apoptosis assays were used to further characterize the biological effects of the TKIs. Changes in downstream signalling events after EGFR and/or HER2 inhibition were also evaluated using a human phosphokinase array.

All three TKIs had concentration dependent antiproliferative effect across the panel of bladder cancer cell lines. A significant correlation was found between EGFR protein expression and sensitivity to erlotinib ($r = - 0.9429$, $p = 0.0167$). Cell cycle analysis revealed that all three TKIs induced G_1 arrest in RT112 cells. They also induced apoptosis, except for erlotinib. The results from the human phosphokinase arrays revealed a significant increase in phospho-p38 MAPK levels after erlotinib and lapatinib treatment. Inhibition of p38 MAPK had a synergistic effect in cell growth inhibition in combination with lapatinib in two bladder cancer cell lines.

Taken together, these data suggest that targeting EGFR and/or HER2 in bladder cancer may provide clinical benefit in these patients. Moreover, p38 MAPK may be a therapeutic target either alone or in combination with EGFR and/or HER2 inhibitors, which may provide a new combination therapy for bladder cancer. These studies could provide the rationale for the use of novel targeted therapies in bladder cancer.

Contents

List of figures

Chapter 6

List of tables

Chapter 6

DECLARATION OF AUTHORSHIP

I, Regina Mora Vidal

declare that the thesis entitled

Investigation of members of the human epidermal growth factor receptor family as potential therapeutic targets for bladder cancer

and the work presented in the thesis are both my own, and have been generated by me as the result of my own original research. I confirm that:

- this work was done wholly or mainly while in candidature for a research degree at this University;
- where any part of this thesis has previously been submitted for a degree or any other qualification at this University or any other institution, this has been clearly stated;
- where I have consulted the published work of others, this is always clearly attributed;
- where I have quoted from the work of others, the source is always given. With the exception of such quotations, this thesis is entirely my own work;
- I have acknowledged all main sources of help;
- where the thesis is based on work done by myself jointly with others, I have made clear exactly what was done by others and what I have contributed myself;
- none of this work has been published before submission.

Signed: ……..

Date:…….

Acknowledgements

I would like to take this opportunity to thank a number of people who made this project possible. First, I would like to thank Dr Simon Crabb for giving me the opportunity to conduct this research under his supervision, and for his guidance and invaluable support during these years. I would also like to thank Professor Graham Packham for his support, advice and helpful discussions on this project.

I would also like to express my gratitude to Dr Annette Hayden for her help during the first months of this research and to Dr Emre Sayan for his interest in this project. I would also like to thank the oncology pharmacy at Southampton General Hospital for providing some of the drugs used in this study and the BBSRC for funding this work.

A big thank you to all past and present members from the Graham Packham group and all people at the Somers building for their help and for providing a friendly environment, and especially to Bea, Vania, Marta, Max and Miao. I would also like to thank my family and friends for always being there for me, and especially to my parents.

I would like to dedicate this work to my grandmother.

Abbreviations

ADAM a disintegrin and metalloprotease

ADCC antibody-dependent cellular cytotoxicity

AR amphiregulin

BCG bacillus Calmette-Guerin

BTC betacellulin

CDC complement-dependent cytotoxicity

CDK cyclin-dependent kinase

CDKI cyclin-dependent kinase inhibitor

CDKN1A cyclin-dependent kinase inhibitor 1A

CIS carcinoma in situ

COX2 cyclooxygenase 2

DMEM Dulbecco's modified Eagles medium

DMSO dimethyl sulfoxide

DTT dithiothreitol

ECM extracellular matrix

EGF epidermal growth factor

EGFR epidermal growth factor receptor

EMT epithelial-to-mesenchymal transition

EPI epiregulin

ERK extracellular signal-regulated kinase

FDA Food and drug administration

FGFR3 fibroblast growth factor receptor 3

FISH fluorescence in situ hybridization

FRET Förster resonance energy transfer

HB-EGF heparin-binding EGF-like growth factor

HER human epidermal growth factor receptor

HRAS Harvey rat sarcoma viral oncogene homolog gene

HRGs heregulins

HRP horseradish peroxidase

IHC immunohistochemistry

IP immunoprecipitation

JAK Janus kinase

KRAS v-Ki-ras2 Kirsten rat sarcoma viral oncogene homolog

mAb monoclonal antibody

MAPK mitogen-activated protein kinase

MMPs matrix metalloproteinases

MSK mitogen-and stress-activated kinase

NF-κB nuclear factor κB

NRG-1 neuregulin-1

NSCLC non-small cell lung cancer

PAGE polyacrylamide gel electrophoresis

PARP poly (ADP-ribose) polymerase

PBS phosphate buffered saline

PCR polymerase chain reaction

PDK1 3-phosphoinositide-dependent protein kinase-1

PI propidium iodide

PI3K phosphatidylinositol 3-kinase

PIP2 phosphatidylinositol-4,5-bisphosphate

PIP3 phosphatidylinositol-3,4,5-trisphosphate

PLCγ phospholipase C-γ

PS phosphatidylserine

PTEN phosphatase and tensin homolog

RB retinoblastoma

RPMI Roswell Park Memorial Institute

SDS sodium dodecyl sulfate

SOS son of sevenless

STAT signal transducer and activator of transcription

TCC transitional cell carcinoma

TGF- α transforming growth factor- α

TKI tyrosine kinase inhibitor

TMA tissue microarray

TSP-1 thrombospondin 1

UC urothelial carcinoma

VEGF vascular endothelial growth factor

VEGF-A vascular endothelial growth factor A

Chapter 1: Introduction

1.1 Molecular biology of cancer

Cancer is considered a multistep process rather than a single event where normal cells transform to malignant cells. In this process, cancer cells need to acquire a series of well-defined biological characteristics or hallmarks: sustained proliferative signalling, evasion of growth suppressors, resistance of cell death, unlimited replicative potential, sustained angiogenesis and the ability to invade and metastasize (Hanahan and Weinberg 2000).

Probably the most characteristic trait of cancer cells is their ability to proliferate autonomously. In normal cells, cell proliferation is tightly regulated and depends on external signals. Cancer cells, however, can produce their own factors to stimulate proliferation (autocrine proliferative stimulation) or can stimulate other cells to produce them for them (paracrine proliferative stimulation). Other mechanisms adopted by cancer cells for this chronic proliferation are the overexpression of membrane receptors or mutations in their structure, which can also result in amplified signals of proliferation, as well as constitutive activation of components downstream of these receptors.

Insensitivity to growth inhibitory signals is another hallmark of cancer. Tumour suppressor genes regulate the cell cycle or promote apoptosis to prevent inappropriate cell division. Cancer cells, however, frequently have inactivation of tumour suppressor genes such as retinoblastoma (RB), which is controlled mainly by external signals, and p53, controlled by intracellular signals.

Another trait of cancer cells is their ability to resist programmed cell death. For instance, more than 50% of human cancers have lost the p53 tumour suppressor function, a DNA-damage sensor that induces apoptosis, giving tumour cells the ability to evade apoptosis. Other strategies of cancer cells to evade apoptosis are the increase of antiapoptotic regulators (e.g. Bcl-2, Bcl-x_L) or the downregulation of proapoptotic factors (e.g. Bax, Bim, Puma).

The potential for unlimited proliferation is another characteristic of cancer cells. Mammalian cells have a finite replicative potential determined by the length of telomeric DNA. Telomeres have a protective function on the ends of chromosomal DNA, but after each cell division there is a progressive shortening of telomeres. This results in unprotected ends of chromosomal DNA, causing end-to-end chromosomal fusions leading to cell death. Cancer cells, however, have acquired unlimited replicative potential by increasing their telomerase activity. Telomerase, a DNA polymerase that adds telomere repeat segments to the ends of telomeric DNA, allows unlimited multiplications of the cells by protecting the ends of chromosomal DNAs from end-to-end fusions.

Another hallmark of cancer cells is their ability to induce angiogenesis. Oxygen and nutrients supply requires the growth of new blood vessels, which is even important in early stages of tumorigenesis. The vascular endothelial growth factor -A (VEGF-A) and thrombospondin-1 (TSP-1) are prototypes of angiogenesis inducers and inhibitors, respectively. Tumours have chronically activated angiogenesis by increasing the expression of VEGF-A or by downregulation of TSP-1.

One of the most damaging phenotype of cancer cells and the major cause of cancer death is the ability of these cells to invade local tissues and metastasize. A common alteration found in cancer cells is the loss of E-cadherin, a key cell-to-cell adhesion molecule. On the other hand, N-cadherin, a molecule associated with cell migration, is found to be upregulated in many invasive carcinoma cells.

Since these hallmarks of cancer were reviewed by Hanahan and Weinberg in 2000, new hallmarks have emerged, such as the ability of cancer cells to reprogram their glucose metabolism (“Warburg Effect” or “aerobic glycolysis”) and the ability to evade immune surveillance, which is responsible for identifying and eradicating cancer cells (Hanahan and Weinberg 2011).

The acquisition of all these hallmarks is possible due to two enabling characteristics; genomic instability and inflammation within tumours. Also of crucial importance are the cells forming the “tumour microenvironment” considered to be active participants of tumorigenesis.

1.2 Bladder cancer

1.2.1 Introduction to bladder cancer

Bladder cancer is the seventh most common cancer in the UK. In 2010, around 10,000 people were diagnosed with bladder cancer and nearly 5,000 died from this disease. More than 90% of bladder cancers present as urothelial carcinoma (UC) or transitional cell carcinomas (TCCs), 8% are squamous cell carcinomas, and less than 2% are adenocarcinomas and other rare subtypes. It is more common in men than in women, affecting mainly people over 65 years old. External risk factors strongly linked to TCCs are tobacco smoking and occupational exposure to aromatic amines, found in dyes, rubber, paints and leather processing (Mitra and Cote 2009). In Egypt and parts of Middle East and Africa, the most common form of bladder cancer is the squamous cell carcinoma, which is associated with *Schistosoma haematobium*, a parasite endemic in these areas. The irritation and inflammation caused by this parasite is thought to play an important role in the carcinogenesis of this particular type of bladder cancer (Mostafa *et al.* 1999).

TCCs can be very heterogeneous in terms of their biology, but they can be grouped into two different phenotypes, which have a very different biological behaviour and prognosis. Approximately 80% of TCC patients present with low grade superficial tumours, when cancer cells are found only in the innermost layer of the bladder (the lining). There are three forms of superficial tumours: CIS (carcinoma in situ) and Ta (papillary carcinoma) are detected in the innermost layer of the bladder lining whereas in T1, the cancer has started to grow into the connective tissue just under the bladder lining. The other 20% of bladder cancer patients present with muscle invasive tumours, when the cancer has spread into the muscle layer of the bladder. In T2 tumours, the cancer has grown through the connective tissue into the muscle. In T3 tumours, the cancer has grown through the muscle into the fat layer. In T4, the cancer has spread outside the bladder to directly invade either other organs (e.g. prostate, uterus, vagina) or the pelvic or abdominal wall. T2-T4 are classified as invasive bladder cancer. Ta and T1 carcinomas are not normally invasive but can frequently recur, whereas CIS more often become invasive.

This project is about TCCs and this can occur anywhere in the urothelial tract (renal pelvis, ureters, urethra). From here on, I will refer to TCC of the bladder as "bladder cancer" or "TCCs".

1.2.2 Pathogenesis of bladder cancer

Alterations of various molecular pathways have been involved in the pathogenesis of TCCs. Some alterations are frequently found in superficial tumours, whereas others are more common in invasive tumours, so it has been proposed that pathogenesis of TCC consists of two alternative molecular pathways (shown in Figure 1.1), which would explain their divergent clinical behaviour (Wu 2005). However, as some superficial tumours can progress to high-grade, invasive carcinomas, it is believed that there may be some overlap between the two pathways (Luis *et al.* 2007).

Superficial, non-invasive tumours are mainly characterized by mutations in the *fibroblast growth factor receptor 3* (*FGFR3*) and the *Harvey rat sarcoma viral oncogene homolog* (*HRAS)* genes. FGFR3 is a member of the FGFR family, which are cell-surface tyrosine kinase receptors. *FGFR3* is mutated in approximately 70% of low grade, non-invasive tumours (Billerey *et al.* 2001). Mutations in the *PI3KCA* gene, which encodes the catalytic p110 subunit of PI3K, occur in 20% of superficial bladder tumours and are associated with *FGFR3* mutations (Lopez-Knowles *et al.* 2006).

FGFR3 mutations lead to constitutive activation of the receptor, activating the Ras-mitogen-activated protein kinase (MAPK) pathway. *HRAS* mutations are also commonly found in superficial bladder cancer (30-40%). *HRAS* codes for a protein anchored to the cytoplasmic side of the cell membrane that is involved in signal transduction, activating also the MAPK pathway. Mutations in the *FGFR3* and *RAS* genes are mutually exclusive in low grade TCCs as it has been found that 80% of these tumours have mutations in either one gene or the other (Jebar *et al.* 2005). This also suggests that activation of the Ras-MAPK pathway is essential for the initiation of superficial bladder cancer (Dovedi and Davies 2009).

It has been proposed that the lower malignant potential of these cancers is due to MAPK signalling activation, which besides its role in cell proliferation, can also stimulate cell

differentiation and induction of inhibitors that lead to cell cycle arrest and senescence, which might explain why these tumours are self-limiting (Schulz 2006).

By contrast, CIS and invasive tumours (T2-T4) contain mutations in the tumour suppressors' *TP53* and/or *retinoblastoma* (*RB*) at a higher frequency to what is seen in superficial tumours. The *TP53* gene encodes p53, a transcription factor which has a critical role in the control of the cell cycle, but it is also important in DNA repair, angiogenesis and apoptosis. p53 inhibits cell cycle progression at G_1-S transition through the transcriptional activation of the *cyclin-dependent kinase inhibitor 1A (CDKN1A)* gene, which encodes the p21 protein, a cyclin-dependent kinase inhibitor (CDKI). Inactivating mutations in p53 are very common (>50%) in invasive bladder tumours (Wright *et al.* 1991), and they can result in loss of p21 expression, leading to tumour progression. Higher p53 expression is associated with higher recurrence and shorter overall survival (Williams and Stein 2004).

It has also been found that 41% of tumours with altered p53 also show downregulation of phosphatase and tensin homolog (PTEN). This combined PTEN and p53 inactivation may promote bladder cancer tumorigenesis due to increased mTOR signalling, leading to an aggressive form of bladder cancer associated with poor patient outcome, with a median survival of 6 months (Puzio-Kuter *et al.* 2009).

The *RB* gene encodes a nuclear phosphoprotein (pRb) that regulates the cell cycle at the G_1-S transition. In its active or dephosphorylated form, pRb blocks cell proliferation by binding and altering the function of E2F, a transcription factor that controls the expression of genes essential for the progression from G_1 to S phase. When Rb is phosphorylated by cyclin/cyclin-dependent kinases (CDK) complexes, E2F is released, allowing transcription of proteins required for the G_1-S transition (Weinberg 1995).

Loss of pRb expression has been associated with shorter survival in bladder cancer patients (Cordon-Cardo *et al.* 1992). Moreover, tumours that contain alterations on both p53 and Rb have a worse prognosis compared with patients with tumours that contain only alterations in one or none of these proteins, indicating a synergism between them to promote tumour progression (CordonCardo *et al.* 1997; Cote *et al.* 1998).

Invasive tumours have also alterations in cadherins (N- and E-cadherins), matrix metalloproteinases (MMPs), vascular endothelial growth factor (VEGF), thrombospondin 1 (TSP-1) and cyclooxygenase 2 (COX2), which can remodel the extracellular matrix (ECM) and promote angiogenesis (Wu 2005).

Deletions on both arms of chromosome 9 are considered to be the earliest event in bladder carcinogenesis and is characteristic of approximately 60% of all grades and stages of TCCs (Cairns *et al.* 1993). Candidates for these alterations are loss of cyclin-dependent kinase inhibitor 2A (*CDKN2A*) gene that encodes $p16^{INK4A}$ on 9p and tuberous sclerosis 1 (*TSC1*) on 9q (Schulz 2006). Invasive tumours have other chromosomal abnormalities as well, whereas superficial tumours show few genetic alterations other than on chromosome 9 (Williams and Stein 2004).

Figure 1.1 is therefore a schematic representation of the two biological states based on current understanding. However, this model is not complete and there is some overlap between both pathways not completely understood. Therefore, more work is needed to elucidate bladder cancer biology. Despite this, this model does seem to correlate with clinically different states (superficial versus high grade/invasive tumours).

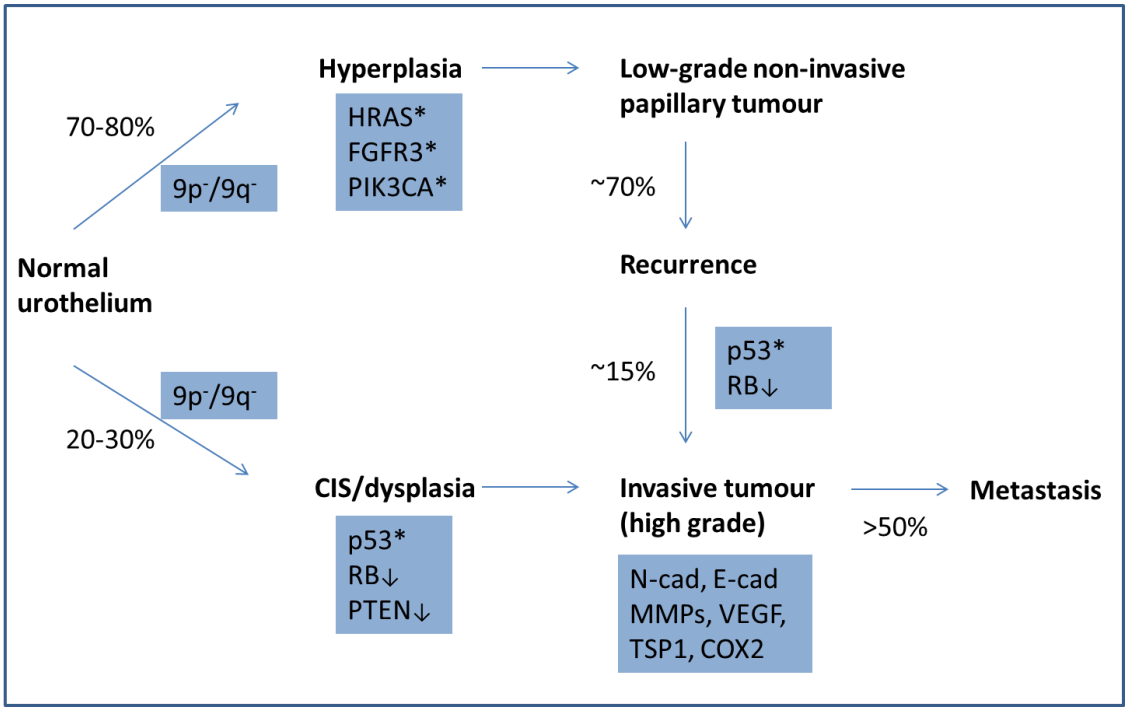

Figure 1.1 Characterization of the divergent molecular pathways proposed for bladder cancer tumorigenesis. Deletion of both arms of the chromosome 9 ($9p^-/9q^-$) are thought to be an early event of both pathways. 70-80% of TCCs present as low-grade, superficial and papillary cancers. Mutations in the *HRAS* gene, *fibroblast growth factor receptor 3* gene (*FGFR3*) and *PI3KCA* gene are commonly found in these tumours. Around 70% of these tumours will recur, and approximately 15% will become invasive. 20-30% of TCCs present as high-grade muscle-invasive tumours. Mutations in the p53 and Rb pathways as well as PTEN loss are commonly found in these tumours and over 50% of them will metastasize. Alterations in genes involved in cell adhesion (N- and E-cadherins), proteases (MMPs) and angiogenesis (VEGF, TSP1, COX2) play an important role in metastases. * indicates mutated proteins. Adapted from (Wu 2005).

1.2.3 Treatment of bladder cancer

Treatment of TCC varies depending on the phenotype of the tumour. Superficial tumours are normally treated by surgery to remove the tumour followed in some cases by intravesical chemotherapy or immunotherapy. Mitomycin C is the agent of choice for chemotherapy, and bacillus Calmette-Guerin (BCG) is used for the immunotherapy (Dovedi and Davies 2009). However, there are frequent recurrences in superficial carcinomas (~70%), and around 15% will progress to be muscle invasive.

Muscle-invasive tumours are usually treated aggressively if this is feasible with chemotherapy followed by radical cystectomy or radiotherapy. They represent the major cause of morbidity and mortality as at least 50% of these patients will develop metastasis and die within 2 years of diagnosis. Metastatic bladder cancer is generally viewed as an incurable disease as the 5-year survival rate is below 10% (Dovedi and Davies 2009).

Cisplatin-based chemotherapy represents the most effective treatment for advanced bladder cancer and remains the first-line treatment for these patients (Stenzl *et al.* 2011). Since its introduction in 1985, systemic chemotherapy with the methotrexate, vinblastine, doxorubicin and cisplatin regimen (MVAC) was considered the standard chemotherapeutic regimen for metastatic bladder cancer, producing a median survival of 14 to 15 months (Sternberg *et al.* 2007). The administration of the gemcitabine and cisplatin (GC) regimen has become preferred over MVAC as it has shown decreased toxicity and better tolerability, but it has not improved the response rate or the overall survival compared to MVAC (von der Maase *et al.* 2000). A second-line chemotherapy has become available with the recent approval of vinflunine (Stenzl *et al.* 2011).

Despite the current treatments available to treat bladder cancer, the high failure rate in both superficial and invasive disease by conventional therapy has led to increased interest in more effective therapies to improve clinical outcome of bladder cancer patients. In recent years, research in bladder cancer has focused on the identification of molecular alterations and biological characteristics of these tumours. The identification of altered molecular pathways in bladder cancer could serve as prognostic markers to predict which superficial tumours will recur or become invasive or which invasive tumours will metastasize. Furthermore, these molecular alterations might potentially be

used as targets for future therapies, ideally based on individual tumour profiles (Youssef *et al.* 2009). Targeted therapy has the potential to improve management of these patients, as it could be used on their own or in combination with standard therapies to enhance overall treatment efficacy. It also has the potential to avoid some of the side effects associated with cytotoxic chemotherapy. There is no targeted therapy currently approved for use in bladder cancer, but there is considerable clinical research currently on-going. The HER family (and especially EGFR and HER2) and their role in bladder cancer will be the main focus in this study.

1.3 The HER family

Members of the human epidermal growth factor receptor (EGFR or HER) family are commonly overexpressed in malignant disease, where they regulate many vital cellular processes. They can be useful as prognostic and/or predictive markers, and they have also become therapeutic targets in recent years. The HER family proteins have also been associated with bladder tumorigenesis, so they could represent an important potential target for therapy in bladder cancer (Bellmunt *et al.* 2003). EGFR and HER2 targeted therapy have significantly changed the prognosis of a wide variety of tumours in the last few years, especially HER2 targeted therapy in breast cancer.

The human epidermal growth factor or HER family of receptors consists of four distinct, but structurally similar members: EGFR (ErbB1/HER1), HER2 (ErbB2/neu), HER3 (ErbB3) and HER4 (ErbB4). They are expressed in epithelial, mesenchymal and neuronal tissues where they play important roles in development, proliferation and differentiation in response to extracellular ligands (Olayioye *et al.* 2000).

These cell surface receptors (shown in Figure 1.2) contain a large and heavily glycosylated extracellular domain for ligand binding, a transmembrane domain and an intracellular domain with tyrosine kinase activity and a carboxy-terminal tail with tyrosine autophosphorylation sites. There are four subdomains in the extracellular region of the HER receptors (I-IV); subdomains I and III are rich in leucine repeats and facilitate ligand binding (also called L1 and L2), whereas subdomains II and IV are rich

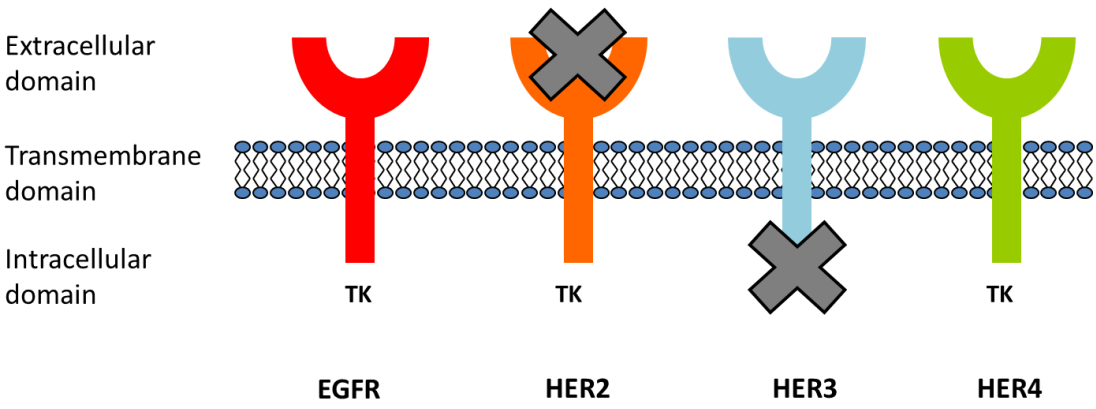

Figure 1.2 The HER family of receptors. The human epidermal growth factor or HER family of receptor consists of 4 different proteins; EGFR, HER2, HER3 and HER4. They all share a similar structure: an extracellular domain for ligand binding, a transmembrane domain and an intracellular domain with tyrosine kinase activity. However, HER2 has no known ligand, and HER3 has no tyrosine kinase activity.

in cysteine (S1 and S2) and are involved in receptor dimerization, which is essential for the activity of these family of receptors. In the absence of ligand, the dimerization domain (domain II) is engaged in intramolecular interactions with domain IV, but after ligand binding, the conformation of the extracellular domain changes, exposing the dimerization domain and making receptor-receptor interactions possible (Burgess *et al.* 2003).

There are approximately thirteen different ligands for these receptors, which contain a conserved epidermal growth factor domain (Citri and Yarden 2006). These include the epidermal growth factor (EGF), transforming growth factor-α (TGF-α), amphiregulin (AR), heparin-binding EGF-like growth factor (HB-EGF), betacellulin (BTC) and epiregulin (EPI), which can bind to EGFR, whereas the heregulins (HRGs) or neuregulins (NRGs) are the ligands for HER3 and HER4. They are produced as glycosylated transmembrane proteins, and proteases at the cell membrane (sheddases) will cleave them to release mature growth factors. ADAM10 and ADAM17 (a disintegrin and metalloprotease 10 and 17) have been found to be the main sheddases to release EGFR ligands (Sahin *et al.* 2004). HER2 has no known activating ligand, which is due to its unique structure; a strong interaction between domains I and III leaves the receptor in a conformation where is unable to bind a ligand. However, the dimerization domain is constitutively exposed, similar to the ligand-bound state, leaving HER2 ready for receptor-receptor interactions (Citri and Yarden 2006).

After ligand binding, the receptor undergoes dimerization, forming either homodimers or heterodimers among other family members. These conformational changes within the receptor complex lead to the activation of the tyrosine kinase domain, which results in the tyrosine autophosphorylation of the C-terminal tail. The phosphorylation on tyrosine residues promotes interaction of the receptor with adaptor molecules in the cytoplasm that activate multiple intracellular signalling pathways, including the mitogen-activated protein kinase pathway (Ras-MAPK) and the phosphatidylinositol 3-kinase (PI3K/Akt) pathway, which play an important role in both cell proliferation and survival respectively (Mendelsohn and Baselga 2000). However, the Janus kinase (JAK)/ signal transducer and activator of transcription-3 (STAT3), Src, phospholipase C-γ (PLCγ) and other pathways are also involved in certain cellular and biological contexts.

To activate the Ras-MAPK pathway, the phosphorylated tyrosine residues provide binding sites for the adaptor protein Grb2 (growth factor receptor-bound protein 2), activating it directly, or indirectly through interaction with Shc (Src-homology-2-domain-containing). Grb2 then recruits SOS (son-of-sevenless), a Ras-activating guanine nucleotide exchange factor, which activates Ras by exchanging GDP for GTP. Activated Ras interacts with Raf, which binds to and phosphorylates MEK1/2, which then phosphorylate ERK1/2 (extracellular signal-regulated kinase 1 and 2) (shown in Figure 1.3). Once activated, ERK1/2 can phosphorylate a wide range of cellular substrates, including membrane proteins, cytoskeletal proteins and nuclear substrates and this signalling pathway has a major role in controlling cellular proliferation (Roux and Blenis 2004).

The other critical pathway activated by the HER family members is the PI3K/Akt pathway (shown in Figure 1.3) which plays a crucial role in cell growth, proliferation and survival (Cantley 2002). PI3K is a heterodimer that consists of a catalytic subunit (p110) and a regulatory subunit (p85). PI3K is activated through the binding of the p85 regulatory subunit to a phosphotyrosine site on the receptor, leading to the activation of the p110 catalytic subunit. Once activated, PI3K phosphorylates phosphatidylinositol-4,5-bisphosphate (PIP2) to phosphatidylinositol-3,4,5-trisphosphate (PIP3), which recruit several proteins to the cell membrane such as Akt (also known as protein kinase B, PKB) and PDK1 (3-phosphoinositide-dependent protein kinase-1). PKB/Akt, a serine threonine kinase, is thought to be the major player in the PI3K pathway; although it can also be activated by other molecules independent of the PI3K pathway. When Akt is recruited to the plasma membrane, it is phosphorylated by PDK1 at threonine 308 (Alessi *et al.* 1997). Activated Akt regulates a number of proteins involved in cell cycle control, apoptosis and cell survival. This pathway is negatively regulated by the tumour suppressor PTEN. PTEN dephosphorylates PIP3 to PIP2, therefore inhibiting the activity of PI3K and preventing Akt activation (Stambolic *et al.* 1998). Many other signalling pathways converge on the PI3K pathway. For example, Ras activates the PI3K pathway by interacting directly with p110 catalytic subunit of PI3K (Rodriguezviciana *et al.* 1994), while Akt also regulates the activity of the Ras–MAPK pathway through phosphorylation and inactivation of Raf (Manning and Cantley 2007).

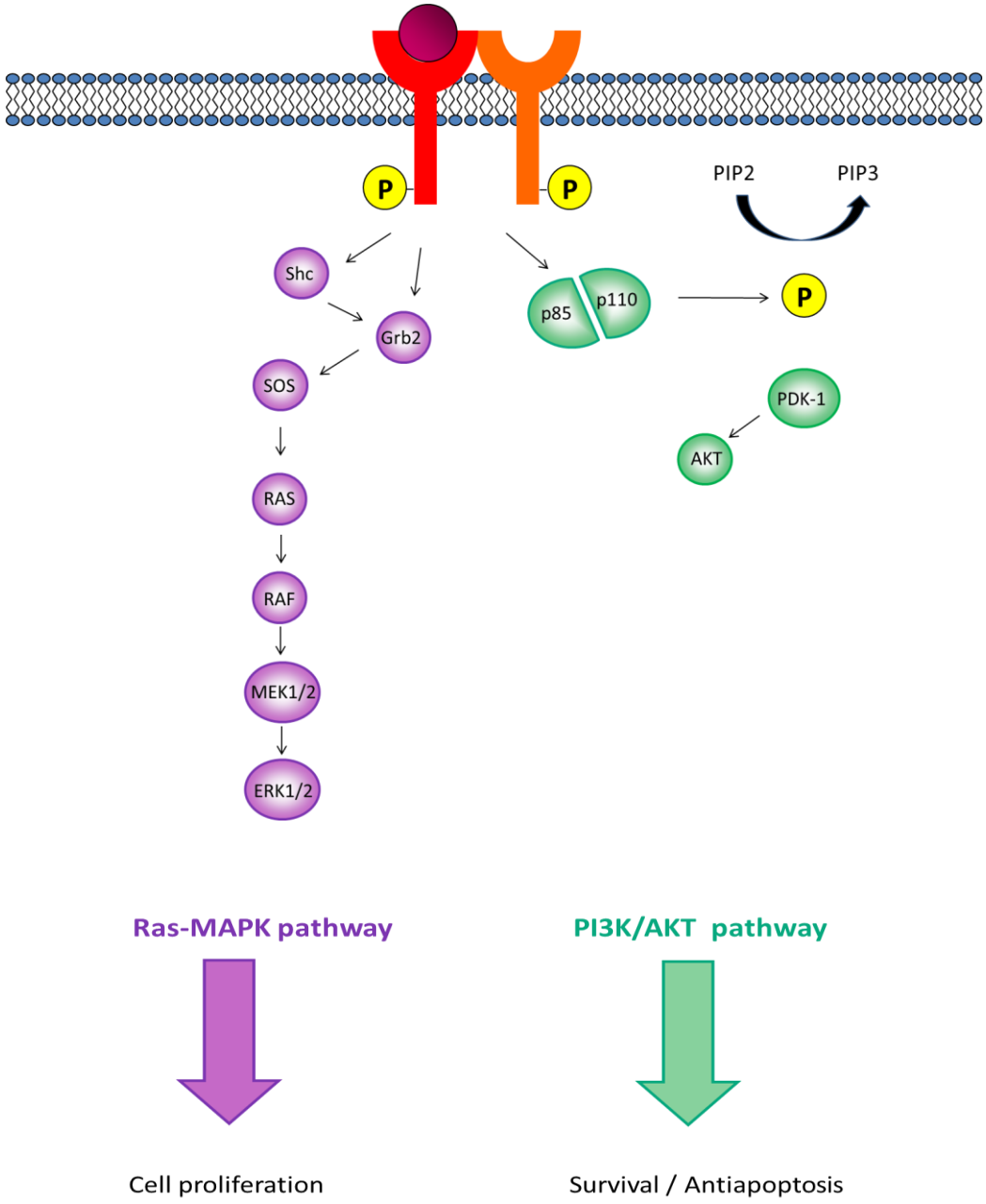

Figure 1.3 Some signalling pathways activated by HER family and their effects in the cell. Phosphorylated receptors activate the Ras-MAPK pathway and the PI3K/Akt pathway. After ligand binding, activated HER receptors bind adaptors molecules such as Shc or Grb2 leading to SOS recruitment and the activation of the Ras-MAPK pathway, which leads to cell proliferation through the activation of different nuclear targets. The PI3K/Akt pathway is activated through p85, the regulatory subunit of PI3K, which activates Akt, leading to enhanced anti-apoptotic and survival signals.

The inactivation of the signalling pathways downstream of HER family members is achieved when the ligand-receptor complex is internalized by endocytosis and the receptor is subsequently degraded or recycled back to the surface (Lemmon and Schlessinger 2010).

The HER family is therefore a complex network due to various numbers of ligands, receptors and the different downstream pathways that can be potentially activated. The type and intensity of the signalling pathways activated will depend on the ligand, the receptor activated and its dimer partner. In fact, a hierarchical relationship has been proposed to establish the potency of HER dimers; heterodimers are more active than homodimers, and HER2-containing heterodimers are particularly active, with the HER2–HER3 heterodimer being the most active (Tzahar *et al.* 1996).

All HER members have binding sites for the adaptor Grb2 and can in theory signal through the Ras/MAPK pathway (Sergina and Moasser 2007). However, EGFR, in contrast to other family members, induces activation of the PI3K pathway relatively weakly since it has no intracellular binding sites for PI3K (Soltoff *et al.* 1994), but it can induce its activation via Ras. On the other hand, EGFR is the only HER member that can activate the phospholipase C-γ pathway (Roskoski 2004).

HER2 is an 'orphan' receptor with no known ligand, but it has strong tyrosine kinase activity and it is thought to be the preferred heterodimeric partner of the other HER receptors (Graus-Porta *et al.* 1997; Tzahar *et al.* 1996), resulting in augmented signal transduction on ligand binding. Like EGFR, it also lacks binding motifs for PI3K (Soltoff *et al.* 1994).

HER3 lacks tyrosine kinase activity due to substitutions in critical residues in its tyrosine kinase domain (Guy *et al.* 1994) and it is then unable to activate downstream signalling pathways on its own or as a homodimer. However, it can be phosphorylated when forming heterodimers and it can then strongly activate the PI3K pathway, as it has seven intracellular binding sites for PI3K (Soltoff *et al.* 1994).

HER4 has one intracellular binding site for PI3K (Schulze *et al.* 2005). This receptor can activate gene expression through signalling pathways, but it can also undergo

proteolysis at the cell membrane, and the released intracellular domain can translocate into the nucleus where it can also regulate gene expression (Ni *et al.* 2001).

1.3.1 The HER family in cancer

Under homeostatic conditions, receptor activation is tightly regulated by the availability of ligands. However, overexpression or inappropriate activation of the HER family receptors can result in the exaggerated activation of signalling pathways, influencing cell proliferation, apoptosis, angiogenesis, migration and invasion (Holbro *et al.* 2003). In particular, EGFR and HER2 overexpression in non-malignant cell lines can transform the phenotype of these cells, and these two receptors have been implicated in the development of numerous types of human cancers (see Table 1.1), and have been associated with more aggressive clinical behaviour (Mendelsohn and Baselga 2000).

EGFR is deregulated in various types of human malignancies mainly due to overexpression or mutations (Yarden and Sliwkowski 2001). This deregulation leads to high tyrosine kinase activity, activating signalling pathways that promote survival and cell cycle progression. Overexpression of EGFR is frequent in glioblastomas and in non-small cell lung cancer (NSCLC), but also in head and neck, ovary, cervix, oesophagus, stomach, endometrium, colon and breast cancer (Sergina and Moasser 2007). The most common mutation, EGFR class III variant or EGFR vIII, deletes part of the extracellular domain, resulting in a constitutively active receptor in the absence of ligands. It is commonly found in glioblastomas, but has also been reported in breast, ovarian and lung carcinomas (Normanno *et al.* 2006). EGFR expression is a strong prognostic indicator for poor clinical outcome in head and neck, ovarian, cervical and oesophageal cancers (Nicholson *et al.* 2001).

HER2 at physiological levels forms heterodimers with other family members activated by their specific ligands. However, like EGFR, HER2 is also involved in human cancers and it is thought that high expression levels of HER2 promotes spontaneous dimerization, causing constitutive HER2 activation and downstream signalling (Holbro *et al.* 2003). HER2 deregulation is well-known in breast cancer, where the protein is found to be overexpressed in 20-30% of patients due to gene amplification. HER2 was first linked to breast cancer in 1987 and its amplification was associated with worse prognosis (Slamon *et al.* 1987), establishing the hypothesis that HER2 overexpression

could be involved in the pathogenesis of some human malignancies. Different *in vitro* and transgenic models studies have found that HER2 overexpression induces malignant transformation, confirming the hypothesis (Moasser 2007). Since then, other cancers are known to overexpress HER2 such as lung, pancreas, colon, oesophagus, gastric and ovarian cancer. HER2 mutations are rare, only seen in a small percentage of lung cancer patients (Stephens *et al.* 2004).

HER3 is overexpressed in breast, colon, prostate and stomach cancers (Roskoski 2004), although it has not been implicated as a driving oncogene. However, its role in cancers driven by EGFR or HER2 is not clear, especially when the HER2-HER3 heterodimer is considered the most powerful in activating signalling pathways (Sergina and Moasser 2007). In *in vitro* models it has been shown that HER3 is not transforming by itself, but it is thought that it may have a critical role as a mediator of the oncogenic functions of other HER family members, and also in providing resistance to targeted therapy in breast and lung tumours (Sithanandam and Anderson 2008).

There is no evidence that HER4 is involved in any type of cancer, and on the contrary, some reports have suggested that it may have antiproliferative effect on breast tumour cells (Sartor *et al.* 2001; Sassen *et al.* 2009).

Gene	Malignancy	Alteration	Frequency
EGFR	Breast cancer	Gene amplification	5%
		Overexpression	20-30%
	Glioblastoma multiforme	Deletions and mutations	40-60%
		Overexpression	40%
	Non-small cell lung cancer	Kinase domain mutations	5-50%
		Gene amplification	5-10%
	Head and neck cancer	Overexpression	80%
	Colorectal cancer	Overexpression	60-80%
HER2	Breast cancer	Gene amplification	20-30%
	Non-small cell lung cancer	Kinase domain mutations	4%
	Oesophageal adenocarcinoma	Gene amplification	15-40%
	Gastrointestinal cancer	Gene amplification	20-30%

Table 1.1 The epidermal growth factor receptor family and cancer. Adapted from (Wieduwilt and Moasser 2008).

1.3.2 The role of the HER family in bladder cancer

Overexpression of EGFR or HER2 has prognostic value and can be used as a therapeutic strategy in various malignancies. However, its significance in bladder cancer remains controversial since contradictory reports have been published over the last 20 years. This could be due to the conditions of the samples used, different methods used when measuring EGFR and/or HER2 expression (immunohistochemistry; IHC, real-time PCR or fluorescence in situ hybridization; FISH), and also the fact that in each study there is a heterogeneous mix of tumour stage and grade. However, most studies report overexpression of EGFR and/or HER2 in subsets of cases and, as in other cancers, their overexpression has been linked in some studies at least to poor prognosis (see Tables 1.2 and 1.3).

Overexpression of EGFR is highly variable in bladder cancer, ranging from 31-96% in the published literature, and it has been associated with high grade and/or stage (Lipponen and Eskelinen 1994; Neal *et al.* 1990; Wright *et al.* 1991). Increased EGFR expression has also been associated with increased probability of progression and death in bladder cancer in some of these reports (Kassouf *et al.* 2008; Lipponen and Eskelinen 1994). Unlike other cancers, mutations within the kinase domain of EGFR or the truncated variant EGFR vIII are rare events in bladder cancer (Blehm *et al.* 2006).

Overexpression of HER2 in bladder carcinoma in the published literature is also very variable, ranging from 9 to 98%, and it has been associated with high tumour grade in some studies (Kruger *et al.* 2002). Prognostic significance of HER2 overexpression in bladder cancer is also uncertain due to conflicting results of different studies, but some reports have shown an association between HER2 expression and poor long term survival (Chow *et al.* 2001; Kruger *et al.* 2002; Mellon *et al.* 1996).

Although HER2 gene amplification is observed rarely in bladder cancer, suggesting that other mechanisms are responsible for HER2 overexpression (Mellon *et al.* 1996), a large study including 1005 muscle invasive tumours showed that 9.2% of tumours overexpressed HER2 and that 5.1% had HER2 gene amplification (Lae *et al.* 2010). Moreover, a recent study identified HER2 amplification in 9% of high-grade non-muscle invasive bladder cancer, and it was associated with higher risk of recurrence and progression (Chen *et al.* 2013).

Besides EGFR and HER2, it is also important to consider the other HER family members, HER3 and HER4. For instance, Chow *et al.* suggested that combination of HER expression levels may be a better prognostic indicator than the expression of individual receptors on their own as they found poor long-term survival with HER2 expression but also with EGFR-HER2 and HER2-HER3 co-overexpression (Chow *et al.* 2001). On the other hand, it has also been suggested that the balance between HER family receptors may have a role in driving the cells towards either proliferation or growth inhibition. For instance, in a study by Rotterud *et al.* it was found that HER2 expression increased and HER4 decreased from normal samples to carcinomas (Rotterud *et al.* 2005). Another report showed that tumours that express high levels of EGFR and low levels of HER4 may identify patients with an adverse prognosis (Kassouf *et al.* 2008).

Memon *et al.* showed that the outcome of patients with EGFR and HER2 expressing tumours is dependent on the expression of HER3 and HER4; expression of EGFR or HER2 on their own showed no correlation with survival. However, when EGFR or HER2 were expressed in the presence of HER3 and HER4, it was associated with a good prognosis (Memon *et al.* 2006). Another study showed that patients who express the HER4 isoform JM-a/CYT2 relate to favourable prognosis but only when the oestrogen receptor α is not co-expressed (Munk *et al.* 2013), suggesting that the co-expression of other receptors other than HER family members may also influence prognosis.

In conclusion, although the available evidence is rather complex, EGFR and HER2 appear to have an important role in bladder tumorigenesis and/or progression and seem to be associated with poor prognosis. This is also supported by a recent systematic review and meta-analysis on the clinical significance of the HER family members in bladder cancer, where the authors reported a significant association between EGFR and HER2 expression with progression and mortality in bladder cancer patients (Tsai *et al.* 2012). Therefore, they could be used as potential therapeutic targets in this disease. The role of HER3 as a prognostic factor is still controversial in bladder cancer, whereas HER4 seems to serve as a good prognostic factor.

Reference	N° of samples	Method	EGFR overexpression	Finding
(Chow *et al.* 2001)	245 (primary human bladder cancer)	IHC	72.2%	No prognostic significance
(Memon *et al.* 2006)	88 (primary human bladder cancer)	qPCR	96%	No correlation with survival
(Korkolopoulou *et al.* 1997)	106 (primary human bladder cancer)	IHC	36.8%	No correlation with tumour grade or stage
(Wright *et al.* 1991)	82 (primary human bladder cancer)	IHC	31%	Strong association with stage and grade
(Lipponen and Eskelinen 1994)	234 (primary human bladder cancer)	IHC	35%	Association with high grade Poor long term survival
(Neal *et al.* 1990)	101 (primary human bladder cancer)	IHC	48%	Significant association with high grade Associated with an adverse prognosis
(Kramer *et al.* 2007)	121 (primary human bladder cancer)	IHC	37%	Associated with poor prognosis

Table 1.2 EGFR expression in bladder cancer. IHC; immunohistochemistry, qPCR; quantitative polymerase chain reaction.

Reference	N° of samples	Method	HER2 overexpression	Finding
(Kruger *et al.* 2002)	138 (muscle invasive bladder cancer)	IHC	41%	Associated with high grade carcinomas Worse disease-related survival
(Jimenez *et al.* 2001)	80 (muscle invasive bladder cancer)	IHC	28%	No prognostic significance to survival
(Chow *et al.* 2001)	245 (primary human bladder cancer)	IHC	44.5%	Poor long term survival
(Memon *et al.* 2006)	88 (primary human bladder cancer)	qPCR	98%	No correlation with survival
(Korkolopoulou *et al.* 1997)	106 (primary human bladder cancer)	IHC	39.6%	No correlation with survival
(Mellon *et al.* 1996)	95 (primary human bladder cancer)	IHC	21%	No association with tumour stage or grade Associated with an adverse prognosis
(Wright *et al.* 1991)	82 (primary human bladder cancer)	IHC	15%	Weak association with stage, no correlation with grade

Table 1.3 HER2 expression in bladder cancer. IHC; immunohistochemistry, qPCR; quantitative polymerase chain reaction.

1.4 Targeting HER family members

Targeted therapy works by inhibiting specific molecules involved in tumour growth and progression. Their specificity towards tumour cells gives the potential advantage of increased efficacy and less toxicity when compared to chemotherapy or radiotherapy. This may ultimately prolong the patient's life and improve its quality. The first targeted cancer therapy was used in breast cancer with the approval of tamoxifen, which targets the cellular receptor for the female sex hormone oestrogen, which many breast cancers require for growth (Atalay *et al.* 2003).

Due to their implication in the development and progression of many cancers, HER family members, and especially EGFR and HER2, have been considered an important target for therapy in certain cancers for many years and recently they have also been investigated as potential targets for therapy in bladder cancer. The understanding of the structure and function of these receptors has led to the rational development of new therapeutic approaches and monoclonal antibodies and tyrosine kinase inhibitors (TKI) have been developed in recent years to block their activity.

Targeted therapies directed at members of the HER family have proven effective against a variety of tumour types. Table 1.4 shows some of the drugs that have been approved for use in oncology.

1.4.1 Monoclonal antibodies (mAb)

Monoclonal antibodies target the extracellular domain of these receptors altering signalling properties, but they may also act by recruiting immune cells that may kill the tumour cell by attacking the antibody-receptor complex (antibody-dependent cellular cytotoxicity, ADCC) or by complement-dependent cytotoxicity (CDC) (Atalay *et al.* 2003). Another possibility is that they may induce receptor internalization and downregulation, enhancing receptor degradation (Ciardiello and Tortora 2008). However, there is still uncertainty in most cases on how they can inhibit tumour growth.

Compound	Company	Structure	Mechanism of action	Indication
Cetuximab (C225/Erbitux™)	ImClone	Monoclonal antibody	Inhibits EGFR	Squamous-cell carcinoma of the head and neck Colorectal cancer
Nimotuzumab (TheraCIM h-R3™)	YM-BioSciences	Monoclonal antibody	Inhibits EGFR	Squamous-cell carcinoma of the head and neck Nasopharyngeal cancer
Panitumumab (ABX-EGF/Vectibix™)	Amgen	Monoclonal antibody	Inhibits EGFR	Colorectal cancer
Trastuzumab (Herceptin™)	Genentech/Roche	Monoclonal antibody	Inhibits HER2	Breast cancer Gastric cancer
Pertuzumab (Perjeta™)	Genentech	Monoclonal antibody	Inhibits HER2	Breast cancer
Gefitinib (ZD-1839/Iressa™)	AstraZeneca	TKI	Inhibits EGFR	Non-small cell lung cancer
Erlotinib (OSI-774/Tarceva™)	Genentech/OSI Pharmaceuticals	TKI	Inhibits EGFR	Non-small cell lung cancer Pancreatic cancer
Lapatinib (GW-572016/Tycerb™)	GlaxoSmithKline	TKI	Inhibits EGFR/HER2	Breast cancer

Table 1.4 EGFR and HER2 targeted therapy drugs approved in oncology. Adapted from (Agarwal *et al.* 2007).

1.4.1.1 Trastuzumab

Trastuzumab is a humanised monoclonal antibody that binds to the extracellular domain of HER2 (domain IV). It was approved by the Food and Drug Administration (FDA) in 1998 as treatment for metastatic breast cancer in patients whose tumours overexpress HER2 and subsequently as an adjuvant treatment and in 2010 for gastric cancer.

Although not completely understood yet, trastuzumab potential mechanisms of action are; i) reduction of the shedding of the extracellular domain, thereby reducing p95, which can activate signal-transduction pathways; ii) inhibition of HER2 signalling by blocking the receptor homodimerization or heterodimerization; iii) recruitment of components of antibody-dependent cell-mediated cytotoxicity (ADCC), leading to tumour cell death or iv) downregulation of HER2 through endocytosis (Hudis 2007). The most serious side effects of this drug although fairly uncommon are cardiomyopathy and pulmonary toxicity.

1.4.1.2 Pertuzumab

Pertuzumab is also a humanised monoclonal antibody that binds to the dimerization domain of HER2 but in a different way to trastuzumab; it targets the dimerization domain of HER2 (domain II) and it is believed that it inhibits HER2 from forming dimers with other HER family members, blocking ligand-activated signalling (Agus *et al.* 2002). It has been approved by the FDA in June 2012 for HER2-positive metastatic breast cancer.

1.4.1.3 Cetuximab

Cetuximab is a chimeric monoclonal antibody that blocks ligand binding to EGFR. It is thought that after the antibody binds to EGFR, the receptor is internalized, leading to receptor downregulation at the cell surface and the inhibition of activation of signalling pathways (Youssef *et al.* 2009). Anti-tumour effects of this antibody have been attributed to different mechanisms, including the inhibition of cell cycle progression, angiogenesis and metastasis, induction of apoptosis and it also may be able to synergistically potentiate chemotherapy and radiotherapy cytotoxic effects (Baselga

2001). It was approved by the FDA in 2004 for patients with metastatic colorectal cancer and in 2006 for squamous-cell carcinoma of the head and neck. It has relatively few side effects, including asthenia, fever, nausea, acne-like rash and diarrhoea (Cunningham *et al.* 2004).

1.4.2 Tyrosine kinase inhibitors (TKIs)

TKIs are cell-permeable molecules that can inhibit the kinase activity of the HER family members by binding to the tyrosine kinase domain of the receptor, inhibiting receptor autophosphorylation and thereby inhibiting downstream signalling pathways. This mechanism of action is important since kinase activity is essential for the oncogenic function of these proteins. Most of these agents are ATP analogs that can bind reversibly or irreversibly within the ATP pocket of the catalytic domain of HER proteins. However, TKIs do not have the specificity of monoclonal antibodies. The catalytic kinase domain of the HER family members share significant homology with other kinase proteins, so specificity for the HER family was a concern for the development of TKIs to target these receptors (Wieduwilt and Moasser 2008). However, it was found that compounds based on the quinazoline structure showed high specificity for the HER family, and three compounds have been approved for clinical use in cancer: gefitinib (Iressa®), erlotinib (Tarceva®) and lapatinib (Tykerb®). Gefitinib and erlotinib show more specificity for the EGFR receptor, whereas lapatinib is specific for both EGFR and HER2. By inhibiting the tyrosine kinase domain of the HER family members, TKIs block the activation of signalling pathways, which results in induction of apoptosis and inhibition of cellular proliferation and angiogenesis (Sridhar *et al.* 2003). TKIs have the advantage that they can usually be given orally to patients, whereas monoclonal antibodies are usually given intravenously. Three different TKIs were used in this study; lapatinib, erlotinib and CP654577. Their structures are shown in Figure 1.4.

1.4.2.1 Lapatinib

Lapatinib is an oral reversible non-covalent dual TKI that targets both EGFR and HER2. It binds to the ATP-binding pocket of the EGFR and the HER2 protein kinase domain, inhibiting autophosphorylation of the receptors and activation of signalling

pathways such as ERK1/2 and Akt, leading to increased cell apoptosis and decreased cell proliferation (Xia *et al.* 2002).

Rusnak *et al*. showed how this drug was a potent inhibitor of both EGFR and HER2-driven tumour growth in tissue culture, showing a 100-fold more potency on these cell lines compared to normal fibroblast cells. It was also found to be highly specific for the HER receptors, being >300-fold selective for EGFR and HER2 over other kinases involved in cellular proliferation (Rusnak *et al.* 2001).

It was approved by the FDA in 2007 for its use in advanced or metastatic breast cancer patients whose tumours overexpress HER2, where it has proved to be effective. The most common adverse effects of lapatinib are diarrhoea, hand-foot syndrome, skin rash, nausea, rash and fatigue, but unlike trastuzumab, no cardiac toxicity has been reported (Medina and Goodin 2008).

1.4.2.2 Erlotinib

Erlotinib is another oral small molecule TKI. It reversibly inhibits the tyrosine kinase function of EGFR, inducing cell cycle arrest in G_1 and apoptosis (Moyer *et al.* 1997). It was approved by the FDA in 2004 for the treatment of chemotherapy-resistant advanced or metastatic non-small-cell lung cancer and in 2005 for pancreatic cancer. The most frequent adverse effects seen with erlotinib are an acneiform skin rash and diarrhoea, but these are dose-dependent and reversible. Skin rash is a common side effect to all EGFR inhibitors, including monoclonal antibodies and in some circumstances can be used as a predictive biomarker for treatment benefit (Ciardiello and Tortora 2008). Erlotinib has also been the first positron emission tomography radiolabeled TKI (TKI-PET) used for imaging TKI and target interactions. Although still in early stages, the first clinical evaluations using this imaging technique have showed promising potential for patient selection and stratification (Poot *et al.* 2013).

1.4.2.3 CP654577

There are a few HER2 TKIs under development, but none of them has been approved for clinical use yet. One of them is CP654577, a potent HER2 TKI. Treatment of

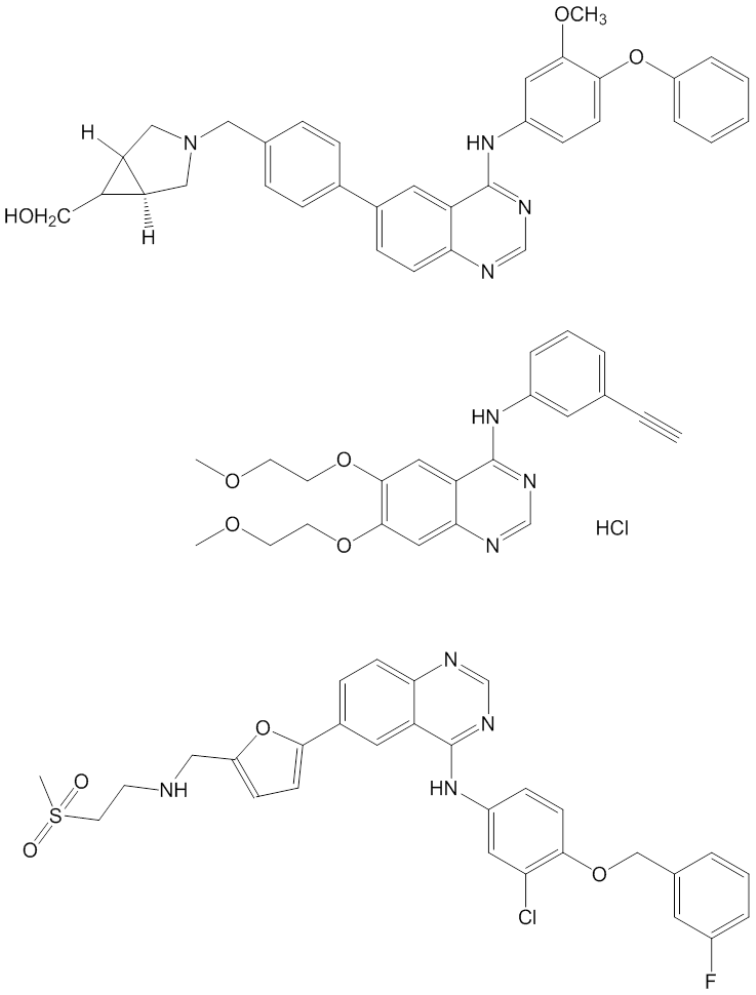

Figure 1.4 Lapatinib, erlotinib and CP654577 chemical structures.

SKBR3 human breast cancer cells with CP654577 resulted in a decreased phosphorylation of HER2 and HER3 and a reduction of activated MAPK and Akt, leading to cycle arrest at G_1 and apoptosis on these cells (Barbacci *et al.* 2003).

1.4.3 Mechanisms of resistance to targeted therapy

Despite some impressive response rates to TKIs in some tumours, some patients may have intrinsic resistance to these therapeutic agents, while others may develop acquired resistance some time after the initial treatment. Different mechanisms of intrinsic or acquired resistance to targeted therapy are already known. For instance, activating mutations in *EGFR* occur in lung cancer and activate the Ras/MAPK pathway. However, mutational activation of *v-Ki-ras2 Kirsten rat sarcoma viral oncogene homolog* (*KRAS),* which result in EGFR-independent activation of the MAPK pathway, is also seen in approximately 20-30% of lung cancers, making these tumours resistant to EGFR TKIs (Massarelli *et al.* 2007). *KRAS* mutations are also found in colorectal cancer (40%), and a strong correlation has been found between mutated *KRAS* and lack of response to cetuximab therapy (Lievre *et al.* 2006). Therefore, KRAS status serves as a predictive factor of response to EGFR targeting therapies in different cancers.

Mutations or loss of PTEN expression may also serve as a marker of primary resistance to gefitinib and erlotinib. PTEN is a phospholipid phosphatase that counteracts PI3K by dephosphorylating PIP3 to PIP2. Inactivation of PTEN resulting in failure to inhibit Akt has been found to lead to *in vitro* resistance towards EGFR TKIs (She *et al.* 2003). The deletion of PTEN is commonly found in glioblastomas and correlates with resistance to TKI therapy, whereas co-expression of PTEN with EGFR vIII (a constitutively active EGFR) identifies patients that will respond to EGFR TKI therapy (Mellinghoff *et al.* 2005). Therefore, PTEN is a response biomarker for anti-EGFR therapy in this malignancy.

Despite these intrinsic mechanisms of resistance, EGFR TKIs have showed considerable clinical promise with the initial impressive response rates obtained. However, patients who firstly respond to TKI therapy may become resistant after prolonged treatment. For instance, gefitinib and erlotinib are highly active in the treatment of a subset of non-small cell lung cancer (NSCLC) patients with activating mutations in the tyrosine kinase domain of EGFR (Lynch *et al.* 2004; Pao *et al.* 2004).

However, the majority of patients who initially respond to these TKIs become resistant to this class of drugs. A secondary mutation within the tyrosine kinase domain of EGFR resulting in the substitution of methionine for threonine in codon 790 (T790M) is thought to block erlotinib or gefitinib binding (Pao *et al.* 2005) and is responsible for TKI resistance in approximately 50% of cases (Kosaka *et al.* 2006).

Another 20% of NSCLC patients may also acquire resistance to EGFR TKI treatment through amplification of MET, a receptor tyrosine kinase. There is increasing evidence that persistent HER3 signalling can mediate resistance to TKIs. MET amplification results in EGFR-independent activation of the PI3K-Akt pathway through the activation of HER3, promoting cell survival in gefitinib-resistant lung cancer cell lines (Engelman *et al.* 2007). MET amplification serves as an example of a cancer adopting a new mechanism to activate downstream signalling events. Interestingly, though, is that these cells may be still dependent on EGFR signalling, and EGFR inhibition may be still necessary in order to prevent cell invasiveness and epithelial-to-mesenchymal transition (La Monica *et al.* 2013).

In breast cancers overexpressing HER2, failure to inhibit PI3K/Akt signalling also seems to lead to TKI resistance. In this case, however, phosphorylation of HER3 is not due to the amplification of another non-HER family receptor. Instead, Sergina *et al*. showed that TKIs are unable to effectively suppress HER3 signalling in these tumours due to an Akt-driven negative feedback signalling, which re-establishes HER3 signalling by inducing a forward shift in HER3 phosphorylation–dephosphorylation steady-state equilibrium, maintaining Akt signalling, which is important for tumour survival. HER3 phosphorylation has been attributed to an incomplete inhibition of the HER2 kinase activity by the TKIs (Sergina *et al.* 2007). A way to overcome this resistance may be by using combinations of different drugs. For instance, Garrett *et al*. found that the combination of an HER3 antibody and a p110α inhibitor blocked PI3K pathway and inhibited cell growth of HER2-overexpressing breast cancer cells (Garrett *et al.* 2013).

Therefore, effective HER targeted therapy requires functional EGFR/HER2 receptors as well as intact downstream signalling pathways dependent on these receptors. However, cancer cells have developed ‘escape routes’ to these inhibitors by different mechanisms,

including the activation of alternative signalling pathways or mutations in the tyrosine kinase domain of the target that disrupt drug binding. These allow tumour cells to grow despite inhibition of EGFR and/or HER2. Understanding the multiple mechanisms by which cancer cells become resistant to TKI therapy is essential to develop future treatments that can be highly effective for cancers driven by this oncogenic family of receptors.

1.5 Preclinical studies using EGFR and/or HER2 targeted therapies in bladder cancer

Targeted therapy against EGFR and/or HER2 has the potential to improve clinical outcome of bladder cancer patients, and preclinical studies have actually confirmed that these agents are active in bladder cancer cell lines and xenograft experimental models.

For instance, different sensitivity to erlotinib has been found within a panel of bladder cancer cell lines. This EGFR TKI inhibited the activation of EGFR, mitogen activated protein kinase and Akt, suggesting it could be a potential therapeutic drug for bladder cancer treatment (Jacobs *et al.* 2007). Gefitinib has also been found to be effective in the inhibition of growth in a subset of EGFR-expressing bladder cancer cells *in vitro* and *in vivo* (Dominguez-Escrig *et al.* 2004; Shrader *et al.* 2007). Kassouf *et al*. found that resistance to gefitinib *in vitro* and *in vivo* nude mice models was associated with the uncoupling of EGFR and MAPK inhibition (Kassouf *et al.* 2005). Different antiproliferative response to cetuximab has also been found in a panel of bladder cancer cells (Black *et al.* 2008). In the same study, resistance to this monoclonal antibody was associated with markers of epithelial-to-mesenchymal transition (EMT) such as loss of E-cadherin.

Lapatinib has also proven to be effective in inhibiting cell growth of bladder cancer cell lines. Havaleshko *et al.* found that 11 out of 39 bladder cancer cell lines were sensitive to this drug (Havaleshko *et al.* 2009) whereas studies by McHugh *et al.* found that lapatinib reduced cell viability in bladder cancer cells and it also enhanced

chemotherapy effects of GTC (gemcitabine, paclitaxel and cisplatin) and GC (gemcitabine and cisplatin) regimens (McHugh *et al.* 2009; McHugh *et al.* 2007).

Taken together, these preclinical studies suggested a possible role of EGFR and/or HER2 in driving at least a subset of bladder cancers, and TKIs and monoclonal antibodies targeting these receptors have entered clinical trials.

1.6 Clinical trials using EGFR and/or HER2 targeted therapies in bladder cancer

There have been some recent reports of clinical trials using drugs that target EGFR in bladder cancer with mixed results. For instance, gefitinib has been evaluated in a phase II study in 31 patients with metastatic bladder cancer, but results from this study showed that gefitinib was ineffective as a second-line treatment for this disease (Petrylak *et al.* 2010). However, results from a phase II clinical trial to evaluate the efficacy of erlotinib as a single-agent for treatment of muscle invasive bladder cancer patients undergoing radical cystectomy suggested a potential clinical effect of erlotinib in these patients (Pruthi *et al.* 2010). Moreover, a phase II study to evaluate cetuximab in 39 metastatic bladder cancer patients treated with or without paclitaxel showed that the combination of cetuximab and paclitaxel may actually increase the effectiveness of paclitaxel (Wong *et al.* 2012). A phase II randomized trial of gemcitabine and cisplatin with or without cetuximab in patients with bladder cancer is currently undergoing (NCT00645593).

Targeting EGFR/HER2 in bladder cancer has also been evaluated. For instance, in a single-arm phase II study using lapatinib as the second-line treatment of patients with locally advanced or metastatic bladder cancer, an objective response rate was observed in 1 out of 59 the patients enrolled (1.7%). Although these results were not considered to be positive, clinical benefit was found to be significantly correlated with EGFR expression, and the median overall survival was significantly prolonged in patients with tumours that overexpressed EGFR and/or HER2 (30.3 weeks compared to 10.6 weeks in patients with tumours with negative or low expression of EGFR and/or HER2), highlighting the importance of EGFR and/HER2 as predictive markers to identify which

subsets of patients may benefit from these treatments (Wulfing *et al.* 2009). Pre-selection of patients likely to benefit from this therapy is therefore of vital importance. Indeed, a phase II/III trial to evaluate the role of lapatinib in EGFR or HER2 overexpressing patients with locally advanced or metastatic bladder cancer as maintenance therapy after first-line chemotherapy compared with placebo is currently on-going in the UK (LaMB study, NCT00949455).

Targeting HER2 specifically with trastuzumab has also been evaluated in a single arm phase II clinical trial in conjunction with carboplatin, gemcitabine and paclitaxel in advanced bladder cancer patients. The results suggested a possible relationship between the overexpression of HER2 and the clinical response (Hussain *et al.* 2007). Another trial to evaluate paclitaxel and radiation therapy with or without trastuzumab in patients who have undergone surgery is also undergoing (NCT00238420).

Despite the mixed results obtained so far, numerous clinical trials are still on-going with EGFR and /or HER2 inhibitors as single agents or in combination with chemotherapy or radiotherapy. The results from these clinical trials in conjunction with further *in vitro* studies will be essential to understand bladder cancer biology and to optimize a potential new therapeutic approach targeting HER family members for this disease.

Chapter 2: Hypothesis and aims

The aim of the project is to investigate the role of EGFR and HER2 as potential therapeutic targets in bladder cancer and to better understand potential resistance mechanisms for these approaches. The hypothesis is that EGFR and/or HER2 may have a major part in driving some subtypes of this disease and that EGFR and HER2 directed therapies could be effective treatments for these patients. In order to investigate this, the following aims will be addressed:

- Characterization of expression levels of HER family members and function in bladder cancer cell lines.
- Study of the effect of EGFR and/or HER2 inhibition using targeted drugs or by protein depletion using siRNA by analysing changes in cell proliferation, cell cycle and induction of apoptosis in bladder cancer cells.
- Investigation of downstream pathways after EGFR and/or HER2 inhibition in bladder cancer cell lines.

The ultimate goal of this study is to provide a rationale to test EGFR and/or HER2 targeted therapy in bladder cancer and support the on-going investigation of the effectiveness of EGFR and/or HER2 as therapeutic targets in bladder cancer.

Chapter 3: Materials and Methods

3.1 Solutions and buffers

All reagents were purchased from Sigma, unless otherwise stated.

3.1.1 General reagents

Phosphate Buffered Saline (PBS)

137 mM NaCl

2.7 mM KCl

4.3 mM Na_2HPO_4

1.47 mM KH_2PO_4

HCl to pH 7.4

Tris (Tris[hydroxymethyl]aminomethane)-Buffered Saline (TBS)

10 mM Tris-HCl pH 8.0

150 mM NaCl

TBS-Tween

10 mM Tris-HCl pH 8.0

150 mM NaCl

0.05% (v/v) Tween-20

Annexin V Buffer (10x)

0.1 M HEPES

1.4 M NaCl

25 mM $CaCl_2$

3.1.2 Protein analysis reagents

Protein Running Buffer

25 mM Tris Base

200 mM Glycine

0.1% (w/v) Sodium Dodecyl Sulfate (SDS)

Transfer Buffer

25 mM Tris Base

200 mM Glycine

0.1% (w/v) SDS

25% (v/v) ethanol

Stripping buffer

25 mM glycine

1% (w/v) SDS

RIPA Lysis Buffer

150 mM NaCl

1% (v/v) NP-40 substitute

0.5% (w/v) Sodium Deoxycholate

0.1% (w/v) SDS

50 mM Tris-HCl pH 8.0

Brij Lysis Buffer

1M Tris-HCl pH 7.5

500 mM EDTA pH 8

4 M NaCl

10% (v/v) Brij 97 (previously warmed at 40°C)

3.1.3 Compounds

Erlotinib was provided by Genentech Inc, dissolved in 100% dimethyl sulfoxide (DMSO) and aliquoted as 10 mM stock until use. Lapatinib was provided by GlaxoSmithKline, dissolved in 100% DMSO, and aliquoted as 100 mM stock until use. CP654577 was provided by Pfizer, dissolved in 100% DMSO and aliquoted as 100 mM stock until use. All the compounds were stored at -20°C. Cetuximab (Erbitux®), trastuzumab (Herceptin®) and rituximab (MabThera®) were kindly provided as excess stock for disposal from the oncology pharmacy at Southampton General Hospital and were kept at 4°C. The epidermal growth factor (EGF) was provided by Sigma, reconstituted with 10mM acetic acid and kept as aliquots of 1mg/ml. Human Neuregulin-1 (NRG-1) was purchased from Cell Signaling, reconstituted with 20mM

citrate and aliquoted as 100 μg/ml stock. Both compounds were stored at -20°C. Caspase inhibitor VI (Z-VAD-FMK) was purchased from Calbiochem, resuspended in DMSO to a final concentration of 10 mM and stored at -20°C.

3.2 Mammalian cell lines

Cell lines used are described in Table 3.1, which were selected to be representative of a range of bladder cancer TCC subtypes. SKBR3, a breast adenocarcinoma cell line, was used as a positive control in some experiments as it overexpresses HER2.

3.2.1 Cell culture

HT1376, T24, UM-UC-3, UM-UC-6 and SKBR3 were maintained in Dulbecco's modified Eagles medium (DMEM; PAA Laboratories GmbH, Austria) supplemented with 10% (v/v) fetal bovine serum (FBS; PAA Laboratories GmbH, Austria), 2mM L-glutamine, 100μg/ml penicillin G and 100μg/ml streptomycin (PAA Laboratories GmbH, Austria). RT112 and RT112CP were cultured in Roswell Park Memorial Institute 1640 media (RPMI; PAA Laboratories GmbH, Austria) containing 10% (v/v) fetal bovine serum, 2mM L-glutamine, 100μg/ml penicillin G and 100μg/ml streptomycin. All cell lines were maintained in 175 cm^2 tissue culture flasks and cultured in a humidified incubator at 37°C and 5% (v/v) CO_2 in a mycoplasma-free environment. Cells were passaged at 70-80% confluence 2 to 3 times per week. Briefly, all media was aspirated from the flask. Five ml PBS was added and aspirated to remove any residual media and 5 ml Trypsin-EDTA (PAA Laboratories GmbH, Austria) was added and incubated at 37°C for 2 to 20 minutes (depending on the cell line) until the cells had detached from the T175 flask. Five ml of complete media was added to resuspend the cells and to inactivate the trypsin and 2 ml of the resuspended cells was added to a new T175 flask. Twenty-five ml of complete media was added to the new flask and cultured. All media was pre-warmed to 37°C before use.

Cell line	Tissue of origin (all human)	Characteristics	References
HT1376	Bladder transitional cell carcinoma, grade 3	Loss of Rb expression	(Rieger *et al.* 1995)
		P53 mutation	(Rieger *et al.* 1995)
		Express E-cadherin	(McHugh *et al.* 2009)
T24	Bladder transitional cell carcinoma, grade 3	HRAS mutation	(Reddy *et al.* 1982)
		PTEN mutation	(Wang *et al.* 2000)
		P53 mutation	(Lopez-Knowles *et al.* 2006)
		Loss of E-cadherin	(McHugh *et al.* 2009)
RT112	Bladder carcinoma epithelial	Express E-cadherin	(McHugh *et al.* 2009)
RT112CP	Bladder carcinoma epithelial, cisplatin resistant	Cisplatin resistant	(Walker *et al.* 1990)
UM-UC-3	Bladder transitional cell carcinoma	PTEN deletion	(Wang *et al.* 2000)
		KRAS mutation	(Platt *et al.* 2009)
		Loss of E-cadherin	(Rieger *et al.* 1995)
		P53 mutation	(Rieger *et al.* 1995)
		Mesenchymal morphology	(Black *et al.* 2008)
UM-UC-6	Bladder transitional cell carcinoma	Mesenchymal morphology	(Black *et al.* 2008)
		Loss of E-cadherin	(Black *et al.* 2008)
SKBR3	Breast adenocarcinoma	Overexpresses HER2	

Table 3.1 Mammalian cell lines. All cell lines were obtained from Dr Simon Crabb, and were originally from the European Collection of Cell Cultures (ECACC). RT112CP were a kind gift from Prof John Masters at University College London (UCL).

3.2.2 Cryopreservation of cells

For cryopreservation, cells were washed with PBS, trypsinised and five ml of complete media was added (as before); cells were removed from the T175 flask and were spun down in a 15 ml falcon tube at 1000 rpm in a Sorvall Legend RT centrifuge for 5 minutes at room temperature. Media was aspirated and cells were resuspended in 5 ml freezing media [90% (v/v) fetal bovine serum and 10% (v/v) DMSO]. One ml of resuspended cells was added to each cryovial, which were placed in a Nalgene cryo 1°C freezing container "Mr Frosty" filled with isopropanolol and incubated at -80°C overnight. Cells were then transferred to liquid nitrogen for long term storage.

3.2.3 Thawing cell for culture

Cells stored in liquid nitrogen were quickly thawed at 37°C, transferred to a 15 ml falcon tube containing 5 ml of pre-warmed media and centrifuged at 1000 rpm in a Sorvall Legend RT centrifuge for 5 minutes at room temperature to remove the DMSO. Media was aspirated and cells were resuspended in 1 ml of pre-warmed media and transferred in a 25 cm^2 tissue culture flask containing 10 ml of pre-warmed media and incubated at 37°C and 5% (v/v) CO_2.

3.3 Western blotting

3.3.1 Preparation of cell lysates

Sodium dodecyl sulphate-polyacrylamide gel electrophoresis (SDS-PAGE) was used to analyse proteins from cell extracts. Cells were normally seeded at a density of $3x10^5$ cells per well in 6-well plates and incubated overnight. The following day cells were treated with the appropriate concentration of drugs, DMSO (equivalent to the highest dose of the drug) as control or left untreated, and incubated for the desired length of time. For experiments where cells were treated with growth factors, cells were plated and incubated in complete media overnight, then the following day cells were washed with PBS and RPMI phenol red free media (Invitrogen Gibco) supplemented with charcoal stripped serum, 2mM L-glutamine, 100µg/ml penicillin G and 100µg/ml streptomycin was added into the wells and incubated for 24 hours. The following day

cells were stimulated with EGF or NRG-1 at the appropriate concentrations for 10 minutes before collecting the cells.

To prepare protein lysates, media was aspirated from the wells, and cells were rinsed with ice cold PBS. Then 1 ml of ice cold PBS was added to the wells and the cells were detached using a plastic cell scraper and transferred into 1.5 ml microcentrifuge tubes. Cells were then collected by centrifugation at 1500 rpm for 5 minutes at 4°C in a Heraeus Biofuge fresco refrigerated microfuge and washed in PBS. Cells were then lysed in 1x RIPA buffer supplemented with 1% (v/v) protease inhibitor cocktail and 1% (v/v) phosphatase inhibitor cocktail 2 and 3 (both from Sigma, UK).

Cell lysates were incubated on ice for 30 minutes and centrifuged at 13000 rpm for 15 minutes at 4°C in a Heraeus Biofuge fresco refrigerated microfuge. The supernatant was transferred into a clean microcentrifuge tube and protein assay reagent (Bio-Rad, UK) was used (diluted 1 in 5) to determine the protein content of the clarified lysate. Bovine serum albumin (BSA) was used as a standard curve for the assay. 3x SDS Red loading buffer (Cell Signaling, UK) supplemented with 0.1 M Dithiothreitol (DTT; Cell Signaling, UK) was added to protein extracts normalized to 20 µg (or 40 µg when blotting for phospho-proteins) in a final volume of 30 µl. The samples were then heated at 95°C in a heating block for 5 minutes and loaded onto Tris-HCl gels. Tables 3.2 and 3.3 show the recipe for the making of the gels. Gels were prepared using glass plates by pouring first the separating gel until it reached 80% of the capacity, then 1 ml distilled water was added to achieve a smooth surface at the interface between the two gels. Once the separating gel had polymerized, the water was removed and the stacking gel was poured to fill up all the capacity. A comb was inserted at the top of the glass plates, which was removed once the stacking gel had polymerized. Proteins were normally resolved in 10% gels except for HER family members (175-185 kDa) when 8.5% gels were used.

3.3.2 SDS-Polyacrylamide Gel Electrophoresis (SDS-PAGE)

Broad range protein markers (Cell Signaling, UK) were used as molecular weight standards. Proteins were separated electrophoretically using mini-protean III cell (Bio-Rad, UK) in 500 ml 1x protein running buffer at 200 Volts for approximately 45 minutes. Proteins from the 10% or 8.5% polyacrylamide gels were then transferred onto

Solution	10%	8.5%
30% (w/v) Acrylamide/Bis-acrylamide	6.6 ml	5.7 ml
1.5 M Tris pH 8.8	5.0 ml	5.0 ml
dH_20	8.3 ml	9.2 ml
10% (w/v) ammonium persulphate (APS)	100 µl	100 µl
TEMED (N, N, N', N'-tetramethylethylenediamine)	15 µl	15 µl

Table 3.2 Recipe for 10% and 8.5% Tris-HCl resolving gels.

Solution	
30% (w/v) Acrylamide/Bis-acrylamide	1.4 ml
1.5 M Tris pH 6.8	2.5 ml
dH_20	6.0 ml
10% APS	100 µl
TEMED	15 µl

Table 3.3 Recipe for Tris-HCl stacking gel.

nitrocellulose membrane (Whatman, Germany). A "sandwich" was prepared, consisting of 1 sponge, 1 filter paper, nitrocellulose membrane, polyacrylamide gel, 1 filter paper and 1 sponge. Transfer onto nitrocellulose membrane was performed in 500 ml 1x transfer buffer in a mini-trans blot cell (Bio-Rad, UK) at 100 Volts for 75 minutes (or 90 minutes when transferring large proteins). The nitrocellulose membrane was incubated in 5% (w/v) dried non-fat milk (Marvel) in TBS with 0.05% (v/v) Tween (TBS-Tween) on an automatic roller inside a 50 ml falcon tube for 1 hour at room temperature to block non-specific protein binding sites. Following this the membrane was incubated with the primary antibody at the appropriate concentration in 3% or 5% (w/v) non-fat milk/TBS-Tween or 5% (w/v) BSA/TBS-Tween at 4°C overnight (see Table 3.4). The following day membranes were washed three times in TBS-Tween for 5 minutes, after which the membranes were incubated with rabbit, mouse or goat horseradish peroxidase (HRP) -conjugated secondary antibody (GE Healthcare, UK) for 1 hour at room temperature at 1/3000 dilution in 3% (w/v) non-fat milk/TBS-Tween. The membranes were then washed as before and protein was detected using a stable peroxide solution and luminol enhancer that form the Supersignal West Pico Chemiluminescent Substrate (Thermo Scientific, UK) or the Supersignal West Femto Chemiluminescent Substrate (Thermo Scientific, UK). Chemilluminescence was detected on a ChemiDoc-It® Imaging System (Ultra-Violet Products, UK) using VisionWorks®LS Image Acquisition and Analysis software (UVP Ltd). Densitometry of the resulting Western blots was done using Quantity One software (Bio-Rad, UK) after background subtraction.

3.3.3 Stripping of membranes

Membranes were incubated with 10 ml stripping buffer for 30 minutes on an automatic roller at room temperature and then washed two times in TBS-Tween for 10 minutes before being re-probed.

Antibody	*Molecular weight*	*Supplier*	*Dilution*	*Blocking*	*2nd Antibody*
EGFR	175 kDa	Santa Cruz Biotechnology, Inc.	1/200	3% dried skimmed milk 0.05%TBS-T	Goat
HER2	185 kDa	Cell Signaling	1/1000	5% BSA 0.05%TBS-T	Rabbit
HER3	185 kDa	Thermo Scientific	1/200	3% dried skimmed milk 0.05%TBS-T	Mouse
HER4	180 kDa	Santa Cruz Biotechnology, Inc.	1/200	3% dried skimmed milk 0.05%TBS-T	Rabbit
p-EGFR (Tyr1068)	175 kDa	Cell Signaling	1/1000	5% dried skimmed milk 0.05%TBS-T	Mouse
p-HER2 (Tyr1221/1222)	185 kDa	Cell Signaling	1/1000	5% BSA 0.05%TBS-T	Rabbit
p-Akt (Ser473)	60 kDa	Cell Signaling	1/1000	5% BSA 0.05%TBS-T	Rabbit
p-Akt (Thr308)	60 kDa	Cell Signaling	1/1000	5% BSA 0.05%TBS-T	Rabbit
Akt	60 kDa	Cell Signaling	1/1000	5% BSA 0.05%TBS-T	Rabbit
p-ERK1/2 (Thr202/Tyr204)	42,44 kDa	Cell Signaling	1/1000	5% BSA 0.05%TBS-T	Rabbit
ERK1/2	42,44 kDa	Cell Signaling	1/1000	5% dried skimmed milk 0.05%TBS-T	Mouse
p-p38 (Thr180/Tyr182)	43 kDa	Cell Signaling	1/1000	5% BSA 0.05%TBS-T	Rabbit
p38 MAPK	43 kDa	Cell Signaling	1/1000	5% BSA 0.05%TBS-T	Rabbit
p-GSK-3α/β (Ser21/9)	46, 51 kDa	Cell Signaling	1/1000	5% BSA 0.05%TBS-T	Rabbit
p-STAT4 (Tyr693)	81 kDa	Cell Signaling	1/1000	5% BSA 0.05%TBS-T	Rabbit
p-MAPKAPK-2 (Thr334)	49 kDa	Cell Signaling	1/1000	5% BSA 0.05%TBS-T	Rabbit
PARP	89, 116 kDa	Cell Signaling	1/1000	5% dried skimmed milk 0.05%TBS-T	Rabbit
MYC	64, 67 kDa	Calbiochem	1/1000	3% dried skimmed milk 0.05%TBS-T	Mouse
Actin	42 kDa	Sigma	1/500	3% dried skimmed milk 0.05%TBS-T	Rabbit

Table 3.4 Primary antibodies used for Western blotting. BSA, bovine serum albumin; TBS-T, Tris (Tris[hydroxymethyl]aminomethane)-Buffered Saline-Tween.

3.4 Immunoprecipitation assays

Immunoprecipitation assays (IP) were performed in order to study dimerization patterns of the HER family in bladder cancer cell lines. For these assays, RT112, T24 and SKBR3 cells were grown to near confluence in cell culture dishes. One ml of ice cold PBS was added to the wells and cells were then collected by scraping and transferred to 1.5 ml microcentrifuge tubes. After two washes in PBS cells were lysed with cold Brij buffer supplemented with 1% (v/v) protease inhibitor cocktail and 1% phosphatase inhibitor cocktail 2 and 3 (both from Sigma, UK). Cells were then incubated on ice for 30 minutes with occasional mix and then centrifuged in a Heraeus Biofuge refrigerated microfuge at 13000 rpm for 15 minutes at 4°C. Protein assay reagent (Bio-Rad, UK) was used to determine the protein content of the clarified lysate. Bovine serum albumin was used as a standard for the assay. For each cell line, 20 µg were kept aside as "whole cell lysate" and between 700-1000 µg were used for the immunoprecipitation. Protein G-Sepharose 4 Fast Flow beads (GE Healthcare) were used for the immunoprecipitation. Beads were washed three times with 500 µl Brij lysis buffer and diluted 50% in PBS before use. Wide bore tips were used when handling the beads to prevent their blockage. After washing the G-Sepharose beads, the cell lysate was "pre-cleared": the cell lysate was incubated with 10 µl of the previously washed protein G beads for 1 hour at 4°C with shaking in order to clean the supernatant and reduce non-specific binding before IP. The protein G beads were removed by centrifugation and the supernatant (pre-cleared lysate) was added to a fresh tube containing the appropriate monoclonal antibody (mAb): 40 µg trastuzumab for HER2 IP, 40 µg cetuximab for EGFR IP or 40 µg rituximab as an isotype-matched control monoclonal antibody. Cell lysates plus antibody were rotated at 4°C overnight. After the overnight incubation a new aliquot (10 µl) of pre-washed protein G beads was added and incubated for 2 hour at 4°C with permanent shaking. Immunocomplexes were then collected by pelleting them with a short centrifugation (1 min at 10000 rpm) and the supernatant was removed. Beads were then washed five times with 500 µl lysis buffer, resuspending each time. After the 4^{th} wash a new 1.5 ml microcentrifuge tube was used to minimize contamination. Beads were resuspended in 30 µl 3x SDS Red loading buffer (Cell Signaling, UK) supplemented with 0.1 M DTT (Cell Signaling) and protein immunocomplexes were dissociated by boiling the samples at 95°C in a heating block

for 10 min. Samples were chilled on ice and stored at -20°C until resolved by electrophoresis on a SDS-polyacrilamide gel.

3.5 Cell proliferation assays (MTS assays)

3.5.1 Cell proliferation assays

Cell proliferation assays were used to measure the effect of different compounds on growth inhibition of cell lines and to determine IC_{50} values (concentration required for 50% inhibition of cell viability). Briefly, cells were seeded at a density of 1000 cells per well (or 2000 cells for HT1376 cell line due to their slow rate of proliferation) in a 96-well cell culture plate with 50 µl complete DMEM or RPMI, depending on the cell line, and incubated at 37°C and 5% (v/v) CO_2 overnight. The outside wells of the 96-well plate were not used to avoid the cells drying out and were filled with media. The following day, 50 µl of different drug concentrations (2x), DMSO (as a control) or media (as the untreated cells) was added to the wells to a total volume of 100 µl. Data points were assessed in triplicate. After 4 days, the media was removed from all the wells and 100 µl of RPMI containing 5 µl of MTS reagent [3-(4,5-dimethylthiazol-2-yl)-5-(3-carboxymethoxyphenyl)-2-(4-sulfophenyl)-2H-tetrazolium, inner salt] contained in the CellTiter 96® AQ_{ueous} One Solution Reagent (Promega, UK) was added to each well. This assay is based on the conversion of MTS into soluble formazan by endogenous dehydrogenase enzymes found in metabolically active cells. After 90 minutes incubation, the absorbance of the formazan product at 490 nm (subtracting 595 nm absorbance) was measured using a Varioskan Flash spectral plate reader (Thermo Scientific, UK). The absorbance is then directly proportional to the number of living cells in culture.

3.5.2 Analysis

The MTS assay was used as an indirect measure to quantify cell proliferation. To calculate this, the data were background-subtracted (all plates contained wells containing only media with no cells or drugs that served as background values). Metabolically active cells were then calculated as a percentage of the controls cells (treated with the equivalent DMSO concentration). In all experiments DMSO was used

at the highest concentration equivalent to the drug being tested, and no difference between DMSO-treated cells and untreated cells was observed in any experiment. The percentage of metabolically active cells was then plotted against the log of the drug concentration. GraphPad Prism4 (GraphPad Software, Inc, USA) was used to generate a non-linear regression sigmoidal curve from which the concentration that inhibits 50% of the cells (IC_{50}) was determined. Statistical analysis was performed using the unpaired Student's t-test.

3.5.2.1 Correlation between TKI IC_{50} and HER family expression

The relative expression levels of EGFR, HER2, HER3 and HER4 previously determined by densitometry using Quantity One software were plotted against the IC_{50} mean values found for erlotinib, lapatinib and CP654577 for each cell line. Correlations were analysed by the Spearman's rho correlation using GraphPad Prism4.

3.5.3 Cell proliferation assays with growth factors

RT112 and T24 cells were seeded at a density of 1000 cells per well in a 96-well cell culture plate with 50 µl RPMI phenol red free supplemented with charcoal stripped serum, and incubated at 37°C and 5% (v/v) CO_2 overnight. The following day, 50 µl of RPMI phenol red free supplemented with charcoal stripped serum plus various concentrations of EGF or NRG-1 was added to the cells to a final volume of 100 µl. Each dose was tested in triplicate, and each experiment was repeated two times for each cell line. After 4 or 7 days in a humidified incubator at 37°C and 5% (v/v) CO_2, the media was removed from all the wells and 100 µl of RPMI containing 5 µl of MTS reagent contained in the CellTiter 96® AQ_{ueous} One Solution Reagent was added to each well to analyse number of viable cells. Results were expressed as absorbance values (OD_{490}-OD_{595}) plotted against the log of the growth factor concentration. GraphPad Prism4 was used to generate a non-linear regression sigmoidal curve.

3.6 Cell cycle analysis

Flow cytometric analysis was performed to measure cell cycle distribution by analysing DNA content per cell using the fluorescent nucleic acid dye propidium iodide (PI). The dye passes through a permeabilized membrane and intercalates into cellular DNA. The

intensity of the PI signal is then directly proportional to DNA content, so it is possible to identify the proportion of cells that are in one of the three interphase stages of the cell cycle (G_1, S phase and G_2M). For these experiments, cells were plated at a density of $1.5x10^5$ in a 6-well plate and then cultured overnight before treating with various concentrations of the relevant drug. The plates also contained wells with untreated cells and DMSO-treated cells as controls (highest concentration equivalent to the drug being tested). Cells were harvested at set time points by washing with PBS before trypsinising the cells, but all fractions were collected. Cells were then pelleted at 1500 rpm in a Sorvall Legend RT centrifuge for 5 minutes at room temperature, washed with PBS and fixed in ice cold 70% (v/v) ethanol for 30 minutes on ice. After fixation cells were pelleted to eliminate the ethanol, and washed with PBS. Cells were spun down before adding PI. Each 500 µl sample contained 2.5 µl PI (1 mg/ml stock) and 50 µl RNase (0.1 mg/ml stock) in PBS. Samples were analysed (10000 events/sample) using a six-colour FACS Canto I (BD Biosciences). Data were analysed using FACS Diva software. Percentage of cells in G_1 phase, S phase or G_2M phase of the total number of cells in the cell cycle was estimated by DNA content after gating histograms generated with the PE-area variable. Events in sub G_1 phase were expressed as percentage of total cells and were used as an indirect measure of cell death.

3.7 Measurement of apoptosis

Flow cytometric analysis was performed to measure apoptosis by Annexin V and propidium iodide (PI) staining. Loss of plasma membrane is one of the earliest features in apoptosis. The membrane phospholipid phosphatidylserine (PS) is translocated from the inner to the outer leaflet of the plasma membrane, thereby exposing PS to the external cellular environment. Annexin V binds in the presence of Ca^{2+} ions with high affinity to negatively charged phospholipids like PS, so it binds to cells undergoing apoptosis which have exposed PS in their membranes. The PI can differentiate between early and late apoptotic cells since necrotic cells that have lost cell membrane integrity will permit PI entry. Therefore, viable cells are Annexin V negative/PI negative; early apoptotic cells are Annexin V positive/PI negative, late apoptotic cells or necrotic cells

are Annexin V positive/PI positive and necrotic cells are Annexin V negative/PI positive.

Cells were plated at a density of $1.5x10^5$ in a 6-well plate and then cultured overnight before treating them with the relevant drug for the desired length of time. The plates also contained wells with untreated cells and DMSO-treated cells as controls (equivalent to the highest drug concentration tested). Cells were harvested by washing with PBS before trypsinising. All fractions were collected and cells were pelleted at 1500 rpm in a Sorvall Legend RT centrifuge for 5 minutes at room temperature. Cells were then washed with PBS and resuspended in 500 µl of 1 x Annexin binding buffer. To each sample, 1.25 µl of Annexin V-FITC and 2.5 µl PI (0.1 mg/ml) were added and samples were incubated for 15 minutes at room temperature in the dark. Samples were analysed (10000 events/sample) using a six-colour FACS Canto I (BD Biosciences). Data were analysed using FACS Diva software and presented as percentage of total cells as viable cells (unstained), early apoptotic cells (Annexin V positive), late apoptotic cells (Annexin V positive/PI positive) or necrotic cells (Annexin V negative/PI positive).

3.8 Protein depletion by siRNA

Small interfering RNA (siRNA) has become a useful approach to silence gene expression. By using siRNA complementary to the target gene, this binds to the complementary mRNA causing mRNA elimination. ON-TARGET plus siRNA SMART pools against EGFR or HER2 and ON-TARGET plus non-targeting pool siRNA used as control were purchased from Dharmacon Research, Inc. The lyophilized siRNA were reconstituted in RNase-free water to 50 µM concentration and stored in aliquots at -20°C as stock solutions. Target sequences of the ON-TARGET plus SMART pool siRNA used in this project to deplete EGFR and HER2 are shown in Table 3.5. RNA interference assay was done according to the INTERFERin siRNA forward transfection protocol (Polyplus-transfection Inc). Optimization experiments were carried out by varying amounts of INTERFERin (transfection reagent) and siRNA concentration in order to determine the optimal amount for each cell line.

	Target sequence
EGFR	CAAAGUGUGUAACGGAAUA
	CCAUAAAUGCUACGAAUAU
	GUAACAAGCUCACGCAGUU
	CAGAGGAUGUUCAAUAACU
HER2	UGGAAGAGAUCACAGGUUA
	GAGACCCGCUGAACAAUAC
	GGAGGAAUGCCGAGUACUG
	GCUCAUCGCUCACAACCAA

Table 3.5 Target sequences of the ON-TARGET plus siRNA SMART pools against EGFR and HER2.

For a 6-well plate assay, $3x10^5$ of RT112 cells or $1.5x10^5$ of T24 cells were added into each well and incubated overnight. The following day, 500 µl of OPTIMEM (Invitrogen Gibco; serum-free cell medium) was incubated with 5 µl INTERFERin and 1.5 µl siRNA for 15 minutes at room temperature and then 500 µl of the siRNA/INTERFERin complex was added into each well. The final volume per well was 1500 µl and the siRNA concentration was 50 nM. The plates were incubated at 37°C and 5% (v/v) CO_2. Cells were collected at set time points after transfection and the relevant protein expression levels were analysed by Western blot.

3.9 Human phosphokinase array

A human phospho-kinase array kit (Proteome Profiler Human Phospho-Kinase Array Kit ARY003, R&D Systems) was used to detect simultaneously the relative phosphorylation levels of 46 proteins after HER family kinase inhibition in cell lines. A layout of the protein antibody array is shown in Table 3.6. The phospho-kinase array was performed according to the manufacturer's protocol. Briefly, cells were plated at a density of $3x10^6$ in a cell culture dish and then cultured overnight before treating them with the relevant drug or the equivalent concentration of DMSO as control cells. After one hour incubation, media was removed and ice cold PBS was added to the dishes to collect the cells by scrapping. Cells were then washed in PBS and lysed with Lysis Buffer 6 for 30 minutes on ice. Cell lysates were then centrifuged in a Heraeus Biofuge refrigerated microfuge at 13000 rpm for 15 minutes at 4°C and supernatant was transferred into a clean microcentrifuge tube. Protein assay reagent was used to determine the protein content of the clarified lysate and 200 µg of protein was used per array part. Nitrocellulose membranes were blocked for 1 hour on a rocking platform at room temperature and then the lysates were added to the membranes and incubated overnight at 4°C on a rocking platform. The following day, the membranes were washed three times with 1x Wash Buffer to remove unbound proteins and then incubated with a cocktail of biotinylated detection antibodies for 2 hours at room temperature on a rocking platform. Membranes were then washed and streptavidin-HRP was added and incubated for 30 minutes at room temperature on a rocking platform. Membranes were washed again and phosphorylated protein bound was detected using

Supersignal West Pico or Femto Chemiluminescent Substrate (Thermo Scientific, UK) on a ChemiDoc-It® Imaging System (Ultra-Violet Products, UK) using VisionWorks®LS Image Acquisition and Analysis software (UVP Ltd). The phospho-antibody array experiment was done once with erlotinib and once with lapatinib.

3.9.1 Data analysis

The positive signals were quantified using Quantity One software. Every spot was subtracted by the averaged background level from the negative controls in each array. Then the data were analysed in three different ways: i) as raw data, ii) as a percentage of the positive control, and iii) as a percentage of the global mean. To analyse the data by percentage of the positive control, the average of positive controls was calculated for each single array. Then, a correction factor was applied to normalise the arrays to be compared (array A untreated vs. treated and array B untreated vs. treated) and spots representing each phosphorylated kinase were expressed as the percentage of their positive control. To calculate the data by percentage of the global mean, the mean of all the positive signals was calculated for each single array. Then, a correction factor was applied to normalise the arrays to be compared (array A untreated vs. treated and array B untreated vs. treated). Spots representing each phosphorylated kinase were expressed as the percentage of the global mean. Statistical analysis was performed using the Student's t-test and presented for p values <0.01 and <0.05. Only statistically significant changes ($p<0.05$) found in all three analyses were considered for further investigation and validation.

ARRAY A	Positive Control	p38α (T180/Y182)	ERK1/2 (T202/Y204, T185/Y187)	JNK pan (T183/Y185, T221/Y223)	GSK-3α/β (S21/S9)
		MEK1/2 (S218/S222, S222/S226)	MSK1/2 (S376/S360)	AMPKα1 (T174)	Akt (S473)
	TOR (S2448)	CREB (S133)	HSP27 (S78/S82)	AMPKα2 (T172)	β-Catenin
	Src (Y419)	Lyn (Y397)	Lck (Y394)	STAT2 (Y689)	STAT5a (Y694)
	Fyn (Y420)	Yes (Y426)	Fgr (Y412)	STAT3 (Y705)	STAT5b (Y699)
	Hck (Y411)	Chk-2 (T68)	FAK (Y397)	STAT6 (Y641)	STAT5a/b (Y694/Y699)
	Positive Control		Negative control		
ARRAY B		p53 (S392)		Positive Control	
	Akt (T308)	p53 (S46)			
	p70 S6 Kinase (T389)	p53 (S15)	p27 (T198)	Paxillin (Y118)	
	p70 S6 Kinase (T421/S424)	RSK1/2/3 (S380/S386/S377)	p27 (T157)	PLCγ-1 (Y783)	
	p70 S6 Kinase (T229)	RSK1/2 (S221/S227)	c-Jun (S63)	Pyk2 (Y402)	
	STAT1 (Y701)	STAT4 (Y693)	eNOS (S1177)	Negative control	

Table 3.6 Layout of Proteome Profiler Human Phospho-Kinase Array Kit ARY003 (R&D Systems) composed of array A and array B.

The residues indicated in parentheses are the phosphorylation sites.

3.10 Synergy assays

Synergism was assessed using the median effect principle derived from the mass-action law principle (Chou and Talalay 1984) using CalcuSyn software (Biosoft, Cambridge, UK) according to the manufacturer's instructions. This software produces a combination index (CI) value that determines whether a combination of drugs is synergistic (CI < 1.0), additive (CI = 1) or antagonist (CI > 1). Potential CI values and their proposed meaning is shown in Table 3.7. The median effect equation states:

$$f_a/f_u = (D/D_m)^m$$

where,

f_a is the fraction affected by the dose

f_u is the fraction unaffected, assuming $f_a + f_u = 1$.

D is the dose of the drug

D_m is the median effect dose that inhibits the system under study by 50% (analogous to the IC_{50})

m is the coefficient signifying the shape of the dose-effect relationship (where m = 1, > 1, < 1, indicates hyperbolic, sigmoidal and negative sigmoidal dose-effect curves, respectively).

Prerequisites for synergy determination are dose-effect curves for each drug alone and for the combination of both. A median-effect plot can then be constructed which linearizes all dose effect curves that followed the mass-action law principle, where x = log (D) versus y = log (f_a/f_u). Then it is possible to know the potency at the x-intercept (the D_m value or IC_{50}) and the slope or shape (the *m* value) for drug 1, drug 2 and the combination (Chou and Talalay 1984). Both D_m and *m* are essential for the determination of synergism or antagonism. Subsequently, the F_a-CI plot can be created; a plot of CI on the y-axis as a function of effect level (f_a) on the x-axis. The growth inhibitory effect of each drug (f_a), the sigmoidicity of the curves and the IC_{50} are included to calculate the combination index (CI).The computer-simulated F_a-CI plot displays synergism or antagonism for the entire spectrum of effect levels (f_a from 0.01 to 0.99).

CI	Description
<0.1	Very strong synergism
0.1-0.3	Strong synergism
0.3-0.7	Synergism
0.7-0.85	Moderate synergism
0.85-0.9	Slight synergism
0.9-1.1	Nearly additive
1.1-1.2	Slight antagonism
1.2-1.45	Moderate antagonism
1.45-3.3	Antagonism
3.3-10	Strong antagonism
>10	Very strong antagonism

Table 3.7 Combination index (CI) values and their proposed degree of synergism or antagonism (Chou 2006).

In order to assess synergy between drugs, cell proliferation assays were used in order to create dose-effect curves for each drug alone and the combination of both. Since the most efficient way for experimental design is to choose the combination drugs at their equipotent ratio (e.g. at the ratio of their IC_{50}), and to have several data points above and below the IC_{50} (Chou 2010), the doses tested for single drugs or the combination of drugs were: $2xIC_{50}$, $1.5xIC_{50}$, $1xIC_{50}$, $0.75xIC_{50}$ and $0.5xIC_{50}$. However, these concentrations had to be varied in some experiments as it was difficult to obtain reproducible IC_{50} values, especially with T24 cells. Cell growth inhibition effect of single drugs and combination of drugs was entered in the Calcusyn programme to generate the dose-effect curves, the median-effect plots and the F_a-CI plots.

Chapter 4: Characterization of HER family expression and function in human bladder cancer-derived cell lines

The overall goal of this project was to understand the biology of bladder cancer, and in particular, to determine whether EGFR and/ or HER2 have roles as potential targets for therapy. Since more than 90% of bladder cancers present as transitional cell carcinomas (TCCs), a panel of six human bladder cancer-derived cell lines (TCCs) were selected for this project and it was first important to characterise HER family expression and function in these cells. Therefore, the aim of the work described in this chapter was to characterize the following parameters in these cells:

- Basal expression of the HER family and basal activation of key downstream signalling pathway molecules (phospho-Akt and phospho-ERK1/2).
- The effect of growth factors on activation of downstream pathways and cell proliferation.
- Dimerization patterns of HER family members.

4.1 Expression levels of HER family and downstream molecules

4.1.1 Protein expression levels of HER family

Bladder cancer patients show great variability in terms of EGFR and HER2 expression (Chow *et al.* 2001; Kassouf *et al.* 2008; Korkolopoulou *et al.* 1997; Memon *et al.* 2006; Memon *et al.* 2004; Wright *et al.* 1991), so the first experiment performed was the analysis of the protein expression levels of HER family members (EGFR, HER2, HER3 and HER4) in the panel of six bladder cancer cell lines (TCCs); HT1376, T24, RT112, RT112CP, UM-UC-3 and UM-UC-6.

Figure 4.1 shows a representative Western blot of HER family expression in the six bladder cancer cell lines and Figure 4.2 shows quantitation of the relative expression levels of EGFR, HER2, HER3 and HER4 in the bladder cancer cell lines after being normalised to β-actin expression. The cell lines expressed variable levels of EGFR, and

HT1376 cell line showed the highest expression. HER2 could be detected in all cell lines except for HT1376, and it was relatively highly expressed in RT112 cells. Only three bladder cancer cell lines, HT1376, RT112 and RT112CP expressed detectable levels of HER3, and all of them expressed HER4, but they also showed different levels of expression.

These results revealed a complex pattern of HER proteins expression among the six bladder cancer cell lines, with no evident interrelationship among them. However, all cell lines expressed either EGFR and/or HER2; there was no cell line that was both EGFR negative and HER2 negative. There was also a possible inverse relationship between HER3 and HER4: the cell lines that had no HER3 expression were the ones which had higher expression levels of HER4 and vice versa; the cell lines with HER3 expression were the ones with lower HER4 expression. Of note is also the different expression levels of EGFR and HER2 between RT112 and RT112CP, a cisplatin-resistant cell line derived from RT112 cells by continuous exposure to increasing concentrations of cisplatin for 14 months (Walker *et al.* 1990).

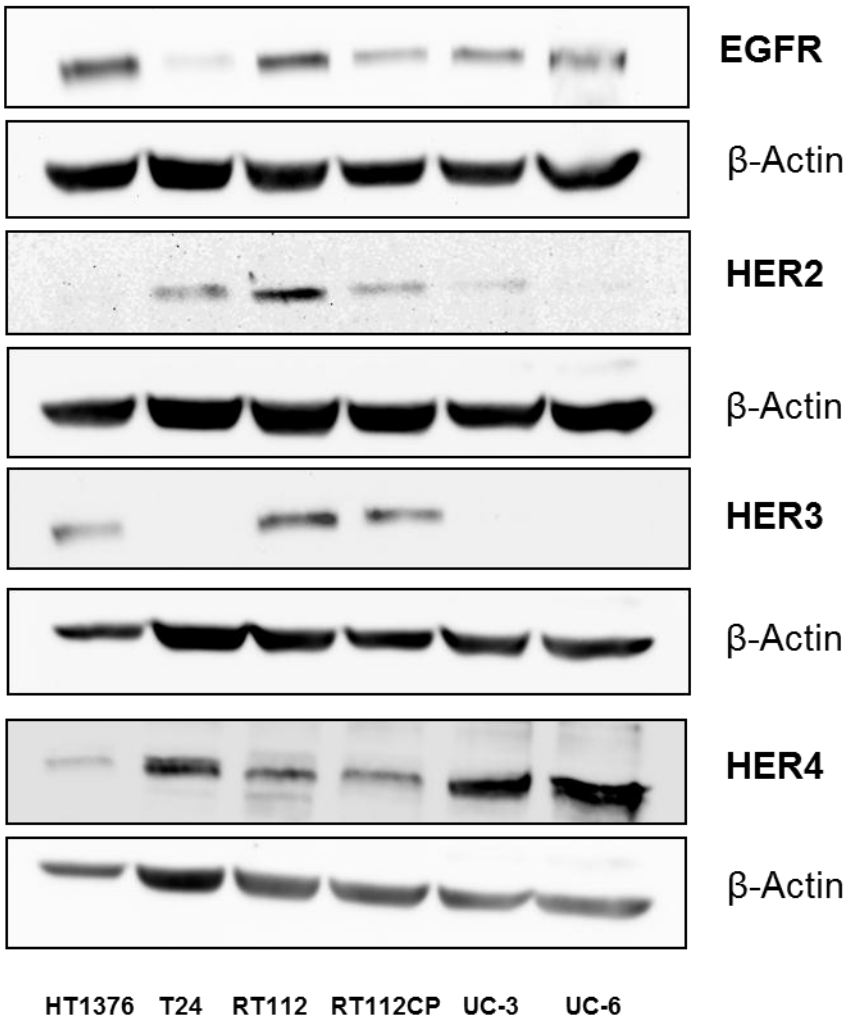

Figure 4.1 EGFR, HER2, HER3 and HER4 expression in a panel of bladder cancer cell lines. Cell lines were grown to near confluence and whole cell lysates were subjected to SDS-PAGE and analysed by Western blot for EGFR (175 kDa), HER2 (185 kDa), HER3 (185 kDa) and HER4 (180 kDa). *β*-actin (42 kDa) was used as a loading control. Representative blots are shown from four independent experiments.

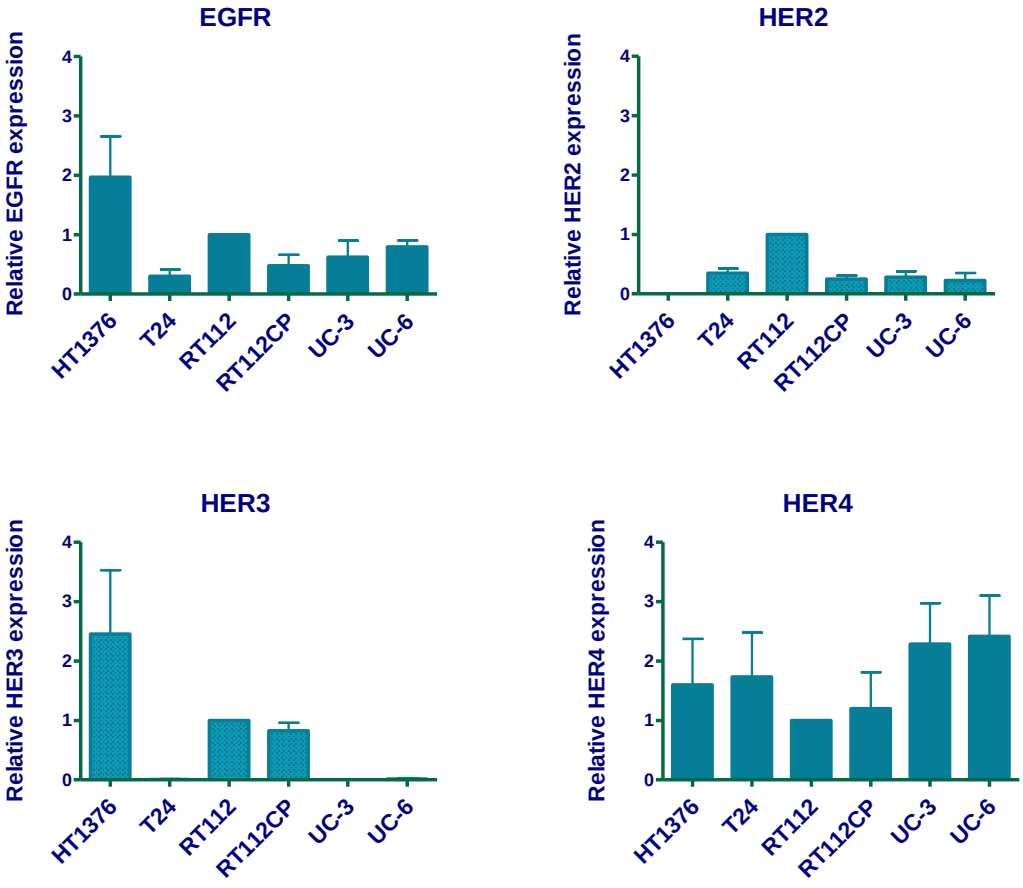

Figure 4.2 Relative expression levels of EGFR, HER2, HER3 and HER4 in the six bladder cancer cell lines. Protein expression levels of EGFR, HER2, HER3 and HER4 were normalized to the levels of *β*-actin in respective samples and RT112 levels were set at 1 for all four proteins. Protein expression levels are presented as the fold difference compared to RT112 cells. Values represent the mean value of four independent experiments. The error bars represent standard deviation.

4.1.2 Protein expression levels of phospho-Akt and phospho-ERK1/2 activation

After analysing the HER expression levels in the panel of bladder cancer cell lines, I analysed activation of downstream signalling pathways normally activated by HER family members. In order to do this, phosphorylation of Akt (PI3K/Akt pathway) and ERK1/2 (Ras-MAPK pathway) were studied, as it is considered that these pathways may have an important role in promoting cancer through these receptors (Sergina and Moasser 2007). Initial experiments were performed using cells grown in 10% serum prior to testing effects of specific growth factors.

Phosphorylation of Akt occurs at two major sites; threonine 308 and serine 473. Phosphorylation of Akt at Thr308 is dependent on the activation of the PI3K pathway, being phosphorylated by PDK1 (Alessi *et al.* 1997), whereas mTOR complex 2 (mTORC2) phosphorylates Akt on Ser473 (Sarbassov *et al.* 2005). Cells were grown to near confluence and phosphorylation of Akt at both sites was studied. Figure 4.3 shows that HT1376 and UM-UC-6 cells had relatively high levels of phosphorylation of Akt at Thr308, whereas levels were somewhat lower in T24, RT112 and UM-UC-3 cell lines. Only low levels of phosphorylation expression could be detected in RT112CP cell line. The cell lines T24, RT112 and UM-UC-3 all contained phosphorylated Akt at Ser473; UM-UC-6 had very low levels of phospho-Akt 473, while no phosphorylation was detected in HT1376 and RT112CP cell lines. No evident relationship between the expression of phosphorylated Akt at Thr308 and Ser473 could be found. However, all cell lines seemed to have one phosphorylation site more predominant than the other, except T24 which had low levels for both phosphorylation sites and RT112CP which did not show any phosphorylation at Akt sites. A possible inverse relationship could be found between phosphorylation of Akt at Thr308 and the expression of HER2.

Levels of expression of phospho-ERK1/2 and total ERK1/2 were also studied in the panel of bladder cancer cell lines. The results showed (Figure 4.4) high expression levels of phospho-ERK1/2 in T24 cell line, moderate expression levels in HT1376 cell line and weakly expression in UM-UC-6 cell line. No expression could be detected in RT112 or RT112CP cell lines; however this was variable as weak levels of phospho-ERK1/2 could be seen in subsequent experiments in RT112 cells. No relation could be found between phosphorylation of ERK1/2 and the expression of HER family receptors.

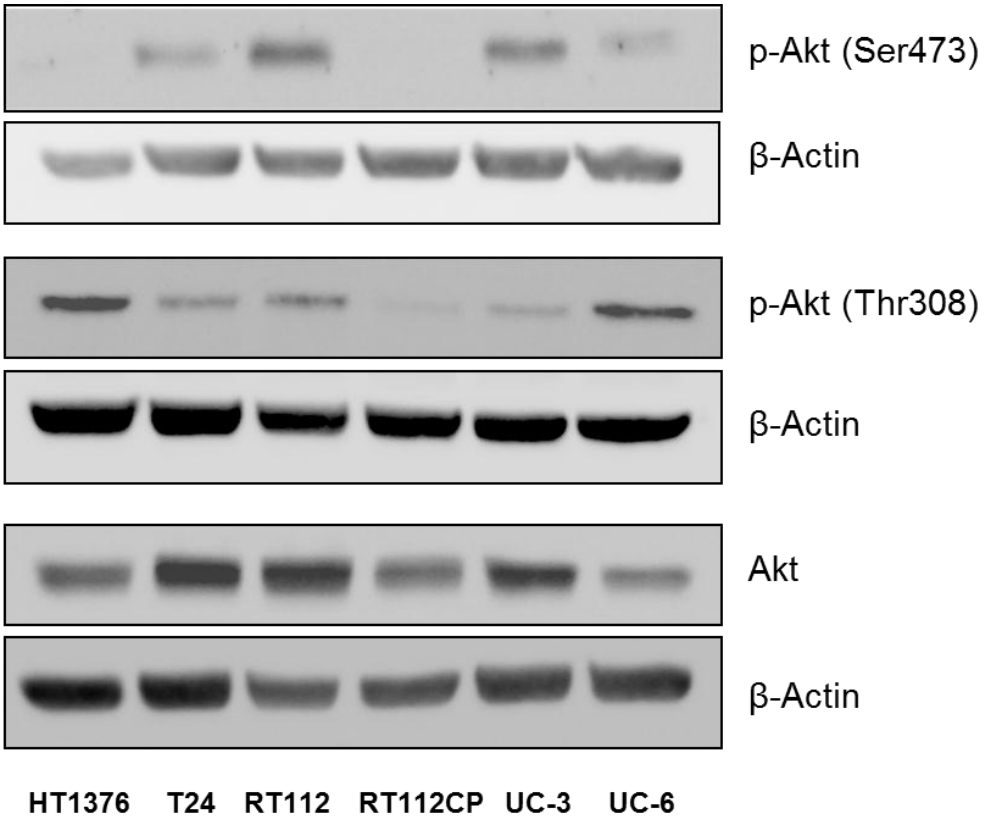

Figure 4.3 Phospho-Akt (Ser473), phospho-Akt (Thr308) and total Akt expression in a panel of bladder cancer cell lines. Cell lines were grown to near confluence and whole cell lysates were subjected to SDS-PAGE and analysed by Western blot for phospho-Akt (Ser473 or Thr308; 60 kDa) and total Akt (60 kDa). *β*-actin (42 kDa) was used as a loading control. Representative blot from two independent experiments.

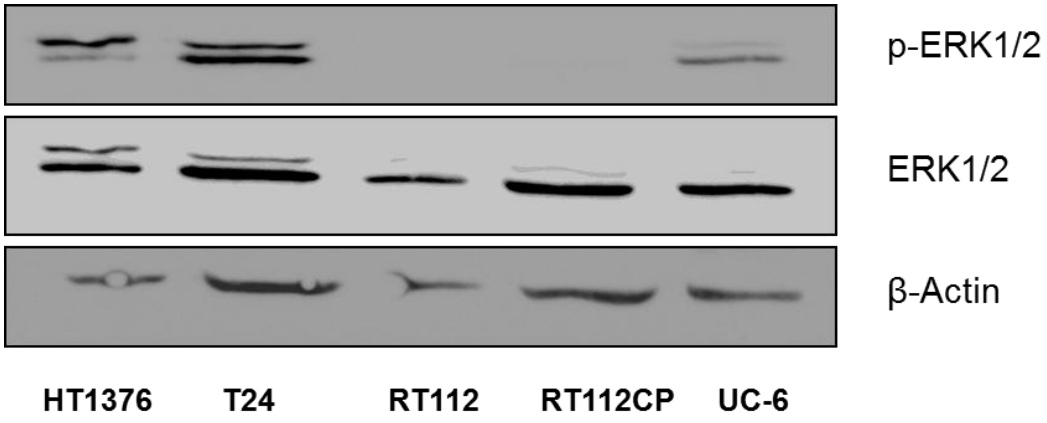

Figure 4.4 Phosphorylated ERK1/2 and total ERK1/2 expression in a panel of bladder cancer cell lines. Cell lines were grown to near confluence and whole cell lysates were subjected to SDS-PAGE and analysed by Western blot for phospho-ERK1/2 (Thr202/Tyr204; 42/44 kDa) and total ERK1/2 (42/44 kDa). *β*-actin (42 kDa) was used as a loading control. Representative blot of two independent experiments. (Note UM-UC-3 cell line was not included in this assay).

4.2 Effect of growth factors in RT112 and T24 cells

Since the HER family of receptors depend on ligand binding in order to be activated, the activation levels of phospho-Akt and phospho-ERK1/2 were studied in three different conditions: in presence of fetal bovine serum (FBS) or charcoal stripped FBS in the media, or in cells grown in charcoal stripped FBS supplemented with epidermal growth factor (EGF) or neuregulin-1 (NRG-1), ligands for EGFR and HER3/HER4, respectively. Charcoal stripping of FBS was used as it removes non-polar material such as growth factors, hormones and cytokines from the serum. Two cell lines were chosen for these experiments; RT112 and T24. RT112 was chosen because it was the cell line with the highest HER2 expression, but it also expressed all the other receptors. T24 was chosen because it also expressed HER2 and EGFR but did not express HER3.

4.2.1 Effect of serum in RT112 and T24 cells

The effect of presence/absence of FBS in the media on bladder cancer cell lines was analysed by studying phosphorylated levels of Akt and ERK1/2 proteins. Cells were grown overnight in media supplemented with FBS or supplemented with charcoal stripped FBS. Cell lysates were collected and phospho-proteins were analysed by Western blot. The results are shown in Figure 4.5. No difference in the phosphorylation of Akt Ser473 or ERK1/2 sites could be seen as a result of adding FBS or charcoal stripped FBS in the media in any of the two cell lines tested, suggesting that the basal levels of phosphorylation were not dependent on ligands present on serum.

4.2.2 Effect of EGF and NRG-1 in RT112 cells

EGF is a known ligand for EGFR, whereas NRG-1 binds to HER3 or HER4. The effect of adding EGF or NRG-1 in RT112 cells supplemented with charcoal stripped FBS was analysed by studying levels of phospho-Akt or phospho-ERK1/2. Increasing concentrations of EGF and NRG-1 were added to the cells for 10 minutes. Figure 4.6 shows how EGF increased levels of phospho-ERK1/2 and slightly increased phospho-Akt (Ser473) in these cells, but levels of phospho-Akt (Thr308) remained the same. On the other hand, NRG-1 increased levels of both phospho-Akt (Ser473) and phospho-Akt (Thr308), but no significant changes were seen in phospho-ERK1/2.

4.2.3 Effect of EGF and NRG-1 in T24 cells

A similar experiment was performed using T24 cells. The addition of EGF in T24 cells increased phospho-ERK1/2 and phospho-Akt (Ser473) in a dose dependent manner and it also seemed to increase levels of phospho-Akt (Thr308). By contrast, NRG-1 did not alter levels of phosphorylated ERK1/2, Akt (Thr308) or Akt (Ser473) (shown in Figure 4.7).

Table 4.1 shows a summary of the effects of EGF and NRG-1 found in phosphorylation of ERK1/2 and Akt in RT112 and T24 cells.

4.2.4 Effect of EGF and NRG-1 in cell proliferation of RT112 and T24 cells

After characterizing the effect of EGF and NRG-1 on two downstream pathways of the HER family (Akt and ERK1/2), the effect of these growth factors on cell proliferation was also studied in RT112 and T24 cells. To study this, cells growing in charcoal stripped FBS were treated continuously with increasing concentrations of EGF and NRG-1. Cell proliferation was measured using the MTS assay at two time points: 4 days and 7 days. This assay is based on the conversion of MTS into soluble formazan by enzymes found in metabolically active cells and therefore, it can be used as an indirect measure of cell number. Since the change in metabolic activity of treated cells was quite small compared to non-treated cells, the results were expressed as OD_{490}-OD_{595} (consistent with the data presented in NRG-1 Cell Signaling datasheet). A dose-dependent increase in cell proliferation could be detected in RT112 cells treated with EGF at both time points, whereas treatment with NRG-1 appeared to increase cell proliferation just at the higher concentration of 100 ng/ml. However for T24 cells, no increase in cell proliferation could be seen after EGF or NRG-1 treatment (shown in Figure 4.8).

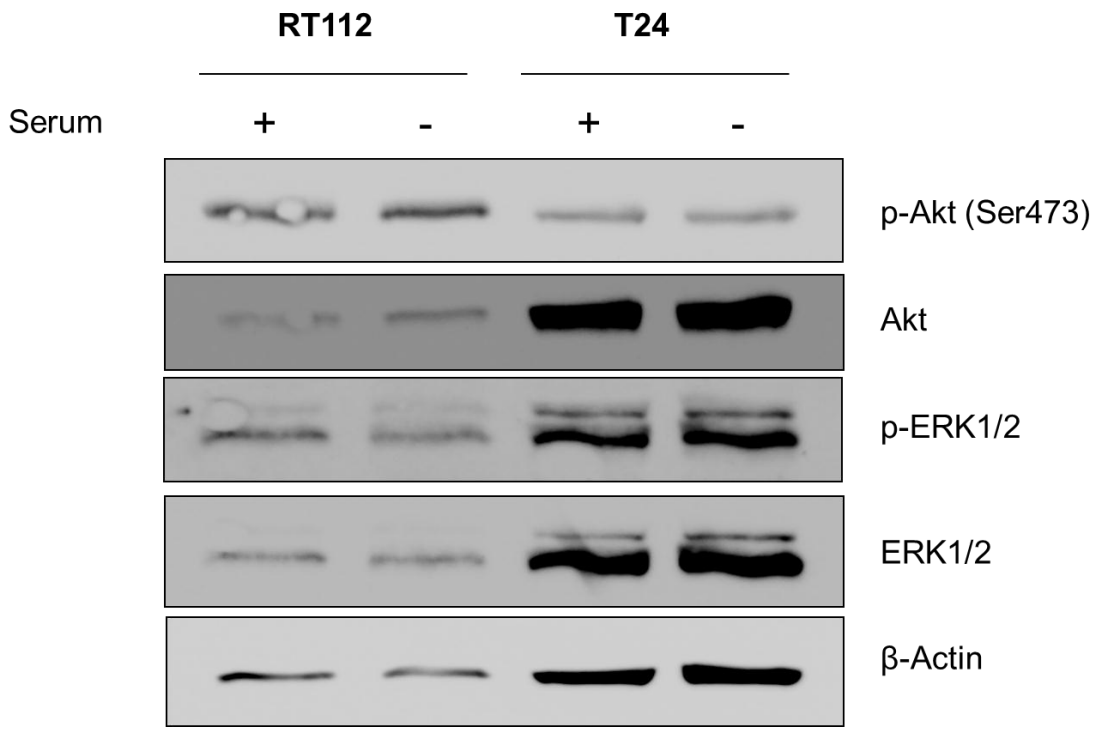

Figure 4.5 Effect of presence of serum in RT112 and T24 cells. Cell lines were grown to near confluence in the presence of fetal bovine serum (FBS) in the media (+) or with charcoal stripped FBS (-). Whole cell lysates were subjected to SDS-PAGE and analysed by Western blot for phospho-Akt (Ser473; 60 kDa) and phospho-ERK1/2 (Thr202/Tyr204; 42/44 kDa) and total expression of Akt and ERK1/2. *β*-actin (42 kDa) was used as a loading control. Representative blot from two independent experiments.

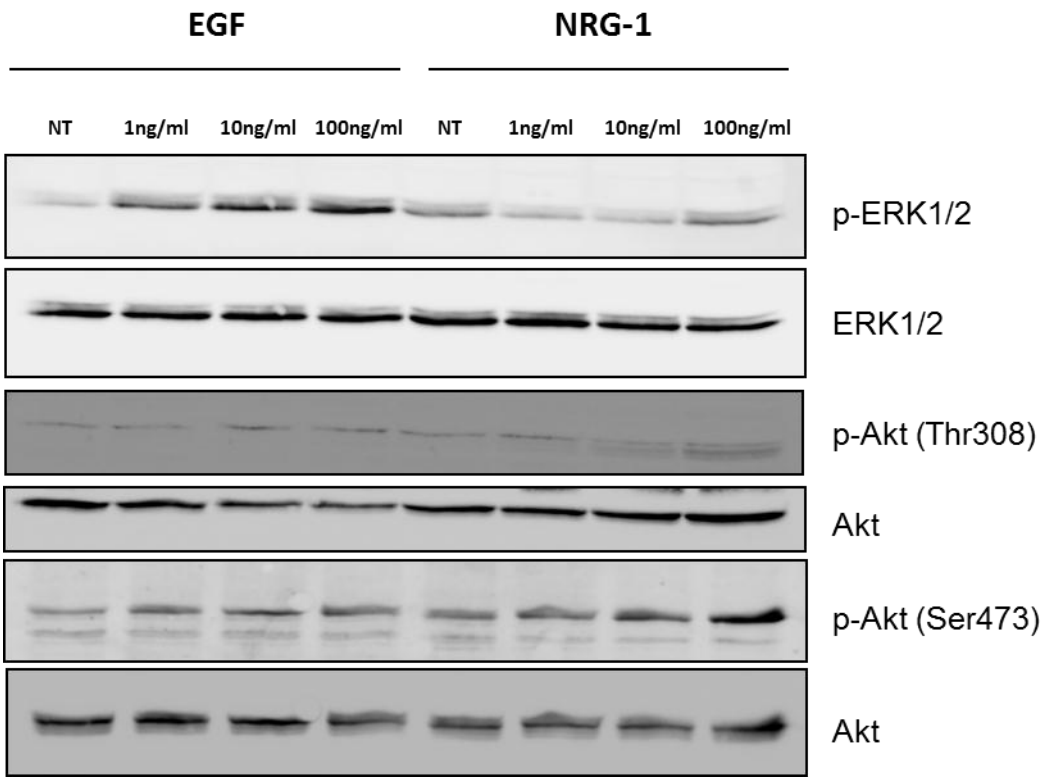

Figure 4.6 Effect of EGF and NRG-1 in RT112 cells. Cell lines were grown to near confluence in media supplemented with charcoal stripped FBS and then stimulated with increasing concentrations of epidermal growth factor (EGF) or neuregulin-1 (NRG-1) for 10 minutes or left untreated (NT). Whole cell lysates were subjected to SDS-PAGE and analysed by Western blot for phospho-Akt (Thr308 or Ser473; 60 kDa) and phospho-ERK1/2 (Thr202/Tyr204; 42/44 kDa) and total expression of Akt and ERK1/2. Representative blot from three independent experiments.

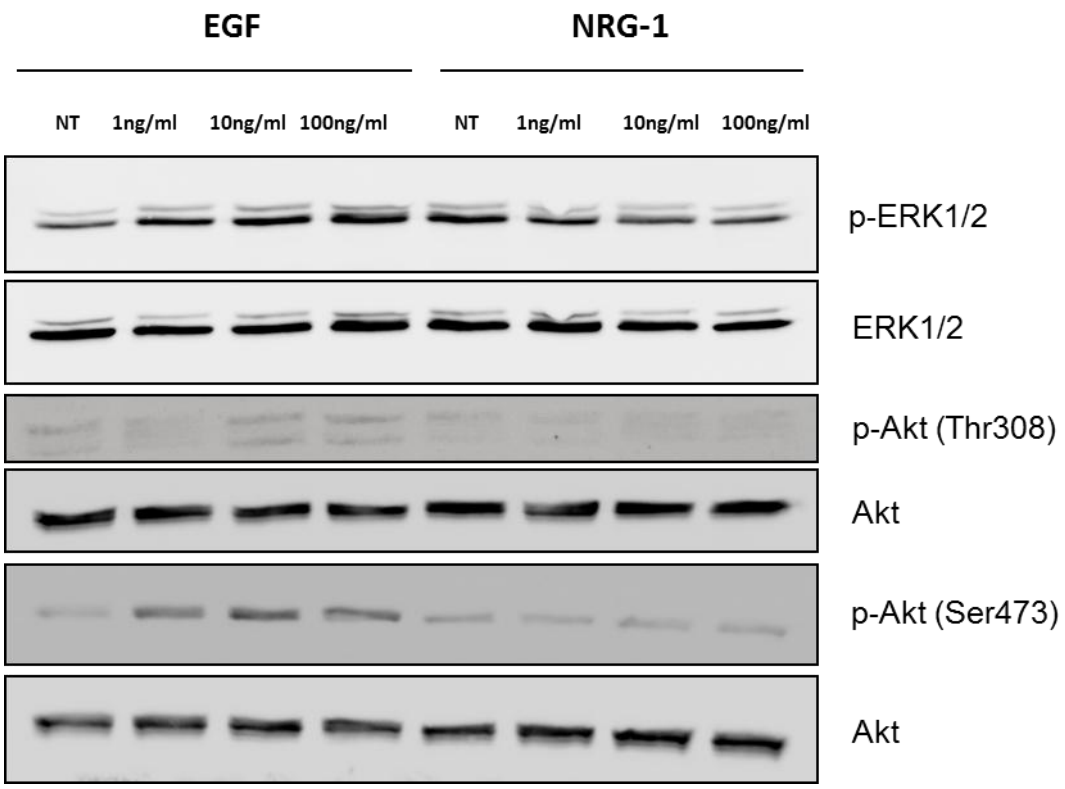

Figure 4.7 Effect of EGF and NRG-1 in T24 cells. Cell lines were grown to near confluence in media supplemented with charcoal stripped FBS and then stimulated with increasing concentrations of epidermal growth factor (EGF) or neuregulin-1 (NRG-1) for 10 minutes or left untreated (NT). Whole cell lysates were subjected to SDS-PAGE and analysed by Western blot for phospho-Akt (Thr308 or Ser473; 60 kDa) and phospho-ERK1/2 (Thr202/Tyr204; 42/44 kDa) and total expression of Akt and ERK1/2. Representative blot from three independent experiments.

RT112 cell line	EGF	NRG-1
p-ERK1/2	↑	≈
p-Akt (Thr308)	≈	↑
p-Akt (Ser473)	↑	↑

T24 cell line	EGF	NRG-1
p-ERK1/2	↑	≈ (or ↑)
p-Akt (Thr308)	≈ (or ↑)	≈
p-Akt (Ser473)	↑	≈

Table 4.1 Effects of epidermal growth factor (EGF) and neuregulin-1 (NRG-1) in downstream signalling pathways in RT112 and T24 cells.

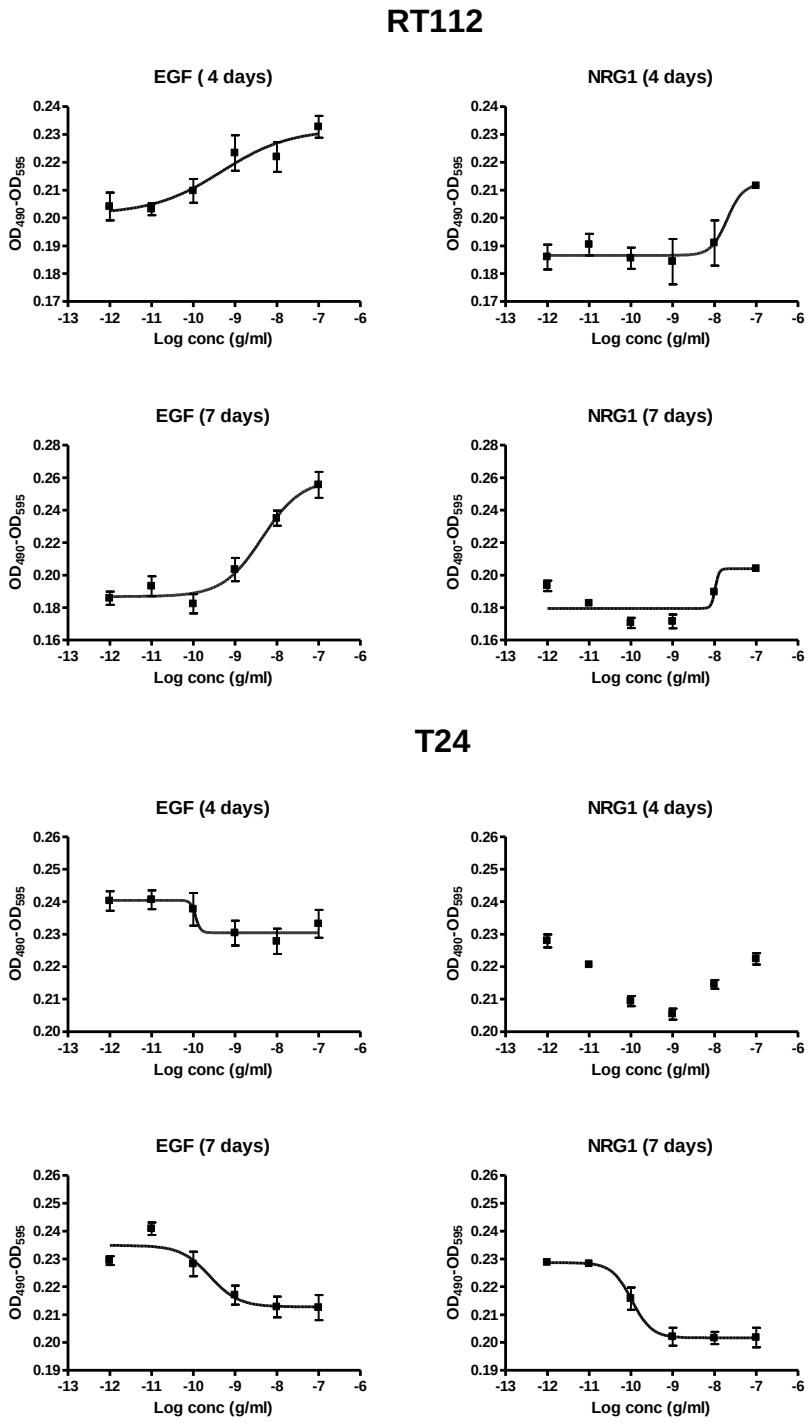

Figure 4.8 Effect of EGF and NRG-1 on cell proliferation of RT112 and T24 cells. Cells were treated with increasing concentrations of EGF or NRG-1 (from 0.001 to 100 ng/ml) continuously for 4 or 7 days. Cell proliferation was measured by MTS assay and the OD_{490}-OD_{595} was determined. GraphPad Prism4 was used to generate a non-linear regression sigmoidal curve. Each data point shows the mean of triplicate determinations ± SD. Representative graph from two independent experiments.

4.3 Dimerization patterns of HER family in bladder cancer

In recent years there has been an increased interest to investigate which HER dimers are present in tumours where these receptors act as oncogenes, as it may serve as a prognostic factor for the disease but also a predictive factor for targeted therapy that might exploit such interactions. Immunoprecipitation assays (IP) were used in order to investigate dimerization patterns of HER family in bladder cancer, which is currently unknown.

4.3.1 HER2 IP with trastuzumab

HER2 was immunoprecipitated in RT112, T24 and SKBR3 cells using trastuzumab, a HER2-specific monoclonal antibody (Carter *et al.* 1992). SKBR3 cells were used as a control as they are known to contain EGFR-HER2 dimers (Gaborit *et al.* 2011) and HER2-HER3 dimers (Sanchez-Martin and Pandiella 2012). Cells were grown to near confluence and lysed with a buffer containing Brij, a non-ionic detergent used to extract intact membrane complexes. Cell lysates were incubated overnight with trastuzumab or rituximab, a monoclonal antibody against CD20, which is found primarily in B cells, and which was used here as an isotype-matched control for trastuzumab. G-Sepharose beads were used for the immunoprecipitation. After the HER2 pull-down, Western blots were used to detect HER2 and co-immunoprecipitating EGFR, HER3 and HER4. The results are shown in Figure 4.9. HER2 was successfully immunoprecipitated in all three cell lines and a strong signal could be seen in SKBR3 cells as these cells are known to overexpress HER2. Associated EGFR could be detected also in SKBR3 cells, but little or no EGFR could be seen in RT112 or T24 cells. A weak band of co-immunoprecipitated HER3 could be seen in RT112 and SKBR3 cells. Results from T24 in the HER3 immunoblot were disregarded as the negative control (rituximab) also showed a band. HER4 results were difficult to interpret as they appeared as a smear rather than bands.

4.3.2 EGFR IP with cetuximab

EGFR was immunoprecipitated in RT112, T24 and SKBR3 cells using cetuximab, an EGFR-specific monoclonal antibody (Goldstein *et al.* 1995). Rituximab was used as an isotype-matched control monoclonal antibody for cetuximab. EGFR was pulled down

and Western blots were used to detect EGFR and co-immunoprecipitating HER2, HER3 and HER4. The results are shown in Figure 4.10. EGFR could be immunoprecipitated in the three cell lines (RT112, T24 and SKBR3) with RT112 showing the most EGFR. However, no HER2 or HER3 co-immunoprecipitated for any of the cell lines. HER4 could not be detected in the whole cell lysates, and a similar smear could be seen in the control and the EGFR-immunoprecipitated lanes for all three cell lines. Of note, however, is that the relative expression levels of EGFR and HER2 between RT112 and SKBR3 whole cell lysates differed significantly between this experiment and the previous HER2 IP, suggesting a technical problem in this experiment.

Since ligand binding is a necessary event for the dimerization of these receptors, another immunoprecipitation assay was performed where cells were plated in a cell culture dish in media supplemented with charcoal stripped FBS, incubated overnight and treated the following day with EGF in order to stimulate receptor dimerization on these cells. EGFR was immunoprecipitated using cetuximab but results were similar to previous ones where cells had not been stimulated (data not shown). As results were not reproducible between experiments and no co-immunoprecipitation of HER members could be seen, EGFR and HER2 immunoprecipitation assays were not investigated any further.

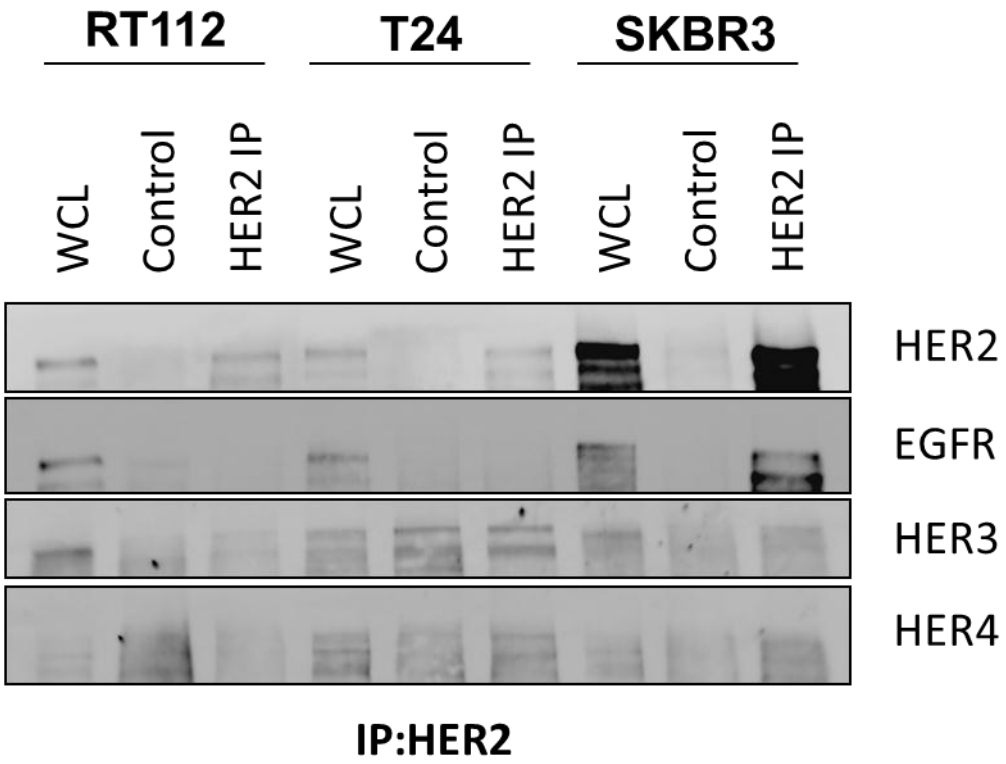

Figure 4.9 Immunoprecipitation of HER2 with trastuzumab. RT112, T24 and SKBR3 cells were subjected to immunoprecipitation for HER2 using trastuzumab and blotted for HER2 (185 kDa), EGFR (175 kDa), HER3 (185 kDa) and HER4 (180 kDa). WCL, whole cell lysate. Rituximab was used as an isotype-matched control mAb for trastuzumab.

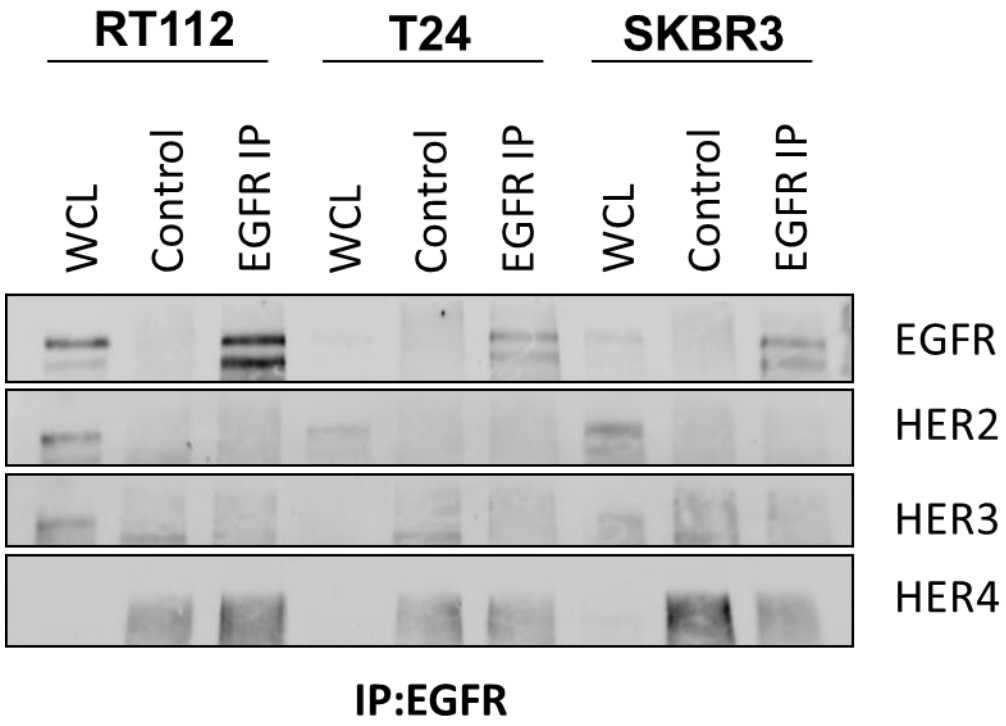

Figure 4.10 Immunoprecipitation of EGFR with cetuximab. RT112, T24 and SKBR3 cells were subjected to immunoprecipitation for EGFR using cetuximab and blotted for EGFR (175 kDa), HER2 (185 kDa), HER3 (185 kDa) and HER4 (180 kDa). WCL, whole cell lysate. Rituximab was used as an isotype-matched control mAb for cetuximab.

4.4 Summary of Chapter 4

In this chapter, characterization of the six bladder cancer cell lines with respect to HER family activity was carried out by analysing basal expression levels of HER family proteins, basal activation of downstream signalling pathways molecules (phospho-Akt and phospho-ERK1/2) and the effect of growth factors EGF and NRG-1 in cell proliferation and activation of downstream pathways. A study on dimerization patterns of HER family members in these cell lines was also performed.

The results showed a complex pattern of HER family expression among the six bladder cancer cell lines and different basal expression levels of phospho-ERK1/2 and phospho-Akt at Ser473 and Thr308, with no evident interrelationship among them. The addition of EGF or NRG-1 in RT112 cells increased phosphorylation of ERK1/2 and Akt, whereas in T24 cells, only EGF could increase phosphorylation of these proteins. When looking at the effects of these growth factors in cell proliferation, a dose-dependent increase could only be seen in RT112 cells treated with EGF.

Immunoprecipitation assays were used in order to investigate dimerization patterns of HER family members in bladder cancer. However, results were not reproducible between experiments and the technique was not sufficiently sensitive to detect co-immunoprecipitation of other HER members. For this reason, immunoprecipitation assays were not investigated any further.

4.5 Discussion

Human TCC cell lines (HT1376, RT112, RT112CP, T24, UM-UC-3 and UM-UC-6) were chosen as model systems in this study and they were selected to be representative of a range of bladder cancer subtypes.

T24, UM-UC-3 and UM-UC-6 are representative of advanced bladder cancer and have been used as models of invasive bladder cancer (Black *et al.* 2008; Imao *et al.* 1999). Interestingly, these cell lines had mesenchymal morphology due to loss of E-cadherin,

and grew as single spindle-shaped cells. On the contrary, HT1376, RT112 and RT112CP grew in well-organized islands that would merge as cells became more confluent. HT1376 and RT112 cells are known to express high levels of E-cadherin (McHugh *et al.* 2009). Expression levels of E-cadherin in RT112CP cells are not known, but since they derived from RT112 cells, they probably also expressed E-cadherin.

4.5.1 Expression levels of HER family and downstream molecules

In order to investigate whether bladder cancer may be driven by EGFR and/or HER2 signalling, initial work analysed the EGFR, HER2, HER3 and HER4 expression levels in the six bladder cancer cell lines. The results showed a complex variability of expression for EGFR and HER2 (and the other family members) among the cell lines consistent with emerging clinical data, where there is a mixture of patients who are $EGFR^{+}/HER2^{+}$, $EGFR^{-}/HER2^{+}$, $EGFR^{+}/HER2^{-}$ and $EGFR^{-}/HER2^{-}$. Only three bladder cancer cell lines, HT1376, RT112 and RT112CP expressed detectable levels of HER3 and all cell lines expressed HER4 but with different levels of expression. This contrasts with findings by McHugh *et al*., who found similar expression levels of HER3 across a panel of 6 bladder cancer cell lines but no expression of HER4 receptor (McHugh *et al.* 2009). A comparison of the different bladder cancer cell lines used is shown in Table 4.2. A possible inverse relationship between HER3 and HER4 expression was also observed, although significance of this needs to be further studied.

The HER receptors signal predominantly through both the mitogen-activated protein kinase (MAPK) pathway, which drives cell proliferation, and through the PI3K/Akt pathway, which drives cellular survival and antiapoptotic signals (Mendelsohn and Baselga 2000), but other pathways may also be relevant. Since overexpression of EGFR and/or HER2 could result in increased activation of these pathways, activation of key molecules of both pathways were analysed across the panel of cell lines first under standard medium conditions (10% FBS) but also after EGF and NRG-1 stimulation.

Akt is a fundamental molecule in the PI3K pathway, and it is frequently activated in a wide variety of cancers (Altomare and Testa 2005), resulting in tumour cell survival and enhanced resistance to apoptosis.

	This study	*(McHugh et al. 2009)*
Bladder cancer cell lines	HT1376	HT1376
	T24	T24
	RT112	RT112
	RT112CP	J82
	UM-UC3	RT4
	UM-UC6	

Table 4.2 Bladder cancer cell lines used to study HER expression levels across a panel of bladder cancer cell lines in this study and a published study by McHugh *et al*.

Phosphorylation of Akt can occur at Thr308 by PDK1 (Alessi *et al.* 1997) and at Ser473 by mTORC2 (Sarbassov *et al.* 2005). Phosphorylation status of Akt at both sites was evaluated in the six bladder cancer cell lines. The results showed different levels of expression among the cell lines, with no evident relationship between the expression of phosphorylated Akt at Thr308 or Ser473 with respect to HER family members. Of note, however, was a possible inverse relationship between HER2 expression and phosphorylation of Akt at Thr308, but this would require further investigation.

Phosphorylation of ERK1/2 at Thr202 and Tyr204 was used to monitor the activation state of the Ras-MAPK pathway. Varying levels of activation were found among the cell lines. Cell lines also expressed preferentially total ERK1 over total ERK2, except for the HT1376 cell line, which expressed both, which is in accordance with another study (Swiatkowski *et al.* 2003). HT1376 also showed higher levels of phosphorylation of ERK2 over ERK1. T24 cell line contain *HRAS* mutation (Reddy *et al.* 1982), and it was the cell line which expressed higher levels of phospho-ERK1/2.

4.5.2 Effect of growth factors in bladder cancer cell lines

RT112 and T24 were the cell lines chosen to test whether EGFR and HER2 signalling pathways were functional in these cells. In order to do this, cells were stimulated with EGF (ligand for EGFR) or NRG-1 (ligand for HER3/HER4). Study on phosphorylation status of HER family members (phospho-EGFR and phospho-HER2) could not be done as the antibodies used were not sensitive enough. One way to overcome this could have been by immunoprecipitating the protein first and then detection of the phosphorylated protein by Western blotting. Although specific activation of the receptors could not be analysed, the effects of EGF and NRG-1 on the activation of molecules downstream of the EGFR/HER2 pathway was studied.

In RT112 cells, phosphorylation of ERK1/2 and Akt increased after the addition of EGF or NRG-1, which is in accordance with other studies (McHugh *et al.* 2009). In T24 cells, however, only EGF could increase phosphorylation of these proteins. The fact that T24 cells did not respond to stimulation of NRG-1, which is the ligand for HER3/HER4, is in accordance to the previous observation that HER3 could not be detected by Western blot in these cells.

The analysis of the effects of these growth factors on cell proliferation showed a dose-dependent increase in RT112 cells treated with EGF, and some increase after NRG-1 stimulation. On the contrary, T24 cells did not respond to EGF or NRG-1, probably because T24 cells are known to have a mutation in *HRAS* (Reddy *et al.* 1982) and phospho-ERK1/2 was found to be constitutively activated in this cell line. These findings contrast with studies by Okuyama *et al.*, where they found that NRG was more important in growth stimulation than EGF in a 3–dimensional culture of primary human urothelial cancer cells (Okuyama *et al.* 2013).

4.5.3 Study of HER family dimerization patterns in bladder cancer

Recently, there has been a growing interest to investigate the dimerization patterns of HER family members in tumours where these receptors act as oncogenes. The presence of specific dimers could serve as a prognostic factor for the disease but also a predictive factor for targeted therapy that might take advantage of such interactions. For instance, pertuzumab is a humanised monoclonal antibody that has been recently approved for HER2-positive metastatic breast cancer. It binds to the dimerization domain of HER2 and it inhibits HER2 from forming dimers with other HER family members (Agus *et al.* 2002). Immunoprecipitation assays were used in order to investigate dimerization patterns of HER family members in bladder cancer, which is currently unknown. Elucidation of dimerization patterns in bladder cancer could also be clinically relevant and could be used as a therapeutic target the same way it has been used in breast cancer.

Cetuximab and trastuzumab were the two monoclonal antibodies chosen to immunoprecipitate EGFR and HER2, respectively. Despite successful immunoprecipitation of these receptors, results were not reproducible between experiments and no co-immunoprecipitation of other HER members could be detected. HER2 IP worked for SKBR3 cells, which were used as a positive control, since these cells have high levels of HER2 expression. However, in bladder cancer cells that have lower expression of this receptor, the technique was probably not sufficiently sensitive.

In studies made by Sanchez-Martin *et al*. they observed very low or undetectable interaction between HER receptors in the absence of ligands, whereas in the addition of NRG-1, HER2-HER3 dimers could be detected in breast cancer cells including SKBR3 (Sanchez-Martin and Pandiella 2012). To test whether this could also be the case in this

bladder cancer model, an immunoprecipitation assay was also performed where cells were treated with EGF in order to stimulate receptor dimerization. However, no co-immunoprecipitation of HER members could be detected even in the presence of ligands and other methods may be needed to study dimerization patterns of HER family members in bladder cancer. A potential alternative to immunoprecipitation assays which might allow this work to be taken forward would be the assessment of receptor dimerization by Förster Resonance Energy Transfer (FRET), which has been successfully used to assess EGFR/HER2 dimers in breast cancer cells (Waterhouse *et al.* 2011).

Chapter 5: Investigation of EGFR and HER2 inhibition in bladder cancer cell line models

After characterizing the HER family expression and function in the panel of bladder cancer cell lines, my next step was to determine whether EGFR and HER2 have a critical role in these cells. To investigate this, EGFR and HER2 activity was inhibited using two different approaches: using tyrosine kinase inhibitors (TKIs) against EGFR and/or HER2 and also knocking down their expression using small interfering RNA (siRNA). Effects on cell proliferation, cell cycle and induction of apoptosis were analysed.

5.1 Cell proliferation assays with TKIs (lapatinib, erlotinib, CP654577)

Cell proliferation assays were used to investigate whether tyrosine kinase inhibitors (TKI) against EGFR and/or HER2 had an impact on the proliferation of these cells. To test this, the panel of six bladder cancer cell lines and one breast cancer cell line (SKBR3) were treated with three different TKIs: lapatinib (EGFR/HER2 TKI), erlotinib (EGFR TKI) or CP654577 (HER2 TKI) at various concentrations continuously for 4 days. Lapatinib and erlotinib are drugs that are already in use in the clinic to treat various cancers. CP654577 was used as a tool to target HER2. Another two HER2 TKI compounds were included in this study: CP724714 (Jani *et al.* 2007) and mubritinib (TAK-165) (Nagasawa *et al.* 2006). However, proliferation assays using these two compounds were not successful (data not shown) due to instability problems with mubritinib and solubility issues with CP721714. These compounds were therefore excluded from the study and CP654577 was chosen as the sole HER2 TKI tested.

The MTS assay was used to quantify cell proliferation. The assay measures metabolic activity of the cell, which can be used as an indirect measure of cell number. The dose-response curves from each drug can be used to calculate the dose achieving IC_{50} (concentration required for 50% inhibition of cell viability). SKBR3 cells are a breast

cancer cell line known to overexpress HER2 and it was included in the study as a positive control as it is a lapatinib sensitive cell line.

All bladder cancer cell lines showed an antiproliferative effect in response to increasing concentrations of lapatinib, erlotinib and CP654577. Representative dose-response curves for each cell line and each drug are shown in Figure 5.1. The IC_{50} values found from all the experiments performed are shown in Figure 5.2. The mean of the IC_{50} values ± standard deviation found for each cell line and each drug are shown in Table 5.1. Lapatinib IC_{50} ranged from 2.2 to 8.6 μM in the bladder cancer cell lines. IC_{50} found for SKBR3 cells was 10.6 μM, so all bladder cancer cell lines were more sensitive to this drug than the SKBR3 breast cancer cell line. Greater variability of response between individual cell lines was observed with erlotinib. IC_{50} values varied from 0.8 to 28.7 μM. In contrast, the IC_{50} values for CP654577 were very similar among the cell lines, varying only from 1.7 to 2.5 μM. There was an initial concern about the specificity of the molecule, as little is known about it with only one paper published (Barbacci *et al.* 2003).

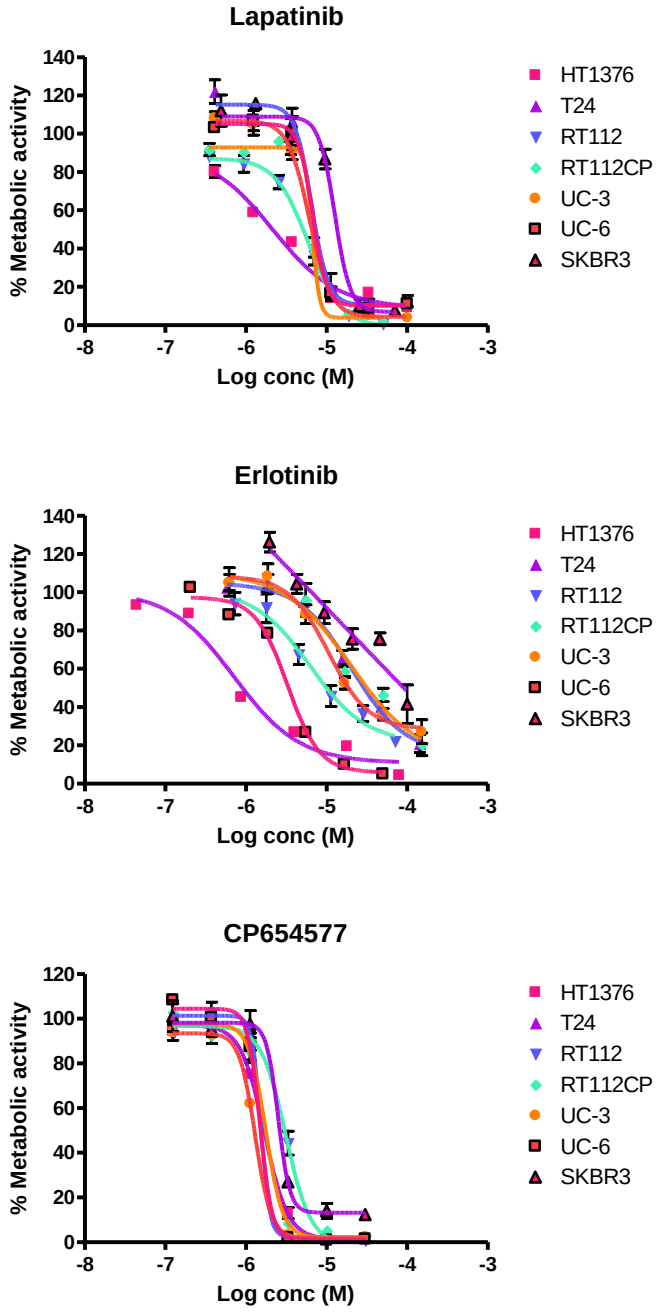

Figure 5.1 Representative dose-response curves of bladder cancer cell lines treated with TKIs. Bladder cancer cell lines and a breast cancer cell line (SKBR3) were treated with lapatinib (EGFR/HER2 TKI), erlotinib (EGFR TKI) and CP654577 (HER2 TKI) at various concentrations continuously for 4 days. Control cells were treated with equal concentrations of DMSO, and the MTS assay was used to measure the % of metabolic activity of treated cells compared to control cells. GraphPad Prism4 was used to generate a non-linear regression sigmoidal curve. Each data point represents the mean of triplicate determinations in a representative experiment ± SD.

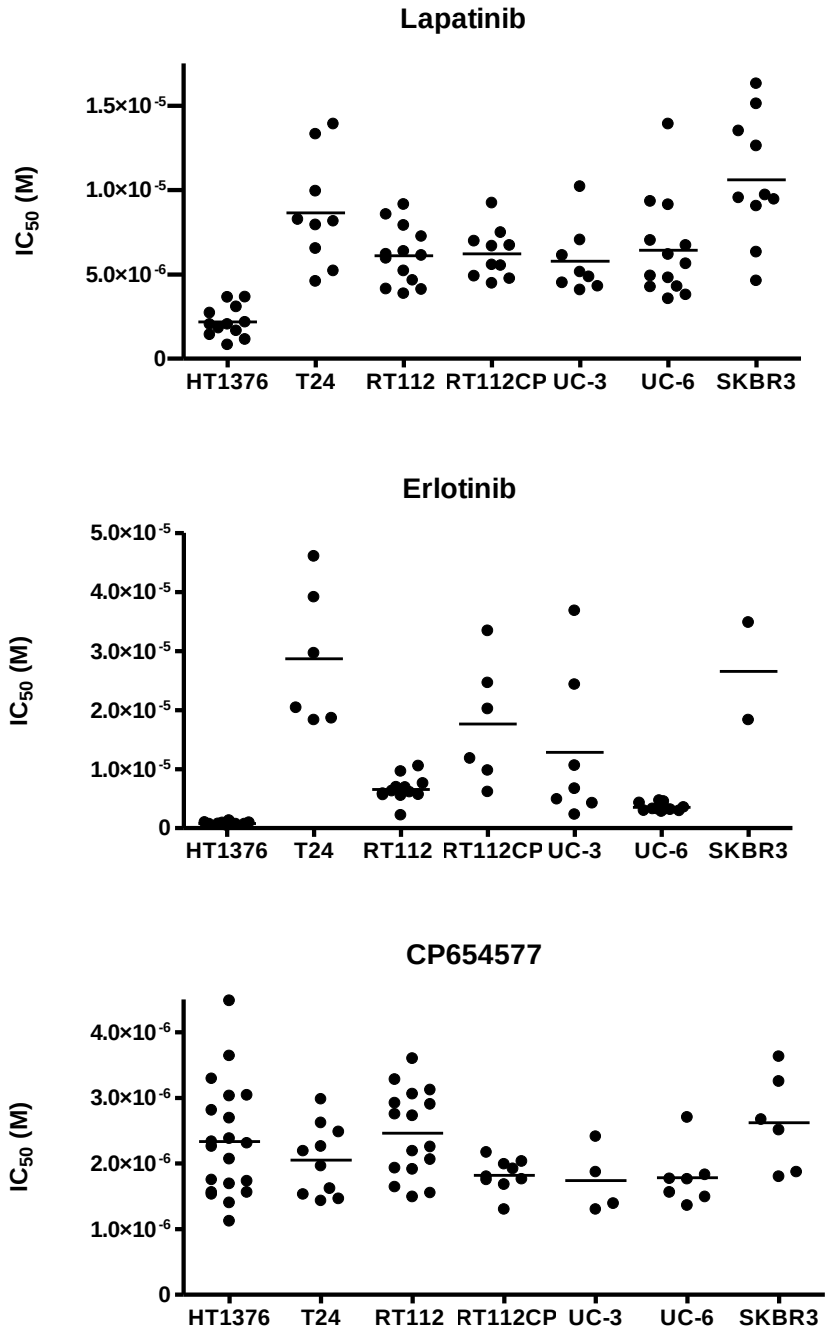

Figure 5.2 Mean IC_{50}values in bladder cancer cell lines for lapatinib, erlotinib and CP654577. IC_{50} values were calculated from dose-response curves generated by a non-linear regression sigmoidal curve using the GraphPad Prism4. All IC_{50} values found and their mean are shown for each drug and each cell line. The horizontal bar represents the mean value for each group.

	Lapatinib		Erlotinib		CP654577	
Cell line	IC_{50} (μM)	± SD	IC_{50} (μM)	± SD	IC_{50} (μM)	± SD
HT1376	2.2	0.9	0.8	0.2	2.3	0.9
T24	8.6	3.3	28.7	11.7	2.1	0.5
RT112	6.1	1.7	6.6	2.1	2.5	0.7
RT112CP	6.2	1.5	17.7	10.3	1.8	0.3
UM-UC-3	5.8	2.1	12.8	12.9	1.7	0.5
UM-UC-6	6.4	2.9	3.5	0.7	1.8	0.4
SKBR3	10.6	3.7	26.6	11.7	2.6	0.7

Table 5.1 IC_{50} values for lapatinib, erlotinib and CP654577 in the bladder cancer cell lines. Mean IC_{50} for lapatinib, erlotinib and CP654577 in the panel of bladder cancer cell lines and the breast cancer cell line SKBR3. Number of experiments performed for each drug; lapatinib n≥8, erlotinib n≥2, CP654577 n≥4. SD, standard deviation.

5.2 Effect of TKIs on downstream signalling pathways

To investigate how effective TKIs were in inhibiting HER family activated downstream pathways, and therefore to clarify the underlying mechanism of action of the TKIs, changes on protein expression of growth and survival signalling pathways were evaluated in T24 cells. This cell line was chosen for these studies in order to keep cell death to a minimum as it was one of the most resistant cell lines against the TKIs. T24 cells growing in media supplemented with charcoal stripped FBS were pre-treated with the three TKIs (lapatinib, erlotinib and CP654577) and then stimulated with growth factors: EGF (ligand for EGFR) or NRG-1 (ligand for HER3 and HER4). Changes in phosphorylation levels of ERK1/2 and Akt (Ser473) were evaluated by Western blot.

5.2.1 Study of TKIs effect on EGF activated pathways

Cells were pre-treated with lapatinib, erlotinib or CP654577 at the IC_{50} dose for 24 hours and then stimulated for 10 minutes with EGF at 100 ng/ml, based on published literature (McHugh *et al.* 2009). The results (see Figure 5.3) showed that stimulation of T24 cells with EGF increased phospho-ERK1/2 and also increased slightly the levels of phospho-Akt (Ser473), which is in accordance of EGFR being able to weakly activate Akt pathway due to the fact that this receptor, in contrast to the other family members, has no intracellular binding sites for PI3K (Soltoff *et al.* 1994).

Downregulation of phospho-ERK1/2 was observed in both lapatinib and erlotinib-treated cells despite EGF stimulation, confirming that this downstream signalling pathway was blocked with these TKIs. However, in CP654577-treated cells downregulation of phospho-ERK1/2 was not observed and phospho-ERK1/2 could be activated after EGF stimulation, suggesting CP654577 specificity for HER2 and therefore not affecting EGF signalling through EGFR.

In contrast, when cells had been previously treated with lapatinib or CP654577, activation of phospho-Akt (Ser473) could still be seen compared to control cells for each treatment. More striking was the increase in phospho-Akt (Ser473) in erlotinib-treated cells, regardless of having been treated with EGF or not.

Quantification of phospho-ERK1/2 and phospho-Akt (Ser473) expression levels is shown in Figure 5.4

5.2.2 Study of TKIs effect on NRG-1 activated pathways

Cells were pre-treated with lapatinib, erlotinib or CP654577 at the IC_{50} dose for 24 hours and then treated for 10 minutes with NRG-1 at 100 ng/ml. The results (see Figure 5.5) showed levels of phospho-ERK1/2 increased in NRG-1-treated cells. This contrasts with the results seen in Chapter 4, where stimulation with NRG-1 did not alter the levels phospho-ERK1/2 in T24 cells (section 4.2.3). T24 cells had no HER3 expression that could be detected by Western blot (as seen in Chapter 4), so it could be that NRG-1 was signalling through HER4 or that even though HER3 could not be detected by Western blot, was still active in these cells and able to activate signalling pathways. Stimulation of T24 cells with NRG-1 had no or little effect in the levels of phospho-Akt (Ser473).

A downregulation of phospho-ERK1/2 could be observed when cells had been previously treated with TKIs (lapatinib, erlotinib or CP654577) despite stimulation of the cells with NRG-1, suggesting that the TKIs were effective at blocking this pathway. Phospho-Akt (Ser473) was upregulated when cells had been treated with erlotinib, regardless of having been treated with NRG-1 or not, confirming the results seen previously.

Quantification of phospho-ERK1/2 and phospho-Akt (Ser473) expression levels is shown in Figure 5.6

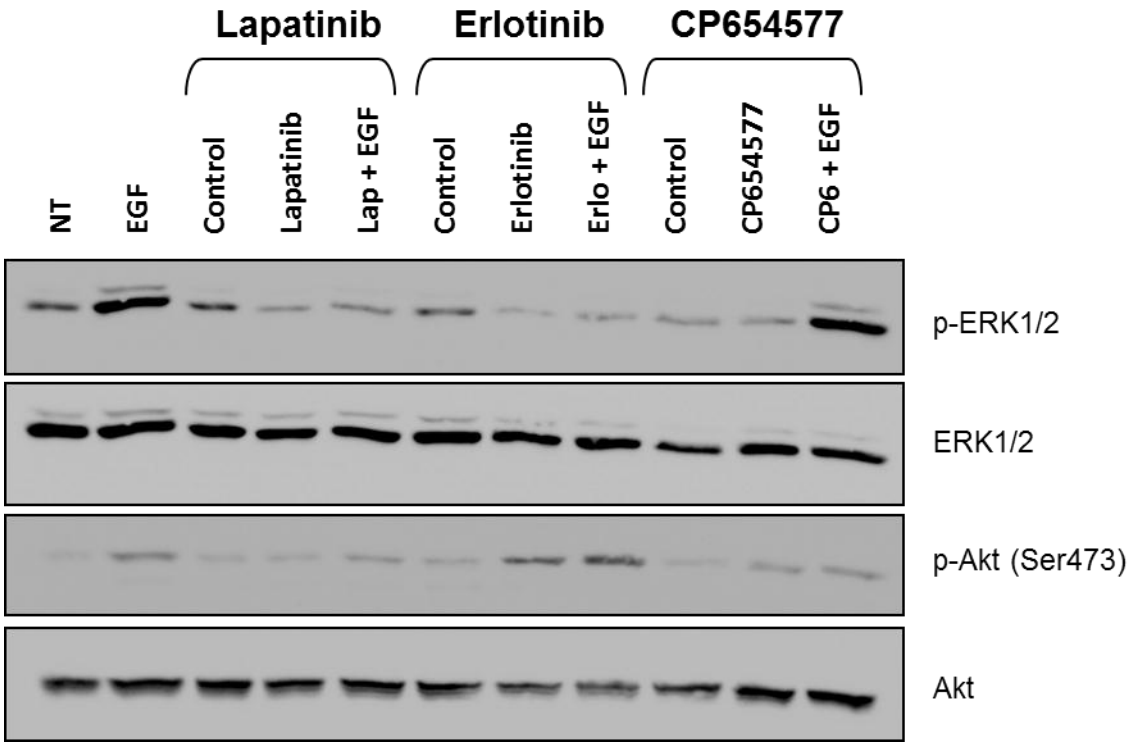

Figure 5.3 Analysis of response of T24 cells after 24 hours pre-treatment with TKIs (lapatinib, erlotinib or CP654577) and subsequent stimulation with EGF. T24 cells growing in media supplemented with charcoal stripped FBS were pre-treated with lapatinib, erlotinib or CP654577 at the IC_{50} dose, DMSO at the equivalent dose (control) or left untreated (NT) for 24 hours and then the indicated samples were treated with EGF at 100 ng/ml for 10 minutes. Whole cell lysate was subjected to SDS-PAGE and analysed by Western blot for phospho-ERK1/2 (Thr202/Tyr204; 42/44 kDa), phospho-Akt (Ser473; 60 kDa), total ERK1/2 and total Akt. Representative of two different experiments.

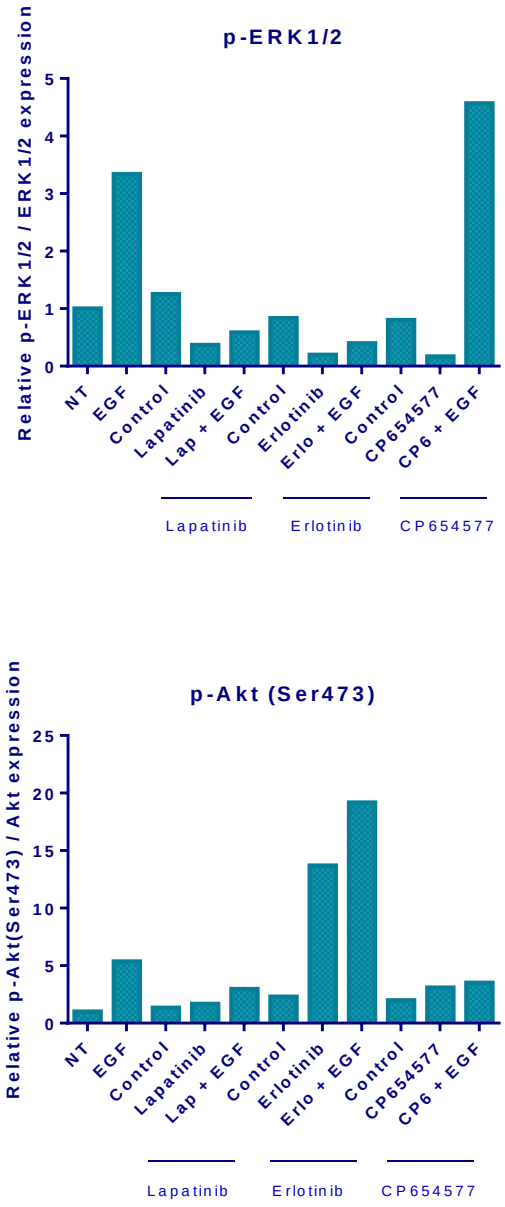

Figure 5.4 Relative expression levels of phospho-ERK1/2 and phospho-Akt (Ser473) in T24 cells after 24 hours pre-treatment with TKIs (lapatinib, erlotinib or CP654577) and subsequent stimulation with EGF. Protein expression levels of phospho-ERK1/2 and phospho-Akt (Ser473) were normalized to the levels of total ERK1/2 and Akt respectively. Protein expression levels are presented as the fold difference compared to untreated cells (NT).

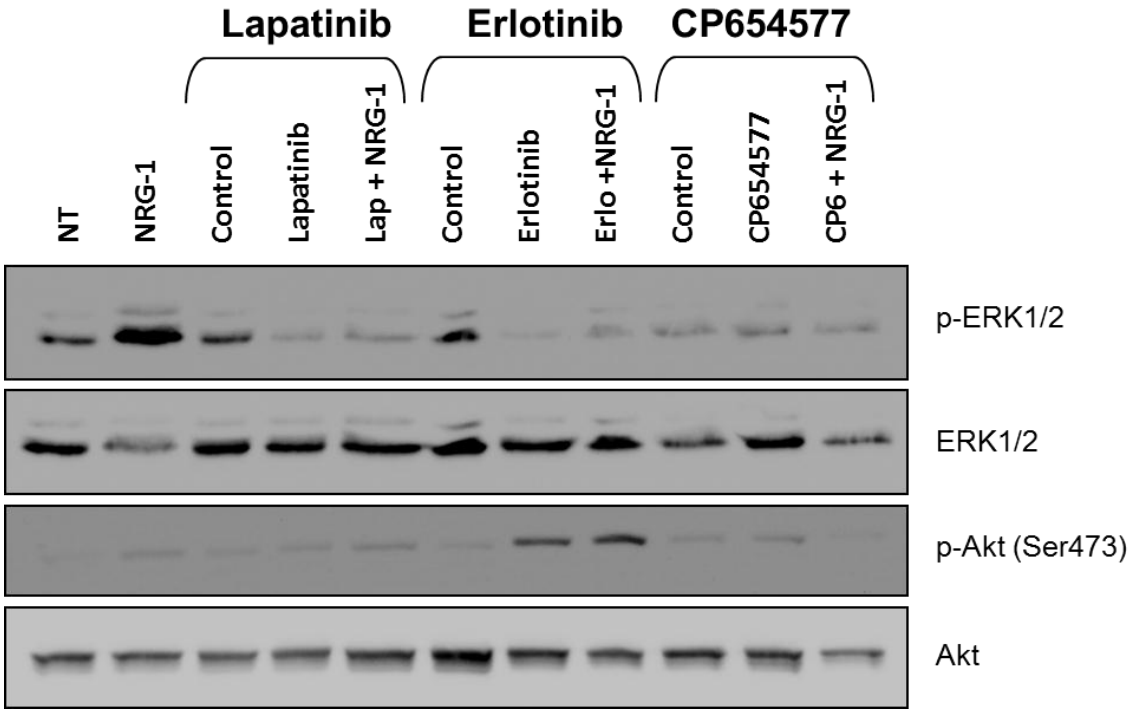

Figure 5.5 Analysis of response of T24 cells after 24 hours pre-treatment with TKIs (lapatinib, erlotinib or CP654577) and subsequent stimulation with NRG-1. T24 cells growing in media supplemented with charcoal stripped FBS were pre-treated with lapatinib, erlotinib or CP654577 at the IC_{50} dose, DMSO at the equivalent dose (control) or left untreated (NT) for 24 hours and then the indicated samples were treated with NRG-1 at 100 ng/ml for 10 minutes. Whole cell lysate was subjected to SDS-PAGE and analysed by Western blot for phospho-ERK1/2 (Thr202/Tyr204; 42/44 kDa), phospho-Akt (Ser473; 60 kDa), total ERK1/2 and total Akt. Representative of two different experiments.

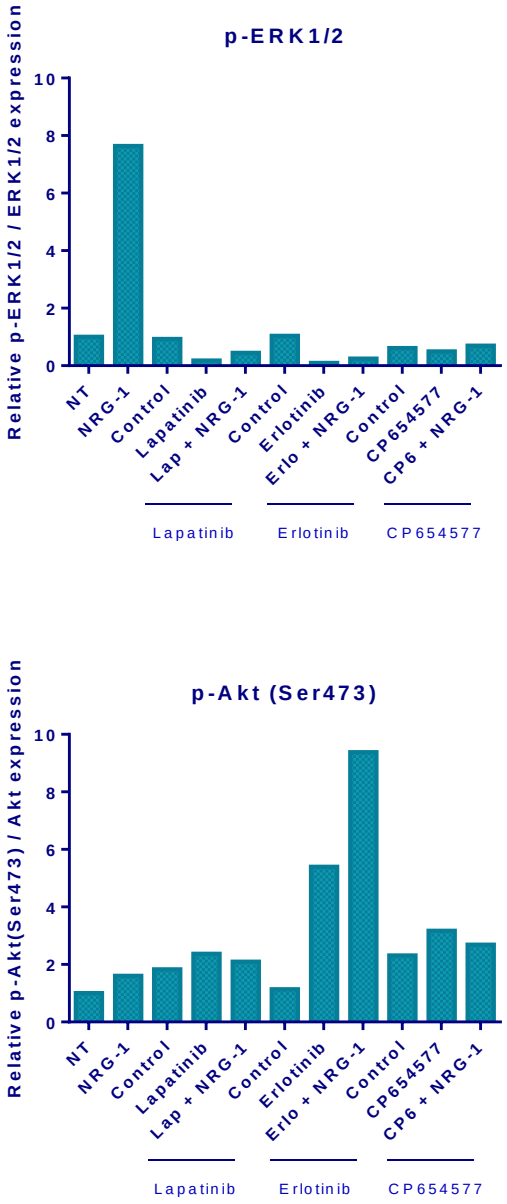

Figure 5.6 Relative expression levels of phospho-ERK1/2 and phospho-Akt (Ser473) in T24 cells after 24 hours pre-treatment with TKIs (lapatinib, erlotinib or CP654577) and subsequent stimulation with NRG-1. Protein expression levels of phospho-ERK1/2 and phospho-Akt (Ser473) were normalized to the levels of total ERK1/2 and Akt respectively. Protein expression levels are presented as the fold difference compared to untreated cells (NT).

5.3 Cell cycle analysis

To better characterize the antiproliferative effect of the TKIs, a study on cell cycle distribution using propidium iodine (PI) staining was performed after treating RT112 cells with lapatinib (EGFR/HER2 TKI), erlotinib (EGFR TKI) or CP654577 (HER2 TKI) at different concentrations (around, below and above their respective IC_{50}). RT112 cell line was chosen as it was the cell line that showed the highest expression of HER2 and it also had high levels of EGFR.

The cell cycle analysis of RT112 cells treated with lapatinib (Figure 5.7A) showed a dose-dependent increase in G_1 population after 24 hours and 48 hours of treatment, suggesting a G_1 arrest in these cells. Representative gating-histograms of this experiment are shown in Figure 5.8. In a separate experiment (shown in Figure 5.7B), RT112 cells were treated with lapatinib in order to study cell death on these cells by analysing the proportion of events with sub G_1 DNA content. After 72 hours, an increase was seen at 25 μM.

RT112 cells were also treated with erlotinib in order to study the effect of this drug on cell cycle distribution. The results (Figure 5.9A) showed a dose-dependent increase in G_1 population after 24, 48 and 72 hours of erlotinib treatment, suggesting a possible G_1 arrest on these cells similar to lapatinib treatment. Representative gating-histograms of this experiment are shown in Figure 5.10. However, the analysis of events with sub G_1 DNA content after erlotinib treatment (Figure 5.9B) showed no or little increase compared to control cells.

RT112 cells treated with CP654577 also showed an increase in G_1 population after 24 and 48 hours of treatment (Figure 5.11A). Representative gating-histograms of this experiment are shown in Figure 5.12. After 72 hours, an increase of events with sub G_1 DNA content was seen at 14 μM (Figure 5.11B).

A

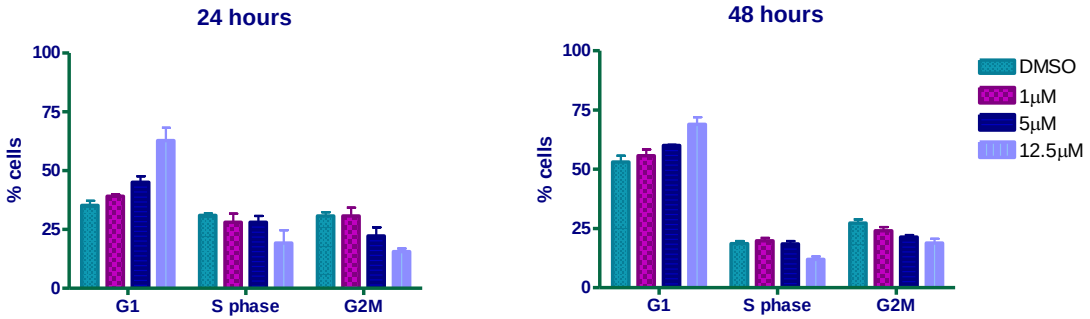

B

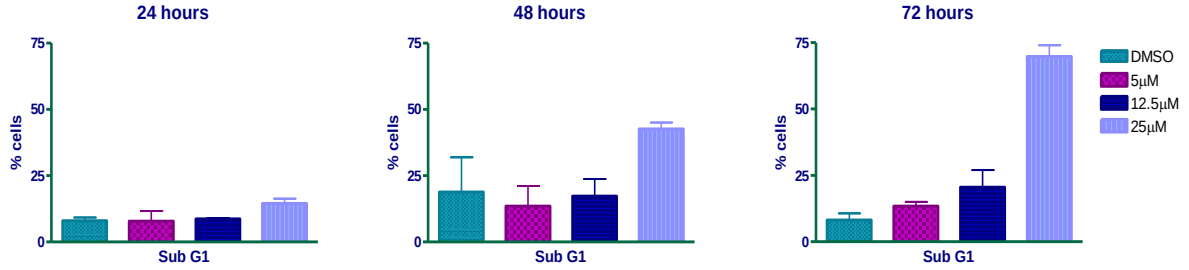

Figure 5.7 Analysis of the cell cycle distribution and cell death after treatment of RT112 cells with lapatinib using PI staining. (A) RT112 cells were treated with 1 μM, 5 μM, 12.5 μM lapatinib or DMSO (as control) over 24 and 48 hours. Cell cycle analysis was performed by propidium iodine (PI) staining. (B) RT112 cells were treated with 5 μM, 12.5 μM, 25 μM lapatinib or DMSO (as control) over 24, 48 and 72 hours to quantify events with sub G_1 DNA content. Values represent the average of one experiment made in duplicate, and the error bars represent standard deviation. Representative of four different experiments.

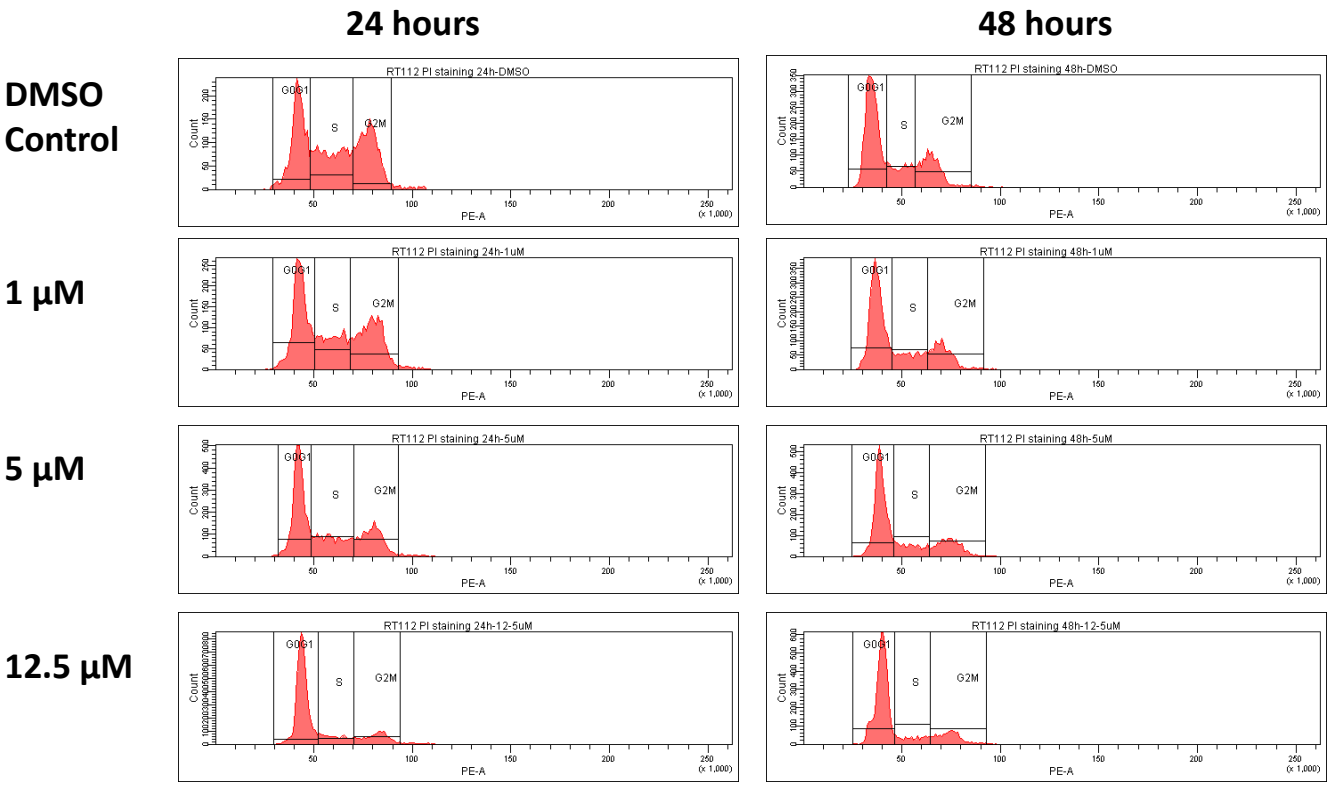

Figure 5.8 Representative gating histograms of the cell cycle analysis study of RT112 cells after lapatinib treatment. Cells were treated with DMSO (control) or lapatinib at the indicated concentrations for 24 and 48 hours, and then they were analysed by flow cytometry after propidium iodine (PI) staining. The cell cycle profile was estimated by gating histograms generated with the PE-area variable.

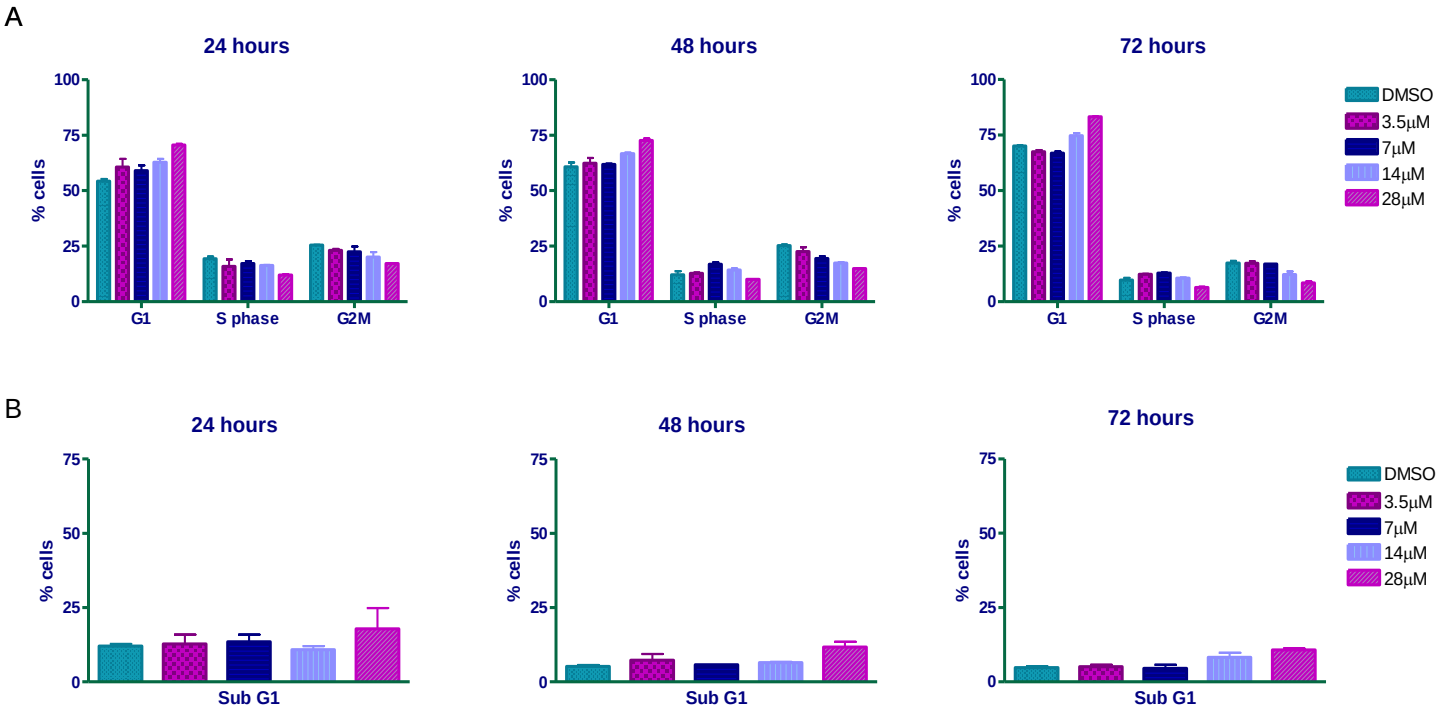

Figure 5.9 Analysis of the cell cycle distribution and cell death after treatment of RT112 cells with erlotinib using PI staining. (A) RT112 cells were treated with 3.5 µM, 7 µM, 14 µM, 28 µM erlotinib or DMSO (as control) over 24, 48 and 72 hours. Cell cycle analysis was performed by PI staining. (B) Analysis of events with sub G_1 DNA content after treating RT112 cells with erlotinib. Values represent the average of one experiment made in duplicate, and the error bars represent standard deviation. Representative of two different experiments.

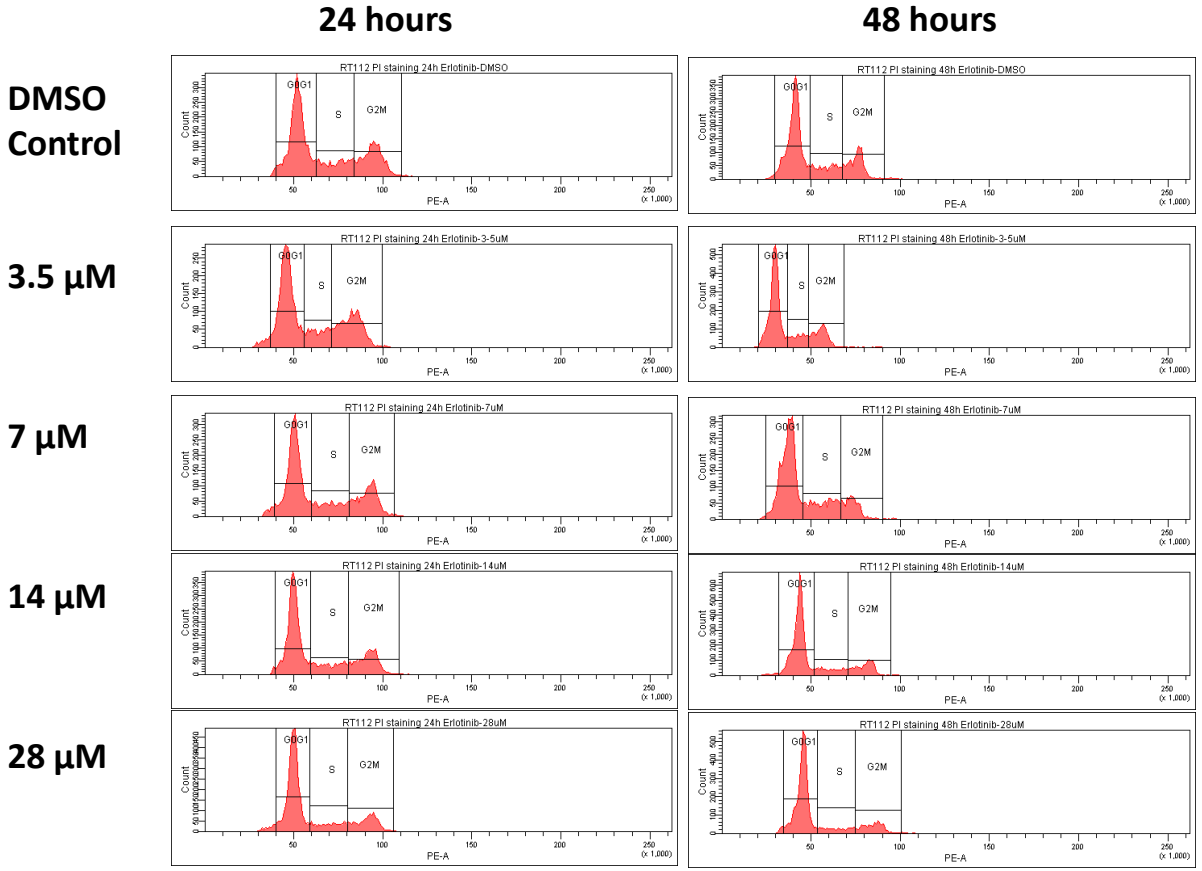

Figure 5.10 Representative gating histograms of the cell cycle analysis study of RT112 cells after erlotinib treatment. Cells were treated with DMSO (control) or erlotinib at the indicated concentrations for 24 and 48 hours, and then they were analysed by flow cytometry after propidium iodine (PI) staining. The cell cycle profile was estimated by gating histograms generated with the PE-area variable.

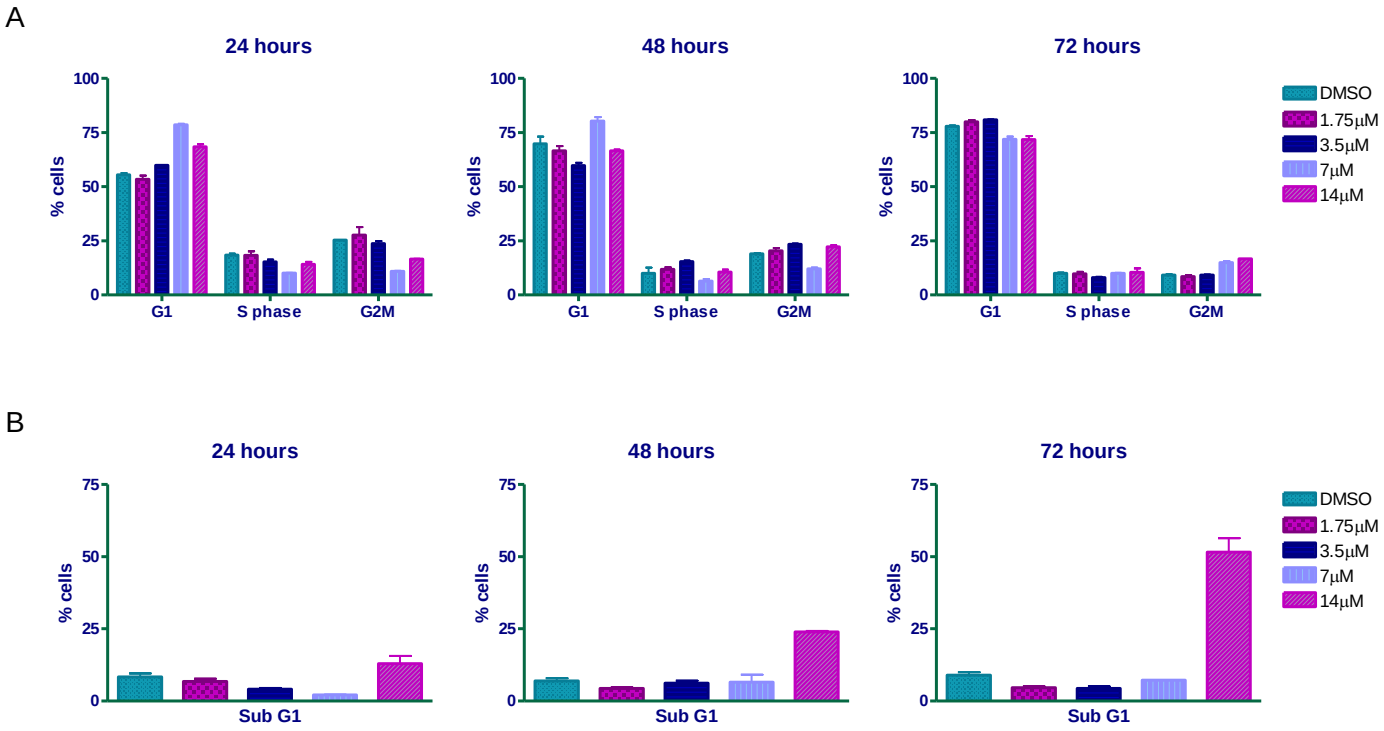

Figure 5.11 Analysis of the cell cycle distribution and cell death after treatment of RT112 cells with CP654577 using PI staining. (A) RT112 cells were treated with 1.75 µM, 3.5 µM, 7 µM, 14 µM CP654577 or DMSO (as control) over 24, 48 and 72 hours. Cell cycle analysis was performed by PI staining. (B) Analysis of events with sub G_1 DNA content after treating RT112 cells with CP654577. Values represent the average of one experiment made in duplicate, and the error bars represent standard deviation. Representative of four different experiments.

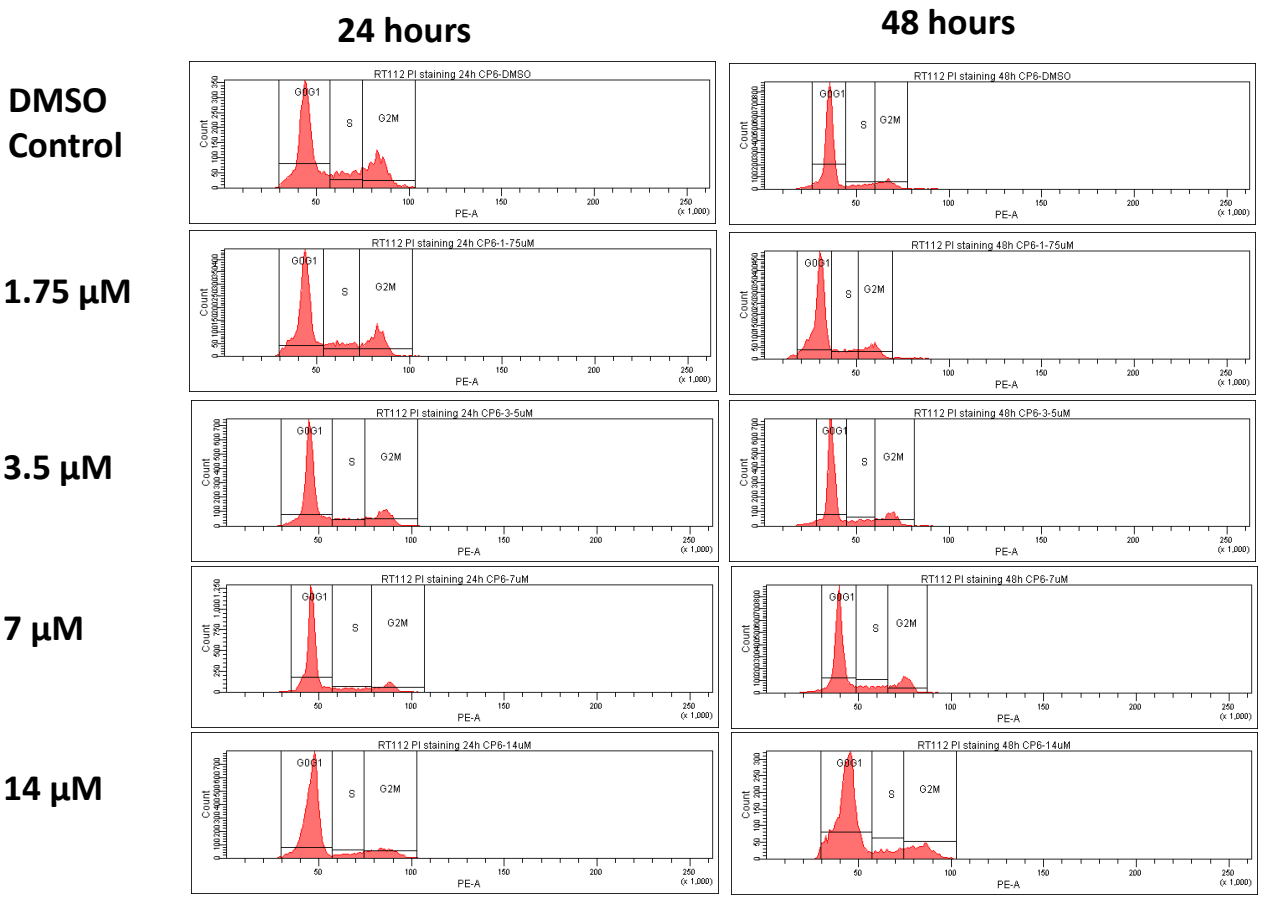

Figure 5.12 Representative gating histograms of the cell cycle analysis study of RT112 cells treated with CP654577. Cells were treated with DMSO (control) or CP654577 at the indicated concentrations for 24 and 48 hours, and then they were analysed by flow cytometry after propidium iodine (PI) staining. The cell cycle profile was estimated by gating histograms generated with the PE-area variable.

5.4 Apoptosis analysis

To further characterize the effects of EGFR and/or HER2 inhibition by TKIs, a study on induction of apoptosis was performed in RT112 cells. As a measure of apoptotic cells, externalization of plasma membrane phosphatidylserine was examined by flow cytometry using Annexin V. PI staining was used to discriminate between early and late apoptotic cells. The intensity of PI staining was plotted versus Annexin V staining and depending on the signal strengths of the channels, viable (Annexin V and PI negative), necrotic (Annexin V negative and PI positive), early apoptotic (Annexin V positive and PI negative) and late apoptotic (Annexin V and PI positive) cells were quantified.

First, RT112 cells were treated for 24, 48 and 72 hours with increasing concentrations of lapatinib. The results (Figure 5.13) showed an increase in early apoptotic cells at 25 μM after 24 hours. After 48 and 72 hours there was an increase in early apoptotic cells at 12.5 μM and 25 μM and a reduction in viable cells. No or little increase in late apoptotic cells or necrotic cells could be seen. Diagrams of Annexin V/PI flow cytometry analysis in a representative experiment are presented in Figure 5.14.

The analysis of RT112 cells treated with erlotinib (Figure 5.15) showed little effect of this drug on apoptosis. Only after 72 hours viable cells decreased at 28 μM due to a modest increase in early and late apoptotic cells. Diagrams of Annexin V/PI flow cytometry analysis in a representative experiment are presented in Figure 5.16.

RT112 cells treated with CP654577 (Figure 5.17) showed an increase in early apoptotic cells and in late apoptotic cells after 24, 48 and 72 hours of treatment at the higher dose (14 μM). After 72 hours, an increase in early apoptotic cells could also be seen in cells treated with CP654577 at 7 μM. Diagrams of Annexin V/PI flow cytometry analysis in a representative experiment are presented in Figure 5.18.

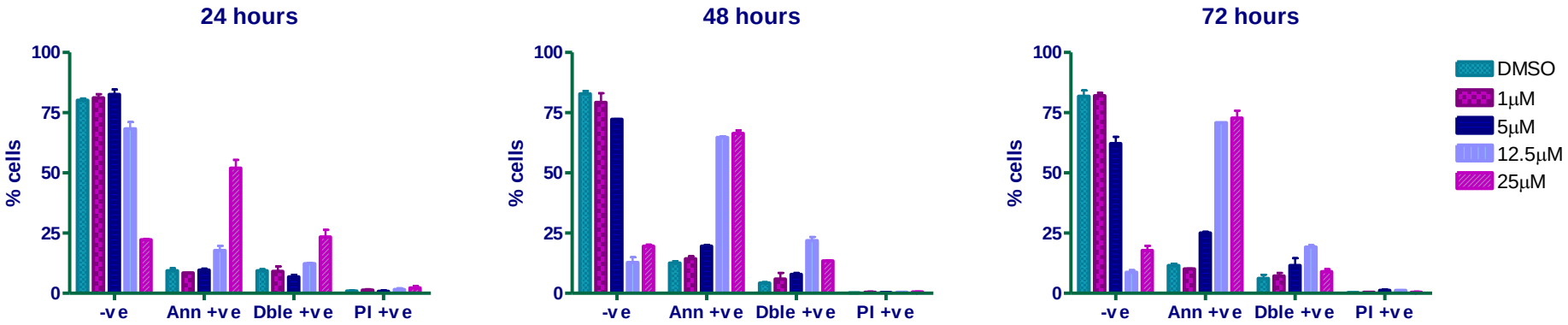

Figure 5.13 Induction of apoptosis by lapatinib in RT112 cells. Cells were treated with lapatinib (1 µM, 5 µM, 12.5 µM and 25 µM) or DMSO (control) for 24, 48 and 72 hours and labeled with Annexin V-FITC and PI. Data are expressed as % Annexin V-negative and PI-negative cells (viable cells), % of Annexin V-positive and PI-negative cells (early stage of apoptosis), % of Annexin V-positive and PI-positive cells (late stage of apoptosis or necrosis) and % Annexin V-negative and PI-positive cells (necrotic cells). Error bars represent the standard deviation of duplicates in one representative experiment. Representative of three different experiments.

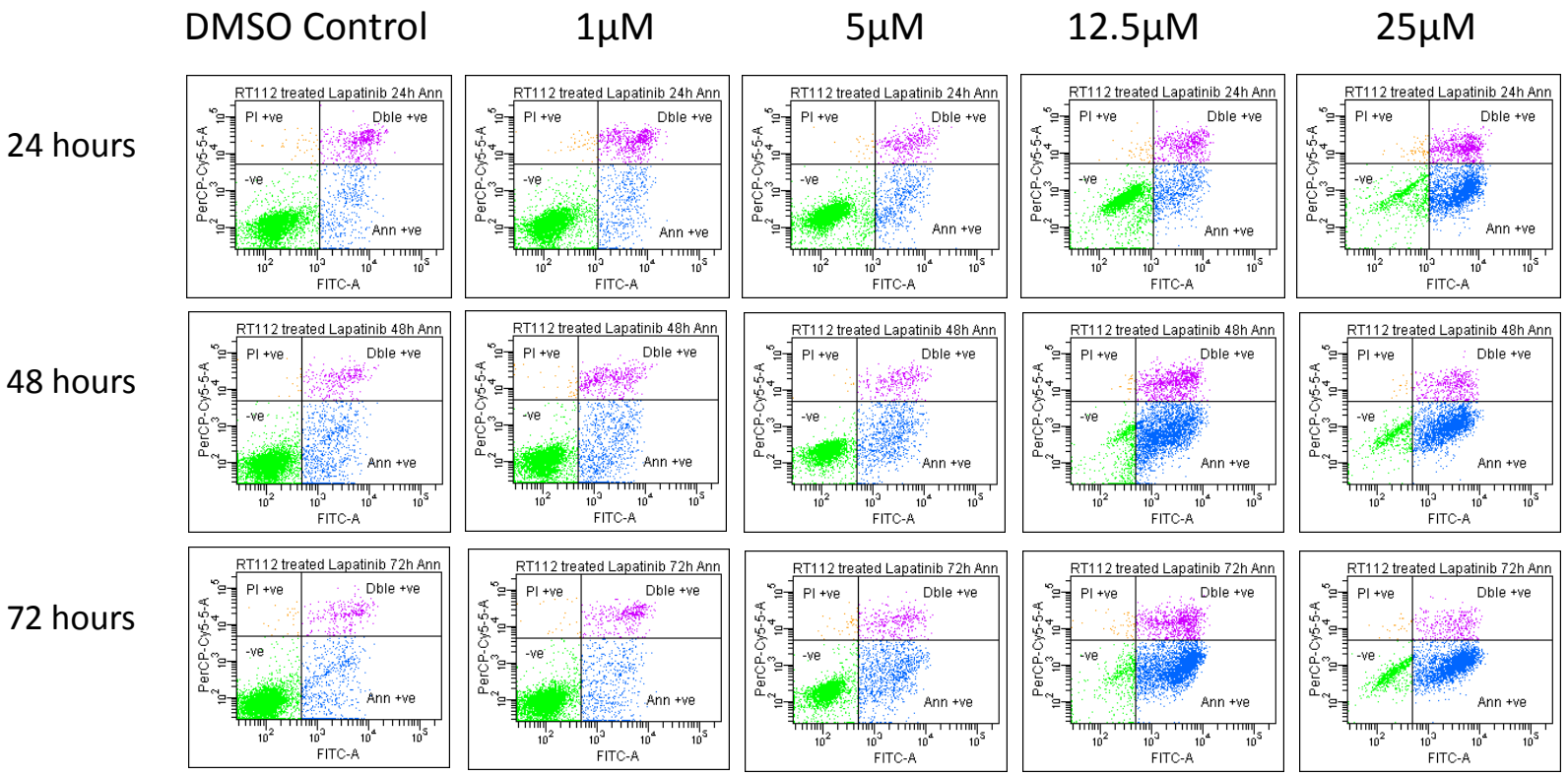

Figure 5.14 Study of induction of apoptosis in RT112 cells treated with lapatinib. RT112 cells were treated with different concentrations of lapatinib (1 µM, 5 µM, 12.5 µM and 25 µM) or DMSO (control) for 24, 48 and 72 hours. Apoptosis was examined with flow cytometry after Annexin V-FITC and PI staining. The lower left quadrants represent the viable cells (Annexin V-negative/PI-negative). The lower right quadrants represent the cells in the early stage of apoptosis (Annexin V-positive). The upper right quadrants contain the cells in the late stage of apoptosis or necrosis (Annexin V-positive/PI-positive) and the upper left quadrant are necrotic cells (Annexin V-negative/PI-positive).

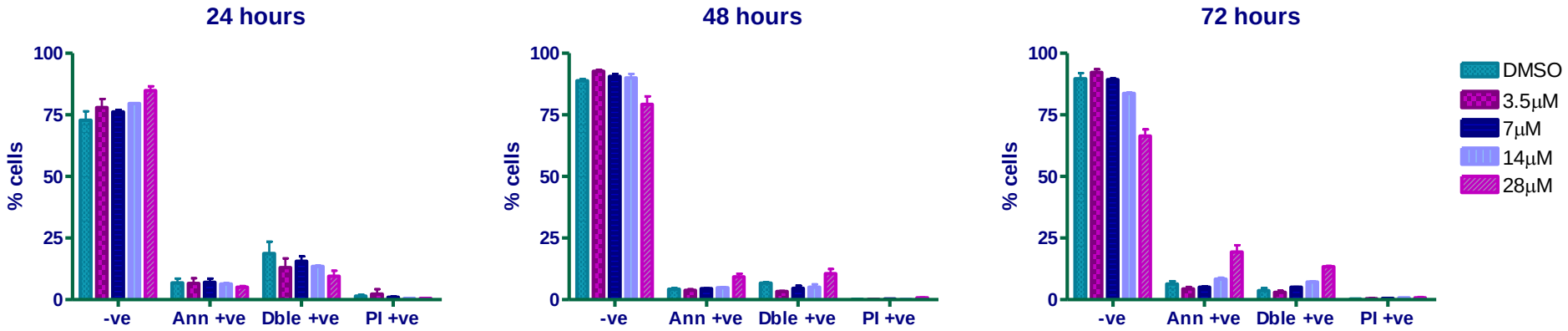

Figure 5.15 Induction of apoptosis by erlotinib in RT112 cells. Cells were treated with erlotinib (3.5 µM, 7 µM, 14 µM and 28 µM) or DMSO (control) for 24, 48 and 72 hours and labeled with Annexin V-FITC and PI. Data are expressed as % Annexin V-negative and PI-negative cells (viable cells), % of Annexin V-positive and PI-negative cells (early stage of apoptosis), % of Annexin V-positive and PI-positive cells (late stage of apoptosis or necrosis) and % Annexin V-negative and PI-positive cells (necrotic cells). Error bars represent the standard deviation of duplicates in one representative experiment. Representative of three different experiments.

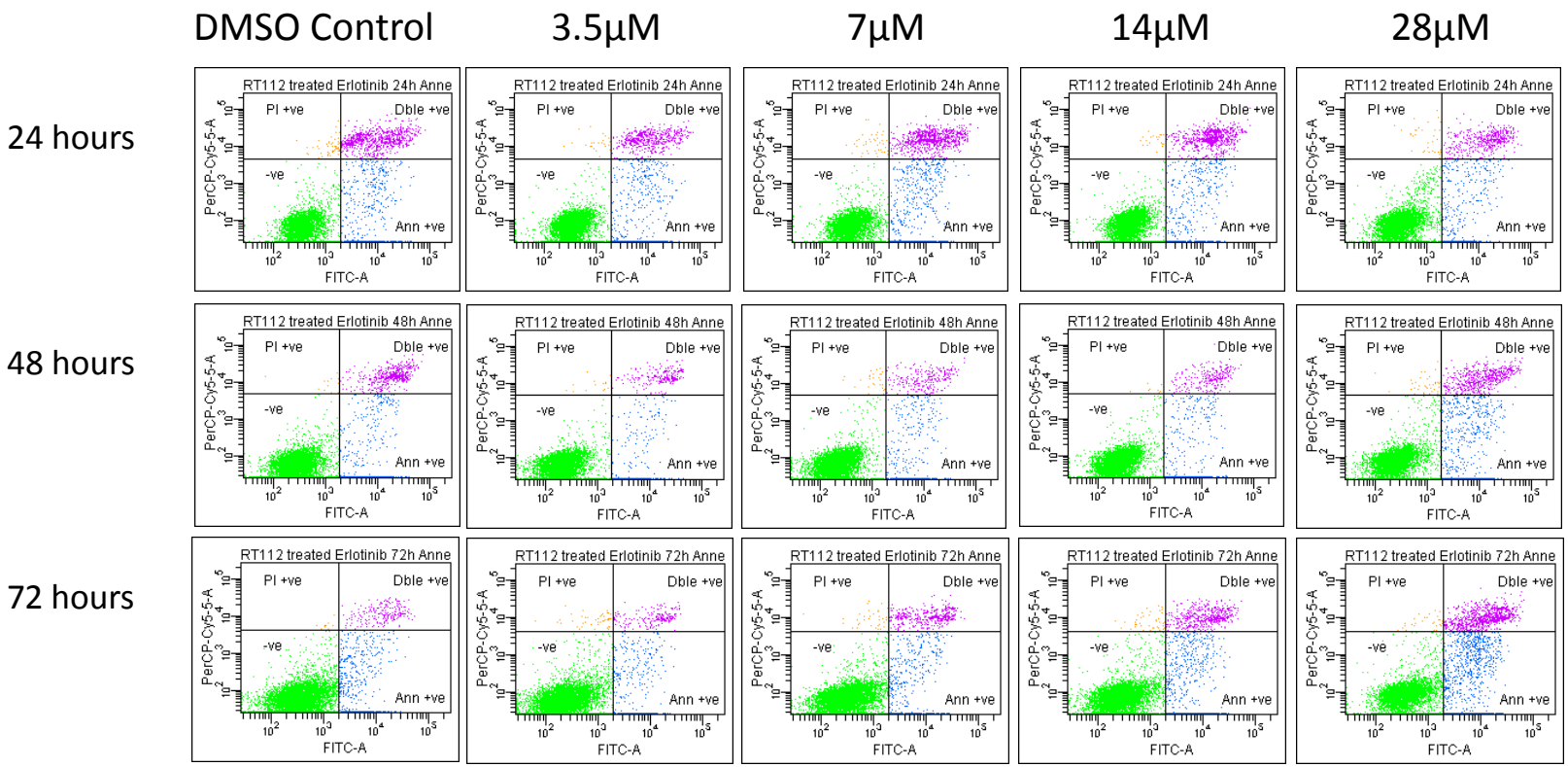

Figure 5.16 Study of induction of apoptosis in RT112 cells treated with erlotinib. RT112 cells were treated with different concentrations of erlotinib (3.5 µM, 7 µM, 14 µM and 28 µM) or DMSO (control) for 24, 48 and 72 hours. Apoptosis was examined with flow cytometry after Annexin V-FITC and PI staining. The lower left quadrants represent the viable cells (Annexin V-negative/PI-negative). The lower right quadrants represent the cells in the early stage of apoptosis (Annexin V-positive). The upper right quadrants contain the cells in the late stage of apoptosis or necrosis (Annexin V-positive/PI-positive) and the upper left quadrant are necrotic cells (Annexin V-negative/PI-positive).

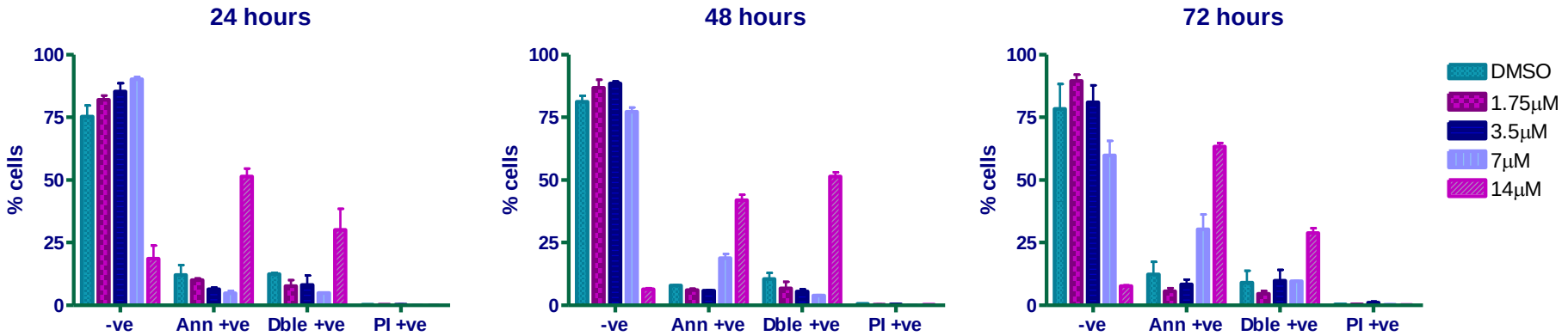

Figure 5.17 Induction of apoptosis by CP654577 in RT112 cells. Cells were treated with CP654577 (1.75 µM, 3.5 µM, 7 µM and 14 µM) or DMSO (control) for 24, 48 and 72 hours and labeled with Annexin V-FITC and PI. Data are expressed as % Annexin V-negative and PI-negative cells (viable cells), % of Annexin V-positive and PI-negative cells (early stage of apoptosis), % of Annexin V-positive and PI-positive cells (late stage of apoptosis or necrosis) and % Annexin V-negative and PI-positive cells (necrotic cells). Error bars represent the standard deviation of duplicates in one representative experiment. Representative of three different experiments.

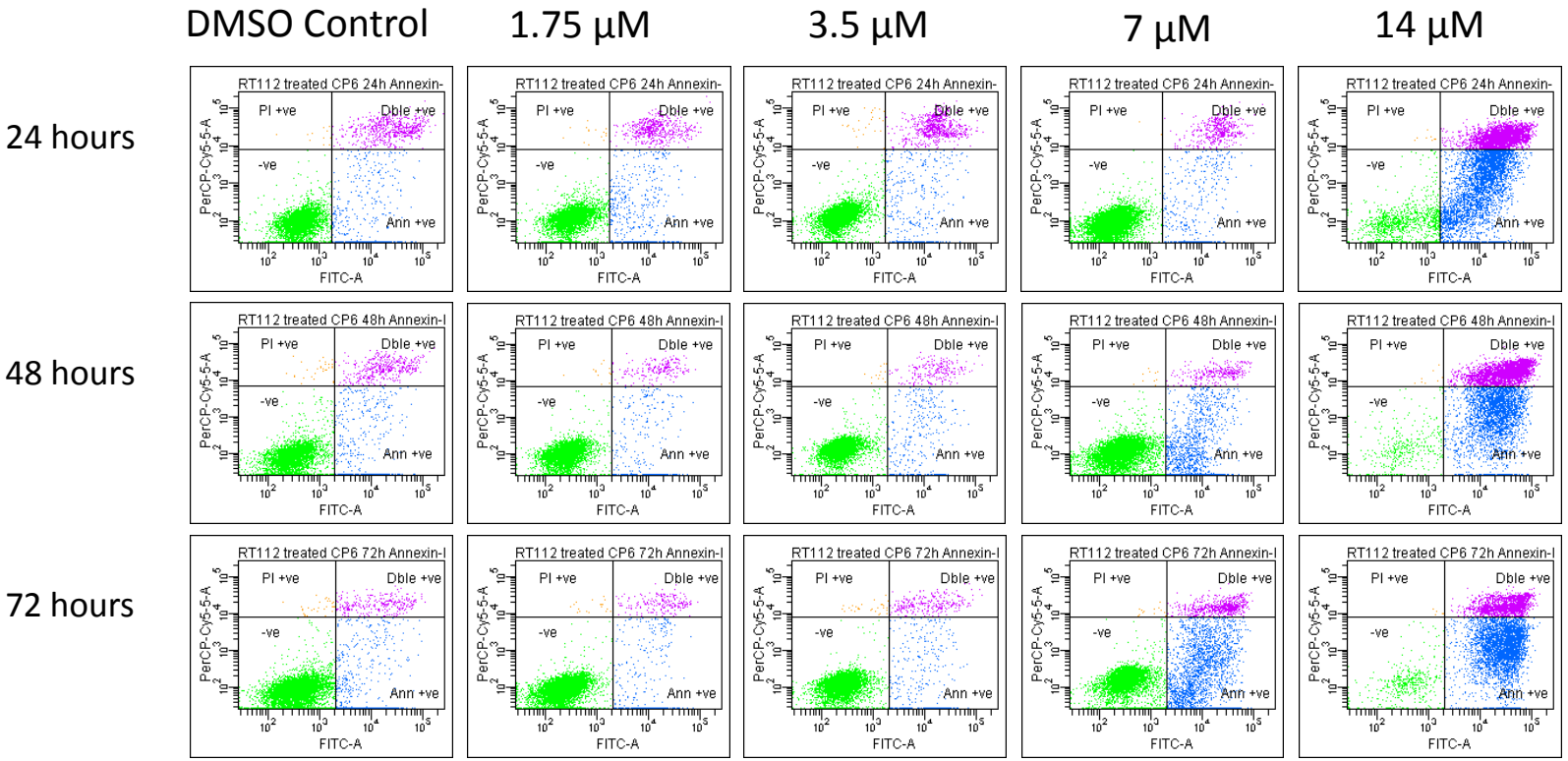

Figure 5.18 Study of induction of apoptosis in RT112 cells treated with CP654577. RT112 cells were treated with different concentrations of CP654577 (1.75 µM, 3.5 µM, 7 µM and 14 µM) or DMSO (control) for 24, 48 and 72 hours. Apoptosis was examined with flow cytometry after Annexin V-FITC and PI staining. The lower left quadrants represent the viable cells (Annexin V-negative/PI-negative). The lower right quadrants represent the cells in the early stage of apoptosis (Annexin V-positive). The upper right quadrants contain the cells in the late stage of apoptosis or necrosis (Annexin V-positive/PI-positive) and the upper left quadrant are necrotic cells (Annexin V-negative/PI-positive).

5.5 Molecular markers for apoptosis and cell cycle arrest

The results obtained from the cell cycle analysis suggested that all three TKIs induced a G_1 arrest in RT112 cells. However, when analysing the induction of apoptosis, only lapatinib and CP654577 induced apoptosis in RT112 cells, whereas no or little apoptosis could be seen after erlotinib treatment. In order to confirm these results, a Western blot was performed to analyse MYC, a marker for cell cycle and PARP cleavage, a marker for apoptosis. RT112 cells were treated with increasing doses of lapatinib or erlotinib for 24, 48 and 72 hours. CP654577 was excluded from this study due to the suspected lack of specificity of the compound.

The results showed that MYC was downregulated with increasing dose and time after lapatinib treatment (see Figure 5.19) and total cleaved PARP was detected after 48 and 72 hours of lapatinib treatment at the higher dose (25 μM), confirming the results obtained in the study of apoptosis by FACS analysis. Quantitation of the relative expression levels of MYC and cleaved PARP after lapatinib treatment is shown in Figure 5.20. RT112 cells treated with erlotinib also showed downregulation of MYC with increasing dose and time (see Figure 5.21). Partial PARP cleavage was detected after 72 hours of erlotinib treatment and appeared in a dose-dependent manner, suggesting some degree of apoptosis in these cells. Quantitation of MYC and cleaved PARP relative expression levels after erlotinib treatment is shown in Figure 5.22.

In order to investigate whether the induction of apoptosis seen in lapatinib-treated cells was caspase-mediated, a study of induction of apoptosis using Z-VAD-FMK, a caspase inhibitor, was performed. RT112 cells were treated for 24, 48 and 72 hours with lapatinib alone or lapatinib plus Z-VAD-FMK. The results showed (see Figure 5.23) that caspase inhibition using Z-VAD-FMK partially reversed the apoptosis induced by lapatinib, as it significantly reduced the number of early apoptotic cells compared to the cells treated with lapatinib only. However, cell viability was not preserved by adding the caspase inhibitor as there was an increase in late apoptotic cells compared to cells treated with lapatinib alone, suggesting other possible mechanisms were activated resulting in cell death.

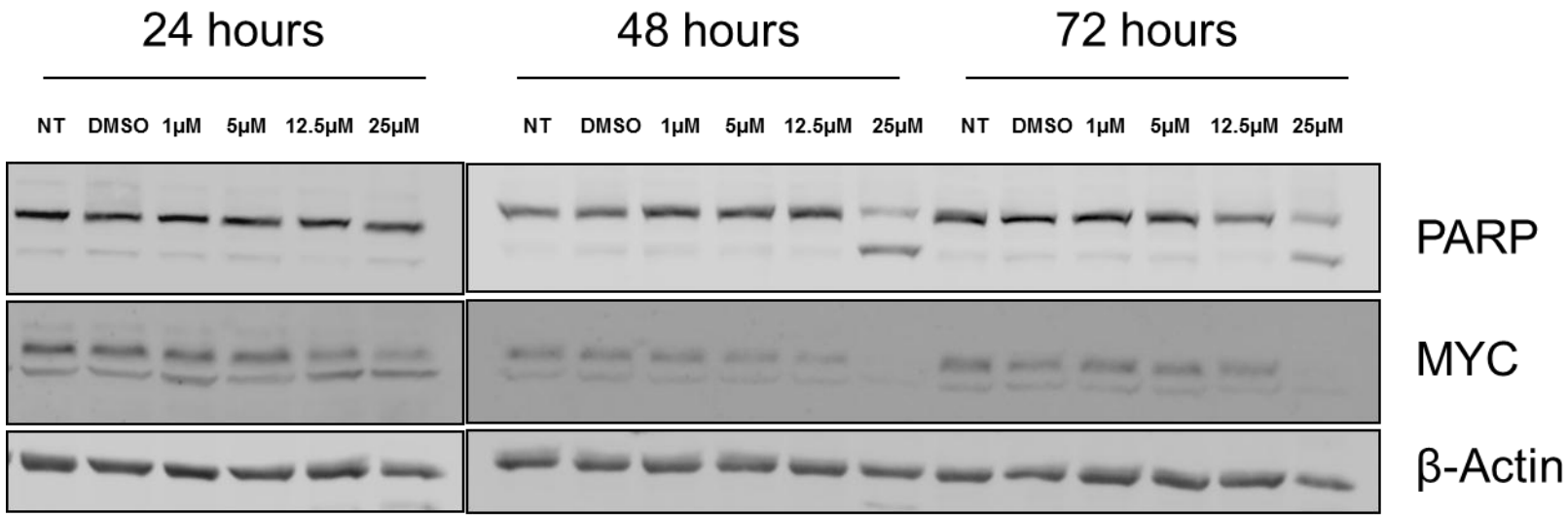

Figure 5.19 Western blot of PARP and MYC in RT112 cells treated with lapatinib. RT112 were treated with increasing concentrations of lapatinib based on previously calculated IC_{50} (1 μM, 5 μM, 12.5 μM and 25 μM), DMSO (as control) or left untreated (NT) for 24, 48 and 72 hours. Whole cell lysate was subjected to SDS-PAGE and analysed by Western blot for PARP and MYC. PARP antibody was used to detect full length PARP (116 kDa), as well as the large fragment (89 kDa) of PARP resulting from caspase cleavage. The sequence of MYC predicts a 45 kDa protein, but MYC migrates under reducing conditions as a 64 – 67 kDa band. β-actin (42 kDa) was used as a loading control. Representative blots from two independent experiments.

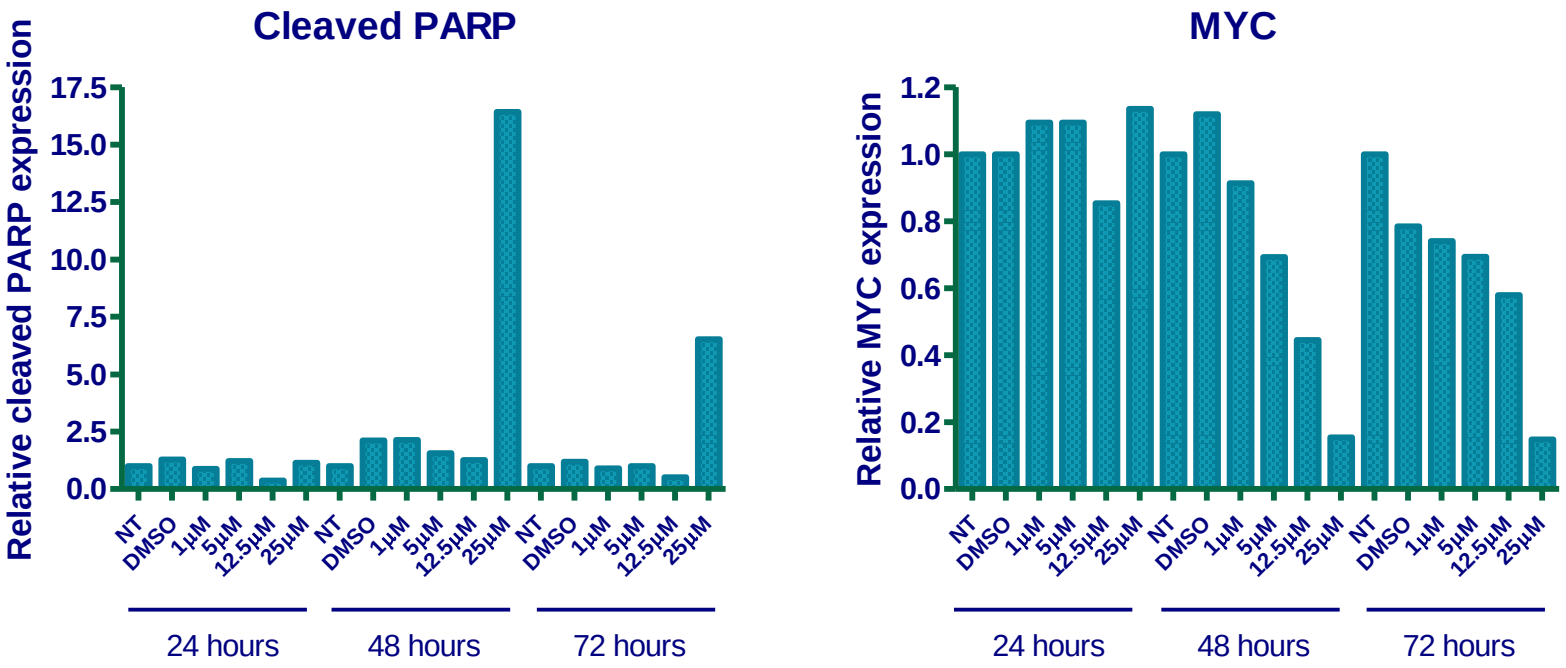

Figure 5.20 Relative expression levels of cleaved PARP and MYC in RT112 cells treated with lapatinib. Protein expression levels of cleaved PARP and MYC were normalized to the levels of *β*-actin in respective samples. Protein expression levels are presented as the fold difference compared to untreated cells (NT) for each time point.

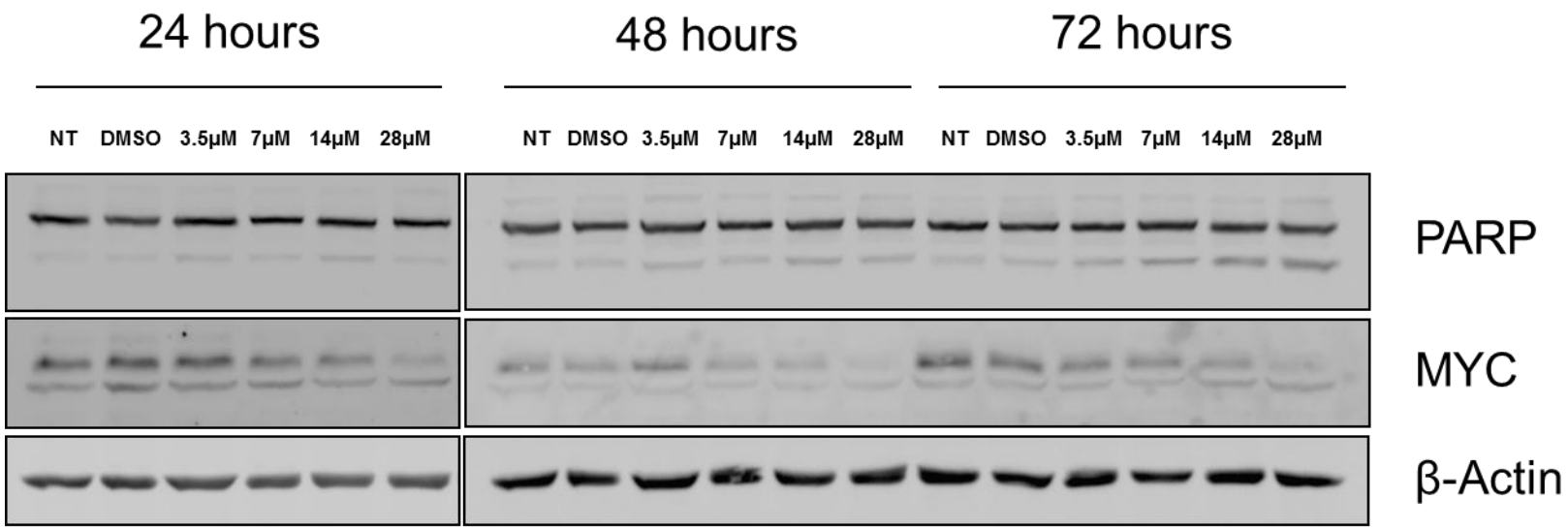

Figure 5.21 Western blot of PARP and MYC in RT112 cells treated with erlotinib. RT112 cells were treated with increasing concentrations of erlotinib based on previously calculated IC_{50} (3.5 μM, 7 μM, 14 μM and 28 μM), DMSO (as control) or left untreated (NT) for 24, 48 and 72 hours. Whole cell lysate was subjected to SDS-PAGE and analysed by Western blot for PARP (116, 89 kDa) and MYC (64, 67 kDa). *β*-actin (42 kDa) was used as a loading control. Representative blots from two independent experiments.

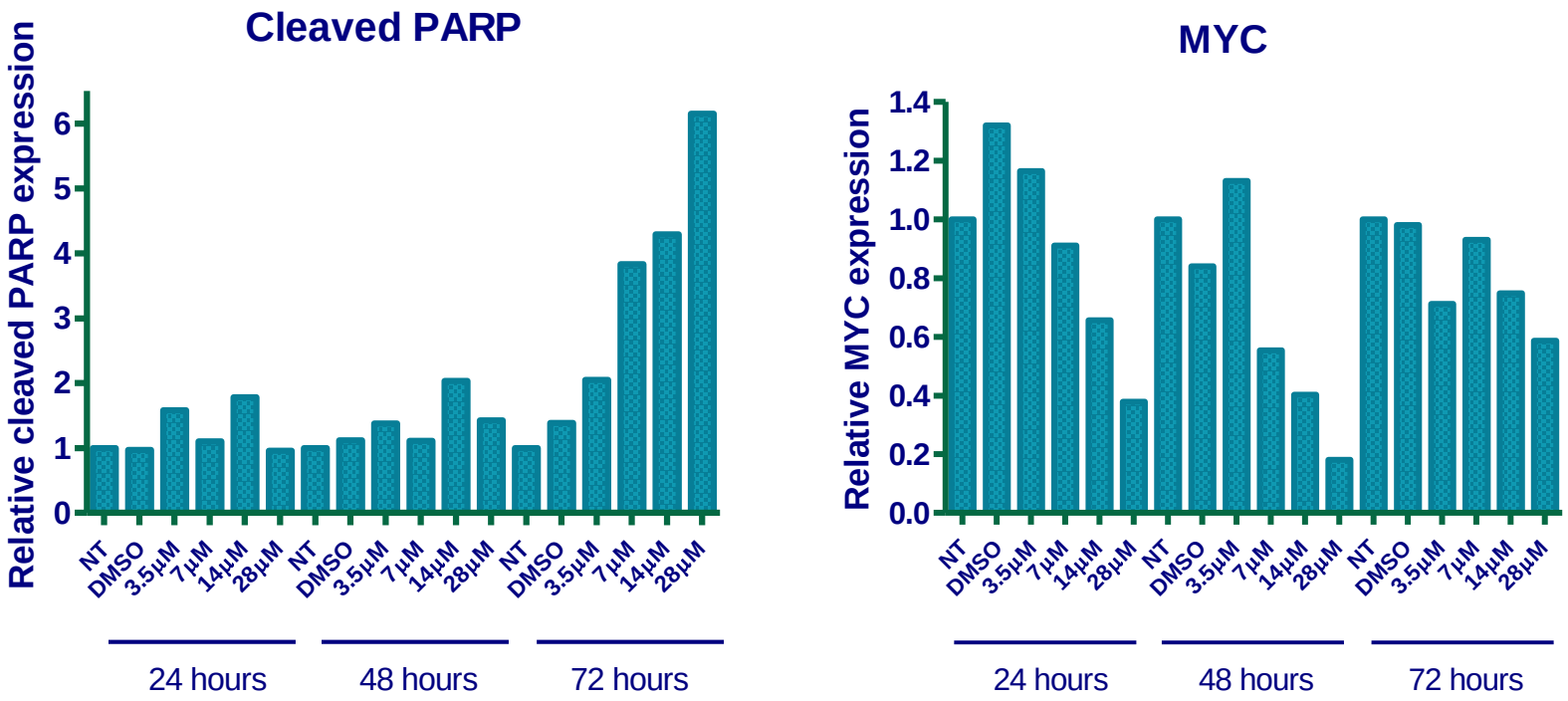

Figure 5.22 Relative expression levels of cleaved PARP and MYC in RT112 cells treated with erlotinib. Protein expression levels of cleaved PARP and MYC were normalized to the levels of *β*-actin in respective samples. Protein expression levels are presented as the fold difference compared to untreated cells (NT) for each time point.

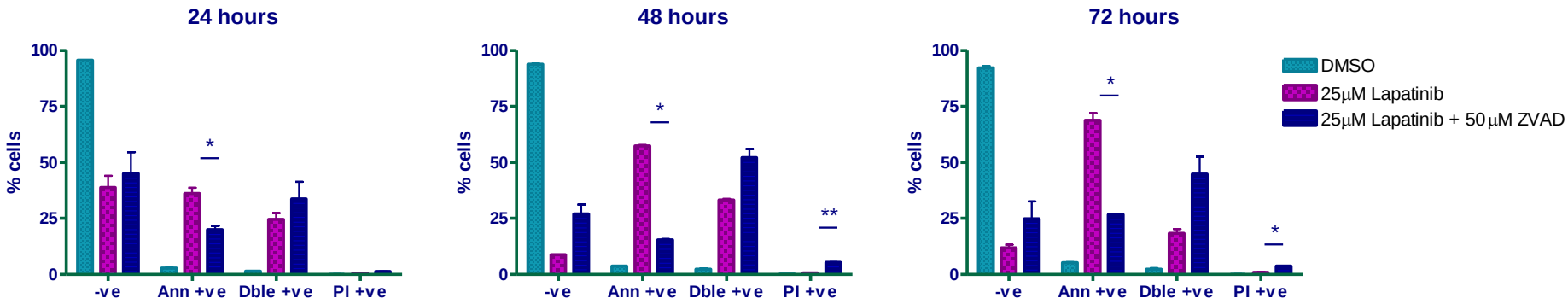

Figure 5.23 Analysis of lapatinib-induced apoptosis in the presence of a caspase inhibitor (Z-VAD-FMK) in RT112 cells. Cells were treated with lapatinib (25 µM), lapatinib (25 µM) plus Z-VAD-FMK (50 µM) or DMSO (as control) for 24, 48 and 72 hours and labeled with Annexin V-FITC and PI. Data are expressed as % Annexin V-negative and PI-negative cells (viable cells), % of Annexin V-positive and PI-negative cells (early stage of apoptosis), % of Annexin V-positive and PI-positive cells (late stage of apoptosis or necrosis) and % Annexin V-negative and PI-positive cells (necrotic cells). Error bars represent the standard deviation of duplicates in one representative experiment. Statistically significant differences between lapatinib treatment and lapatinib plus Z-VAD-FMK treatment are indicated (* $p < 0.05$, ** $p < 0.01$). Representative of two different experiments.

5.6 Correlation between TKI IC_{50} and HER family expression

After obtaining the results from the growth inhibition effect caused by the different TKIs, I investigated whether there was any correlation between the relative expression of all HER family members (EGFR, HER2, HER3 and HER4) and the response found *in vitro* to the three TKIs.

Statistical analysis (Spearman's rho correlation) was used to correlate the growth inhibitory effect (IC_{50}) of lapatinib, erlotinib and CP654577 with the relative expression levels of the HER family members. The results (shown in Table 5.2) revealed a significant direct correlation between EGFR expression and sensitivity to erlotinib ($r = -0.9429$, $p = 0.0167$). Graphs for all correlations studied are shown in Figure 5.24. The correlation graph between EGFR expression and erlotinib IC_{50} is shown in Figure 5.25. These results indicated that high levels of expression of EGFR were associated with higher sensitivity to erlotinib across the various cell lines tested. No other statistically significant relationship between IC_{50} of the TKIs used and expression levels of HER family members was found. However, the r value between EGFR expression and sensitivity to lapatinib suggested correlation ($r = -0.7143$), although it was not statistically significant ($p = 0.1361$).

	EGFR	HER2	HER3	HER4
LAPATINIB				
Spearman r	-0.7143	0.3143	-0.4286	0.2571
P value (two-tailed)	0.1361	0.5639	0.4194	0.6583
Is the correlation significant?	No	No	No	No
ERLOTINIB				
Spearman r	-0.9429	0.6	-0.6	-0.08571
P value (two-tailed)	0.0167	0.2417	0.2417	0.9194
Is the correlation significant?	**Yes**	No	No	No
CP654577				
Spearman r	0.4286	0.2571	0.7714	-0.7714
P value (two-tailed)	0.4194	0.6583	0.1028	0.1028
Is the correlation significant?	No	No	No	No

Table 5.2 Correlation studies between HER family expression and sensitivity to the TKIs lapatinib, erlotinib and CP654577 in the panel of 6 bladder cancer cell lines. Correlations were analysed by the Spearman's rho correlation for nonparametric data using GraphPad Prism4.

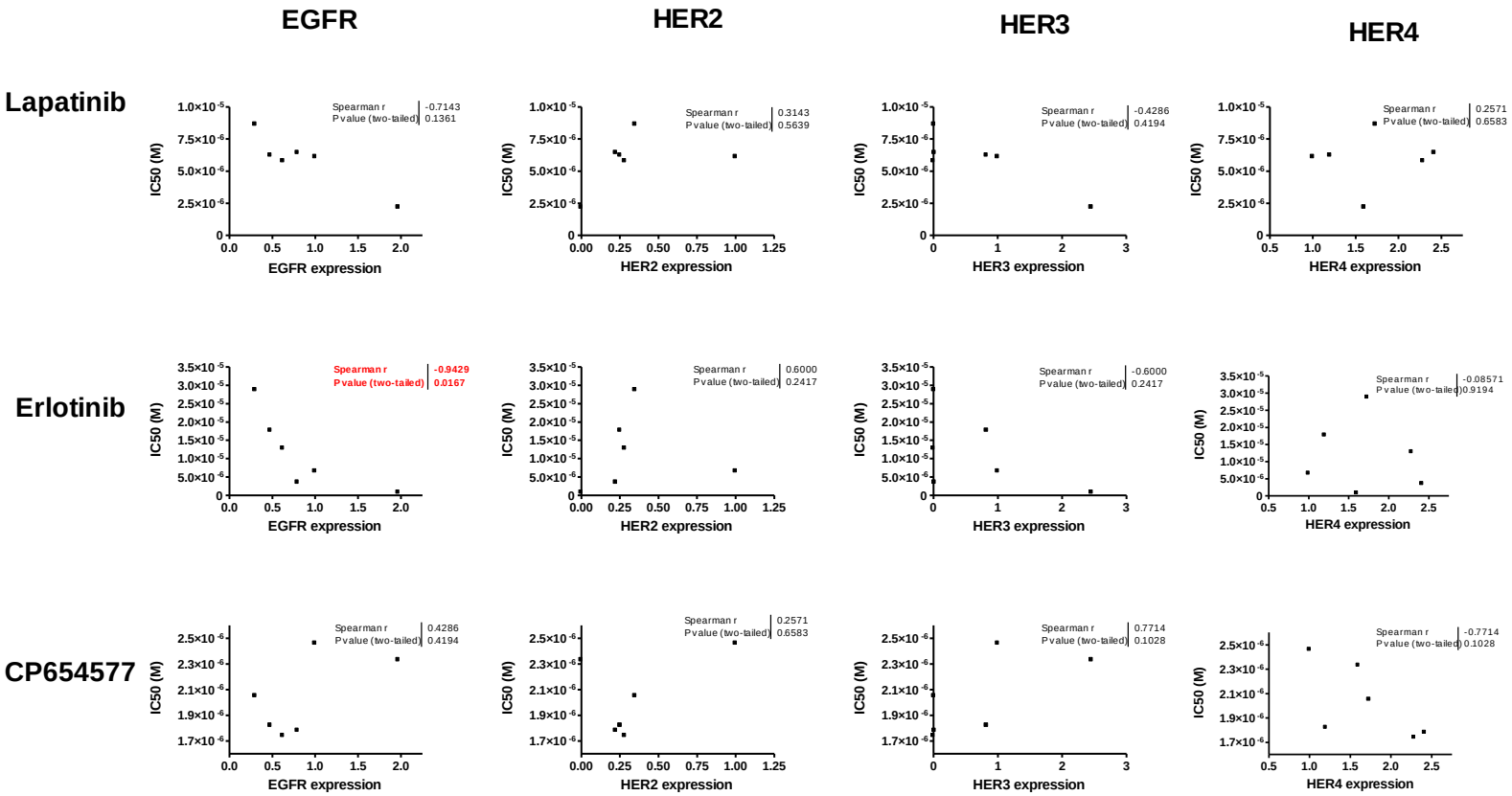

Figure 5.24 Correlation graphs between HER family expression and IC_{50} of lapatinib, erlotinib and CP654577 in the panel of 6 bladder cancer cell lines. Quantitation of immunoblots was done in order to determine the relative expression levels of EGFR, HER2, HER3 and HER4. These individual values were then plotted against the IC_{50} mean value found for each cell line. Correlations were analysed by the Spearman's rho correlation for nonparametric data (n=6). Values in red show statistical significant correlation.

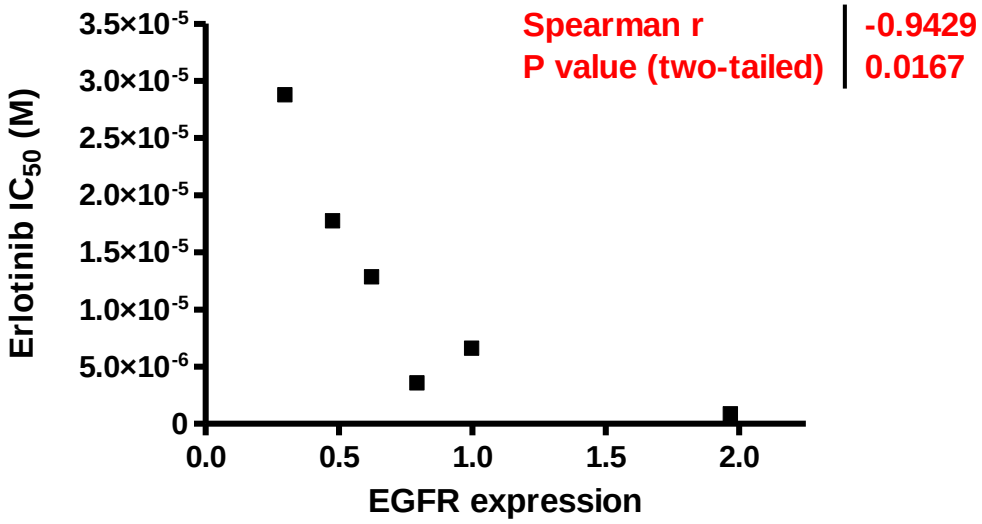

Figure 5.25 Correlation graph between EGFR expression and erlotinib sensitivity across the panel of bladder cancer cell lines. Graph showing statistical correlation (r = - 0.9429, p = 0.0167) between EGFR expression and erlotinib IC_{50} in the 6 bladder cancer cell lines. Correlation was analysed by the Spearman's rho correlation for nonparametric data (n=6).

5.7 EGFR/ HER2 knockdown in RT112 and T24 cells

5.7.1 HER2 siRNA knockdown in RT112 and T24 cells

RNA interference (RNAi) has become an excellent tool in recent years to silence gene expression. Transient knockdown of HER2 expression by small interfering RNA (siRNA) was used here in order to determine the biological role of HER2 in two different bladder cancer cell lines: RT112 and T24. RT112 was chosen as the cell line with the highest HER2 expression, followed by the T24 cell line. The first thing tested was the ability of the siRNA to silence the expression of HER2 at the protein level. The transfection was performed following the INTERFERin forward transfection protocol, where cells are plated on day 1 and transfected the following day. The reverse transfection protocol was also tried on these cells, where cells are transfected the same day they are plated; however there was a high percentage of cell death using this method, especially in RT112 cells, and the forward transfection protocol was chosen for future experiments.

Depletion of HER2 in RT112 cells was confirmed at the protein level by Western blot analysis (Figure 5.26A) which showed moderately decreased HER2 expression at 24 and 48 hours after the transfection, and significantly decreased HER2 expression at 72 hours and 6 days. Specific inhibition of HER2 expression in T24 cells was also confirmed by Western blot analysis (Figure 5.26B) which showed decreased HER2 expression at the two time points tested: 24 hours and 48 hours.

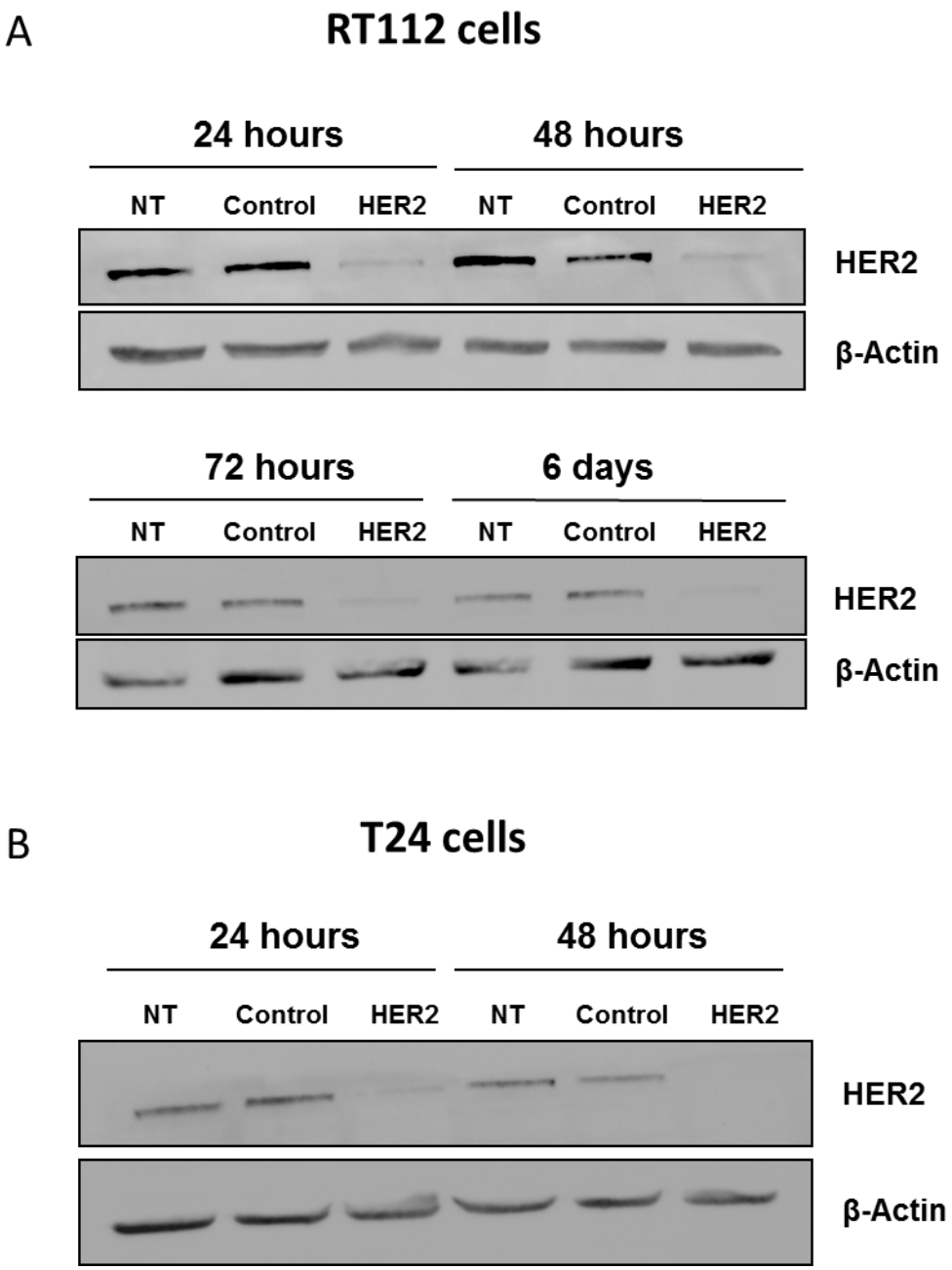

Figure 5.26 (A) HER2 expression levels after HER2 siRNA knockdown in RT112 cells and (B) T24 cells. Cells were transfected with control siRNA, HER2 siRNA or left untreated (NT) and incubated for 24, 48, 72 hours and/or 6 days. Whole cell lysate was subjected to SDS-PAGE and analysed by Western blot for HER2 (185 kDa). *β*-actin (42 kDa) was used as a loading control. Representative of four different experiments.

5.7.2 EGFR siRNA knockdown in RT112 and T24 cells

EGFR knockdown was also performed in RT112 and T24 cell lines. The knockdown was achieved using siRNA against EGFR and using the INTERFERin forward transfection protocol as previously. Depletion of EGFR was confirmed at the protein level by Western blot analysis (Figure 5.27) which showed significantly decreased EGFR expression at 24 and 48 hours after the transfection for both cell lines. When looking at downstream effects of EGFR knockdown, no significant changes could be detected in phospho-ERK1/2 expression levels. However, an increase in the expression levels of phospho-Akt (Ser473) could be seen in both EGFR siRNA and control siRNA transfected cells, suggesting that the transfection was causing this effect rather than the EGFR knockdown. Two different approaches were taken in order to reduce this cellular toxicity; reduce the incubation time of INTERFERin/siRNA complexes with the cells by changing the medium 5 hours after the transfection or decrease the volume of INTERFERin used in the transfection assay. However, none of these two approaches resolved the problem (data not shown).

5.7.3 Cell cycle analysis in RT112 and T24 cells after EGFR/HER2 knockdown

To characterize the effect of the EGFR and HER2 knockdown in RT112 and T24 cells, a study on cell cycle distribution using PI staining was performed. RT112 and T24 cells were transfected with EGFR siRNA, HER2 siRNA or non-targeting siRNA (control) using the INTERFERin forward transfection and incubated for 24, 48 and 72 hours. The results for RT112 cells (Figure 5.28) and T24 cells (Figure 5.29) did not show any significant change in the cell cycle distribution compared to non-treated cells. However, an increased sub G_1 population in T24 cells was seen after 72 hours of HER2 siRNA knockdown (Figure 5.29B), suggesting a possible increase in cell death in these cells.

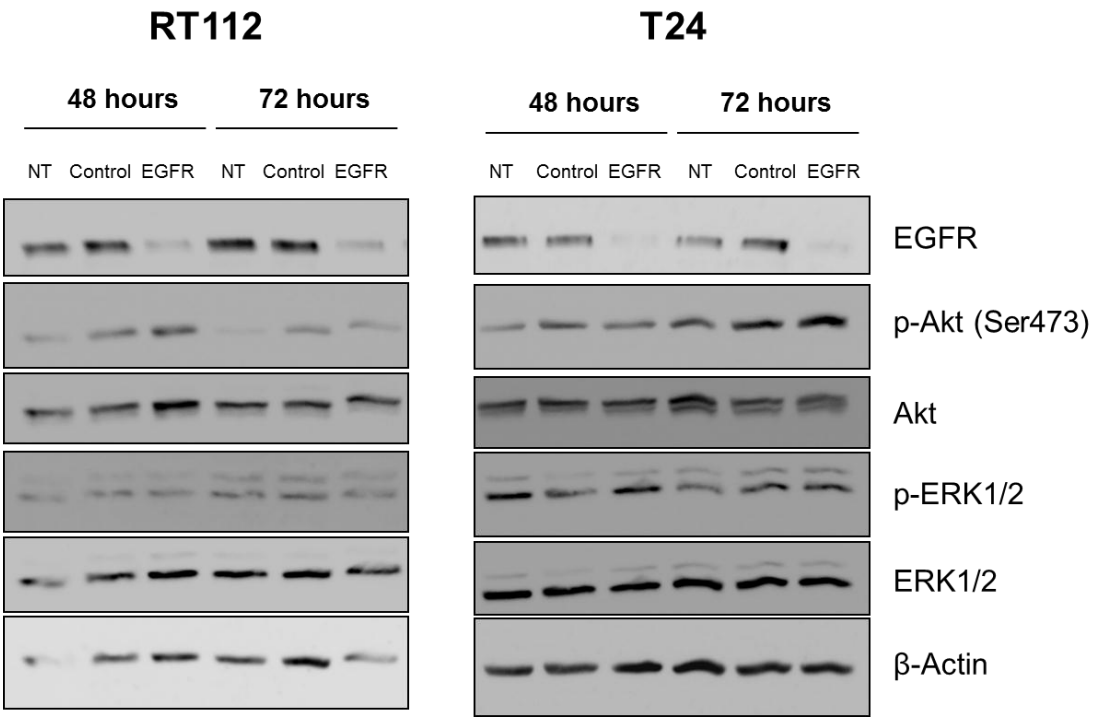

Figure 5.27 EGFR expression levels and downstream effects after EGFR siRNA knockdown in RT112 and T24 cells. Cells were transfected with control siRNA, EGFR siRNA or left untreated (NT) and incubated for 48 and 72 hours. Whole cell lysate was subjected to SDS-PAGE and analysed by Western blot for EGFR (175 kDa), phospho-ERK1/2 (Thr202/Tyr204; 42/44 kDa), phospho-Akt (Ser473; 60 kDa), total ERK1/2 and total Akt. *β*-actin (42 kDa) was used as a loading control. Representative of four different experiments.

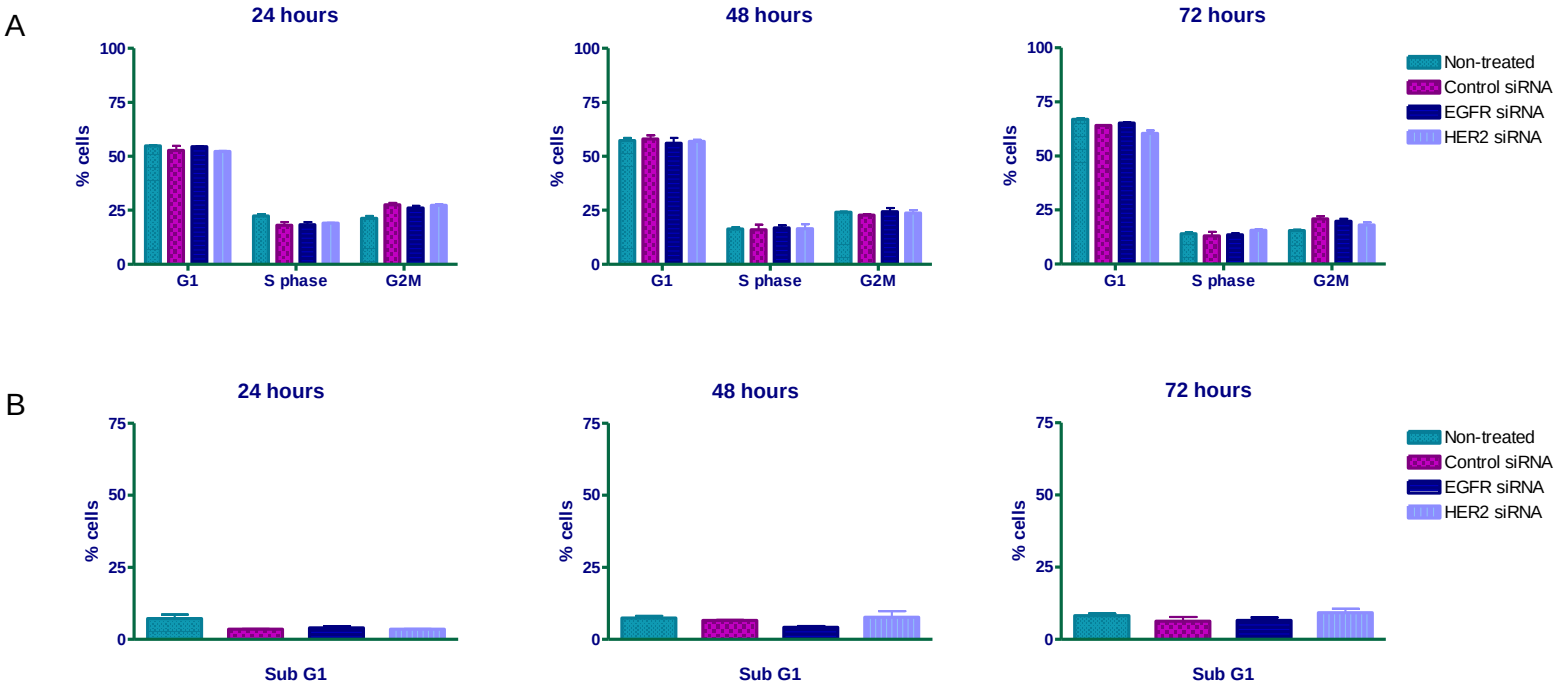

Figure 5.28 Analysis of the cell cycle distribution and cell death after EGFR and HER2 siRNA knockdown in RT112 cells. (A) RT112 cells were transfected with EGFR siRNA, HER2 siRNA or non-targeting siRNA (as control) using the INTERFERin forward transfection protocol. Cells were incubated over 24, 48 and 72 hours and cell cycle was analysed by PI staining. (B) Percentage of events with sub G_1 DNA content in order to quantify cell death. Values represent the average of one experiment made in duplicate, and the error bars represent standard deviation.

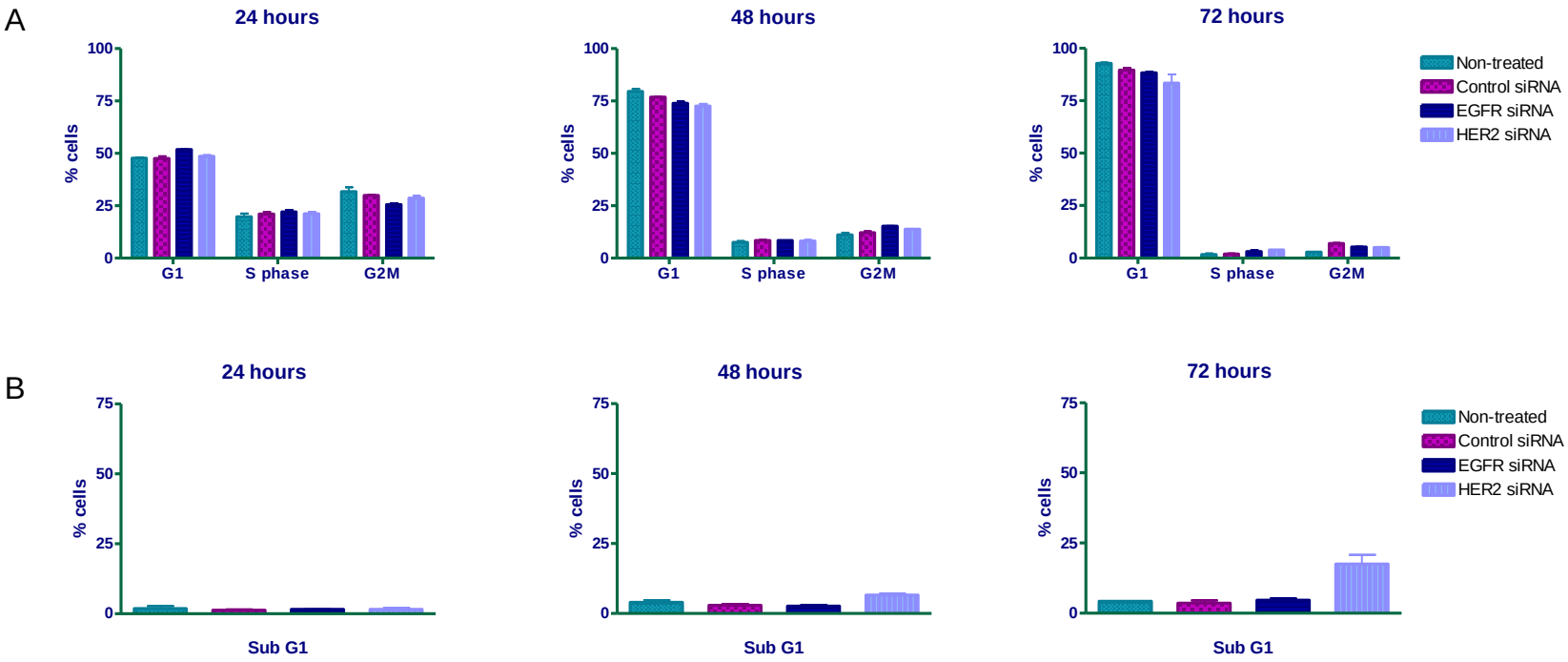

Figure 5.29 Analysis of the cell cycle distribution and cell death after EGFR and HER2 siRNA knockdown in T24 cells. (A) T24 cells were transfected with EGFR siRNA, HER2 siRNA or non-targeting siRNA (as control) using the INTERFERin forward transfection protocol. Cells were incubated over 24, 48 and 72 hours and cell cycle was analysed by PI staining. (B) Percentage of events with sub G_1 DNA content in order to quantify cell death. Values represent the average of one experiment made in duplicate, and the error bars represent standard deviation.

5.8 Summary of Chapter 5

In this chapter, the effects of inhibiting EGFR and HER2 in the panel of bladder cancer cell lines were analysed. Two approaches were used in order to do this: use of tyrosine kinase inhibitors (TKIs) to target the receptors, and use of small interfering RNA (siRNA) to silence their expression. For the first approach, the three TKIs used were: lapatinib (dual EGFR/HER2 TKI), erlotinib (EGFR TKI) and CP654577 (HER2 TKI). All three TKIs had an inhibitory growth effect in the bladder cancer cell lines.

In order to clarify the underlying mechanism of action of the TKIs, changes on protein expression of growth and survival signalling pathways were evaluated in T24 cells. Downregulation of phospho-ERK1/2 was observed after all three TKI treatments despite EGF or NRG-1 stimulation, except for CP654577, which did not inhibit activation of phospho-ERK1/2 after EGF stimulation. Lapatinib and CP654577 had no effect on expression levels of phospho-Akt (Ser473). However, erlotinib significantly increased phosphorylation of Akt at this site, a finding that has not been published before. Since Akt is known to play an important role in cell survival, this could explain why T24 were the most resistant cells compared to the other bladder cancer cell lines.

Since a decrease in cell viability could be due to an increase in cell cycle arrest, increase in apoptosis, or a combination of both, the RT112 cell line was chosen to further characterize the antiproliferative effect of the TKIs. The results showed how all three TKIs induced cell cycle arrest at G_1 phase, which is a known mechanism of action of these TKIs. This was confirmed by downregulation of MYC by Western blot. Downregulation of phospho-ERK1/2 seen in lapatinib and erlotinib treated T24 cells could possibly explain the cell cycle arrest at G_1 phase seen in RT112 cells analysed by FACS. CP654577 also increased G_1 population in RT112 cells, but in T24 cells it did not downregulate phosphorylation of ERK1/2 after EGF stimulation, so it should be further investigated whether downregulation of phospho-ERK1/2 occurs in RT112 cells after CP654577 treatment to explain G_1 arrest seen in these cells.

Apoptosis studies showed increase in apoptotic cells after lapatinib and CP654577 treatment. Apoptosis in lapatinib-treated cells was confirmed by an increase in PARP

cleavage and it was found to be caspase dependent. No or little apoptosis was seen after erlotinib treatment, suggesting that EGFR inhibition alone was not sufficient to induce apoptosis in these cells. On the other hand, if the increase in phospho-Akt (Ser473) observed in T24 cells treated with erlotinib was not cell-dependent and occurred also in RT112 cells, it could also explain the apoptosis resistance seen in erlotinib-treated RT112 cells compared to lapatinib and CP654577 treatment.

The growth inhibition effect of erlotinib was found to be significantly correlated to the levels of EGFR expression of the cell lines, suggesting that EGFR expression could be a potential predictor for TKI sensitivity in bladder cancer. A summary of all the finding of the mechanism of action of the drugs is shown in Table 5.3. CP654577 IC_{50} values among the bladder cancer cell lines were very constant which raised concerns about its specificity. For this reason, the compound was not included in subsequent experiments.

The second approach to understand the role of EGFR and HER2 in bladder cancer cell lines was silencing their expression in the cells. EGFR and HER2 knockdown by siRNA decreased effectively the protein expression levels of both receptors in RT112 and T24 cell lines, although it did not affect cell cycle distribution on these cells. A possible increase in cell death was observed in T24 cells after HER2 siRNA knockdown. However, the analysis of downstream signalling pathways showed an increase in phospho-Akt (Ser473) in both EGFR siRNA and control siRNA treated cells, suggesting that the transfection was causing this effect rather than the EGFR knockdown. For this reason, it was decided not to continue using this method.

Drug	Specificity	Cell cycle effect	Apoptosis	Correlation with HER family expression
Lapatinib	EGFR/HER2	G_1 arrest	Apoptosis	-
Erlotinib	EGFR	G_1 arrest	None or little apoptosis	EGFR
CP654577	HER2	G_1 arrest	Apoptosis	-

Table 5.3 Summary of effects of TKIs in bladder cancer cell lines.

5.9 Discussion

5.9.1 Effect of EGFR and/or HER2 tyrosine kinase inhibitors in bladder cancer cell lines

The MTS assay measures metabolic activity of the cells, and was used as an indirect measure to estimate number of viable cells after TKI treatment. All three TKIs tested inhibited cell proliferation in all bladder cancer cell lines in a concentration-dependent manner which was in accordance with other studies for erlotinib (Jacobs *et al.* 2007) and lapatinib (McHugh *et al.* 2009). The present study is, however, the first to study EGFR and/or HER2 inhibition in a panel of bladder cancer cell lines using different TKIs directed specifically to these receptors, in order to study patterns of sensitivity or resistance in relation to the receptors.

The IC_{50} values found for erlotinib varied among the individual cell lines tested (0.8 to 28.7 μM). This is in agreement with the erlotinib IC_{50} values found by Jacobs *et al.* in 5 bladder cancer cell lines, which ranged from 1 to 40 μM (Jacobs *et al.* 2007). Lapatinib seemed also cell line-dependent, with IC_{50} values from 2.2 to 8.6 μM. Havaleshko *et al.* studied lapatinib IC_{50} in 39 bladder cancer cell lines, which ranged from values below 0.5 μM to more than 20 mM (Havaleshko *et al.* 2009). The authors defined sensitive cell lines by $IC_{50} < 8$ μM. By these criteria, all cell lines in this study were sensitive to lapatinib except T24 cell line, which IC_{50} was 8.6 μM. In contrast, CP654577 IC_{50} values were very similar in all cell lines (between 1.7 to 2.5 μM). Taken together, these results suggested that EGFR and/or HER2 targeted therapy could be of potential use in bladder cancer treatment.

SKBR3 cells were used as a positive control for lapatinib, as it is known to be a sensitive cell line. However, after analysing the results, there was a concern about the behaviour of SKBR3 cells. The lapatinib IC_{50} found in this study (10.6 μM) contrasts with the value found by Rusnak *et al*. (0.03 μM). In the same study, some bladder cancer cell lines were also tested for lapatinib; they found that lapatinib IC_{50} for HT1376 and T24 was 3.3 μM and 8.2 μM, respectively (Rusnak *et al.* 2007), which was similar to the IC_{50} values obtained in my work; 2.2 μM and 8.6 μM. In another study, lapatinib IC_{50} for SKBR3 was found to be 0.05 μM (Zhang *et al.* 2008). This was not

limited to lapatinib since CP654577 IC_{50} for SKBR3 was 2.6 μM, whereas the IC_{50} found by Barbacci *et al*. was 55 nM (Barbacci *et al.* 2003). This suggested a problem with the SKBR3 cell line, whose characteristics may have changed probably due to long passage number, becoming more resistant to the TKIs. Therefore, this would need to be repeated.

5.9.2 Effect of EGFR and/or HER2 kinase inhibition after stimulation with growth factors in T24 cells

Since all three TKIs had an antiproliferative effect on bladder cancer cell lines, it was important to understand how effective these inhibitors were in blocking signalling pathways downstream of EGFR and HER2 after the stimulation of the receptors with growth factors. Changes in phosphorylation levels of ERK1/2 and Akt were studied since MAPK and PI3K/Akt pathways are considered the main effectors of oncogenic HER signalling (Sergina and Moasser 2007). In order to keep cell death to a minimum, T24 cell line was chosen to study this as it was one of the most resistant cell lines against the TKIs.

The results from this experiment showed how both EGF and NRG-1 stimulation increased phosphorylation levels of ERK1/2. When the cells had been pre-treated with the TKIs, lapatinib and erlotinib inhibited activation of phospho-ERK1/2 after EGF and NRG-1 stimulation. This however contrasts with other studies where lapatinib did not inhibit ERK1/2 phosphorylation after EGF or NRG-1stimulation in RT112 or J82 bladder cancer cell lines (McHugh *et al.* 2009). On the other hand, CP654577 could not inhibit activation of phospho-ERK1/2 after EGF stimulation, which is in accordance with studies by Barbacci *et al.* in SKBR3 cells (Barbacci *et al.* 2003). This is consistent with CP654577 specificity for HER2 and could imply that EGFR-HER2 dimers were not relevant in this particular cell line or that EGFR phosphorylation was not dependent on the kinase activity of HER2.

Stimulation of T24 cells with EGF and NRG-1 increased slightly the phosphorylation of Akt (Ser473). Cells pre-treated with lapatinib and CP654577 had no effect on expression levels of phospho-Akt (Ser473). However, erlotinib significantly increased phosphorylation of Akt at this site. Jacobs *et al*. found that erlotinib treatment did not downregulate phospho-Akt in bladder cancer cell lines resistant to this TKI after EGF

stimulation (Jacobs *et al.* 2007). These cells lines had loss of PTEN, so they attributed the uncoupling between EGFR and Akt signalling as a determinant in the sensitivity of bladder cancer cells to erlotinib.

This has also been observed in other cancer types; PTEN loss and subsequent activation of phospho-Akt has been shown to be involved in erlotinib resistance in epidermoid cancer cells (Yamasaki *et al.* 2007), and also in EGFR-mutant non-small cell lung cancer (NSCLC) cell lines (Sos *et al.* 2009). PTEN loss has not only been observed in cell lines as it has also been shown to be involved in intrinsic resistance to EGFR inhibitors in glioblastoma patients (Mellinghoff *et al.* 2005).

Interestingly, in this study, the T24 cell line was the cell line more resistant to erlotinib treatment among the other bladder cancer cell lines (IC_{50} found was 28.7 μM) and it is known to have a *PTEN* mutation (Wang *et al.* 2000). However, in this case, erlotinib was not only failing to downregulate phospho-Akt expression after EGF and NRG-1 stimulation, as there was an increase of expression levels of phospho-Akt, suggesting erlotinib was activating other pathways. Since Akt is known to play an important role in cell survival, this increase could make these cells resistant to apoptosis to this particular drug. Indeed, it would be necessary to elucidate whether this effect is drug-specific, since these findings contrast with another study where gefitinib (another EGFR TKI) inhibited phosphorylation of ERK1/2 and Akt (Ser473) in T24 cells after EGF stimulation (Dominguez-Escrig *et al.* 2004), although the pre-treatment time with the TKI was 10 minutes, whereas in this study was 24 hours.

5.9.3 Effect of EGFR and/or HER2 kinase inhibition on cell cycle on bladder cancer cell lines

To evaluate further the effect of EGFR and/or HER2 kinase inhibition on bladder cancer cell lines, cell cycle analysis was performed in RT112 cells after lapatinib, erlotinib and CP654577 treatment. The doses chosen for this were multiples from the IC_{50} values, so that results could be comparable between treatments. The results showed a G_1 arrest after 24, 48 and 72 hours of treatment with all three TKIs, with a subsequent decrease in the S phase proportion. These results were confirmed by MYC reduction in RT112 cells after erlotinib and lapatinib treatment, which was found to be enhanced over time and dose.

Lapatinib induction of G_1 arrest in RT112 cells is in agreement with another study, which reported a 20% increase in the G_1 phase after 48 hours of treatment in the same cell line (McHugh *et al.* 2009). EGFR inhibition using gefitinib has also been found to increase G_1 phase in 253J B-V, a sensitive bladder cancer cell line (Kassouf *et al.* 2005). Barbacci *et al*. also showed that CP654577 treatment of SKBR3 cells inhibited cell cycle progression at G_1. CP654577 treatment led to decreased phosphorylation of HER2 and HER3 in these cells, resulting in decreased levels of activated ERK1/2 and Akt. This led to a decreased cyclin D and increased $p27^{kip1}$, inhibiting phosphorylation of RB, which is required to enter into the S phase (Barbacci *et al.* 2003).

5.9.4 Effect of EGFR and/or HER2 kinase inhibition on cell death and apoptosis on bladder cancer cell lines

As an indirect measure of cell death, events occurring with sub G_1 DNA content were analysed after each TKI treatment during the cell cycle studies. Lapatinib and CP654577 showed an increase on these events, especially after 72 hours of treatment. This however contrasts with the findings by McHugh *et al.*, where they showed little accumulation of RT112 cells at the sub G_1 phase after lapatinib treatment. On the other hand, erlotinib showed little increase on these events. This is in agreement with studies by Kassouf *et al.* who also found that EGFR inhibition with gefitinib did not increase the sub G_1 population in 253J B-V cells (Kassouf *et al.* 2005).

To explore whether cells arrested in G_1 then progressed to apoptosis, cells were stained with Annexin V and PI and were analysed by flow cytometry. This study showed that RT112 cells arrested in G_1 phase by lapatinib and CP654577 treatment then progressed to apoptosis. Apoptosis in lapatinib-treated cells was confirmed by an increase in PARP cleavage. Since apoptosis can be caspase-dependent and caspase–independent (Leist and Jaattela 2001), Z-VAD-FMK was used in order to confirm that the apoptosis observed was caspase-dependent. This caspase inhibitor partially reversed the apoptosis induced by lapatinib, as it significantly reduced the number of early apoptotic cells compared to the cells treated with lapatinib only. However, cell viability was not preserved by adding Z-VAD-FMK as there was an increase in late apoptotic cells compared to cells treated with lapatinib alone, suggesting other possible mechanisms were activated resulting in cell death.

RT112 cells treated with erlotinib showed no or little apoptosis, confirming the results observed when sub G_1 DNA content was analysed before, and suggesting that EGFR inhibition alone was not sufficient to induce apoptosis in these cells.

Induction of apoptosis in HER2-dependent tumour cells by lapatinib has been associated with the inhibition of phospho-Akt (Xia *et al.* 2002). Similarly, CP654577 induction of apoptosis in SKBR3 and BT474 breast cancer cells, which express high levels of HER2, has been attributed to the inhibition of Akt, but no apoptosis was observed in MCF7 cells, which express low levels of HER2 (Barbacci *et al.* 2003). Activation of the Akt pathway, which plays an important role in regulating cell survival, appears to be more dependent on HER2 signalling than EGFR (Tari and Lopez-Berestein 2000). Therefore, the different effect of erlotinib compared to lapatinib and CP654577 treatment in apoptosis could be explained by the fact that erlotinib, since it only targets EGFR, fails to downregulate Akt activated by HER2.

On the other hand, the different effects between erlotinib and lapatinib in inducing apoptosis in RT112 cells could also be explained by the different ways of binding of these TKIs to EGFR. Lapatinib is known to bind to an inactive-like conformation of EGFR. The complex has a slow dissociation rate, which in tumour cells reflects as a prolonged downregulation of receptor phosphorylation (15% of control levels 96 hours after TKI washout). On the contrary, erlotinib binds to an active-like conformation of EGFR and it has a higher dissociation rate compared to lapatinib; in tumour cells, receptor phosphorylation is recovered to control levels just 24 hours after TKI washout. Therefore, lapatinib is more potent compared to erlotinib in supressing EGFR activity (Wood *et al.* 2004). Consequently, erlotinib may actually inhibit phosphorylation of Akt, but due to the quick dissociation of the complex TKI-EGFR and quick recovery of phospho-EGFR, Akt pathway may be recovered quicker than with lapatinib.

Another possibility, however, is that erlotinib may actually upregulate Akt. If the increase in phospho-Akt (Ser473) observed in T24 cells treated with erlotinib was not cell-dependent and occurred also in RT112 cells, it could explain the apoptosis resistance seen in erlotinib-treated RT112 cells compared to lapatinib and CP654577 treatment. Therefore, expression levels of phospho-Akt (Ser473) should be analysed after erlotinib and lapatinib treatment at different time points to investigate this further.

5.9.5 Test of potential factors for sensitivity to EGFR and/or HER2 TKIs

Growth of bladder cancer cells with high levels of EGFR and/or HER2 expression may be dependent on the growth stimulatory signals via these receptors. If this was the case, inhibition of their signalling by treatment with EGFR and/or HER2 TKIs might be expected to significantly reduce cell growth. In the present study, all bladder cancer cell lines were sensitive to all three TKIs tested (erlotinib, lapatinib and CP654577), suggesting that bladder cancer cell lines are indeed dependent on growth stimulatory signals via these receptors. Although CP654577 inhibited cell growth in a similar way for all the cell lines, the antiproliferative effect of lapatinib and erlotinib differed widely in the panel of bladder cancer cell lines. This different response of sensitivity to EGFR and/or HER2 TKIs made these cells a useful model system to study molecular markers of response to these TKIs.

Statistical analysis was used to study whether the sensitivity of bladder cancer cells to EGFR and/or HER2 TKIs could be predictable by the expression levels of HER family members. The Spearman correlation test was used to compare the growth-inhibitory effect (IC_{50}) of the three TKIs used and the relative expression levels of HER proteins. The results revealed a direct and linear correlation between EGFR expression and sensitivity to erlotinib ($r = -0.9429$, $p = 0.0167$). Some correlation between lapatinib and EGFR expression was also found, although it was not statistically significant ($r = -0.7143$, $p = 0.1361$).

The correlation found between EGFR expression and sensitivity to erlotinib contrasts with other studies (see Table 5.4). Jacobs *et al*. found no correlation between EGFR expression or activation and erlotinib sensitivity in a panel of bladder cancer cell lines (Jacobs *et al.* 2007). No correlation was found either between EGFR expression levels and gefitinib sensitivity, which also targets EGFR, in a panel of 10 bladder cancer cell lines (Kassouf *et al.* 2005). However, in another study, bladder cancer cell lines that were gefitinib sensitive expressed higher surface EGFR levels than the resistant cell lines, but the correlation was not perfect (Shrader *et al.* 2007). No correlation between EGFR expression, EGFR activation or ligand secretion and cetuximab sensitivity (monoclonal antibody that targets EGFR) was found in a panel of eleven bladder cancer cell lines either (Black *et al.* 2008).

Reference	*This study*	*(Jacobs et al. 2007)*	*(Kassouf et al. 2005)*	*(Shrader et al. 2007)*	*(Black et al. 2008)*
Bladder cancer cell lines	HT1376 T24 RT112 RT112CP UM-UC3 UM-UC6	J82 MGHU1 5637 EJ BC16.1	KU7 253J P 253J B-V RT4 UM-UC1 UM-UC3 UM-UC5 UM-UC6 UM-UC13 UM-UC14	KU7 253J B-V RT4 UM-UC1 UM-UC2 UM-UC3 UM-UC4 UM-UC5 UM-UC7 UM-UC9 UM-UC10 UM-UC11 UM-UC12 UM-UC13 UM-UC14 UM-UC15 UM-UC17	KU7 253J P 253J B-V UM-UC3 UM-UC5 UM-UC6 UM-UC9 UM-UC10 UM-UC12 UM-UC13 UM-UC14
EGFR inhibitor	Erlotinib	Erlotinib	Gefitinib	Gefitinib	Cetuximab
Correlation with EGFR expression	Significant correlation	No correlation found	No correlation found	Some correlation found	No correlation found

Table 5.4 Correlation studies of EGFR expression and EGFR inhibitors sensitivity in bladder cancer cell lines.

In other cancers, effect of EGFR inhibitors was also found to be not well correlated with the levels of EGFR expression nor levels of activated EGFR in a panel of lung cancer cell lines (Suzuki *et al.* 2003). However, mutations in the tyrosine kinase domain of EGFR were found later to be correlated with the clinical response of gefitinib in NSCLC patients (Lynch *et al.* 2004; Paez *et al.* 2004). Such mutations are not found in bladder cancer, but these findings highlighted the importance to find biomarkers of response in order to select the subsets of patients who can benefit for these treatments.

In respect to lapatinib, suggested correlation between lapatinib sensitivity and EGFR expression was also found in the six bladder cancer cell lines, although it was not statistically significant ($r = -0.7143$, $p = 0.1361$). This also contrasts with other studies on bladder cancer cell lines (see Table 5.5). Havaleshko *et al*. did not find any significant correlation between EGFR or HER2 expression and lapatinib IC_{50} in 39 bladder cancer cell lines (Havaleshko *et al.* 2009). Another study also found that the effect of lapatinib on the cell growth of two bladder cancer cell lines was independent of EGFR/HER2 expression levels (McHugh *et al.* 2009).

Lack of correlation between lapatinib and EGFR expression has also been found in other cancer cell lines, such as in upper gastrointestinal cancer cell lines (Wainberg *et al.* 2010) or in breast cancer cell lines, where sensitivity to lapatinib was found to be directly related to expression of HER2, but not EGFR expression (Konecny *et al.* 2006). However, in endometrial cancer cells, lapatinib activity correlated with HER2 and EGFR expression (Konecny *et al.* 2008), suggesting that EGFR may play a different role in these malignancies, and therefore, studies to investigate whether EGFR expression can be a predictive markers to TKI treatment need to be performed for each cancer cell type.

Due to limited publications with CP654577, no correlation studies have been done with CP654577 sensitivity and HER2 expression. In this study, no statistical correlation could be found between CP654577 sensitivity and expression of HER2 (or any other HER family member). This finding was not surprising since CP654577 IC_{50} values among the bladder cancer cell lines were very similar (range from 1.7 to 2.5 μM), despite having different levels of HER2 expression.

Reference	*This study*	*(Havaleshko et al. 2009)*		*(McHugh et al. 2009)*
Bladder cancer cell lines	HT1376 T24 RT112 RT112CP UM-UC3 UM-UC6	253J LAVAL UM-UC6 1A6 MGHU4 VMCUB2 5637 Hs172.T MGHU3 UM-UC3 SL4 SW1710 T24T T24 KK47 UM-UC3E VMCUB3 TCCSUP SCABER SW780 UM-UC9	HT1376 CUBIII BC16.1 HT1197 253JP 253JBV PSI UM-UC14 575A Hs228.T FL3 J82 JON KU7 RT4 UM-UC1 UM-UC13D UM-UC2 VMCUB1	J82 RT112
Correlation with EGFR/HER2 expression	Some correlation with EGFR expression	No correlation found		No correlation found

Table 5.5 Correlation studies of EGFR/HER2 expression and lapatinib sensitivity in bladder cancer cell lines.

This raised concerns about the compound specificity, and for this reason, CP654577 was not included in more experiments. New tyrosine kinase inhibitors specific for HER2 are in development and could be used instead of CP654577 for future experiments.

5.9.6 Development of siRNA as an experimental tool

A second approach taken to understand the role of EGFR and/or HER2 in bladder cancer cell lines was to silence their expression in the cells by using small interfering RNA (siRNA). Since the discovery that transfections of siRNA generated by chemical synthesis (21 nucleotides duplexes) into mammalian cells could transiently downregulate target genes (Elbashir *et al.* 2001), siRNA has been widely used as an experimental tool to analyse the function of mammalian genes.

This approach could be useful to demonstrate the dependence of the bladder cancer cell lines on EGFR and/or HER2 and therefore, confirm the effects observed with the inhibitors, while it also offers some advantages versus the use of TKIs; by using siRNA it is possible to specifically inhibit the function of EGFR or HER2. This is not possible when using TKIs, as they can have off-targets due to the similarity of tyrosine kinase proteins. The advantages of using TKIs, however, is that they are small molecules that can be given orally to patients, they are relatively safe and can be combined with chemotherapy or radiotherapy. Some of the limitations of siRNA for its use *in vivo* is that is a transient model, the toxicity of the transfection reagent and siRNA, and that siRNA can be quickly degraded by RNAses (Arrington *et al.* 2009).

However, Brummelkamp *et al*. described a vector system that allowed a stable, long term expression of siRNA in mammalian cells (Brummelkamp *et al.* 2002), which has been used as an experimental tool and has also led to a growing interest in the development of therapeutic approaches based on RNAi technology, although they are not available yet.

In this study, siRNA technique was used as a tool to investigate the impact of EGFR/HER2 modulation on the biology of these cells. EGFR and HER2 knockdown by siRNA decreased effectively the protein expression levels of both receptors in RT112

and T24 cell lines. In RT112 cells HER2 expression remained supressed up to six days after the transfection.

Cell cycle analysis in RT112 and T24 cells after EGFR and HER2 knockdown showed no difference in cell cycle distribution. This contrasts with the findings by Faltus *et al.*, where they showed that in HER2-overexpressing cancer cells, HER2 siRNA knockdown inhibited cell proliferation, induced cell cycle arrest at G_1 phase on SKBR3 cells 72 hours after the transfection and apoptosis 96 hours after the transfection. They also found that cell lines that did not overexpress HER2 were not sensitive to HER2 knockdown (Faltus *et al.* 2004). In another study, HER2 knockdown using siRNA in SKBR3 cells also caused accumulation of cells in the late G_1/S phase (Choudhury *et al.* 2004).

A possible increase in cell death was observed in T24 cells after HER2 siRNA knockdown as there was an increase in the sub G_1 events 72 hours after the transfection, suggesting an induction of apoptosis. This would be in accordance with studies by Arrington *et al.*, where they studied HER2 siRNA knockdown in oesophageal and gastrointestinal adenocarcinomas cell lines with known HER2 overexpression. They found that HER2 suppression increased levels of apoptosis without affecting cell cycle distribution (Arrington *et al.* 2009). However, this effect was not observed in RT112 cells, despite having 2-fold levels of HER2 expression compared to T24 cells.

In another study, the effects of downregulation of HER2 with antisense oligonucleotides were studied in a panel of cancer cell lines with different levels of HER2 expression. Their results showed that in cell lines that overexpressed HER2, the downregulation of HER2 resulted in cell growth inhibition and increase in apoptosis, suggesting that these cells depend on HER2 for cell proliferation and survival. The T24 cell line was included in this study as a cell line with modest HER2 levels and no effect was observed in this cell line or other cell lines with none or low levels of HER2 (Roh *et al.* 2000).

Effects on downstream signalling pathways were also analysed in RT112 and T24 cells after EGFR knockdown. Phosphorylation of ERK1/2 did not seem to change 48 or 72 hours after the transfection with EGFR siRNA, although longer time points may also be needed to check this. However, phosphorylation of Akt (Ser473) increased in both

EGFR siRNA and control siRNA treated cells, suggesting that the transfection itself was causing this effect rather than the EGFR knockdown. Despite two different approaches taken in order to reduce this cellular toxicity, none of these resolved the problem. For this reason, it was decided not to continue using this method to evaluate EGFR or HER2 inhibition.

Taken together, these results suggested that EGFR and HER2 depletion using siRNA was not sufficient to induce changes in cell cycle distribution or apoptosis in these cell lines. This contrasts with the findings obtained when EGFR and/or HER2 were inhibited using TKIs. The differences between these two approaches could be explained by the fact that siRNA can take up to 48 hours to silence gene expression and that gene knockdown may not be 100%; residual activity of EGFR or HER2 may be sufficient to still activate signalling pathways. On the other hand, TKIs can act within minutes targeting only a specific function of these receptors, but these differences need to be investigated further.

Chapter 6: Identification and functional role of p38 MAPK in bladder cancer

6.1 Introduction

HER family receptors have been linked to tumour progression in different tumours. It is believed that their oncogenic activity is mediated primarily by Akt and ERK1/2 signalling, although other signalling pathways are potentially also involved. In the previous chapter, changes in Akt and ERK1/2 pathways have been studied after inhibiting the receptors with TKIs. However, a global understanding of the signalling events downstream EGFR and HER2 receptors was needed in order to understand better their potential biological role in bladder cancer. Since phosphorylation is fundamental to many aspects of cell signalling, the initial approach was to use a human phospho-antibody array to allow simultaneous assessment of potential key nodes involved in several signalling pathways, including Akt, ERK1/2, signal transducer and activator of transcription (STAT) family, Src family kinase, focal adhesion (FAK), cell cycle/check point proteins, transcription factors and others. This phosphoproteomic profiling was used as a novel approach that could potentially highlight key components in oncogenic signalling of EGFR and/or HER2 in these cells and was used here to screen for those suitable for further analysis.

The prospectively defined plan for this phospho-kinase screen is represented in Figure 6.1. In the first step, the phosphokinase array would be performed with erlotinib (EGFR TKI) to identify proteins with significant changes in their phosphorylation status compared to control cells. In the second step, the phosphokinase array would be performed using lapatinib (EGFR/HER2 TKI), and downstream analysis would focus on the proteins with significant changes in phosphorylation identified with both treatments. This way, changes occurring after the inhibition of both receptors (EGFR and HER2) would be elucidated. The third step would be the validation of these phospho-proteins by Western blot in order to rule out any false positive that could have

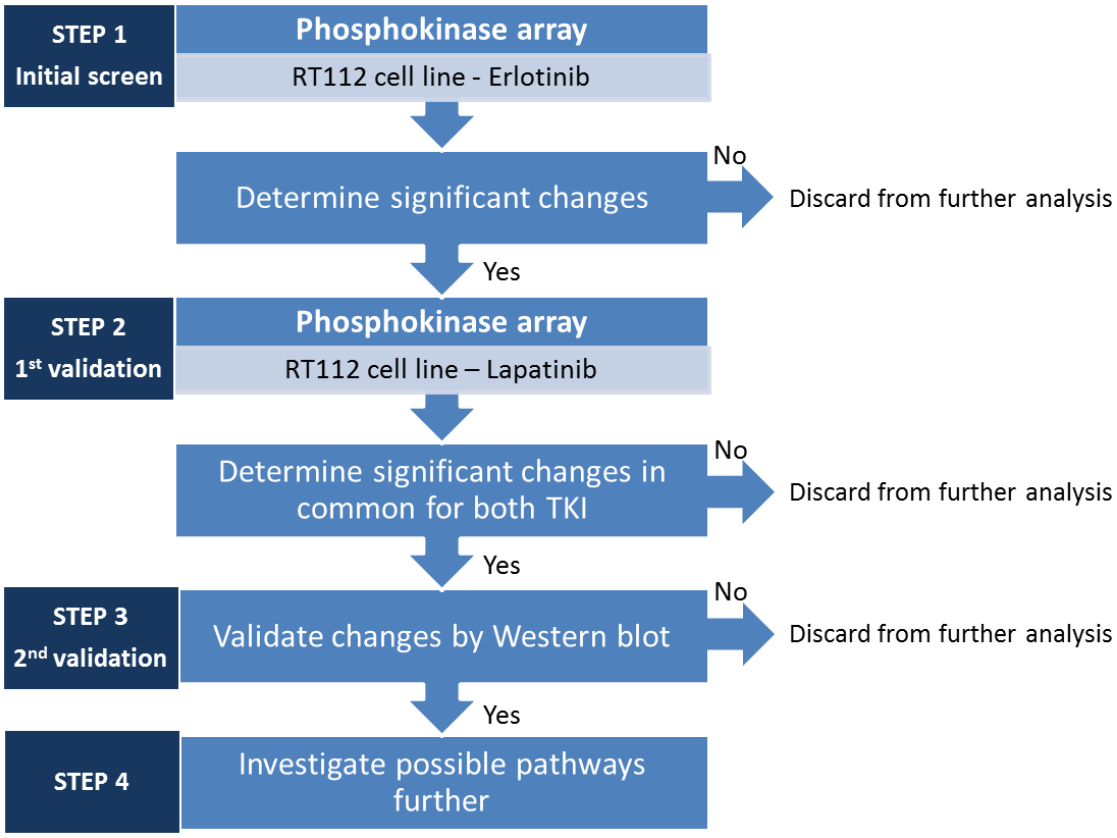

Figure 6.1 Schematic overview of the approach taken to study key signalling pathways after targeting EGFR/HER2 in a bladder cancer cell line.

been generated using the phosphokinase array. Only the changes confirmed by Western blot would be investigated further in the final step.

6.1.1 Statistical analysis

The analysis of the positive signals on the array would be performed in three different ways: by pixel density ("raw data"), by percentage of positive control and by percentage of global mean. Only statistically significant changes using the Student's t-test ($p<0.05$) found in all the analyses would be considered for further investigation and validation.

6.2 Preliminary Western blot to study best time point for the array

In order to optimize the time point to perform the phosphokinase array, a Western blot was performed to investigate when changes in selected phospho-proteins involved in EGFR/HER2 signalling could be detected. RT112 was the cell line chosen to perform the phosphokinase studies. Cells were treated with a high dose of erlotinib ($5xIC_{50}$) and the changes on phosphorylation on two signalling pathways (Akt and ERK1/2) were analysed after short incubation time points. The results showed (Figure 6.2) that downregulation of phospho-Akt (Ser473) and phospho-ERK1/2 was detected after 1 hour and 2 hours of treatment. In order to minimize off-target effects of the drug, one hour treatment was the time point chosen to perform the phosphokinase array.

6.3 Step 1: Phosphokinase array results with erlotinib

The antibody array was used to interrogate 46 phosphorylated signalling proteins to compare RT112 control cells versus RT112 cells treated with erlotinib for 1 hour at $5xIC_{50}$. The analysis of the positive signals on the array A and B revealed the expression of 11 phospho-proteins with stronger or weaker signals in erlotinib treated cells compared to the control cells (shown in Figure 6.3). Phospho-proteins found to be upregulated were: p38α (Thr180/Tyr182), GSK-3α/β (Ser21/9), MEK1/2 (Ser218/222,

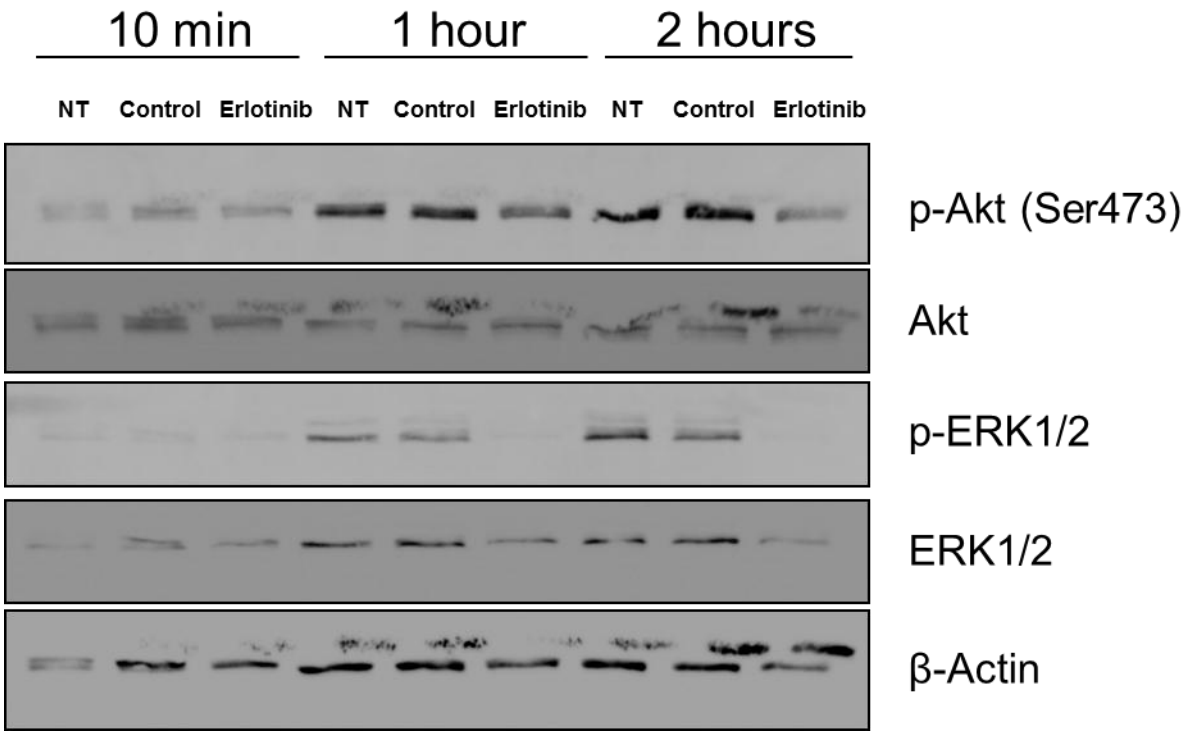

Figure 6.2 Akt and ERK1/2 phosphorylation in response to erlotinib in RT112 bladder cancer cells. RT112 cells were treated with erlotinib at the 5xIC_{50} dose as defined in Chapter 5, DMSO (as control) or left untreated (NT) for the indicated time points followed by Western blot for phospho-Akt (Ser473; 60 kDa) and phospho-ERK1/2 (Thr202/Tyr204; 42/44 kDa) and total expression of Akt and ERK1/2. *β*-actin (42 kDa) was used as a loading control. Representative of two different experiments.

PIXEL DENSITY

	DMSO		ERLOTINIB		T TEST
p38α	708561	873635.8	2545743	2202311	0.014179
GSK-3α/β S21/S9	1571250	1518457	2196120	2162857	0.002408
MEK1/2 S218/S222 S222/S226	782965.6	706422.3	1506723	1544544	0.002975
Akt S473	808405.1	817635.3	1123105	1136388	0.000651
TOR S2448	901045.1	1140468	2050912	2037236	0.013453
Src Y419	866431.7	828160	1409299	1386167	0.001646
p53 S392	6566691	6535567	7143636	7170258	0.001141
p27 T198	323677.2	359810.2	869161.4	820421.2	0.003617
p27 T157	662212.8	663169.6	1030409	1129915	0.013909
PLCγ-1 Y783	661818.8	583080.5	1139427	1028889	0.020924
STAT4 Y693	1434513	1395904	1133855	1155580	0.00664

% POSITIVE CONTROL

	DMSO		ERLOTINIB		T TEST
p38α	13.47865	16.6188	44.01317	38.07559	0.016284
GSK-3α/β S21/S9	29.88922	28.88497	37.96856	37.39348	0.004832
MEK1/2 S218/S222, S222/S226	14.89402	13.43797	26.04962	26.70351	0.004245
Akt S473	15.37794	15.55353	19.41729	19.64693	0.001261
TOR S2448	17.1402	21.69464	35.45808	35.22163	0.0199
Src Y419	16.48176	15.75373	24.36526	23.96534	0.002653
p53 S392	119.0968	118.5324	112.0364	112.4539	0.002843
p27 T198	5.870374	6.5257	13.63139	12.86698	0.005059
p27 T157	12.01023	12.02758	16.1603	17.72089	0.024229
PLCγ-1 Y783	12.00308	10.57504	17.87007	16.13646	0.036522
STAT4 Y693	26.01706	25.31682	17.78268	18.1234	0.002538

% GLOBAL MEAN

	DMSO		ERLOTINIB		T TEST
p38α	46.55232	57.3977	129.5671	112.0879	0.021594
GSK-3α/β S21/S9	103.2308	99.76236	111.7728	110.0799	0.039421
MEK1/2 S218/S222, S222/S226	51.44069	46.4118	76.68554	78.61049	0.008673
Akt S473	53.11205	53.71848	57.16111	57.83713	0.012138
TOR S2448	59.19848	74.92854	104.3824	103.6863	0.042477
Src Y419	56.92439	54.40995	71.72709	70.54978	0.007955
p53 S392	318.3362	316.8274	298.364	299.4759	0.002512
p27 T198	15.69104	17.44267	36.30174	34.26604	0.005107
p27 T157	32.10237	32.14875	43.03648	47.1925	0.024655
PLCγ-1 Y783	32.08327	28.26624	47.58977	42.97301	0.037135
STAT4 Y693	69.54149	67.66981	47.35705	48.26442	0.002492

Figure 6.3 Analysis of the human phospho-antibody array in erlotinib treated cells. Quantitation of phosphorylated protein was performed using Quantity One software. Data were analysed in three different ways: by pixel density, by % of positive control and by % of global mean. Statistical analysis was performed using the Student's t-test (statistical significant changes are highlighted in pink $p<0.01$ and in yellow $p<0.05$). Only statistically significant changes ($p<0.05$) found in all three analyses are shown.

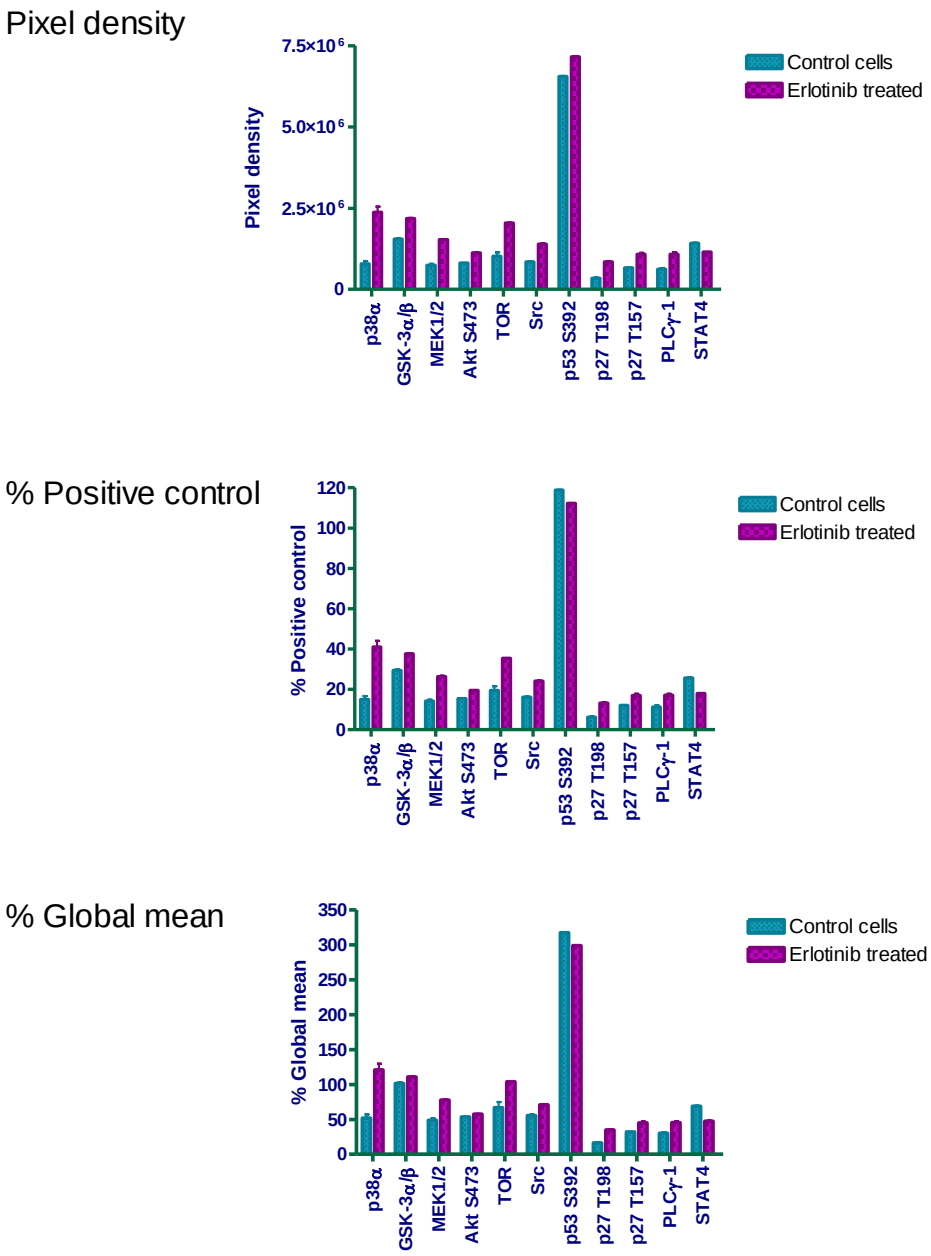

Figure 6.4 Bar charts showing those phospho-proteins reaching pre-determined criteria for statistical significance after erlotinib treatment. Proteins that showed a statistical significant change in their phosphorylation status in RT112 cells after erlotinib treatment were detected using the human phospho-antibody array. Error bars represent the standard deviation of duplicates.

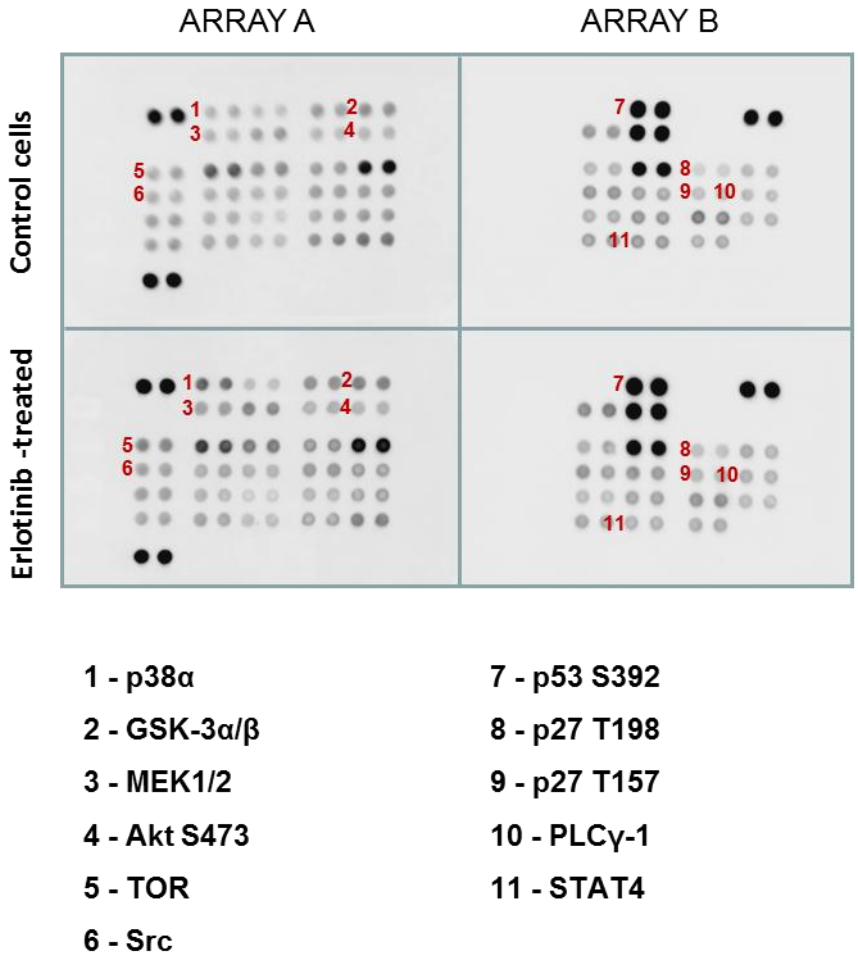

Figure 6.5 Representative human phospho-antibody array image of erlotinib treated RT112 bladder cancer cells. RT112 cells were treated with erlotinib at 5xIC_{50} or the equivalent dose of DMSO (control) for 1 hour and the array was performed as per manufacturer's instructions. Proteins that showed a statistical significant change in their phosphorylation status are shown. The experiment was done once.

Ser222/226), Akt (Ser473), TOR (Ser2448), Src (Tyr419), p27 (Thr198), p27 (Thr157), PLCγ-1 (Tyr783).

Phosphorylation of STAT4 (Tyr693) was found to be downregulated, whereas there was some discrepancy with the phosphorylation status of p53 (Ser392), since it appeared to be upregulated when analysed by pixel density, but downregulated when analysed by percentage of the positive control or percentage of the global mean. The changes of these proteins are shown in Figure 6.4. A representative image of the human phospho-antibody array of erlotinib treated cells is shown in Figure 6.5. Full analysis of the phosphokinase array results with erlotinib is shown in the Appendix.

6.4 Step 2: Phosphokinase array results with lapatinib

After identifying the statistically significant changes in the phospho-proteome of RT112 cells after erlotinib treatment, the screening moved to step 2: the phosphokinase array was performed with lapatinib (EGFR/HER2 TKI) but focusing only on those proteins that reached the criteria for subsequent progression after step 1. The analysis of the positive signals on the arrays A and B revealed the expression of 3 phospho-proteins with stronger or weaker signals in lapatinib treated cells compared to the control cells that were in common with the erlotinib phosphokinase array results: p38α (Thr180/Tyr182), GSK-3α/β (Ser21/9) were upregulated whereas STAT4 (Tyr693) was downregulated (shown in Figure 6.6). The changes of these proteins are shown in Figure 6.7 and a representative image of the human phospho-antibody array of lapatinib treated cells is shown in Figure 6.8. Therefore, these three proteins were taken forward for analysis in step 3 while all the others were removed from further analysis. Full analysis of the phosphokinase array results with lapatinib is shown in the Appendix.

PIXEL DENSITY

	DMSO		LAPATINIB		T TEST
p38α	505375.9	586958.5	953983.6	1026729	0.014803
GSK-3α/β S21/S9	962493.1	797282.6	1538453	1462157	0.020838
STAT4 Y693	2606841	2847884	1752713	1814691	0.016949

% POSITIVE CONTROL

	DMSO		LAPATINIB		T TEST
p38α	9.997423	11.6113	19.33021	20.80421	0.013636
GSK-3α/β S21/S9	19.04018	15.77197	31.17309	29.62714	0.01881
STAT4 Y693	47.60712	52.00913	32.94059	34.10541	0.018991

% GLOBAL MEAN

	DMSO		LAPATINIB		T TEST
p38α	41.72129	48.45634	69.22253	74.50103	0.0246
GSK-3α/β S21/S9	79.45858	65.81964	111.6325	106.0964	0.038886
STAT4 Y693	92.52893	101.0847	68.63297	71.05991	0.026141

Figure 6.6 Analysis of the human phospho-antibody array in lapatinib treated cells. Quantitation of phosphorylated protein was performed using Quantity One software. Data were analysed in three different ways: by pixel density, by % of positive control and by % of global mean. Statistical analysis was performed using the Student's t-test (statistical significant changes are highlighted in yellow $p<0.05$). Only statistically significant changes found in all three analyses and in common with the phosphokinase array results with erlotinib are shown.

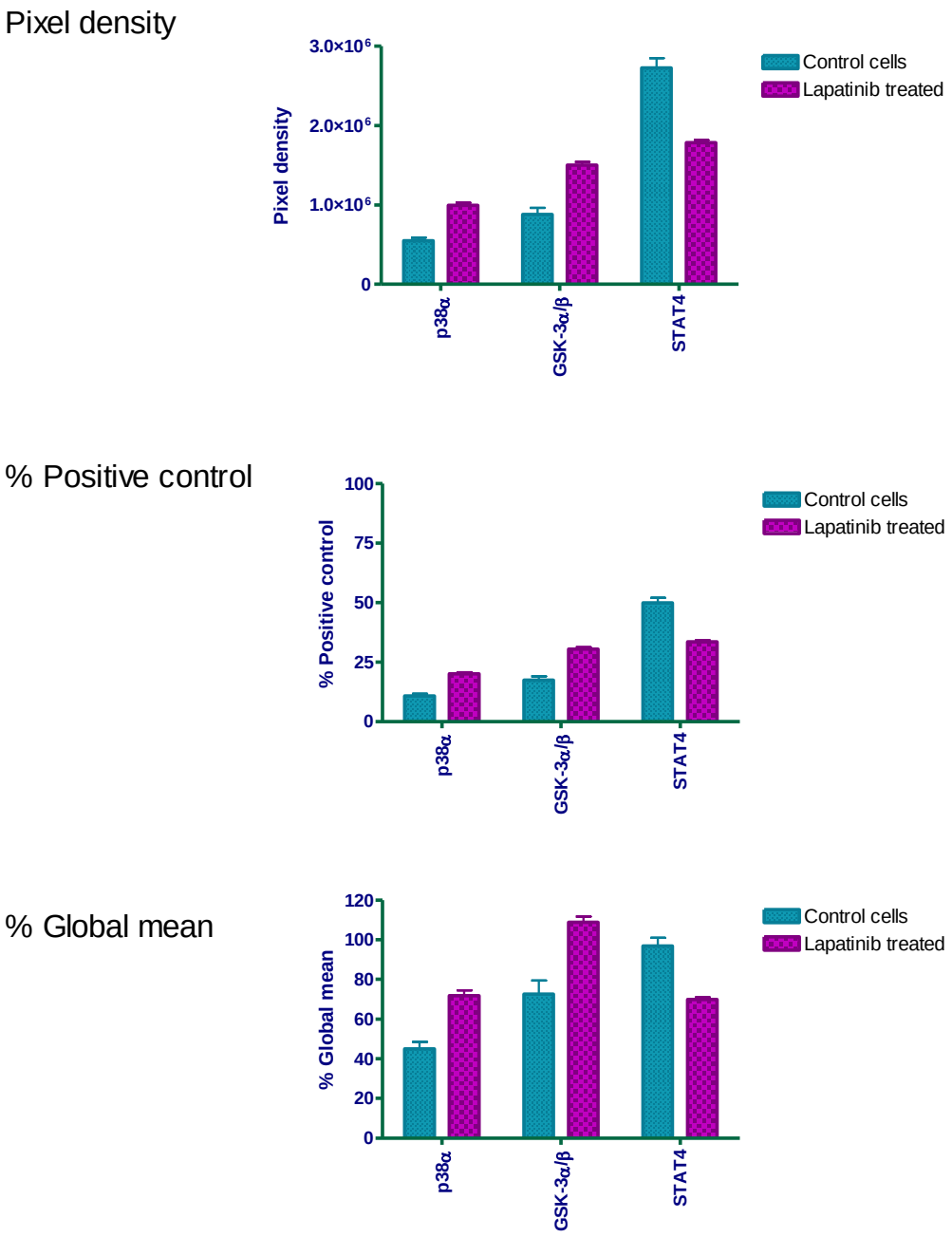

Figure 6.7 Bar charts showing changes in protein phosphorylation reaching pre-determined criteria for statistical significance after lapatinib treatment. Proteins that showed a statistical significant change in their phosphorylation status in RT112 cells after lapatinib treatment were detected using the human phospho-antibody array. Error bars represent the standard deviation of duplicates.

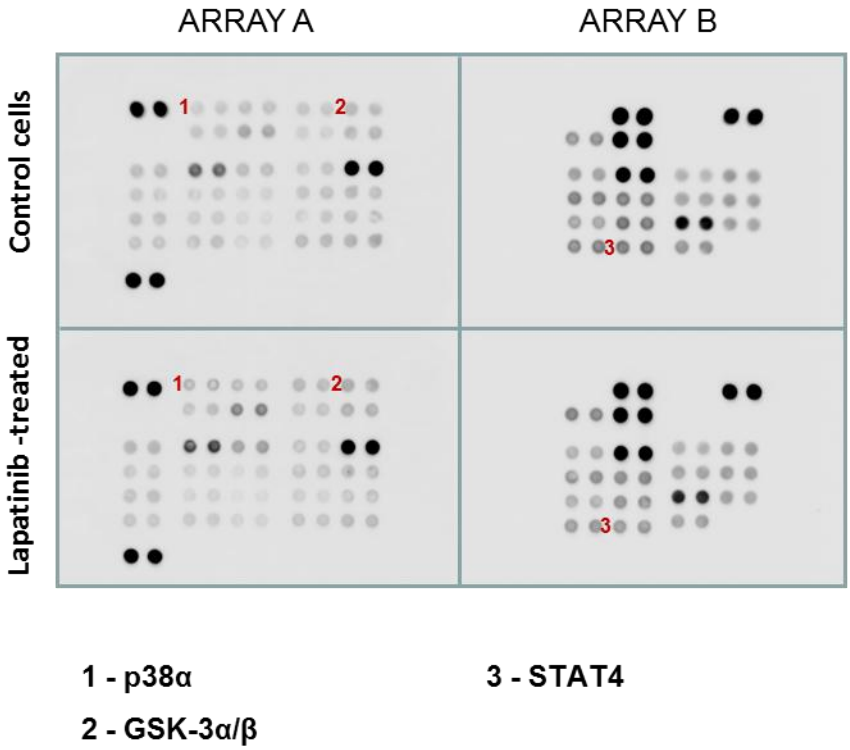

Figure 6.8 Representative human phospho-antibody array image in lapatinib treated cells. RT112 cells were treated with lapatinib at 5xIC_{50} or the equivalent dose of DMSO (control) for 1 hour and the array was performed as per manufacturer's instructions. Proteins that showed a statistical significant change in their phosphorylation status are shown. The experiment was done once.

6.5 Step 3: Study of p38 MAPK, GSK-3α/β and STAT4

Three proteins were detected by the phosphokinase array that changed their phosphorylation status after both erlotinib and lapatinib treatment; phosphorylation of p38α and GSK-3α/β was found to be upregulated and phosphorylation of STAT4 was found to be downregulated.

p38 MAPK is one of the members of the family of mitogen-activated protein kinases (MAPKs). There are four isoforms known of p38 MAPK (α, β, γ and δ) and they are normally activated by stress signals and cytokines (Roux and Blenis 2004). Glycogen synthase kinase-3 (GSK-3α/β) is a serine/threonine kinase that regulates glycogen synthase function. It plays a crucial role in the Wnt signalling pathway and it is also a critical component in receptor tyrosine kinases and G-protein-coupled receptors signalling (Doble and Woodgett 2003). STAT4 is a member of the signal transducers and activators of transcription (STATs). It transduces signals from IL-12, which is the main activator of STAT4, but also IL-23 and IFN-α, and has a central role in pro-inflammatory immune responses (Korman *et al.* 2008).

Validation of the results obtained with the phosphokinase array was necessary before investigating further their possible role in bladder cancer cells.

6.5.1 Study of p38 MAPK, GSK-3α/β and STAT4 after TKI treatment

To validate the phosphokinase array results, a Western blot was performed to detect the increase in phosphorylation of p38α and GSK-3α/β and the downregulation of STAT4 phosphorylation in response to erlotinib or lapatinib treatment. RT112 cells were treated with erlotinib or lapatinib at $2xIC_{50}$ or $5xIC_{50}$ for 30 minutes, 1 hour or 2 hours. The results are shown in Figure 6.9. An increase in phospho-p38 MAPK was observed at $5xIC_{50}$ at all time points after erlotinib and lapatinib treatment, providing validation of the phosphokinase array results. An increase of phospho-p38 MAPK was also detected at $2xIC_{50}$ after 2 hours treatment with erlotinib or lapatinib. Quantification of phospho-p38 MAPK expression levels is shown in Figure 6.10.

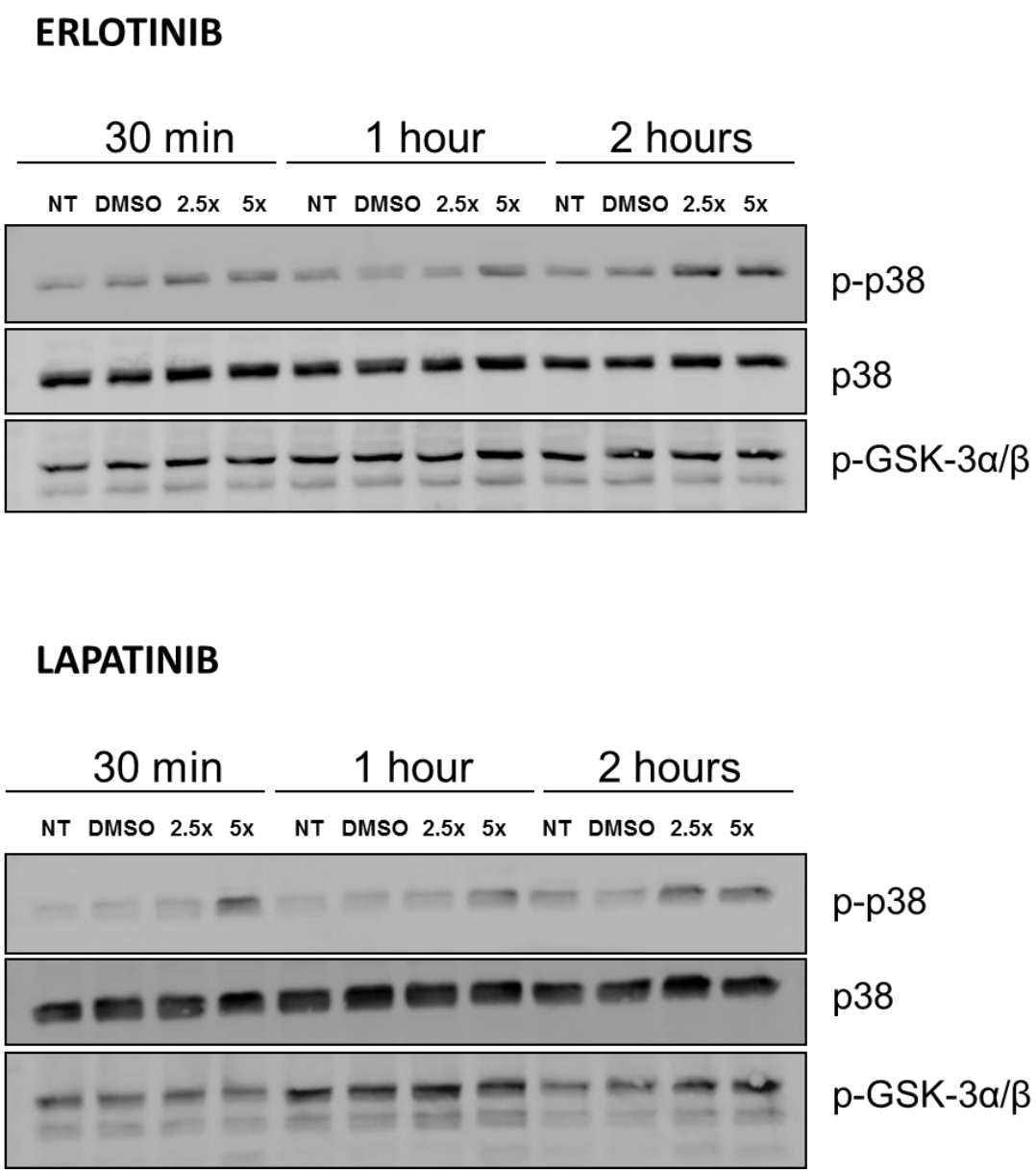

Figure 6.9 Changes in phosphorylation of p38 MAPK and GSK-3α/β in RT112 bladder cancer cells after erlotinib and lapatinib treatment. RT112 cells were treated with 2.5xIC_{50} and 5xIC_{50} of erlotinib or lapatinib, DMSO (as control) or left untreated (NT) for the indicated time points. Cell lysates were analysed by Western blot for phospho-p38 MAPK (Thr180/Tyr182; 43 kDa), total p38 MAPK and phospho-GSK-3α/β (Ser21/9; 46/51 kDa). Representative blot from three independent experiments.

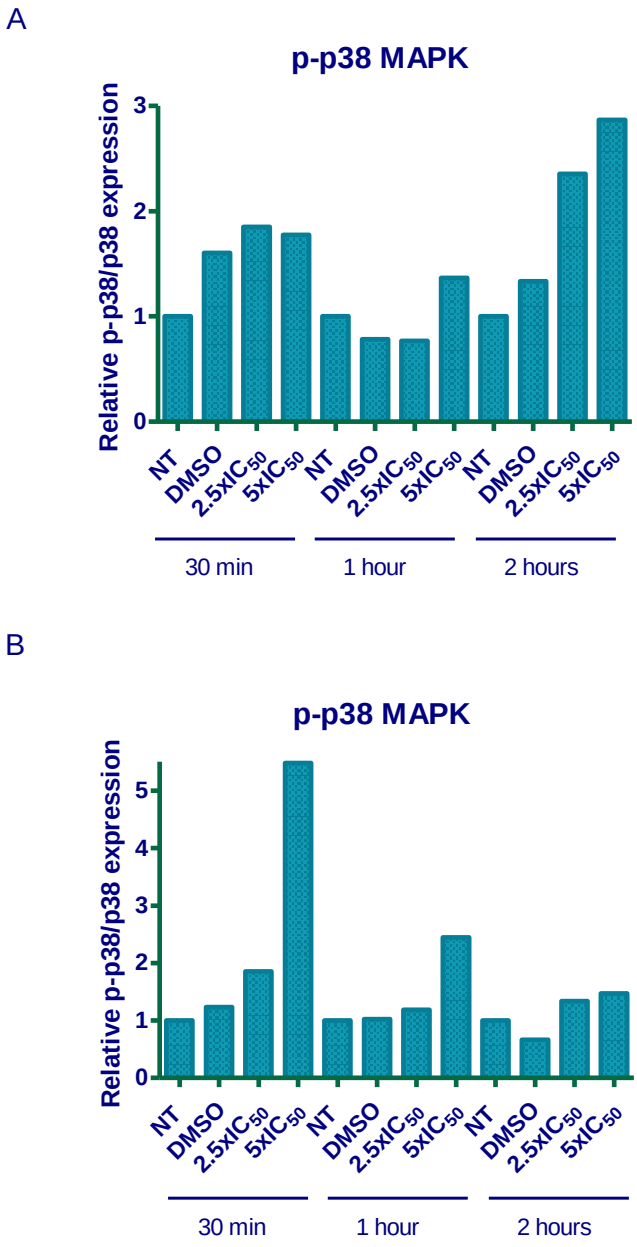

Figure 6.10 Relative expression levels of phospho-p38 MAPK in RT112 bladder cancer cells after erlotinib (A) and lapatinib (B) treatment. Protein expression levels of phospho-p38 MAPK were normalized to the levels of total p38 MAPK in respective samples. Protein expression levels are presented as the fold difference compared to untreated cells (NT) for each time point.

However, no obvious difference was found in the phosphorylation status of GSK-3α/β when analysed by Western blot, although a possible increase in phosphorylation was observed after 2 hours treatment with lapatinib. Phosphorylation of STAT4 could not be detected by Western blot due to the antibody not being sensitive enough (not shown) so it was not possible to validate the downregulation of STAT4 after the TKIs treatment.

To study whether the activation of phospho-p38 MAPK by TKIs was sustained in time, a Western blot was performed where RT112 cells had been treated with erlotinib or lapatinib for longer time points (24, 48 and 72 hours). The results (Figure 6.11) showed no upregulation of phospho-p38 MAPK after erlotinib treatment at these time points. However, phospho-p38 MAPK was still upregulated at 12.5 μM and 25 μM after 24 hours of lapatinib treatment, and still upregulated 48 and 72 hours after treatment at 25 μM, suggesting that HER2 inhibition was potentially responsible for this difference.

The phosphokinase array experiments and the Western blots to confirm the results were all done in RT112 cells. To investigate whether the increase of phospho-p38 MAPK was cell line dependent, a Western blot analysing phospho-p38 MAPK after erlotinib or lapatinib treatment was performed using T24 cells. The results are shown in Figure 6.12. Increase in phospho-p38 MAPK levels was observed after 2 hours treatment with erlotinib or lapatinib at both doses tested ($2xIC_{50}$ and $5xIC_{50}$). Upregulation of phospho-p38 MAPK was also detected at $5xIC_{50}$ dose after 30 minutes and 1 hour of lapatinib treatment. Quantification of phospho-p38 MAPK expression levels is shown in Figure 6.13. No difference was found in the phosphorylation status of GSK-3α/β.

In summary, validation by Western blot confirmed that p38 MAPK was upregulated after erlotinib or lapatinib treatment in RT112 cells, whereas the upregulation of GSK-3α/β was not validated by work to date. STAT4 downregulation could not be validated by Western blot due to the antibody not being sensitive enough. Due to time limitations, this particular pathway could not be investigated further, but its involvement in EGFR/HER2 signalling in bladder cancer cannot be ruled out, and it requires further investigation.

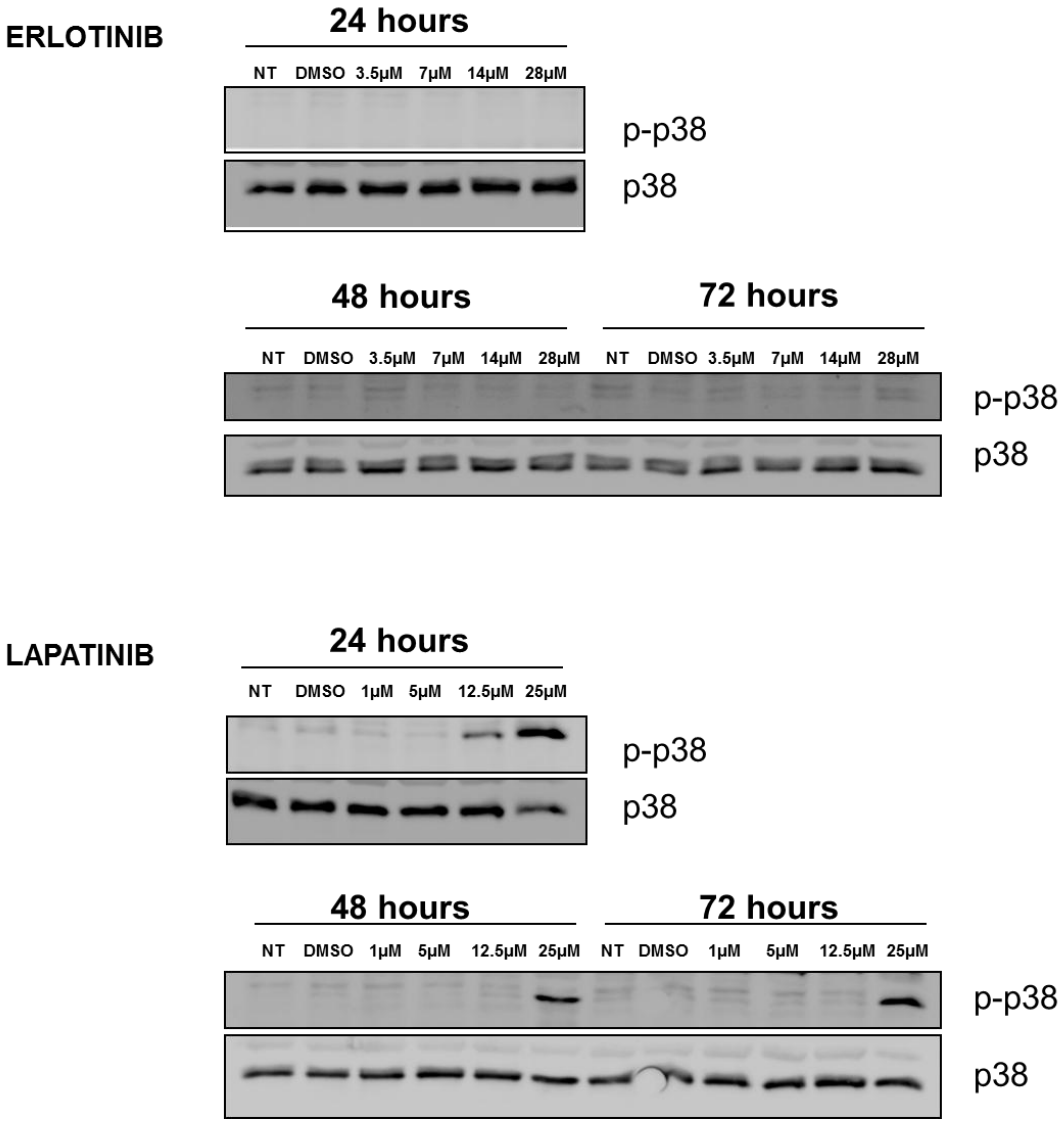

Figure 6.11 Changes in phosphorylation of p38 MAPK in RT112 bladder cancer cells after erlotinib and lapatinib treatment at longer time points. RT112 cells were treated with increasing concentrations of erlotinib, lapatinib, DMSO (as control) or left untreated (NT) for the indicated time points. Cell lysates were analysed by Western blot for phospho-p38 MAPK (Thr180/Tyr182; 43 kDa) and total p38 MAPK. Experiment was done once.

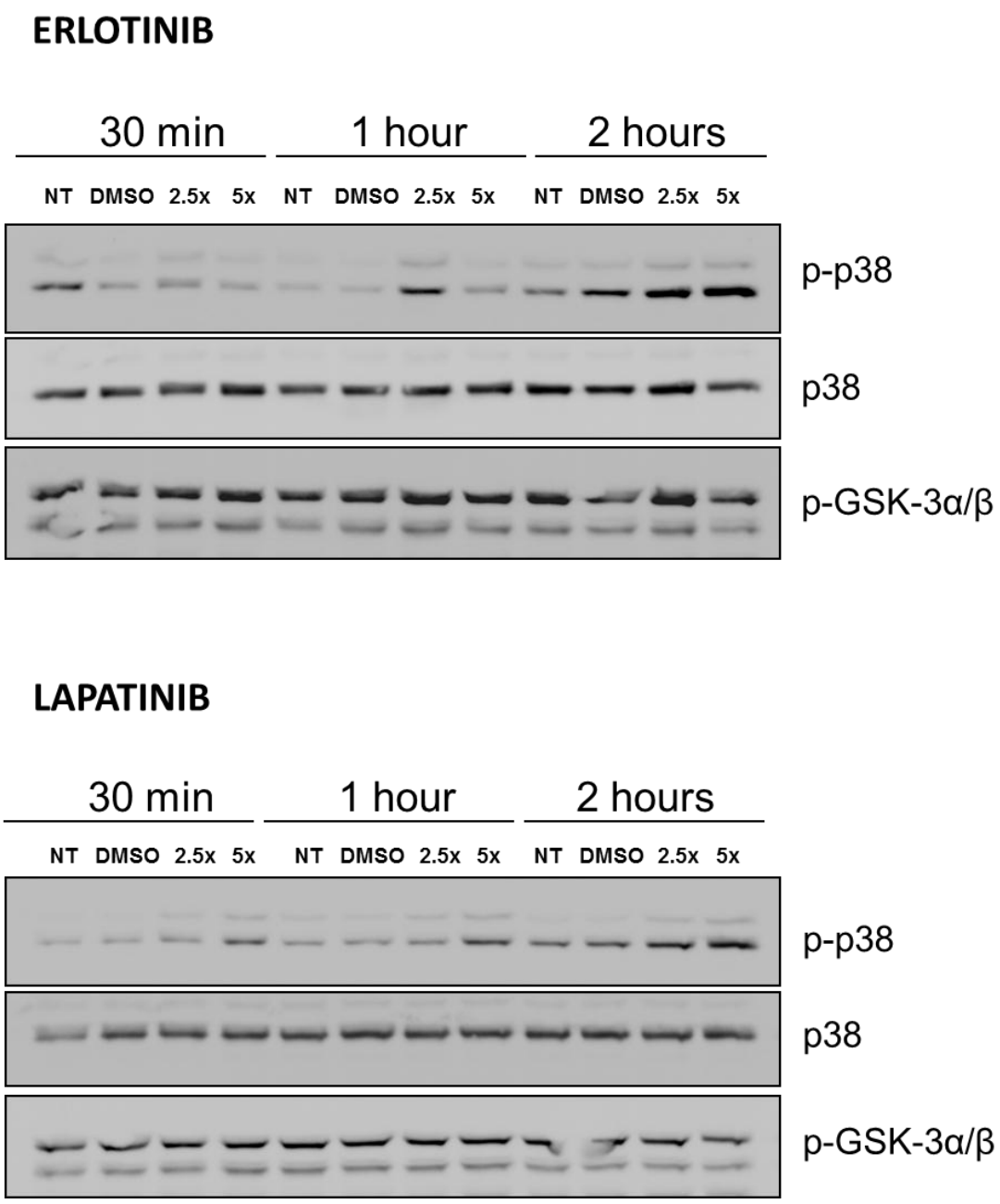

Figure 6.12 Changes in phosphorylation of p38 MAPK and GSK-3α/β in T24 bladder cancer cells after erlotinib and lapatinib treatment. T24 cells were treated with 2.5xIC_{50} and 5xIC_{50} of erlotinib or lapatinib, DMSO (as control) or left untreated (NT) for the indicated time points. Cell lysates were analysed by Western blot for phospho-p38 MAPK (Thr180/Tyr182; 43 kDa), total p38 MAPK and phospho-GSK-3α/β (Ser21/9; 46/51 kDa). Representative blot from two independent experiments.

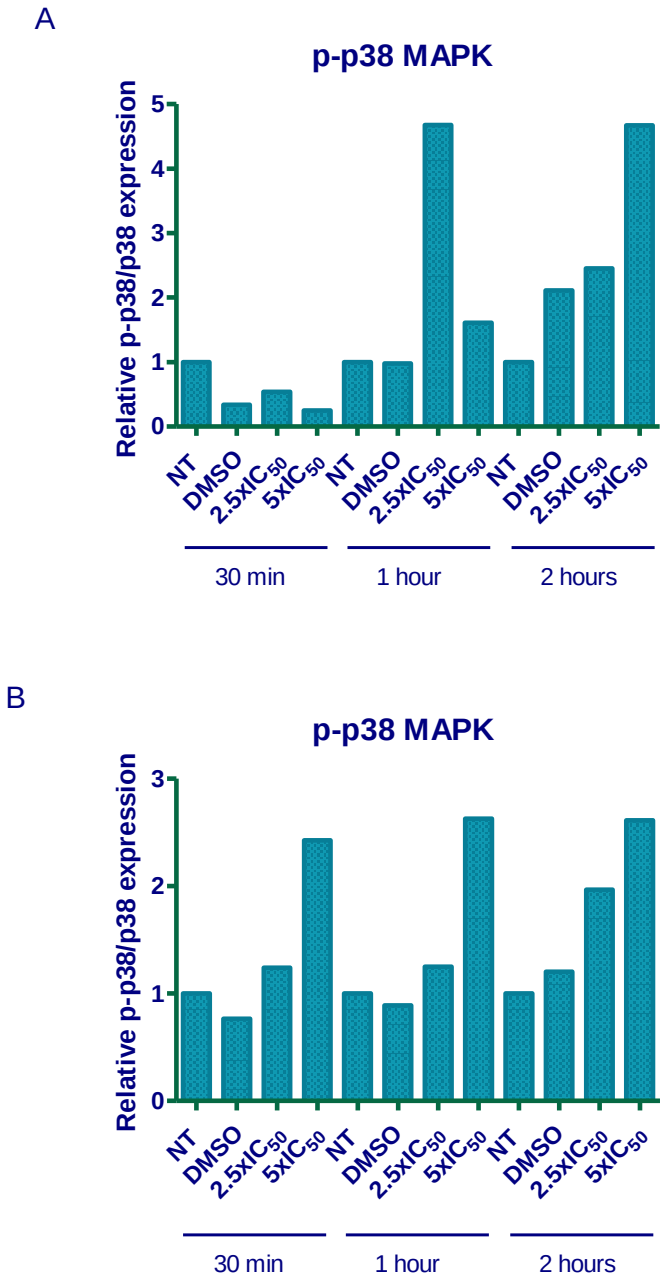

Figure 6.13 Relative expression levels of phospho-p38 MAPK in T24 bladder cancer cells after erlotinib (A) and lapatinib (B) treatment. Protein expression levels of phospho-p38 MAPK were normalized to the levels of total p38 MAPK in respective samples. Protein expression levels are presented as the fold difference compared to untreated cells (NT) for each time point.

6.5.2 Study of p38 MAPK and GSK-3α/β after EGFR/HER2 knockdown

To investigate further the upregulation of phospho-p38 MAPK observed after erlotinib and lapatinib treatment in RT112 cell line, levels of phospho-p38 MAPK were analysed after knocking down EGFR and HER2 expression using siRNA. This would validate further whether the upregulation of phospho-p38 MAPK was due to the inhibition of EGFR/HER2 signalling. The results showed (Figure 6.14) how the transfection downregulated modestly EGFR and HER2 expression levels in this cell line, but a 2-3-fold increase in phospho-p38 MAPK levels in EGFR and also HER2 knockdown cells was observed (shown in Figure 6.15). Levels of phospho-GSK-3α/β were also investigated, but no changes could be detected.

Therefore, after these studies, only p38 MAPK was selected to study further. Phospo-GSK-3α/β upregulation after EGFR and/or HER2 inhibition was viewed as having failed validation, whereas STAT4 was discarded because of technical failure, but it may require further investigation in the future.

6.6 Step 4: Investigation of p38 MAPK role in bladder cancer cell lines

6.6.1 Inhibition of p38 MAPK in bladder cancer cell lines

There were different possibilities for the role of activated p38 MAPK observed after erlotinib and lapatinib treatment in RT112 cells. For instance, its activation could be triggering apoptosis in these cells as p38 MAPK is well-known for being a pro-apoptotic molecule. The fact that phospho-p38 MAPK was upregulated at longer time points after lapatinib treatment would support this hypothesis, since lapatinib induced apoptosis on these cells (as seen in Chapter 5). However, activation of phospho-p38 MAPK could alternatively be a survival mechanism induced by the EGFR/HER2 TKIs. To investigate the role of p38 MAPK in bladder cancer cell lines, its activity was first tested by chemical inhibition. SB203580 is a pyridinyl imidazole inhibitor of p38 MAPK (Cuenda *et al.* 1995), which has been routinely used to investigate the function of p38 MAPK. RT112 and T24 cell lines were treated with increasing concentrations of the p38 MAPK inhibitor for 4 days and the MTS assay was used to assess its effect on cell proliferation.

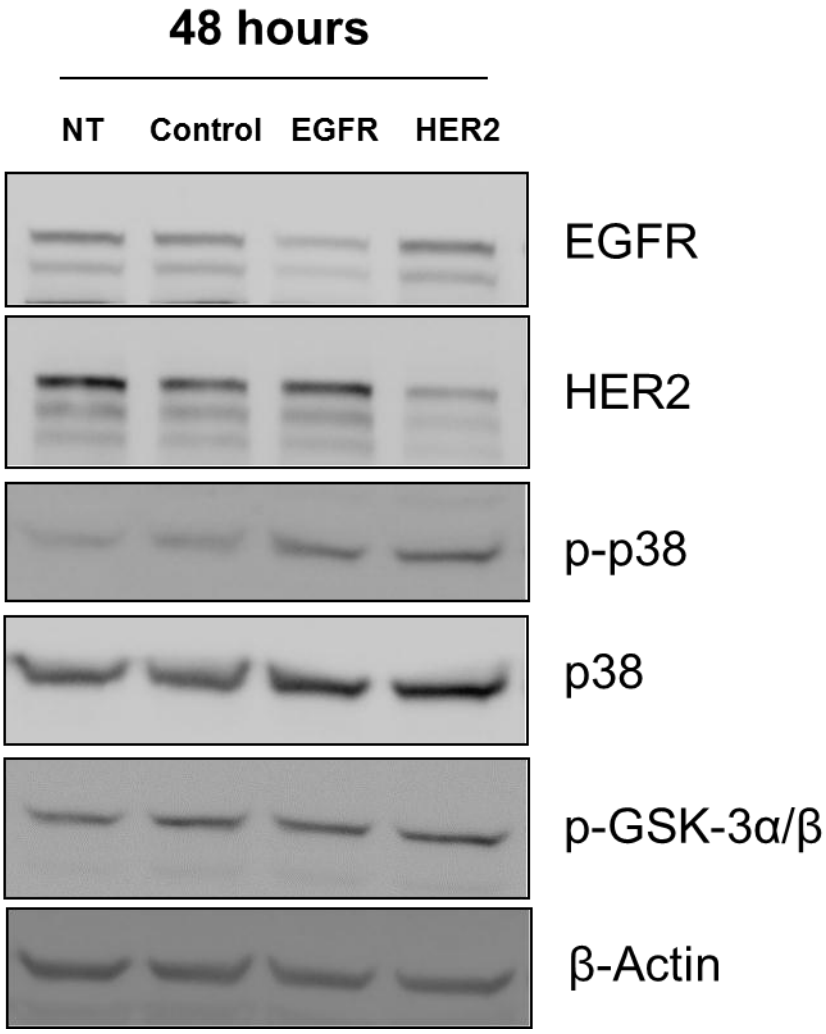

Figure 6.14 Analysis of phospho-p38 MAPK and phospho-GSK-3α/β after EGFR/HER2 knockdown in RT112 bladder cancer cells. Cells were transfected with control siRNA, EGFR siRNA, HER2 siRNA or left untreated (NT) and incubated for 48 hours. Cell lysates were analysed by Western blot for EGFR (175 kDa), HER2 (185 kDa), phospho-p38 MAPK (Thr180/Tyr182; 43 kDa), total p38 MAPK and phospho-GSK-3α/β (Ser21/9; 46/51 kDa). *β*-actin (42 kDa) was used as a loading control. Experiment was done once.

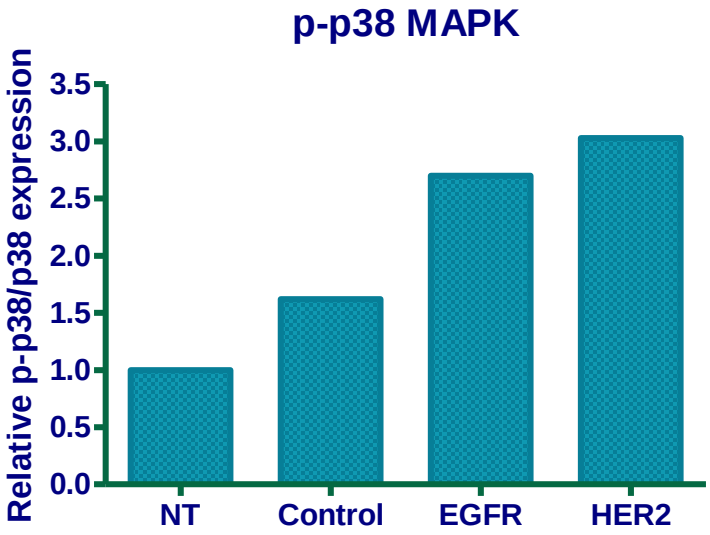

Figure 6.15 Relative expression levels of phospho-p38 MAPK in RT112 bladder cancer cells after EGFR and HER2 siRNA knockdown. Protein expression levels of phospho-p38 MAPK were normalized to the levels of total p38 MAPK in respective samples. Protein expression levels are presented as the fold difference compared to untreated cells (NT).

The compound had an antiproliferative effect in both cell lines; the IC_{50} found for RT112 cells was 36.5 µM, and for T24 cells was 70.1 µM. A representative dose-response curve is shown in Figure 6.16 and the mean IC_{50} values are shown in Figure 6.17.

To help elucidate its role after TKI treatment, my first step was to investigate the effect of dual inhibition of EGFR/HER2 and p38 MAPK using lapatinib and SB203580. A dose-response curve of RT112 cells treated with lapatinib alone or lapatinib in combination with fixed doses of SB203580 were generated. The results (shown in Figure 6.18) demonstrated that RT112 cells exhibited a left shift of the dose-response curve in the presence of SB203580; the IC_{50} changed from 3.73 µM when cells were treated with lapatinib alone to 2.5 µM when 10 µM SB203580 was added to the cells to 1.4 µM when 20 µM SB203580 was added to the cells.

To confirm these results, RT112 cells were treated with a single dose of lapatinib, a single dose of SB203580, and the combination of both. The effect of erlotinib and its combination with SB203580 was also studied. The results showed (Figure 6.19) how cell growth inhibition when these drugs were combined was greater than the effect with either drug alone and that this difference was statistically significant ($p<0.0001$). This raised the possibility of a synergistic effect of SB203580 when combined with EGFR and/or HER2 inhibition, which was more profound with lapatinib. Therefore, the consequences of single and combined inhibition of EGFR/HER2 and p38 MAPK were examined further with synergy assays.

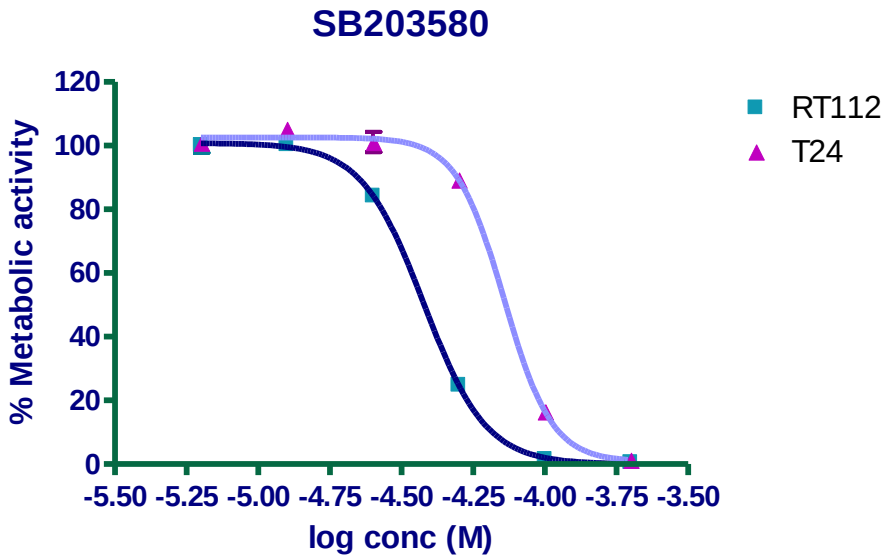

Figure 6.16 Representative dose-response curves of RT112 and T24 bladder cancer cell lines treated with SB203580. Cells were treated with the p38 MAPK inhibitor, SB203580, at various concentrations continuously for 4 days. Control cells were treated with equal concentrations of DMSO, and the MTS assay was used to measure the % of metabolic activity of treated cells compared to control cells. Each data point represents the mean of triplicate determinations in a representative experiment ± SD.

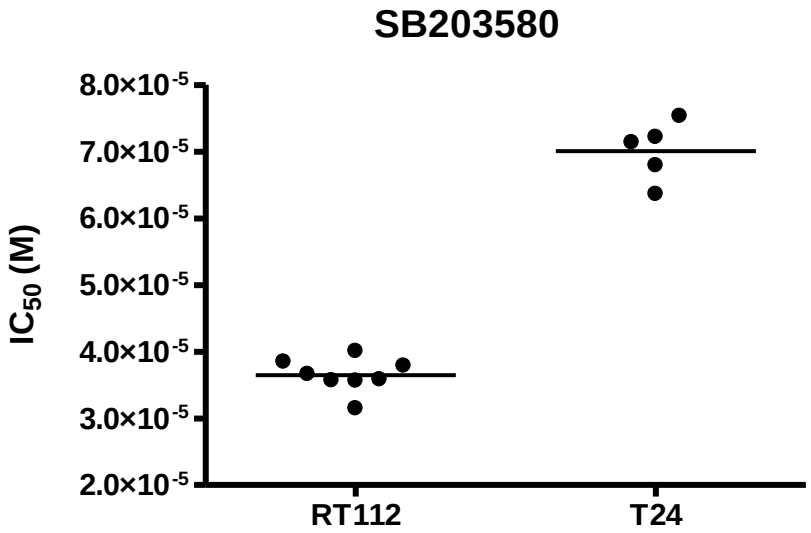

Figure 6.17 Mean IC_{50} values in RT112 and T24 bladder cancer cell lines for SB203580. IC_{50} values were calculated from dose-response curves generated by a non-linear regression sigmoidal curve using the GraphPad Prism4. All IC_{50} values found and their mean (represented by the horizontal bar) are shown for both cell lines.

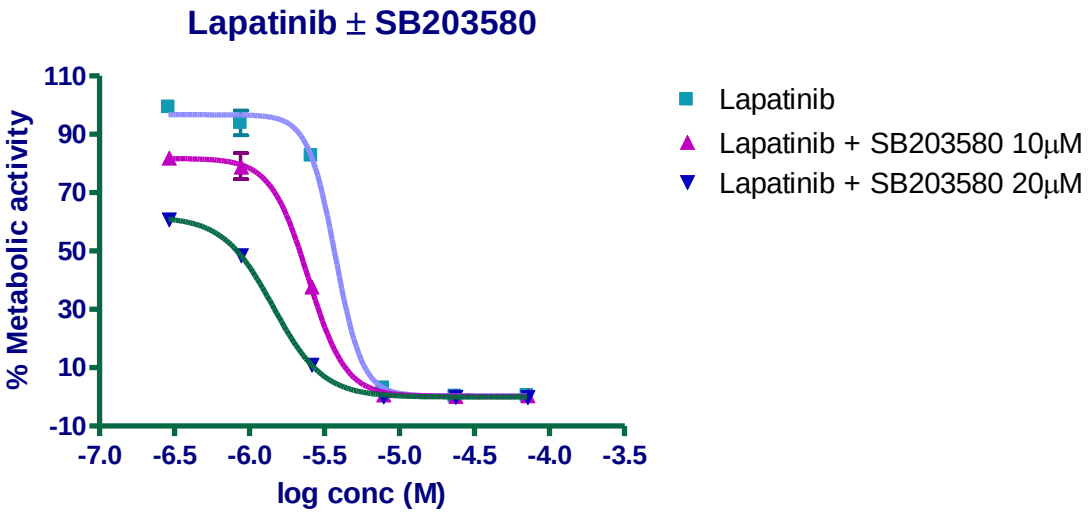

Figure 6.18 Representative dose-response curves of RT112 bladder cancer cell line treated with lapatinib alone or in combination with SB203580. Cells were treated with lapatinib alone or lapatinib and a fixed dose of SB203580 below the IC_{50} (10 μM or 20 μM) continuously for 4 days. Control cells were treated with equal concentrations of DMSO and the MTS assay was used to measure the % of metabolic activity of treated cells compared to control cells. Each data point represents the mean of triplicate determinations in a representative experiment ± SD. Representative of three independent experiments.

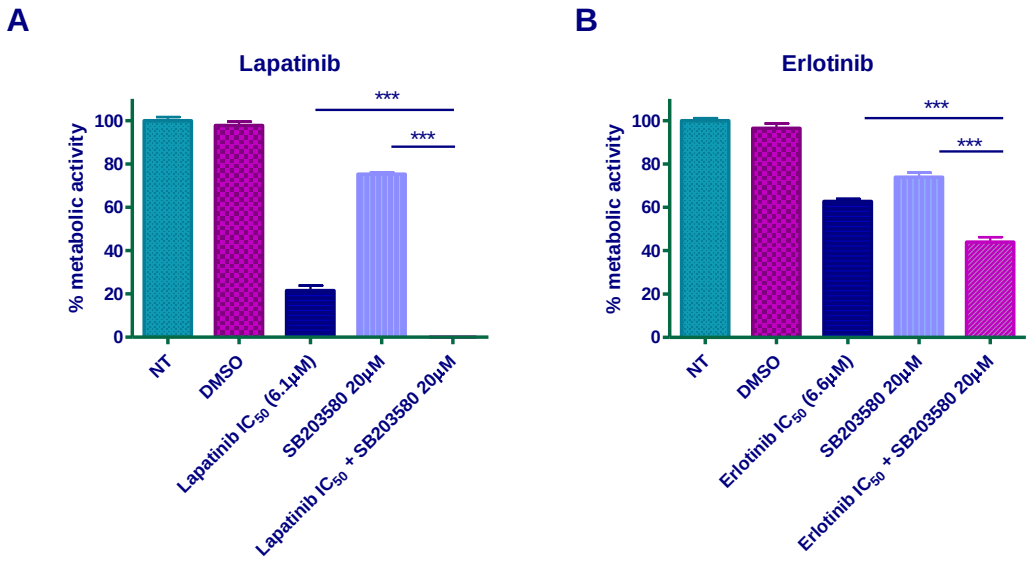

Figure 6.19 Effect of combining lapatinib or erlotinib with SB203580 in RT112 bladder cancer cells. Cells were treated with (A) lapatinib (IC_{50}), SB203580 (20 µM) or a combination of both or (B) erlotinib (IC_{50}), SB203580 (20 µM) or a combination of both continuously for 4 days. Control cells were treated with DMSO (same concentrations as the drug combination) and the MTS assay was used to measure the % of metabolic activity of treated cells compared to non-treated cells (NT). Each histogram represents 6 replicates ± SD. Statistical analysis was performed using the unpaired Student's t-test (*** $p<0.0001$). Representative of two independent experiments.

6.6.2 Synergy effect of lapatinib and SB203580 combination in bladder cancer cells

Synergism was studied using the method of Chou and Talalay by assessing the combination index (CI) where synergism is defined by values CI < 1, antagonism as CI > 1 and additive effect by CI = 1 (Chou and Talalay 1984). A basic requirement for synergy determination is the dose-effect curves for each drug alone and the combination of both. RT112 and T24 cell lines were chosen to study synergy effects of lapatinib and SB203580 combined. Since the experimental design is most efficient when drugs are combined at their equipotent ratio (IC_{50}), combinations of both drugs were done at a fixed molar ratio: approximately 1:4 for RT112 cells and 1:6 for T24 cells. Cell growth inhibition was examined using the MTS assay after 4 days of treatment.

Figure 6.20A shows the cell growth inhibition effect in RT112 cells treated with lapatinib, SB203580 or the combination of both. In order to study synergism, the dose-effect curves showing the fractional inhibitions of lapatinib, SB203580 or the combination of both were analysed first (shown in Figure 6.20B). Then, the sigmoidal dose effects curves were transformed into the corresponding linear forms by the median effect plot (shown in Figure 6.20C). The parameters *m*, D_m and r can be obtained automatically from the median effect plot, where *m* is a coefficient signifying the sigmoidicity of the dose-effect curve, D_m is the dose required to produce the median effect (equivalent to the IC_{50}) and r is the linear correlation coefficient. For lapatinib, *m* = 4.48, D_m = 8.6 µM, r = 0.95, for SB203580 *m* = 2.73, D_m = 31.6 µM, r = 0.99, and for the combination of lapatinib and SB203580 the parameters were: *m* = 5.2, D_m = 2.7 µM, r = 0.74 (shown in Table 6.1), which already suggested that the combination of both drugs was possibly synergistic since the median-effect plot for the combination was situated on the left of both parent compounds (as the IC_{50} for lapatinib, SB203580 or the combination as calculated from the median-effect plot were 8.6, 31.6 and 2.7 µM respectively).

In the F_a-CI plot (Figure 6.20D), the combination index (CI) is plotted as a function of the fractional inhibition (f_a) by computer simulation from f_a = 0.01 to 0.99. The combination index (CI) showed from slight synergism to synergism between the two drugs at all values of fractional inhibition. Of note is that 4 out of the 5 dose combinations tested (the actual combination data points are shown by X in the graph) achieved 100% cell growth inhibition, so the fraction affected = 1 for all these points.

The calculated CI values at ED50, ED75 and ED90 were 0.66, 0.59 and 0.53 respectively, all showing synergism (see Table 6.1). The synergism effect was also clearly observed at 0.75xIC_{50} dose of lapatinib and SB203580 where they inhibited around 40% of cell growth. However, when the drugs were combined together cell growth was inhibited by 100% (Figure 6.20A).

The cell growth inhibition effect in T24 cells treated with lapatinib, SB203580 or the combination of both is shown in Figure 6.21A. The dose-effect curves showing the fractional inhibitions of lapatinib, SB203580 or the combination of both are shown in Figure 6.21B. The transformation of the sigmoidal dose effects curves into the corresponding linear forms by the median effect plot is shown in Figure 6.21C. For lapatinib, *m* = 5.56, D_m = 15.6 µM, r = 0.99, for SB203580 *m* =1.65, D_m = 125.4 µM, r = 0.97, and for the combination of lapatinib and SB203580 the parameters were: *m* = 6.5, D_m = 5.7 µM, r = 0.93, (shown in Table 6.1), which showed that the combination of both drugs was possibly synergistic in these cells as well since the IC_{50} for lapatinib, SB203580 or the combination as calculated from the median-effect plot were 15.6, 125.4 and 5.7 µM respectively. The F_a-CI plot showed from slight antagonism to synergism between the two drugs at different values of fractional inhibition (Figure 6.21D). This probably reflected the experimental difficulties when using this cell line as it was difficult to obtain reproducible IC_{50} effects on cell growth inhibition and some of the doses tested did not have the expected effect. However, treatment with either inhibitor alone at 1.5xIC_{50} had little effect on cell growth inhibition (5% for lapatinib and 20% for SB203580), but when lapatinib and SB203580 were combined resulted in cell growth inhibition of 85%, showing the synergistic interaction between the two drugs. This was also corroborated with the calculated CI values at ED50, ED75 and ED90 which were 0.64, 0.53 and 0.45 respectively, all showing synergism (Table 6.1).

Synergy assays showed that the combination of lapatinib and SB203580 had a synergistic effect in cell growth inhibition against both cell lines, with mean CI values of 0.59 in RT112 cells and 0.54 in T24 cells.

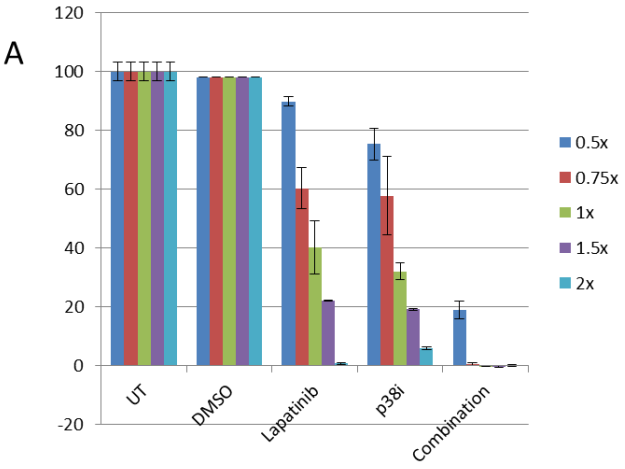
A
120
100
80
60
40
20
0
-20
UT
DMSO
Lapatinib
p38i
Combination
0.5x
0.75x
1x
1.5x
2x

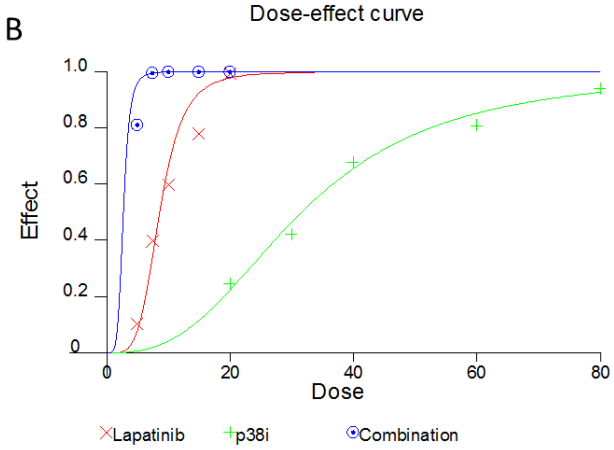
B
Dose-effect curve
Effect
1.0
0.8
0.6
0.4
0.2
0
0
20
40
60
80
Dose
Lapatinib
p38i
Combination

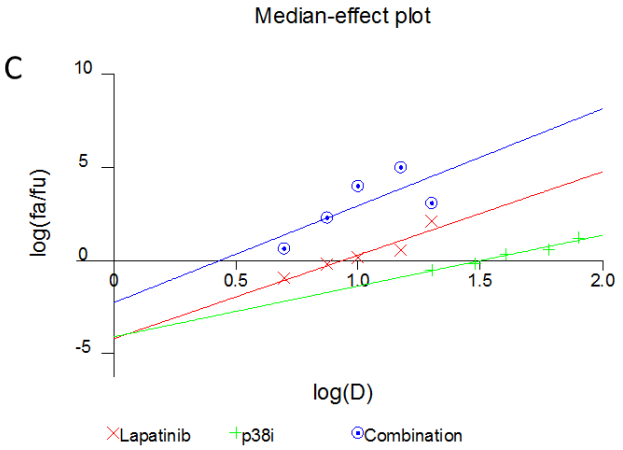
C
Median-effect plot
log(fa/fu)
10
5
0
-5
0
0.5
1.0
1.5
2.0
log(D)
Lapatinib
p38i
Combination

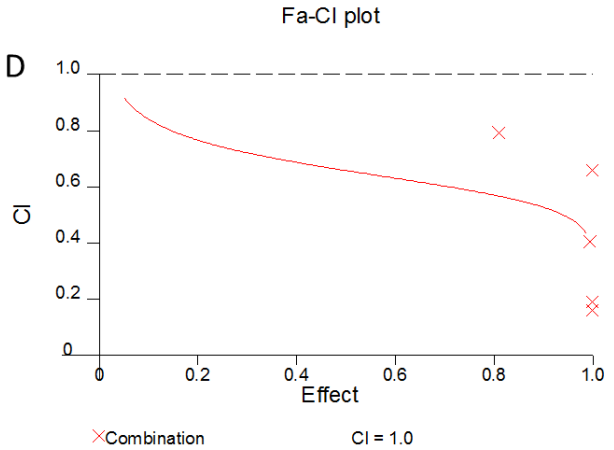
D
Fa-CI plot
CI
1.0
0.8
0.6
0.4
0.2
0
0
0.2
0.4
0.6
0.8
1.0
Effect
Combination
CI = 1.0

Figure 6.20 Lapatinib and SB203580 have synergistic effects in cell growth inhibition in RT112 bladder cancer cells. A) RT112 cells were treated with lapatinib at the following doses: 2xIC_{50} (20µM), 1.5xIC_{50} (15µM), 1xIC_{50} (10µM), 0.75xIC_{50} (7.5µM) and 0.5xIC_{50} (5µM), SB203580 at the following doses 2xIC_{50} (80µM), 1.5xIC_{50} (60µM), 1xIC_{50} (40µM), 0.75xIC_{50} (30µM) and 0.5xIC_{50} (20µM), a combination of both drugs, treated with equivalent concentrations of DMSO as controls or left untreated (UT). The histograms represent the percentage of metabolic activity of RT112 cells compared to untreated cells following exposure to lapatinib, SB203580 or both. Data are mean ± SD of duplicate experiments. B) Dose-effect curves showing the fractional inhibitions of lapatinib, SB203580 or the combination of both drugs in RT112 cells. C) Computer generated median-effect plot showing the inhibition in cell growth by lapatinib, SB203580, or their mixture in a constant molar ratio of 1:4. D) F_a-CI plot: Computer generated graphical presentation of the combination index (CI) with respect to fraction affected (f_a) for the inhibitory effect of lapatinib and SB203580 in RT112 cells. It shows the actual combination data points (in X) and the line is the computer simulation from f_a = 0.01 to 0.99. CI < 1, = 1, > 1 indicate synergism, additive effect and antagonism, respectively. B, C and D graphs were generated using Calcusyn software.

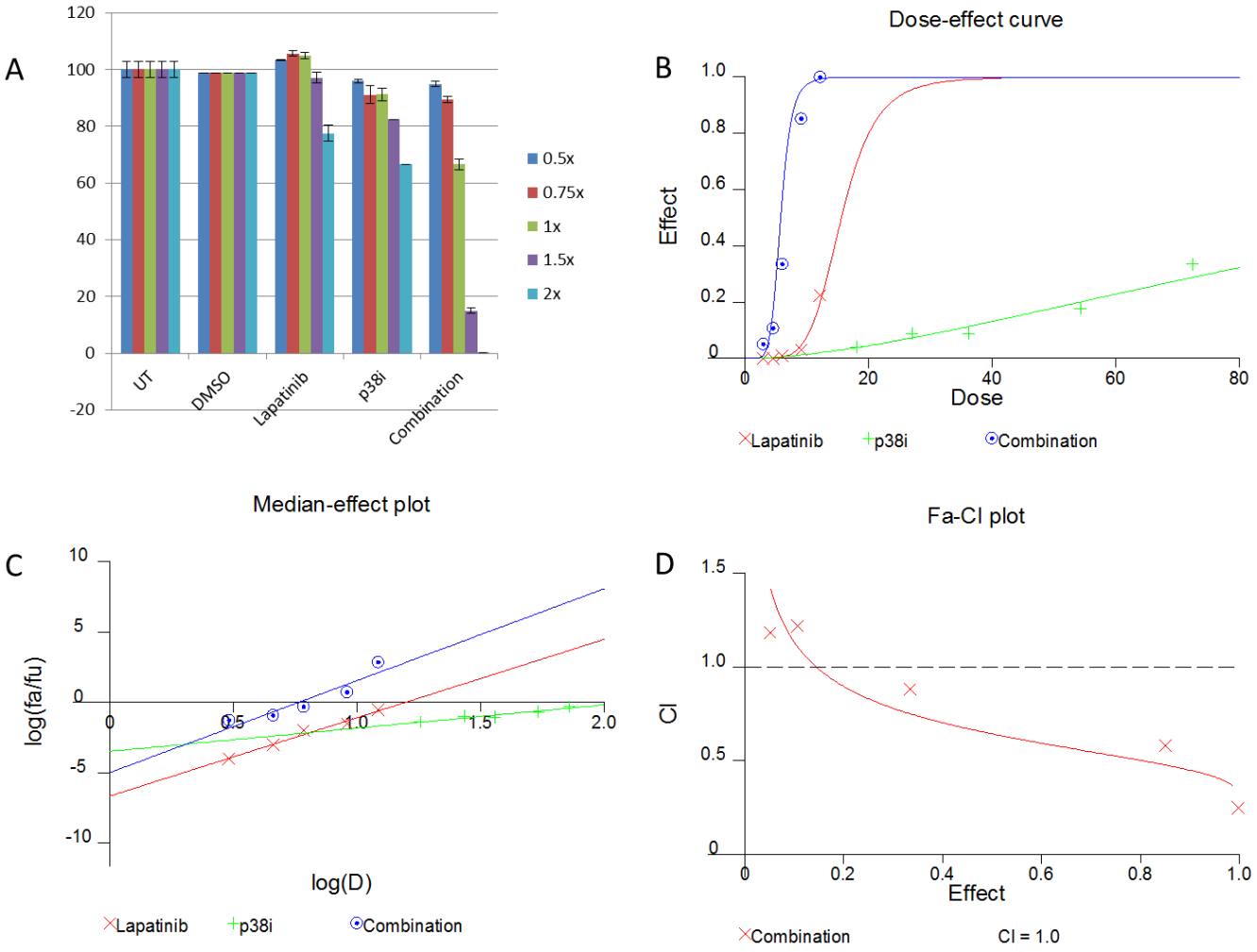
A
120
100
80
60
40
20
0
-20
UT
DMSO
Lapatinib
p38i
Combination
0.5x
0.75x
1x
1.5x
2x
B
Dose-effect curve
Effect
Dose
1.0
0.8
0.6
0.4
0.2
0
0
20
40
60
80
Lapatinib
p38i
Combination
C
Median-effect plot
log(fa/fu)
log(D)
10
5
0
-5
-10
0
0.5
1.0
1.5
2.0
Lapatinib
p38i
Combination
D
Fa-CI plot
CI
Effect
1.5
1.0
0.5
0
0
0.2
0.4
0.6
0.8
1.0
Combination
CI = 1.0

Figure 6.21 Lapatinib and SB203580 have synergistic effects in cell growth inhibition in T24 bladder cancer cells. A) T24 cells were treated with lapatinib at the following doses: 2xIC_{50} (12.2µM), 1.5xIC_{50} (9.2µM), 1xIC_{50} (6.1µM), 0.75xIC_{50} (4.6µM) and 0.5x IC_{50} (3.1µM), SB203580 at the following doses 2xIC_{50} (72.5µM), 1.5xIC_{50} (54.4µM), 1xIC_{50} (36.2µM), 0.75xIC_{50} (27.2µM) and 0.5xIC_{50} (18.1µM), a combination of both drugs, treated with equivalent concentrations of DMSO as controls or left untreated (UT). The histograms represent the percentage of metabolic activity of T24 cells compared to untreated cells following exposure to lapatinib, SB203580 or both. Data are mean ± SD of duplicate experiments. B) Dose-effect curves showing the fractional inhibitions of lapatinib, SB203580 or the combination of both drugs. C) Computer generated median-effect plot showing the inhibition in cell growth by lapatinib, SB203580, or their mixture in a constant molar ratio of 1:6. D) F_a-CI plot: Computer generated graphical presentation of the combination index (CI) with respect to fraction affected (f_a) for the inhibitory effect of lapatinib and SB203580 in T24 cells. It shows the actual combination data points (in X) and the line is the computer simulation from f_a = 0.01 to 0.99. CI < 1, = 1, > 1 indicate synergism, additive effect and antagonism, respectively. B, C and D graphs were generated using Calcusyn software.

		CI Values at					
		ED50	**ED75**	**ED90**	**D_m**	***m***	**r**
RT112	**Lapatinib**	N/A	N/A	N/A	8.60	4.48	0.95
	(Not a combination)						
	SB203580	N/A	N/A	N/A	31.60	2.73	0.99
	(Not a combination)						
	Combination	0.66	0.59	0.53	2.71	5.20	0.74
	(0.25:1)						
T24	**Lapatinib**	N/A	N/A	N/A	15.61	5.56	0.99
	(Not a combination)						
	SB203580	N/A	N/A	N/A	125.39	1.65	0.97
	(Not a combination)						
	Combination	0.64	0.53	0.45	5.77	6.52	0.93
	(0.17:1)						

Table 6.1 Summary of the results generated with Calcusyn software to analyse synergism of lapatinib and SB203580 in RT112 and T24 bladder cancer cells. RT112 and T24 cells were treated with lapatinib, SB203580 or the combination of both in a molar ratio of 1:4 for RT112 cells or 1:6 for T24 cells. Calculated CI values at ED50, ED75 and ED90 are shown (ED; effective dose), as well as D_m, *m* and r parameters generated from the median-effect plot.

6.7 Summary of Chapter 6

In order to investigate potential signalling pathways involved in EGFR or HER2 signalling in bladder cancer, a screening process was defined with predetermined criteria for validation of relevant downstream signalling pathways nodes. In step 1 and 2, a phospho-kinase array was used to simultaneously assess the phosphorylation status of various kinases and signalling molecules in control RT112 cells and RT112 cells treated with TKIs (erlotinib or lapatinib). After this screening process, three proteins were identified whose phosphorylation status changed upon erlotinib or lapatinib treatment: p38 MAPK, GSK-3α/β and STAT4. Only p38 MAPK was investigated further, as it was the only change that could be validated by Western blot. In RT112 cells, increase in phosphorylation of p38 MAPK was observed after short time points (1 and 2 hours) and relatively high doses of erlotinib or lapatinib. This increase in phospho-p38 MAPK was sustained at longer time points (24, 48 and 72 hours) with lapatinib treatment only, but not with erlotinib, suggesting that HER2 inhibition may be critical for this. The increase in phospho-p38 MAPK was not cell-dependent, as T24 cells also showed upregulation of phosho-p38 MAPK after erlotinib or lapatinib treatment.

To address whether this increase in phospho-p38 MAPK observed after erlotinib and lapatinib treatment could be due to an off-target effect of the drugs rather than inhibition of EGFR/HER2, transient downregulation of the expression of these receptors using siRNA was performed to analyse the effect on phospho-p38 MAPK in RT112 cells. The results confirmed an increase in phospho-p38 MAPK in RT112 cells after EGFR and HER2 knockdown.

In order to investigate further the role of p38 MAPK in these cells, SB203580, a p38 MAPK inhibitor, was used to help to elucidate its function on these cells. Cell proliferation assays of RT112 and T24 cells with SB203580 showed that this compound had an inhibitory growth effect on these cells. The IC_{50} for RT112 and T24 was 36.5 μM and 70.1 μM respectively.

The next step was to determine the role of the activation of p38 MAPK after TKI treatment. In order to do this, RT112 cells were treated with different concentrations of lapatinib or with lapatinib combined with a fixed dose of SB203580. The results showed how cells exhibited a left shift of the dose-response curve in the presence of the p38 MAPK inhibitor. This suggested that the phospho-p38 MAPK upregulation could be a mechanism of survival of the cell induced by the EGFR/HER2 inhibition, since when this pathway was blocked with SB203580 there was less cell proliferation. This effect was confirmed in an experiment where RT112 cells were treated with a single dose of lapatinib or lapatinib and SB203580. Combination of both drugs seemed to have a synergistic effect on cell growth inhibition. This effect was also found when SB203580 was combined with erlotinib, although this was less potent. This led to study of the combination of these drugs in synergy assays. The combination of SB203580 and lapatinib was found to have a synergistic effect on cell growth inhibition in both RT112 and T24 cells, with CI values of 0.59 and 0.54 respectively.

The findings of this study could provide a rationale both for p38 MAPK as a therapeutic target in bladder cancer treatment and also for the combination of a p38 MAPK inhibitor with an EGFR/HER2 inhibitor, which showed a synergistic effect in cell growth inhibition of RT112 and T24 cells.

6.8 Discussion

In this study, a screening process was designed in order to investigate which signalling pathways were relevant downstream EGFR and HER2 receptors in bladder cancer. A human protein antibody array was used to analyse the effects of EGFR and/or HER2 inhibition on the intracellular phospho-proteome of RT112 cells by treating them with erlotinib or lapatinib. In this array, some of the signalling pathways or key nodes investigated were Akt and ERK1/2, JAK/STAT, members of the Src family of kinases, p53, p27 and p70S6, among others. A benefit of using this approach was the simultaneous assessment of the phosphorylation of multiple proteins without the need to assess each individually. However, one of the limitations of the phosphokinase array

approach is the potential false positives and false negatives it can generate and therefore, results needed to be validated.

6.8.1 A novel screening approach to identify EGFR/HER2 downstream pathways

The analysis of the phosphokinase array results revealed three proteins which significantly changed their phosphorylation status after one hour treatment with erlotinib or lapatinib in RT112 cells and which held up all the validation steps; p38α and GSK-3α/β were found to be upregulated and STAT4 was found to be downregulated. These changes were also analysed by Western blot in order to be validated, since one of the limitations of the phosphokinase array is, as mentioned before, the false positives or false negatives it can produce. For instance, the preliminary Western blot performed in order to study the best time point for the phosphokinase array showed a clear downregulation of phospho-ERK1/2 after 1 and 2 hours treatment with erlotinib. This change, however, was not detected by the phosphokinase array.

Glycogen synthase kinase-3 (GSK-3α/β) is a serine/threonine kinase that regulates glycogen synthase function but it also plays a crucial role in the Wnt signalling pathway, receptor tyrosine kinases and G-protein-coupled receptors signalling. It has a wide range of functions, including glycogen metabolism, transcription, translation, cell cycle progression and apoptosis. It is normally active in cells and it is regulated through inhibition of its activity via Ser9 and Ser21 phosphorylation (Doble and Woodgett 2003). GSK-3α/β is a downstream element of the PI3K/Akt pathway; Akt activation in response to insulin results in the phosphorylation of both isoforms of GSK-3, inhibiting its activity (Cross *et al.* 1995). Dysregulation of GSK-3α/β has been linked to diabetes, Alzheimer's disease, bipolar disorder and cancer (Doble and Woodgett 2003). In bladder cancer, nuclear accumulation of GSK-3β has been suggested as a new prognostic marker; Naito *et al*. showed that GSK-3β nuclear expression in bladder carcinomas was associated with high-grade tumours, advanced stage of bladder cancer, metastasis and worse survival (Naito *et al.* 2010).

The phosphokinase array results showed that phosphorylation of GSK-3α/β in RT112 cells increased after one hour treatment with erlotinib or lapatinib. However, these results could not be validated by Western blot, and only a possible increase in phosphorylation was observed after 2 hours treatment with lapatinib in RT112 cells. In

contrast with these results, Kassouf *et al.* found that the antiproliferative effects of gefitinib in bladder cancer cells were associated with GSK-3β activation (dephosphorylation) and cyclin D1 degradation, resulting in cell cycle arrest (Kassouf *et al.* 2005). Interestingly, however, GSK-3β has been found to be phosphorylated by p38 MAPK in brain and thymocytes, resulting in β-catenin accumulation and cell survival (Thornton *et al.* 2008). No further investigation was done in this particular signalling pathway but future work is warranted to address this.

The phosphokinase array also revealed another potential molecule involved in EGFR/HER2 signalling: STAT4. Signal Transducers and Activators of Transcription (STATs) is a family of seven transcription factors that were first discovered for their role in cytokine signalling, but they also participate in growth factor signalling. Activation of STATs results in their dimerization and translocation to the nucleus where they regulate expression of genes that control cell proliferation, survival, differentiation, development and immune responses (Bowman *et al.* 2000).

It has been found that constitutive signalling by STATs contributes to malignant progression by stimulating cell proliferation and survival. Inappropriate activation of STATs (and particularly STAT3 and STAT5) has been found in human blood malignancies (lymphomas and leukemias), multiple myelomas, melanomas, head and neck squamous carcinoma cell, prostate, renal cell, lung, ovarian and pancreatic cancer (Bowman *et al.* 2000).

Increased STAT3 activation has been found to increase proliferation of head and neck squamous carcinoma cells and oesophageal carcinoma cell lines via TGF-α mediated activation of EGFR, suggesting that constitutive activation of STAT3 may have a role in the progression of human tumours through EGFR signalling (Quesnelle *et al.* 2007).

STAT4 expression is tissue-restricted and is found mainly in thymus, testis and spleen (Zhong *et al.* 1994). IL-12 is the most potent activator of STAT4, but it can also be activated by IL-23 and IFN-α. STAT4 has a central role in pro-inflammatory immune responses and it has been associated with susceptibility to rheumatoid arthritis and systemic lupus erythematosus (Korman *et al.* 2008). In contrast with other STAT members, STAT4 does not appear to contribute to oncogenesis. However, in prostate

cancer, STAT3 and STAT6 have been found to be significantly activated, as well as higher levels of activated STAT4, although these were not statistically significant (Ni *et al.* 2002). The phosphokinase array results showed that STAT4 phosphorylation was downregulated in RT112 cells after erlotinib or lapatinib treatment. These results could not be validated by Western blot due to the antibody not being sensitive enough. Due to time constrains this pathway could not be investigated further, so it remains unknown whether STAT4 activation may be dependent to EGFR and/or HER2 signalling and whether it may have a role in bladder cancer progression. Therefore, this particular pathway would require further investigation.

6.8.2 Identification of p38 MAPK as a key node downstream EGFR/HER2 signalling

The third molecule identified by the human phosphokinase array was p38α. p38 MAPK is one of the members of the family of mitogen-activated protein kinases (MAPKs), which also includes ERK1/2 (extracellular signal-regulated kinases 1 and 2) and JNKs (c-Jun-N-terminal kinases). MAPKs can be activated by different stimuli, but in general, mitogens and growth factors activate ERK1/2 whereas p38 MAPK and JNK are activated by cytokines and cellular stress such as osmotic shock, ionizing radiation or UV light (Roux and Blenis 2004).

There are four isoforms known of p38 MAPK (α, β, γ and δ), which are encoded by different genes. p38α is expressed at high levels in most cell types whereas p38β is expressed at lower levels. The expression of the other two members, p38γ and p38δ, seem to be tissue-specific (Trempolec *et al.* 2013). Extracellular signals will activate the MAPK cascade that will phosphorylate p38α in threonine and tyrosine residues, resulting in a conformational change that will activate its kinase activity (Trempolec *et al.* 2013). Activated p38α has been shown to phosphorylate up to 66 cellular targets, including DNA and RNA-binding proteins involved in the regulation of gene expression, transcription factors (ATF2, MEF2A, SAP1, CHOP, Elk-1, STAT1, STAT4 and p53) serine and threonine kinases (GSK-3β, MK2, MK3, MSK1 and MSK2) and regulatory proteins involved in cell cycle regulation (cyclin D1, cyclin D3 and $p57^{kip2}$) apoptosis (Bax and BimEL) and cell survival (caspase-3 and caspase-8) (Trempolec *et al.* 2013).

Among its functions, p38 MAPK is well-known for its role in normal immune and inflammatory responses (Ono and Han 2000). Activation of p38 MAPK by cellular stress has been associated with cell cycle arrest (Ambrosino and Nebreda 2001) and apoptosis (Xia *et al.* 1995). It is also thought to have a role as a tumour suppressor (Han and Sun 2007). On the other hand, some reports suggest that p38 MAPK is also activated in mitogenic pathways. For instance, p38 MAPK has been shown to mediate proliferation in breast cancer cells (Chen *et al.* 2009), which contrasts with the role of p38 MAPK in stress and cell cycle arrest.

Therefore, p38 MAPK can control a wide variety of cellular processes. After the activation of p38α, cellular response will depend not only on stimulus, but also signal intensity and duration, cell type and cross-talk with other signalling pathways. For instance, cellular stress will normally trigger high and sustained p38 MAPK activation, resulting in apoptosis, whereas homoeostatic functions resulting in transient and lower p38 MAPK activation tends to be associated with cell survival. This could explain for the opposing effects observed after p38 MAPK activation (Cuadrado and Nebreda 2010). While most studies have shown these different effects in different cell lines, Faust *et al*. tried to address how different stimuli could induce different p38 MAPK signalling pathways in the same cell type and how the level and/or duration of p38 MAPK activation might determine the outcome. Their results showed how after mitogenic stimulation, there was a weak and transient phosphorylation of p38 MAPK which regulated the retinoblastoma pathway through cyclin D1, resulting in cell proliferation. However, a strong and sustained activation of p38 MAPK induced by cellular stress led to cell cycle arrest in murine fibroblast cell lines by increasing the phosphorylation of CREB (Faust *et al.* 2012).

Besides the importance of strength and duration of p38 MAPK activation in cellular outcome, cross-talk between pathways may also be important. Studies by Xia *et al.* showed that activation of p38 MAPK and JNKs with concurrent ERK inhibition induced apoptosis in neuronal cell and that it was this balance that may ultimately lead

to apoptosis or cell survival (Xia *et al.* 1995). A schematic representation of this MAPK pathway is shown in Figure 6.22.

The role of p38 MAPK in bladder cancer is poorly understood, but a recent study including 91 primary human bladder cancer samples found that p38 MAPK expression was associated with higher tumour grade and its expression was also higher in muscle invasive tumours compared to superficial tumours (Ozbek *et al.* 2011). In preclinical models, Kumar *et al*. have suggested that p38 MAPK may play an important role regulating invasion of bladder cancer cells by modulating matrix metalloproteinases 2 and 9 (MMP-2 and MMP-9) (Kumar *et al.* 2010). On the other hand, Otto *et al.* suggested that defects in the p38 MAPK pathway may confer resistance to apoptosis and a survival advantage to bladder cancer cells (Otto *et al.* 2012), so p38 MAPK role as oncogenic or tumour suppressor in bladder cancer remains controversial.

In this study, an increase in phosphorylation of p38 MAPK was observed after short time points (1 and 2 hours) and relatively high doses of erlotinib or lapatinib in RT112 cells and T24 cells. This is in accordance with a study by Wang *et al*., who also found an activation of p38 in glioblastoma multiforme cells after treating them with a high concentration of GW2974, a dual EGFR and HER2 inhibitor (Wang *et al.* 2013). In the present study, transient downregulation of the expression of EGFR and HER2 using siRNA also showed a possible increase in phospho-p38 MAPK in RT112 cells. However, this experiment was only done once and it requires further investigation in order to achieve a better EGFR and HER2 knockdown at longer time points. Nevertheless, the p38 MAPK pathway was investigated further in this bladder cancer cell model.

6.8.3 Investigation of a p38 MAPK role in bladder cancer

In order to investigate further the role of p38 MAPK, a p38 MAPK inhibitor (SB203580) was used to help clarify its function on these cells. SB203580 is a pyridinyl-imidazole inhibitor of p38 MAPK that competes with ATP for binding to p38 MAPK and inhibits its activity (Frantz *et al.* 1998). This compound has been widely used to study p38 MAPK functions (Cuadrado and Nebreda 2010).

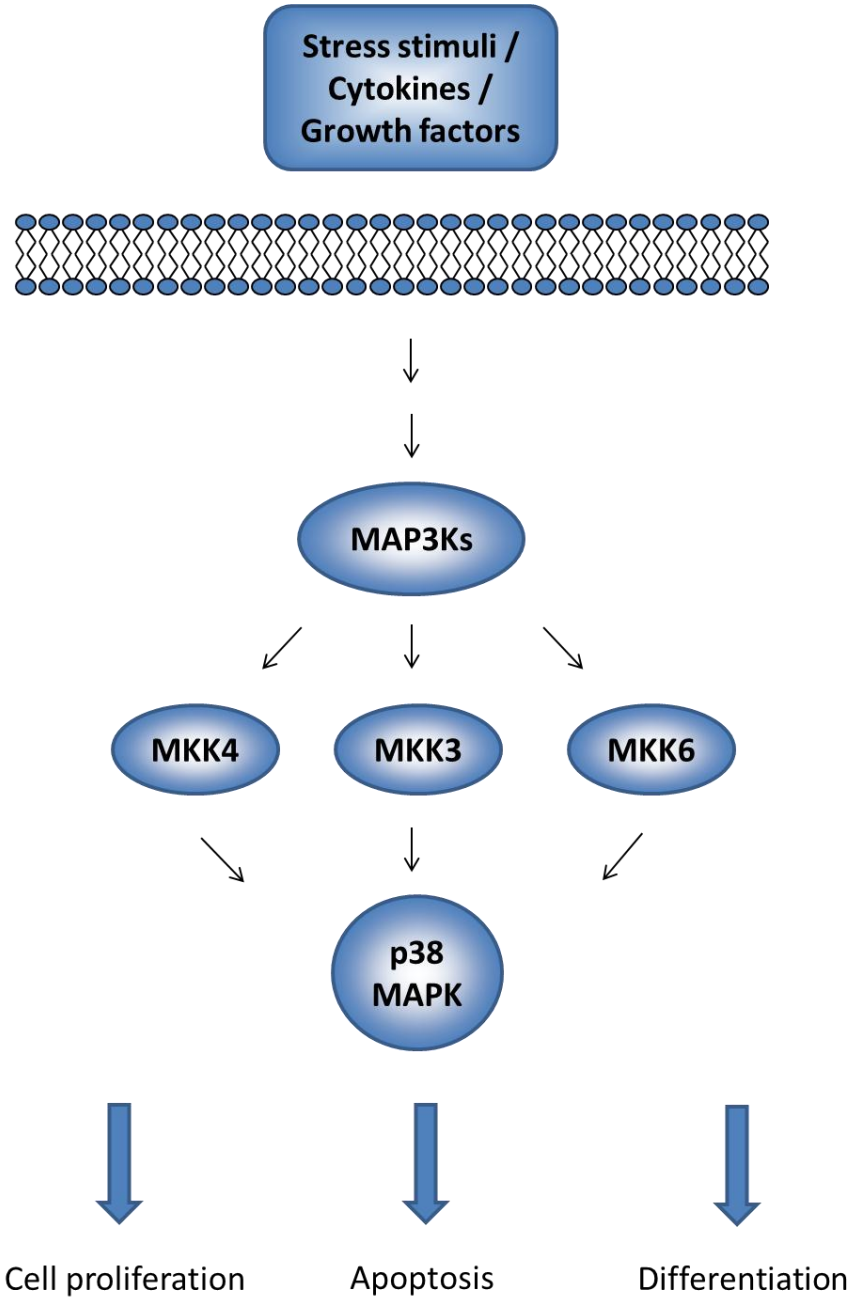

Figure 6.22 Schematic representation of p38 MAPK pathway and its effects in the cell. MAP3Ks can be activated by different stimuli, including stress, cytokines and growth factors. Once activated, they can phosphorylate downstream MAP2Ks, which include MKK3, MKK6 and MKK4. MAP2Ks will phosphorylate and activate p38 MAPK, which depending on the stimuli type, intensity and duration, will lead to different cellular responses.

First, p38 MAPK was studied as a single target in bladder cancer. SB203580 supressed the viability of RT112 and T24 cells in a dose-dependent manner. The IC_{50} for RT112 and T24 was 36.5 µM and 70.1 µM respectively. The reason for this two-fold difference in the IC_{50} was not investigated further, but studies by Kumar *et al.* attributed different sensitivity to SB203580 in bladder cancer cell lines to different signalling mechanisms in different stages of cancer progression. In HTB9, derived from grade 2 bladder cancer, SB203580 caused G_2/M arrest due to a downregulation of cyclin B1 and increased apoptosis whereas in HTB5, derived from a grade 4 bladder cancer, it caused G_1 arrest due to upregulation of p21 but no apoptosis was observed. HTB5 was found to be more resistant to the inhibitor than HTB9 (Kumar *et al.* 2009).

Secondly, p38 MAPK was studied as a key node downstream of EGFR/HER2 inhibition since p38 MAPK was found to be activated after EGFR/HER2 TKI treatment. Studies by Sheng *et al.* showed that EGFR inhibition by siRNA or gefitinib increased p38 MAPK activation in intestinal epithelial cells, and this p38 MAPK activation was associated with mitochondrial translocation of Bax and induction of apoptosis (Sheng *et al.* 2007). The fact that phospho-p38 MAPK was upregulated at longer time points after lapatinib treatment but not with erlotinib would support this hypothesis, since lapatinib but not erlotinib induced apoptosis on these cells. However, the antiproliferative effect of SB203580 observed in the two bladder cancer cell lines did not support this hypothesis. Alternatively, increase of phospho-p38 MAPK could be an activated pathway to confer a natural survival response to the EGFR and/or HER2 inhibition in these cells.

The dose-response curve generated for RT112 cells treated with lapatinib or with lapatinib combined with a fixed dose of SB203580 supported the hypothesis that the phospho-p38 MAPK upregulation could be a survival response induced by the EGFR/HER2 TKI, since when SB203580 blocked the p38 MAPK pathway, there was less cell proliferation. Moreover, when RT112 cells were treated with a single dose of lapatinib or lapatinib and SB203580, cell growth inhibition was greater when both drugs were combined. This effect was also found when SB203580 was combined with erlotinib, but was less marked. This raised the possibility of a synergistic effect of SB203580 when combined with EGFR and/or HER2 inhibition, which was studied further in synergy assays.

6.8.4 Evaluation of synergy between lapatinib and SB203580

Synergism can be defined as a more than expected additive effect. The median-drug effect analysis method is one of the most widely used ways to evaluate synergism of drug combinations (Chou and Talalay 1984). Therefore, the effects of combination of lapatinib and the p38 MAPK inhibitor SB203580 were analysed using this median effect/combination index (CI) method for multiple drug effect analysis. Calcusyn software was used to calculate the combination index (CI) values, which determines whether a combination of drugs is synergistic (CI < 1.0), additive (CI = 1) or antagonist (CI > 1). Since fraction inhibition values lower than 0.5 are generally considered as less clinically relevant, CI values are normally calculated at 0.5, 0.75 and 0.9. The combination of SB203580 and lapatinib showed a synergistic effect on cell growth inhibition in both RT112 and T24 cells, with mean CI values of 0.59 and 0.54 respectively.

There are, however, some limitations when using the Calcusyn programme to calculate the combination index. For instance, negative growth values or values greater than 100% growth cannot be entered into the programme, which can occur when performing replicates for non-treated cells or control cells. Another drawback is that dose-effect curves for single drugs need to have a similar shape and IC_{50} to use a constant ratio concentration when combined. This was particularly important for the combination of lapatinib and SB203580 in T24 cells, whose IC_{50} were very different; 8.6 and 70.1 µM respectively. When IC_{50} values are not similar, combinations with a non-fixed ratio are recommended. However, this design does not provide the F_a-CI plot simulation. In order to compare both cell lines, it was decided to use a constant ratio concentration in both cell lines. The F_a-CI plot is a computer generated graphical presentation of the combination index (CI) with respect to fraction affected (f_a) from 0.01 to 0.99 for the inhibitory effect of the drug combination. The sigmoidicity (*m*) of the dose-effect curves and the IC_{50} are included to calculate the combination index (CI).

The F_a-CI plot for T24 cells showed from slight antagonism to synergism between the two drugs at different values of fractional inhibition. This probably reflected the experimental difficulties when using this cell line; after some experimental repetitions it was still difficult to obtain reproducible IC_{50} effects on cell growth inhibition and none of the doses tested had the expected effect. For instance, the IC_{50} dose used for lapatinib

and SB203580 had 0% and 10% cell growth inhibition respectively. Despite this, calculated CI values at ED50, ED75 and ED90 were 0.64, 0.53 and 0.45 respectively, all showing synergism.

The F_a-CI plot for RT112 cells showed from slight synergism to synergism between the two drugs at all values of fractional inhibition. Four out of the 5 dose combinations tested ($2xIC_{50}$, $1.5xIC_{50}$, $1xIC_{50}$, $0.75xIC_{50}$) achieved 100% cell growth inhibition. The calculated CI values at ED50, ED75 and ED90 were 0.66, 0.59 and 0.53 respectively, all showing synergism. However, one flaw in these results was that the linear correlation coefficient (r) of the median effect plot for the combination of drugs was 0.74, and for tissue culture systems it is expected to be > 0.9.

These findings could provide a rationale for both the use of p38 MAPK inhibitors and the combined use of EGFR and/or HER2 inhibitors and p38 MAPK inhibitors for bladder cancer treatment. A schematic representation of a possible mechanism for this synergistic effect is shown in Figure 6.23. Lapatinib inhibits the phosphorylation of EGFR and/or HER2 receptors, inhibiting the activation of Ras-MAPK and PI3K/AKT pathways, leading to cell cycle arrest and apoptosis. At the same time, however, p38 MAPK is activated as a survival mechanism to this inhibition. The addition of SB203580 blocks p38 MAPK activity, inhibiting the survival mechanism and leading to a greater inhibition of cell growth.

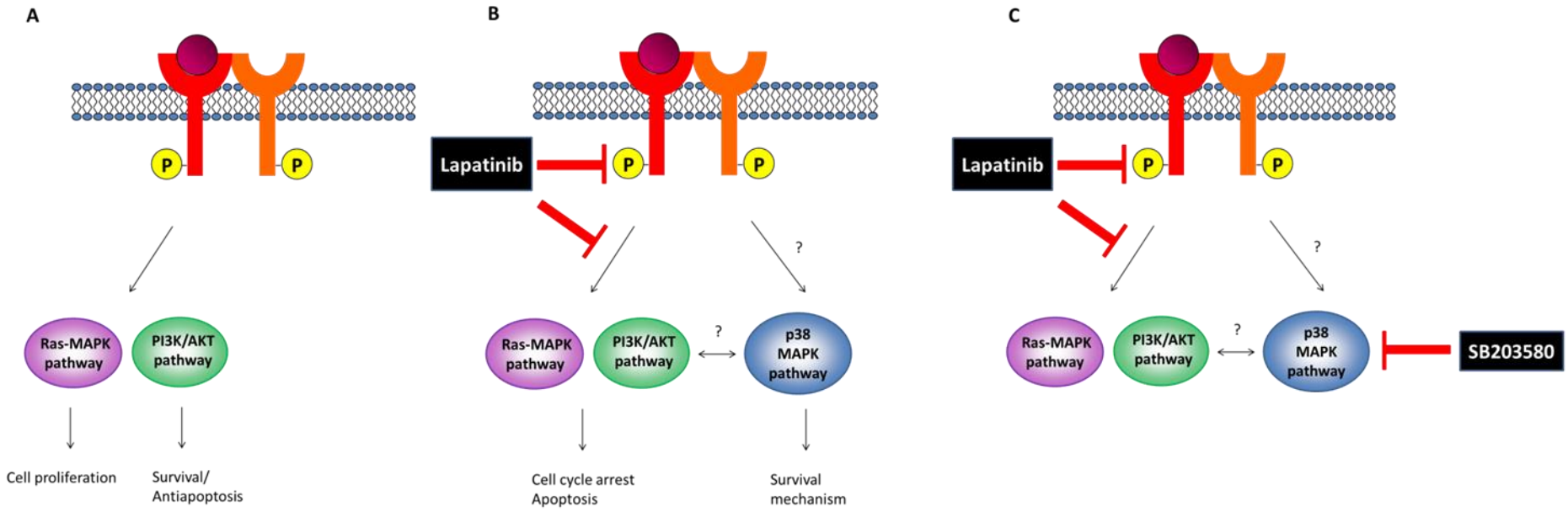

Figure 6.23 A schematic representation of a possible mechanism for the synergistic effect between lapatinib and SB203580. A) After ligand binding, HER receptors signal through Ras-MAPK and PI3K/Akt pathways. B) Lapatinib inhibits the phosphorylation of EGFR and/or HER2 receptors, inhibiting the activation of Ras-MAPK and PI3K/Akt pathways, leading to cell cycle arrest and apoptosis. At the same time, p38 MAPK is activated as a survival mechanism to this inhibition. C) SB203580 inhibits the catalytic activity of p38 MAPK, inhibiting the survival mechanism and leading to a synergistic effect on cell growth inhibition.

Chapter 7: Conclusion

7.1 Overview of results and discussion

Bladder cancer patients with invasive and advanced disease are currently treated with surgery and/or chemotherapy or radiotherapy, but treatment outcomes still remain far from optimal. The prospective use of targeted therapy in bladder cancer, consisting of the inhibition of molecular targets that play crucial roles in carcinogenesis, tumour progression and metastasis, could offer an advantage over conventional therapy as well as reducing side effects. Identification of novel molecular targets in bladder cancer in order to improve therapy has therefore become a priority and several targets have been identified during recent years. Among them are members of the HER family; they have been implicated in many tumours, including breast, colorectal, ovarian and non-small cell lung cancer, and they are normally associated with poor prognosis. EGFR and HER2 signalling are also suspected to have a role in the initiation and progression of bladder cancer. This has been supported not only with *in vitro* studies but also in very early clinical trial data. Therefore, therapeutic approaches involving the inhibition of the HER family are of potential interest for bladder cancer therapy. These therapies have already proved effective in breast, lung and colorectal cancer, so they could also be an effective treatment in bladder cancer.

It is therefore important to understand the molecular mechanisms that cause urothelial cell malignant transformation and progression in order to optimise treatment of bladder cancer patients. The main objective of this study was to investigate whether EGFR and/or HER2 inhibition could be effective as a novel treatment for these patients. Bladder cancer cell lines were chosen as a model system to investigate this. Here I will summarize key results of this study:

- Complex variability of expression of EGFR and HER2 (and the other HER family members) was found in a panel of six bladder cancer cell lines.

- Varying levels of ERK1/2 and Akt activation were also found among the cell lines, with no evident correlation with HER expression levels.

- Tyrosine kinase inhibitors (TKIs) directed at EGFR and/or HER2 (lapatinib, erlotinib and CP654577) had an antiproliferative effect in bladder cancer cells.

- EGFR and/or HER2 kinase inhibition using TKIs induced a cell cycle arrest at G_1 phase in bladder cancer cells.

- Lapatinib and CP654577 induced cell death and apoptosis in RT112 cells, whereas erlotinib induced little apoptosis on the same cells, potentially indicating differences relating to EGFR inhibition versus HER2 and/or EGFR inhibition.

- Sensitivity to EGFR inhibition in bladder cancer cells correlated to expression levels of EGFR.

- p38 MAPK was identified as a key downstream signalling node after EGFR and/or HER2 inhibition in bladder cancer cells.

- p38 MAPK inhibition had both activity as a single intervention and a synergistic effect when combined with lapatinib on cell growth inhibition in bladder cancer cells.

Overall, results were consistent with the initial hypothesis that EGFR and/or HER2 may play a major role in driving some subtypes of bladder cancer and that EGFR and/or HER2 directed therapies could be effective treatments for these patients.

Variable expression levels of EGFR and HER2 were found among the cell lines. Adding more cell lines in order to study EGFR/HER2 expression levels in bladder cancer would probably add complexity to these findings, so another potential approach would be to screen human tissue microarrays (TMA) for HER expression. Cell lines are generally used as preclinical models as they are easy to manipulate and can represent the heterogeneity of patients. However, use of TMA would be more clinically relevant despite its high-cost and ethical approval needed. TMA from the on-going LaMB trial

will be available in the near future (personal communication from Dr Simon Crabb) and may help elucidate expression levels of EGFR and HER2 in bladder cancer, which has been contradictory in the published literature. This trial (NCT00949455) tests lapatinib in EGFR or HER2 overexpressing patients with locally advanced or metastatic bladder cancer as maintenance therapy after first-line chemotherapy compared with placebo.

The HER receptors signal predominantly through both the mitogen-activated protein kinase (MAPK) pathway, which drives cell proliferation, and through the PI3K/Akt pathway, which drives cellular survival and antiapoptotic signals (Sergina and Moasser 2007). Characterization of the cell lines was limited to Akt and ERK1/2, but more nodes could have been investigated for both PI3K/Akt and Ras-MAPK pathways respectively, as well as other signalling pathways that can be activated by the HER receptors. This was addressed using a human phosphokinase array (described in Chapter 6).

Akt is known to be highly phosphorylated in a subset of primary human bladder tumours, suggesting that activation of the PI3K/Akt pathway may be important in the progression of some bladder tumours. Studies by Wu *et al*. showed that 55% of primary tumours from various stage/grades had high levels of phosphorylated Akt (Ser473), although this was done on a relatively small sample (20 patients). They also found a correlation between PI3K pathway activation and the invasive potential of bladder cancer cells lines. Such correlation could not be found with ERK1/2 pathway activation (Wu *et al.* 2004). *PTEN*, a tumour suppressor gene that inhibits the PI3K pathway by dephosphorylating PIP3, has also been found to be mutated or deleted in invasive bladder tumours (23%, also from a small sample of 35 cases) (Wang *et al.* 2000). A more recent study using tissue arrays analysed 887 samples and found that both high expression of phospho-Akt (Ser473) and loss of PTEN correlated significantly with high grade and advanced stage (Sun *et al.* 2011). In a study of 92 bladder tumours, mutations in the *PIK3CA* gene, which encodes the catalytic subunit of PI3K, p110, were found in 27% of the cases (Platt *et al.* 2009). Complexity of these data is in agreement with the results in this study. All together, these findings indicate that multiple components of the PI3K/Akt pathway can be altered in some bladder tumours and may be involved in bladder tumorigenesis and/or progression. The PI3K/Akt pathway is currently being investigated as a possible target for bladder cancer therapies (Ching and Hansel 2010).

Regarding the Ras-MAPK pathway, its activation through *FGFR3* and *HRAS* mutations is thought to be essential for the generation of superficial bladder cancer (Dovedi and Davies 2009). However, proliferation of TCC cell lines has been found to be less dependent on MAPK signalling pathways, despite being active in some cell lines (Swiatkowski *et al.* 2003). Moreover, a recent study found high levels of phospho-ERK1/2 in 60% of high grade tumours and 42% in low grade tumours. Surprisingly, these increased levels of phospho-ERK1/2 were not associated with *FGFR3* mutations and only tumours with *RAS* mutations showed slightly higher phospho-ERK1/2 levels (Juanpere *et al.* 2012).

Investigation of EGFR/HER2 inhibition was not done in combination with chemotherapy reagents, which could have been clinically relevant. Some preclinical data with lapatinib combined with chemotherapy agents (gemcitabine, paclitaxel and cisplatin, GTC or gemcitabine and cisplatin, GC) has showed promising activity in transitional cell carcinoma cell lines (McHugh *et al.* 2009; McHugh *et al.* 2007). Despite this, in the LaMB study, lapatinib is being tested as maintenance therapy after first-line chemotherapy and not in combination with chemotherapy as some unpublished data suggest it may be more effective in this way (personal communication from Dr Simon Crabb). On the other hand, gefitinib (EGFR TKI) has also been shown to be effective in combination with radiation in bladder cancer cell lines (Maddineni *et al.* 2005). Therefore, further work on combination or sequencing of these drugs with chemotherapy or radiotherapy is warranted.

All three TKIs induced G_1 arrest on RT112 cells and lapatinib and CP654577 also induced cell death and apoptosis. Even though targeting EGFR with erlotinib in RT112 bladder cancer cell line had little effect on apoptosis, these small molecules can enhance apoptosis when combined with other therapies. For instance, gefitinib (another EGFR TKI) was found to modestly induce apoptosis in two bladder cancer cell lines, but a significant induction of apoptosis was observed when gefitinib was given combined with ionizing radiation (Maddineni *et al.* 2005). Another study found that no apoptosis was induced in RT4 and T24 bladder cancer cell lines treated with gefitinib. However, the combination of gefitinib with etoposide (a topoisomerase inhibitor) might also improve the efficacy of this genotoxic drug by enhancing apoptosis (Munk *et al.* 2007).

Although a statistically significant correlation was found between EGFR expression and erlotinib sensitivity in the six bladder cancer cell lines, the discrepancy of most of the correlation studies done so far has led to the belief that EGFR and/or HER2 expression levels may not be the best biomarkers to assess sensitivity to TKIs against these receptors. One explanation for this is that expression of these receptors may not necessarily mean that they are transmitting signals. The HER family involves a complex interaction between ligands and receptors, which can subsequently activate different signalling pathways. Therefore, phosphorylated status of these proteins or dimerization patterns among HER family members could be a better prediction factor for TKI sensitivity, as well as key molecules downstream HER signalling. For instance, in colorectal cancer cell lines, sensitivity to gefitinib correlated with constitutive EGFR phosphorylation but not with EGFR expression levels (Van Schaeybroeck *et al.* 2005). Moasser *et al*. showed that in HER2-overexpressing human breast cancer cells, sensitivity to gefitinib (a TKI that selectively inhibits EGFR) correlated well with HER2 rather than EGFR expression levels (Moasser *et al.* 2001), suggesting that HER2 may require phosphorylation by EGFR in EGFR-HER2 dimers in these cell lines. In NSCLC cancer cell lines, gefitinib sensitivity correlated with EGFR-dependent activation of ERK1/2 and Akt on these cells for proliferation and survival (Ono *et al.* 2004). Another predictive marker of response to EGFR inhibition is E-cadherin; its expression in bladder cancer cell lines has been found to correlate to cetuximab sensitivity (Black *et al.* 2008) and to some extent to gefitinib sensitivity (Shrader *et al.* 2007).

There is an urgent need for biomarkers to predict which bladder cancer patients may respond to EGFR and/or HER2 targeted therapy. Further characterization of cell lines should reveal markers of response that can be translated into clinical practice by validation in patient samples. However, if the correlation found between erlotinib responsiveness with expression of EGFR protein can be confirmed, it could already provide a guide for selection of patients suitable for EGFR TKI therapy. Future experiments to confirm this correlation would be to increase the number of cell lines since the study was limited to only six and to check whether the correlation is maintained. Another possibility would be to induce depletion of EGFR in these cells to see whether cell lines resistant to erlotinib remain unaffected to this depletion and sensitive cell lines decrease their cell proliferation rate. Moreover, results from the LaMB study may also provide markers for therapeutic responses to lapatinib treatment

in bladder cancer patients. EGFR expression will be assessed in this trial as a potential predictive biomarker for lapatinib sensitivity (personal communication from Dr Simon Crabb).

The screening process used to investigate potential signalling pathways involved in EGFR or HER2 signalling in bladder cancer identified p38 MAPK as a key node downstream of these receptors. Further investigation of this pathway led to synergy assays, which showed that lapatinib combined with the p38 MAPK inhibitor SB203580 had a synergistic effect in cell growth inhibition in both RT112 and T24 cells. Determination of synergism of two drugs *in vitro* can be achieved relatively quickly, but the key issue is to understand the mechanism, which in most cases it cannot be predicted from the mechanism of action of the drugs (Chou 2010). Although the mechanism of action requires further investigation, the combination of lapatinib and the p38 MAPK inhibitor SB203580 was not an empirical finding since p38 MAPK pathway was indeed highlighted as a key component after EGFR and/or HER2 inhibition from the screening process set up in Chapter 6 using a human phosphokinase array. A possible explanation for this synergistic effect would be that lapatinib inhibits the activation of Ras-MAPK and PI3K/Akt pathways, leading to cell cycle arrest and apoptosis, but at the same time, p38 MAPK may be activated as a survival mechanism to this inhibition. The addition of a p38 MAPK inhibitor may lead to a greater inhibition of cell growth by inhibiting this survival mechanism.

The findings of this study could provide a rational for the combination of these drugs in bladder cancer treatment. Some of the potential advantages of using drug combinations are that they can mutually enhance the therapeutic effects, decrease side effects by using lower doses of the drug while maintaining the same efficacy or to delay or prevent drug resistance. However, combination of drugs can also increase toxicity, cost of the treatment, and it still potentially allows other resistance mechanisms to emerge. p38α is already an interesting pharmaceutical target due to its role in inflammatory diseases such as asthma, rheumathoid arthritis, chronic obstructive pulmonary disease or inflammatory bowel disease, but also for its suspected role in cancer (Yong *et al.* 2009). Several studies have showed good anti-inflammatory effects of p38 MAPK inhibitors, but these compounds have failed in clinical trials due to liver and neural side effects which could be due to off-target effects of these drugs or due to the wide range of p38

physiological functions in the cell (Cuadrado and Nebreda 2010). This might be overcome in the future by new p38 MAPK inhibitors that are in clinical development and which are increasingly selective for p38α, or by targeting p38 MAPK substrates specific for each disease. Combination of an EGFR/HER2 inhibitor with an inhibitor of p38 MAPK may be then a powerful therapeutic strategy for the treatment of bladder cancer patients that could be tested in clinical trials. Predictive biomarkers are needed (both preclinical and clinical) in order to identify which bladder cancer patients might be most likely to benefit from this combined approach to targeted therapy.

7.2 Drawbacks of this study

One of the main drawbacks of this study was that cell lines were chosen as the model system in which to study effects of EGFR and/or HER2 inhibition in bladder cancer. An alternative approach to this would be to use clinical samples or *in vivo* models. The use of *in vivo* models would offer the advantage that treatments could be tested, and also pathogenesis of bladder cancer could be investigated by using knockout models, such as $EGFR^{-/-}$ or $HER2^{-/-}$. These models are however more complex and costly. Another drawback is the use of tyrosine kinase inhibitors, which may have off-targets. This was addressed using siRNA knockdown in order to inhibit EGFR or HER2 specifically, although there was a reagent toxicity problem and this could not be investigated further.

7.3 Future work

The main findings of this study have been the discovery of p38 MAPK as a key molecule activated after EGFR and HER2 inhibition and the synergy effect in cell growth inhibition found between an EGFR/HER2 inhibitor and a p38 MAPK inhibitor in bladder cancer cell lines. The phosphokinase array results also showed that STAT4 phosphorylation was downregulated in RT112 cells after erlotinib or lapatinib treatment. Since these results could not be validated by Western blot due to the antibody sensitivity problem, it remains unknown whether STAT4 activation may be dependent to EGFR and/or HER2 signalling and whether it may have a role in bladder cancer

progression. Therefore this pathway would require further investigation. Another pathway that needs further studying is GSK-3α/β, which was also identified in the human phosphokinase array but whose upregulation was uncertain in the Western blot validation step.

Regarding the role of p38 MAPK in this bladder cancer model, future work should be aimed to elucidate three questions raised from these findings; i) understand further the biology of p38 MAPK in bladder cancer, ii) investigate the relationship between p38 MAPK and EGFR/HER2 signalling pathways and iii) understanding further the mechanisms of action responsible for the synergy effect on cell growth inhibition between EGFR/HER2 inhibitors and p38 MAPK inhibitors in bladder cancer cells.

7.3.1 Biology of p38 MAPK in bladder cancer

A first step to developing the findings here should be to examine the expression status of p38 MAPK in bladder cancer tumours, and to investigate whether it may be overexpressed or mutated. To take this forward, our group are currently staining for p38 MAPK in a tissue microarray derived from 200 bladder cancer cystectomies, which is on-going in the Histochemistry Research Unit (HRU) at the University of Southampton. This tissue microarray was collected by Dr James Douglas and information about grades and survival rates of these patients is available. The next step would be to determine the phosphorylated status of p38 MAPK in these samples.

Cell-based assays to investigate p38 MAPK role in bladder cancer would involve the inhibition, knockdown and overexpression of p38 MAPK in these cells and determine any changes in cell proliferation, cell cycle distribution, apoptosis and invasion. If any changes occur, it would also be necessary to study the p38 MAPK pathway to determine which the upstream and downstream effectors are. p38 MAPK is activated by dual phosphorylation in Thr180 and Tyr182 and MKK3 and MKK6 are the most relevant upstream kinases known for p38 MAPK, which show a high degree of specificity for p38 MAPK (Raingeaud *et al.* 1996). Inhibition of p38 MAPK by targeted drugs or siRNA knockdown would be used to evaluate possible changes in expression or phosphorylation levels of known p38 MAPK substrates. Since SB203580 had an inhibitory growth effect in RT112 and T24 cells, p38 MAPK inhibitors may be a

therapeutic strategy to be considered for bladder cancer treatment, which has also been suggested by other authors (Kumar *et al.* 2010).

7.3.2 Investigation of the cross-talk between EGFR/HER2 signalling and p38 MAPK

Further studies are needed to understand the precise mechanism by which EGFR/HER2 modulate p38 MAPK activity in bladder cancer cell lines. In the present study, EGFR and/or HER2 inhibition using erlotinib and lapatinib increased phosphorylation levels of p38 MAPK in RT112 and T24 cell lines. This should be confirmed by repeating EGFR/HER2 knockdown in these cells, which could only be done once. If this is confirmed, other bladder cancer cell lines should be also investigated. Levels of phosphorylated ERK1/2, JNKs and Akt should be checked as possible pathways involved in this cross-talk.

On the other hand, tissue microarrays from the LaMB study could be an invaluable source to investigate the significance of phospho-p38 MAPK upregulation prior to lapatinib treatment.

7.3.3 Synergy effect of dual inhibition on EGFR/HER2 and p38 MAPK

Synergy between lapatinib and the p38 MAPK inhibitor SB203580 could be due to the inhibition of p38 MAPK or because an off-target of the drug. Despite being highly specific for p38α and p38β, SB203580 can also target additional proteins due to the similarity in the ATP-binding site of different kinases such as CSNK1E, FRK, GAK, JNK1-2 and 3, PTK6, RIPK2, SLK, STK36, TNIK and EGFR (Fabian *et al.* 2005). This implies that SB203580 may have effects in the cell independent of p38 MAPK inhibition. For instance, studies by Lali *et al*. showed how the antiproliferative effects of SB203580 in IL-2 stimulated T cells were not dependent on p38 MAPK inhibition. Instead, they found that this drug inhibited phosphorylation of Akt by PDK-1 at Thr308, which blocked phosphorylation of Rb. They also ruled out a role for p38 MAP kinase in Akt activation (Lali *et al.* 2000).

Although there are other p38 MAPK inhibitors available that could also be tested, the next step would be to determine whether p38 MAPK knockdown has also a synergy effect in cell growth inhibition of RT112 and T24 cell lines treated with lapatinib.

In the same way, effect of EGFR or HER2 knockdown in conjunction to SB203580 should be investigated in synergy assays in bladder cancer cell lines. Although lapatinib is considered a tyrosine kinase with reasonable specificity, only binding weakly to STK10 and SLK in addition of its primary targets EGFR and HER2 (Fabian *et al.* 2005), it would rule out any off-target effect of this drug, and it could potentially reveal whether inhibition of one receptor is more important than the other for the synergy effect.

Next, work should be aimed at addressing the mechanism of these agents responsible for the synergy effect. It would be necessary to check effects on cell cycle progression and apoptosis. For instance, inhibition of phospho-Akt and phospho-ERK1/2 may be greater when both drugs are combined than with either drug alone, which may results in increased cell cycle arrest and/or apoptosis. Therefore, cell cycle progression markers and apoptosis markers should be studied. On the other hand, investigation of how cross-talk with other signalling pathways may contribute to the synergy observed here should also be sought.

Finally, other bladder cancer cell lines should also be tested for synergy effects between these two compounds. This could help to elucidate which are the predictive markers for this synergy effect and could potentially be used to select patients eligible for this treatment.

Appendix

PIXEL DENSITY

ARRAY A	DMSO		ERLOTINIB		T TEST
Positive Control	4846744	4976868	6078558	6065838	0.003159
*p38α	708561	873635.8	2545743	2202311	0.014179
ERK1/2 T202/Y204, T185/Y187	558006.9	523224.7	780629.9	717425.4	0.028674
JNK pan T183/Y185 T221/Y223	1360024	1192304	1819481	1865238	0.022768
*GSK-3α/β S21/S9	1571250	1518457	2196120	2162857	0.002408
*MEK1/2 S218/S222 S222/S226	782965.6	706422.3	1506723	1544544	0.002975
MSK1/2 S376/S360	1112721	1283424	1973525	1791171	0.031735
AMPKα1 T174	740247.7	663254	1149333	1252666	0.016251
*Akt S473	808405.1	817635.3	1123105	1136388	0.000651
*TOR S2448	901045.1	1140468	2050912	2037236	0.013453
CREB S133	2736398	2787783	3594556	3252306	0.062149
HSP27 S78/S82	1548625	1683026	2257523	2292531	0.010916
AMPKα2 T172	1197820	1243802	1632569	1849085	0.042432
β-Catenin	4185150	4551151	5170731	5279411	0.046214
*Src Y419	866431.7	828160	1409299	1386167	0.001646
Lyn Y397	899187.8	997624.8	1215126	1423313	0.084393
Lck Y394	817016.2	835082.7	1166161	1118321	0.006476
STAT2 Y689	1272393	1263613	1704835	1821958	0.013763
STAT5a Y694	1226580	1251963	1589907	1535370	0.008541
Fyn Y420	1165345	1211496	1484041	1451004	0.010181
Yes Y426	895585.7	916972.8	1079768	985946.3	0.1192
Fgr Y412	437957.6	348413.1	596644.4	592141.9	0.046225
STAT3 Y705	939823.3	1129268	1058269	1052303	0.847073
STAT5b Y699	1240312	1246391	1315421	1512351	0.225574
Hck Y411	1089927	1268397	1187098	1267750	0.670914
Chk-2 T68	1096118	1110977	1423088	1320148	0.035633
FAK Y397	715765	665336.5	908727.5	908221	0.013125
STAT6 Y641	1403192	1649088	1324482	1369057	0.287627
STAT5a/b Y694/Y699	2167838	2144762	2175971	2185201	0.189863
Positive Control	5661481	5542557	5463059	5528740	0.258644

% POSITIVE CONTROL

ARRAY A	DMSO		ERLOTINIB		T TEST
Positive Control	92.19754	94.67283	105.0917	104.8718	0.011382
*p38α	13.47865	16.6188	44.01317	38.07559	0.016284
ERK1/2 T202/Y204, T185/Y187	10.61473	9.95308	13.49625	12.40352	0.052887
JNK pan T183/Y185, T221/Y223	25.87116	22.68069	31.45688	32.24797	0.043976
*GSK-3α/β S21/S9	29.88922	28.88497	37.96856	37.39348	0.004832
*MEK1/2 S218/S222, S222/S226	14.89402	13.43797	26.04962	26.70351	0.004245
MSK1/2 S376/S360	21.16682	24.41403	34.12013	30.96743	0.049842
AMPKα1 T174	14.08142	12.6168	19.87073	21.65726	0.023418
*Akt S473	15.37794	15.55353	19.41729	19.64693	0.001261
*TOR S2448	17.1402	21.69464	35.45808	35.22163	0.0199
CREB S133	52.05333	53.03081	62.14602	56.22888	0.157022
HSP27 S78/S82	29.45883	32.01548	39.03016	39.6354	0.022569
AMPKα2 T172	22.78561	23.66031	28.22537	31.96871	0.070066
β-Catenin	79.61233	86.57461	89.39639	91.27536	0.182337
*Src Y419	16.48176	15.75373	24.36526	23.96534	0.002653
Lyn Y397	17.10487	18.97739	21.00823	24.60756	0.143211
Lck Y394	15.54175	15.88542	20.16167	19.33458	0.012098
STAT2 Y689	24.20419	24.03717	29.47477	31.49969	0.024529
STAT5a Y694	23.3327	23.81555	27.48779	26.54491	0.022868
Fyn Y420	22.16786	23.04577	25.65748	25.0863	0.034048
Yes Y426	17.03635	17.44318	18.66804	17.04595	0.537275
Fgr Y412	8.331081	6.627714	10.31534	10.2375	0.081689
STAT3 Y705	17.87786	21.48159	18.29633	18.19319	0.509478
STAT5b Y699	23.59393	23.70956	22.74221	26.14693	0.687373
Hck Y411	20.73322	24.12818	20.52365	21.91803	0.577469
Chk-2 T68	20.85099	21.13363	24.60366	22.82395	0.094352
FAK Y397	13.61569	12.65641	15.71093	15.70217	0.033101
STAT6 Y641	26.69233	31.36989	22.89887	23.66953	0.136206
STAT5a/b Y694/Y699	41.23786	40.7989	37.6202	37.77978	0.004916
Positive Control	107.6959	105.4337	94.45043	95.58599	0.011802

% GLOBAL MEAN

ARRAY A	DMSO		ERLOTINIB		T TEST
Positive Control	318.4301	326.9792	309.3718	308.7244	0.086011
*p38α	46.55232	57.3977	129.5671	112.0879	0.021594
ERK1/2 T202/Y204, T185/Y187	36.66094	34.37576	39.73062	36.51379	0.317724
JNK pan T183/Y185, T221/Y223	89.35331	78.33413	92.60357	94.93241	0.220069
*GSK-3α/β S21/S9	103.2308	99.76236	111.7728	110.0799	0.039421
*MEK1/2 S218/S222, S222/S226	51.44069	46.4118	76.68554	78.61049	0.008673
MSK1/2 S376/S360	73.10557	84.32072	100.4437	91.16273	0.143383
AMPKα1 T174	48.63413	43.57566	58.49597	63.75519	0.054245
*Akt S473	53.11205	53.71848	57.16111	57.83713	0.012138
*TOR S2448	59.19848	74.92854	104.3824	103.6863	0.042477
CREB S133	179.7808	183.1568	182.9471	165.528	0.50064
HSP27 S78/S82	101.7443	110.5745	114.898	116.6797	0.165959
AMPKα2 T172	78.69651	81.71754	83.09057	94.1103	0.279555
β-Catenin	274.9635	299.0098	263.1674	268.6987	0.23003
*Src Y419	56.92439	54.40995	71.72709	70.54978	0.007955
Lyn Y397	59.07646	65.54375	61.84457	72.44035	0.517728
Lck Y394	53.6778	54.86477	59.35245	56.91763	0.104047
STAT2 Y689	83.59597	83.01913	86.76859	92.72961	0.164399
STAT5a Y694	80.58604	82.2537	80.91928	78.14357	0.363732
Fyn Y420	76.56293	79.59505	75.53115	73.84969	0.189813
Yes Y426	58.83981	60.24494	54.95544	50.18032	0.107239
Fgr Y412	28.77373	22.89067	30.36657	30.13741	0.272071
STAT3 Y705	61.74621	74.1927	53.8612	53.55757	0.149093
STAT5b Y699	81.48828	81.88763	66.94911	76.97199	0.191992
Hck Y411	71.608	83.33344	60.41805	64.52287	0.137083
Chk-2 T68	72.01475	72.99094	72.4289	67.18972	0.418503
FAK Y397	47.02562	43.71248	46.25023	46.22445	0.652484
STAT6 Y641	92.18945	108.3447	67.41029	69.67898	0.060208
STAT5a/b Y694/Y699	142.4265	140.9105	110.7473	111.2171	0.000668
Positive Control	371.9582	364.1449	278.0456	281.3885	0.002306

Analysis of the human phospho-antibody array A in erlotinib treated cells. Quantitation of phosphorylated protein was performed using Quantity One software. Data were analysed in three different ways: by pixel density, by % of positive control and by % of global mean. Statistical analysis was performed using the Student's t-test (statistical significant changes are highlighted in pink $p<0.01$ and in yellow $p<0.05$).

* Shows statistically significant changes ($p<0.05$) found in all three analyses.

PIXEL DENSITY

	ARRAY B	DMSO		ERLOTINIB		T TEST
*	p53 S392	6566691	6535567	7143636	7170258	0.001141
	Positive Control	5496209	5531272	6390753	6361599	0.000698
	Akt T308	1429617	1439466	1962831	2368455	0.069112
	p53 S46	6054638	5907911	6561119	6607551	0.015894
	p70 S6 Kinase T389	772525.3	829876.6	1090462	1208147	0.033588
	p53 S15	5019557	5105556	5931212	5751166	0.016023
*	p27 T198	323677.2	359810.2	869161.4	820421.2	0.003617
	Paxillin Y118	693280.4	706056.4	1337314	1081006	0.057966
	p70 S6 Kinase T421/S424	1480383	1524620	1823027	1459896	0.526756
	RSK1/2/3 S380/S386/S377	1276642	1117871	1657052	1524564	0.06261
*	p27 T157	662212.8	663169.6	1030409	1129915	0.013909
*	PLCγ-1 Y783	661818.8	583080.5	1139427	1028889	0.020924
	p70 S6 Kinase T229	922291.5	1006095	918802	798640.1	0.286557
	RSK1/2 S221/S227	1519611	1399900	1399393	1440873	0.595514
	c-Jun S63	2057441	1762130	1825785	1923378	0.841937
	Pyk2 Y402	811753.8	839388.2	1005476	857117	0.296178
	STAT1 Y701	1237301	1290882	1359940	1221148	0.75614
*	STAT4 Y693	1434513	1395904	1133855	1155580	0.00664
	eNOS S1177	907883.3	1060407	1206571	1287392	0.093024

% POSITIVE CONTROL

	ARRAY B	DMSO		ERLOTINIB		T TEST
*	p53 S392	119.0968	118.5324	112.0364	112.4539	0.002843
	Positive Control	99.68203	100.318	100.2286	99.77138	1
	Akt T308	25.92825	26.10688	30.78383	37.14538	0.129825
	p53 S46	109.81	107.1489	102.9005	103.6287	0.063395
	p70 S6 Kinase T389	14.01091	15.05106	17.10213	18.94783	0.080918
	p53 S15	91.03724	92.59696	93.02145	90.19772	0.9094
*	p27 T198	5.870374	6.5257	13.63139	12.86698	0.005059
	Paxillin Y118	12.57369	12.8054	20.97361	16.95384	0.089373
	p70 S6 Kinase T421/S424	26.84897	27.65129	28.59123	22.89611	0.652638
	RSK1/2/3 S380/S386/S377	23.15383	20.27428	25.98817	23.91032	0.210015
*	p27 T157	12.01023	12.02758	16.1603	17.72089	0.024229
*	PLCγ-1 Y783	12.00308	10.57504	17.87007	16.13646	0.036522
	p70 S6 Kinase T229	16.72715	18.24705	14.40992	12.52538	0.079974
	RSK1/2 S221/S227	27.56044	25.38929	21.94722	22.59776	0.065643
	c-Jun S63	37.3148	31.95888	28.63448	30.16506	0.200807
	Pyk2 Y402	14.72238	15.22357	15.76926	13.44249	0.786892
	STAT1 Y701	22.44032	23.41208	21.32845	19.15173	0.152962
*	STAT4 Y693	26.01706	25.31682	17.78268	18.1234	0.002538
	eNOS S1177	16.46583	19.23208	18.92312	20.19066	0.378274

% GLOBAL MEAN

	ARRAY B	DMSO		ERLOTINIB		T TEST
*	p53 S392	318.3362	316.8274	298.364	299.4759	0.002512
	Positive Control	266.442	268.1418	266.9188	265.7011	0.446739
	Akt T308	69.30412	69.78159	81.9804	98.92184	0.132412
	p53 S46	293.5132	286.4003	274.0343	275.9736	0.055743
	p70 S6 Kinase T389	37.45004	40.23028	45.54466	50.45996	0.08328
	p53 S15	243.3352	247.5042	247.7254	240.2055	0.767368
*	p27 T198	15.69104	17.44267	36.30174	34.26604	0.005107
	Paxillin Y118	33.60845	34.22779	55.8548	45.14975	0.090545
	p70 S6 Kinase T421/S424	71.76514	73.90966	76.14128	60.97461	0.632535
	RSK1/2/3 S380/S386/S377	61.88833	54.19151	69.20908	63.67555	0.218274
*	p27 T157	32.10237	32.14875	43.03648	47.1925	0.024655
*	PLCγ-1 Y783	32.08327	28.26624	47.58977	42.97301	0.037135
	p70 S6 Kinase T229	44.71031	48.7729	38.37505	33.35632	0.077953
	RSK1/2 S221/S227	73.66683	67.86353	58.44762	60.18008	0.063356
	c-Jun S63	99.73944	85.42352	76.25646	80.33256	0.19489
	Pyk2 Y402	39.35173	40.69138	41.99512	35.79869	0.756659
	STAT1 Y701	59.98117	62.57861	56.79978	51.00297	0.14582
*	STAT4 Y693	69.54149	67.66981	47.35705	48.26442	0.002492
	eNOS S1177	44.01184	51.40581	50.39414	53.76974	0.39447

Analysis of the human phospho-antibody array B in erlotinib treated cells. Quantitation of phosphorylated protein was performed using Quantity One software. Data were analysed in three different ways: by pixel density, by % of positive control and by % of global mean. Statistical analysis was performed using the Student's t-test (statistical significant changes are highlighted in pink $p<0.01$ and in yellow $p<0.05$).

* Shows statistically significant changes ($p<0.05$) found in all three analyses.

PIXEL DENSITY

	ARRAY A	DMSO		LAPATINIB		T TEST
	Positive Control	5019123	4944603	5084131	4994521	0.428041
*	p38α	505375.9	586958.5	953983.6	1026729	0.014803
	ERK1/2 T202/Y204, T185/Y187	729515.8	726196.9	889844.4	909680.5	0.003404
	JNK pan T183/Y185, T221/Y223	633384.2	602819.6	1179011	1049266	0.017578
*	GSK-3α/β S21/S9	962493.1	797282.6	1538453	1462157	0.020838
	MEK1/2 S218/S222, S222/S226	666457.1	653644.7	719038.1	903428.7	0.243503
	MSK1/2 S376/S360	1437787	1322321	2145576	2313989	0.014131
	AMPKα1 T174	408318.1	370922.9	778430.6	844113.4	0.007937
	Akt S473	874311.3	1003979	1333995	1291814	0.0317
	TOR S2448	884731.1	950452.5	1166546	1217834	0.022275
	CREB S133	3194012	3067123	3302358	3528968	0.159321
	HSP27 S78/S82	878633.6	819395.5	1520045	1717363	0.017444
	AMPKα2 T172	512322.4	673558	796144.1	799077.1	0.12643
	β-Catenin	4742576	4881120	4897193	4792108	0.742234
	Src Y419	641990.1	488318.4	665511.6	718999.6	0.258638
	Lyn Y397	421786.6	536828	490576	539934.7	0.623734
	Lck Y394	347845.1	349195.8	323281.6	590566.8	0.502468
	STAT2 Y689	678111.8	754175.8	802588.9	872362.5	0.143092
	STAT5a Y694	983409.7	753211	1151187	1036492	0.221556
	Fyn Y420	827615.5	784277.2	730538.4	923187.6	0.85185
	Yes Y426	543697.3	534744.1	379355.1	475023.6	0.144957
	Fgr Y412	275177.2	183290.7	211790.5	327719.6	0.63877
	STAT3 Y705	327700.3	580475.1	573046.2	443147	0.740454
	STAT5b Y699	779916.4	603977.4	643475.9	793867.2	0.838845
	Hck Y411	679153.8	697947.9	796761.6	661884	0.6101
	Chk-2 T68	732911.8	829197.8	648994.4	634908.5	0.103667
	FAK Y397	305625.9	383465.1	407449.8	414396.3	0.231464
	STAT6 Y641	932739	1010578	794754.8	771870	0.043393
	STAT5a/b Y694/Y699	1135808	1469741	1037689	1009131	0.237426
	Positive Control	5173412	5083108	4842895	4819238	0.02379

% POSITIVE CONTROL

	ARRAY A	DMSO		LAPATINIB		T TEST
	Positive Control	99.28906	97.81489	103.0178	101.2021	0.093174
*	p38α	9.997423	11.6113	19.33021	20.80421	0.013636
	ERK1/2 T202/Y204, T185/Y187	14.43139	14.36574	18.03058	18.43251	0.00281
	JNK pan T183/Y185, T221/Y223	12.5297	11.92507	23.88985	21.26088	0.016569
*	GSK-3α/β S21/S9	19.04018	15.77197	31.17309	29.62714	0.01881
	MEK1/2 S218/S222, S222/S226	13.18396	12.9305	14.5696	18.30583	0.212765
	MSK1/2 S376/S360	28.44252	26.15835	43.47498	46.88748	0.01293
	AMPKα1 T174	8.077411	7.337653	15.77304	17.10395	0.007518
	Akt S473	17.29576	19.86087	27.03023	26.17554	0.027227
	TOR S2448	17.50188	18.802	23.63728	24.67651	0.01867
	CREB S133	63.18443	60.67429	66.91442	71.50613	0.108523
	HSP27 S78/S82	17.38126	16.20941	30.80009	34.79828	0.016525
	AMPKα2 T172	10.13484	13.32443	16.13196	16.19139	0.108793
	β-Catenin	93.81836	96.55906	99.22996	97.10066	0.228425
	Src Y419	12.69995	9.65999	13.48501	14.56881	0.219739
	Lyn Y397	8.343846	10.61961	9.940356	10.94049	0.521179
	Lck Y394	6.881125	6.907845	6.550532	11.96643	0.47473
	STAT2 Y689	13.41451	14.91922	16.26255	17.67635	0.113122
	STAT5a Y694	19.45396	14.90013	23.32605	21.00205	0.190355
	Fyn Y420	16.37202	15.51469	14.80262	18.7062	0.724141
	Yes Y426	10.7555	10.57839	7.686729	9.625223	0.174789
	Fgr Y412	5.443597	3.625884	4.291431	6.640458	0.594674
	STAT3 Y705	6.482618	11.48305	11.61142	8.979319	0.687923
	STAT5b Y699	15.42842	11.94797	13.03851	16.08583	0.741873
	Hck Y411	13.43512	13.80691	16.14448	13.4115	0.489794
	Chk-2 T68	14.49857	16.40332	13.15033	12.86491	0.126525
	FAK Y397	6.045939	7.585766	8.256	8.396754	0.189939
	STAT6 Y641	18.45158	19.99141	16.10381	15.64011	0.053079
	STAT5a/b Y694/Y699	22.46872	29.07463	21.02629	20.44764	0.268213
	Positive Control	102.3412	100.5548	98.12973	97.65039	0.061404

% GLOBAL MEAN

	ARRAY A	DMSO		LAPATINIB		T TEST
	Positive Control	414.3536	408.2015	368.9124	362.4102	0.00949
*	p38α	41.72129	48.45634	69.22253	74.50103	0.0246
	ERK1/2 T202/Y204, T185/Y187	60.22515	59.95116	64.56849	66.00783	0.019276
	JNK pan T183/Y185, T221/Y223	52.28901	49.76575	85.55087	76.13638	0.02569
*	GSK-3α/β S21/S9	79.45858	65.81964	111.6325	106.0964	0.038886
	MEK1/2 S218/S222, S222/S226	55.01935	53.96162	52.17452	65.55418	0.581439
	MSK1/2 S376/S360	118.6964	109.1642	155.6863	167.9066	0.025222
	AMPKα1 T174	33.70869	30.62153	56.48413	61.25018	0.011118
	Akt S473	72.17874	82.88345	96.79673	93.73604	0.086004
	TOR S2448	73.03894	78.46457	84.64638	88.36794	0.082183
	CREB S133	263.6816	253.2062	239.6242	256.0674	0.390525
	HSP27 S78/S82	72.53557	67.64517	110.2968	124.6146	0.024573
	AMPKα2 T172	42.29476	55.60556	57.76945	57.98227	0.311939
	β-Catenin	391.5232	402.9607	355.3479	347.7228	0.021873
	Src Y419	52.99947	40.31311	48.29056	52.17172	0.643907
	Lyn Y397	34.82058	44.31782	35.59696	39.1785	0.709192
	Lck Y394	28.71634	28.82785	23.45781	42.85244	0.695574
	STAT2 Y689	55.9815	62.26096	58.23709	63.29997	0.722527
	STAT5a Y694	81.18536	62.18131	83.53188	75.20949	0.535847
	Fyn Y420	68.32377	64.74598	53.009	66.98792	0.460574
	Yes Y426	44.88492	44.14578	27.5266	34.46845	0.060672
	Fgr Y412	22.71724	15.13155	15.36785	23.77984	0.919181
	STAT3 Y705	27.05329	47.9211	41.58112	32.15543	0.961802
	STAT5b Y699	64.38597	49.86133	46.6916	57.60423	0.638816
	Hck Y411	56.06752	57.61906	57.81425	48.02733	0.511522
	Chk-2 T68	60.50551	68.4544	47.09204	46.06995	0.046642
	FAK Y397	25.23094	31.65695	29.56519	30.06924	0.711512
	STAT6 Y641	77.00223	83.42825	57.66864	56.00808	0.019563
	STAT5a/b Y694/Y699	93.76658	121.3344	75.2963	73.22411	0.13768
	Positive Control	427.0909	419.6358	351.4079	349.6914	0.002748

Analysis of the human phospho-antibody array A in lapatinib treated cells. Quantitation of phosphorylated protein was performed using Quantity One software. Data were analysed in three different ways: by pixel density, by % of positive control and by % of global mean. Statistical analysis was performed using the Student's t-test (statistical significant changes are highlighted in pink $p<0.01$ and in yellow $p<0.05$).

* Shows statistically significant changes ($p<0.05$) found in all three analyses.

PIXEL DENSITY

ARRAY B	DMSO		LAPATINIB		T TEST
p53 S392	6120064	6107869	5753849	5643361	0.017438
Positive Control	5450152	5501325	5262115	5379549	0.136749
Akt T308	1922497	2102025	2532996	2398698	0.055999
p53 S46	5602859	5565734	5307151	5326447	0.006061
p70 S6 Kinase T389	1575945	1553214	1202398	1295712	0.022389
p53 S15	4984584	5022404	4801293	4783811	0.009613
p27 T198	1111495	959444.3	1186343	1054399	0.48777
Paxillin Y118	1773379	1565100	1451197	1641647	0.475873
p70 S6 Kinase T421/S424	2476788	2474125	1705825	2166222	0.143837
RSK1/2/3 S380/S386/S377	2658361	2605684	2241437	2464689	0.13551
p27 T157	1570426	1614459	1592828	1543277	0.538415
PLCγ-1 Y783	1761879	1545187	1727590	1608651	0.91683
p70 S6 Kinase T229	1466036	1384762	1156242	1125060	0.022576
RSK1/2 S221/S227	2882154	2600705	1922246	1877557	0.027492
c-Jun S63	4110446	4107359	3784946	3808293	0.001419
Pyk2 Y402	1497102	1355201	1649365	1307907	0.803195
STAT1 Y701	2168480	2521785	1723731	1891141	0.11066
*STAT4 Y693	2606841	2847884	1752713	1814691	0.016949
eNOS S1177	1947273	1937355	1564618	1592443	0.001644

% POSITIVE CONTROL

ARRAY B	DMSO		LAPATINIB		T TEST
p53 S392	111.7669	111.5442	108.1381	106.0616	0.04873
Positive Control	99.53273	100.4673	98.89647	101.1035	1
Akt T308	35.10936	38.38797	47.60527	45.08125	0.043483
p53 S46	102.3215	101.6435	99.74288	100.1055	0.03316
p70 S6 Kinase T389	28.78049	28.36538	22.59792	24.35168	0.02985
p53 S15	91.03034	91.72102	90.23576	89.9072	0.076272
p27 T198	20.29854	17.52173	22.2962	19.81643	0.368116
Paxillin Y118	32.38612	28.58245	27.27388	30.8532	0.640958
p70 S6 Kinase T421/S424	45.23203	45.1834	32.05936	40.71209	0.178286
RSK1/2/3 S380/S386/S377	48.54799	47.58597	42.12569	46.3215	0.216072
p27 T157	28.67971	29.48386	29.9357	29.00443	0.592462
PLCγ-1 Y783	32.17609	28.21879	32.46842	30.23307	0.662231
p70 S6 Kinase T229	26.7733	25.28905	21.73047	21.14444	0.028868
RSK1/2 S221/S227	52.63497	47.49506	36.1268	35.28691	0.031354
c-Jun S63	75.06651	75.01013	71.13447	71.57327	0.003585
Pyk2 Y402	27.34064	24.74919	30.99826	24.58087	0.664199
STAT1 Y701	39.60159	46.0538	32.39589	35.54221	0.132342
*STAT4 Y693	47.60712	52.00913	32.94059	34.10541	0.018991
eNOS S1177	35.56183	35.3807	29.40551	29.92845	0.002265

% GLOBAL MEAN

ARRAY B	DMSO		LAPATINIB		T TEST
p53 S392	217.2295	216.7967	225.3099	220.9834	0.106026
Positive Control	193.4513	195.2676	206.0546	210.6531	0.029817
Akt T308	68.23836	74.61064	99.18739	93.9285	0.025968
p53 S46	198.8715	197.5538	207.8181	208.5737	0.005738
p70 S6 Kinase T389	55.93761	55.1308	47.08363	50.73765	0.071359
p53 S15	176.9261	178.2685	188.0096	187.3251	0.005551
p27 T198	39.45213	34.05514	46.45499	41.28828	0.19701
Paxillin Y118	62.94548	55.5527	56.82617	64.28381	0.826786
p70 S6 Kinase T421/S424	87.91272	87.8182	66.79689	84.82519	0.312939
RSK1/2/3 S380/S386/S377	94.3576	92.48783	87.77047	96.51261	0.801367
p27 T157	55.74173	57.30466	62.37218	60.43183	0.059445
PLCγ-1 Y783	62.53728	54.84588	67.64919	62.99176	0.278303
p70 S6 Kinase T229	52.03643	49.15165	45.27627	44.05524	0.063253
RSK1/2 S221/S227	102.301	92.31113	75.27155	73.52161	0.045666
c-Jun S63	145.8989	145.7893	148.2114	149.1256	0.025557
Pyk2 Y402	53.13912	48.10238	64.58605	51.21518	0.415401
STAT1 Y701	76.96943	89.5099	67.49808	74.05355	0.220196
*STAT4 Y693	92.52893	101.0847	68.63297	71.05991	0.026141
eNOS S1177	69.11777	68.76573	61.26751	62.35706	0.006387

Analysis of the human phospho-antibody array B in lapatinib treated cells. Quantitation of phosphorylated protein was performed using Quantity One software. Data were analysed in three different ways: by pixel density, by % of positive control and by % of global mean. Statistical analysis was performed using the Student's t-test (statistical significant changes are highlighted in pink $p<0.01$ and in yellow $p<0.05$).

* Shows statistically significant changes ($p<0.05$) found in all three analyses.

References

Agarwal, P. K., Black, P. C., McConkey, D. J., and Dinney, C. P. N. (2007). Emerging drugs for targeted therapy of bladder cancer. *Expert Opinion on Emerging Drugs* **12,** 435-48.

Agus, D. B., Akita, R. W., Fox, W. D., Lewis, G. D., Higgins, B., Pisacane, P. I., Lofgren, J. A., Tindell, C., Evans, D. P., Maiese, K., Scher, H. I., and Sliwkowski, M. X. (2002). Targeting ligand-activated ErbB2 signaling inhibits breast and prostate tumor growth. *Cancer Cell* **2,** 127-37.

Alessi, D. R., James, S. R., Downes, C. P., Holmes, A. B., Gaffney, P. R. J., Reese, C. B., and Cohen, P. (1997). Characterization of a 3-phosphoinositide-dependent protein kinase which phosphorylates and activates protein kinase B alpha. *Current Biology* **7,** 261-9.

Altomare, D. A., and Testa, J. R. (2005). Perturbations of the AKT signaling pathway in human cancer. *Oncogene* **24,** 7455-64.

Ambrosino, C., and Nebreda, A. R. (2001). Cell cycle regulation by p38 MAP kinases. *Biology of the Cell* **93,** 47-51.

Arrington, A. K., Dahlberg, P. S., Davydova, J., Vickers, S. M., and Yamamoto, M. (2009). ERBB2 suppression decreases cell growth via apoptosis in gastrointestinal adenocarcinomas. *Surgery* **146,** 213-9.

Atalay, G., Cardoso, F., Awada, A., and Piccart, M. J. (2003). Novel therapeutic strategies targeting the epidermal growth factor receptor (EGFR) family and its downstream effectors in breast cancer. [Review] [188 refs]. *Annals of Oncology* **14,** 1346-63.

Barbacci, E. G., Pustilnik, L. R., Rossi, A. M., Emerson, E., Miller, P. E., Boscoe, B. P., Cox, E. D., Iwata, K. K., Jani, J. P., Provoncha, K., Kath, J. C., Liu, Z., and Moyer, J. D. (2003). The biological and biochemical effects of CP-654577, a selective erbB2 kinase inhibitor, on human breast cancer cells. *Cancer Research* **63,** 4450-9.

Baselga, J. (2001). The EGFR as a target for anticancer therapy - focus on cetuximab. *European Journal of Cancer* **37,** S16-S22.

Bellmunt, J., Hussain, M., and Dinney, C. P. (2003). Novel approaches with targeted therapies in bladder cancer. Therapy of bladder cancer by blockade of the epidermal growth factor receptor family. [Review] [207 refs]. *Critical Reviews in Oncology-Hematology* **46,** Suppl-104.

Billerey, C., Chopin, D., Aubriot-Lorton, M. H., Ricol, D., Gil Diez de, M. S., Van, R. B., Bralet, M. P., Lefrere-Belda, M. A., Lahaye, J. B., Abbou, C. C., Bonaventure, J., Zafrani, E. S., van der Kwast, T., Thiery, J. P., and Radvanyi, F. (2001). Frequent FGFR3 mutations in papillary non-invasive bladder (pTa) tumors. *American Journal of Pathology* **158,** 1955-9.

Black, P. C., Brown, G. A., Inamoto, T., Shrader, M., Arora, A., Siefker-Radtke, A. O., Adam, L., Theodorescu, D., Wu, X., Munsell, M. F., Bar-Eli, M., McConkey, D. J., and Dinney, C. P. (2008). Sensitivity to epidermal growth factor receptor inhibitor requires E-cadherin expression in urothelial carcinoma cells. *Clinical Cancer Research* **14,** 1478-86.

Blehm, K. N., Spiess, P. E., Bondaruk, J. E., Dujka, M. E., Villares, G. J., Zhao, Y. J., Bogler, O., Aldape, K. D., Grossman, H. B., Adam, L., McConkey, D. J., Czerniak, B. A., Dinney, C. P., and Bar-Eli, M. (2006). Mutations within the kinase domain and truncations of the epidermal growth factor receptor are rare events in bladder cancer: Implications for therapy. *Clinical Cancer Research* **12,** 4671-7.

Bowman, T., Garcia, R., Turkson, J., and Jove, R. (2000). STATs in oncogenesis. *Oncogene* **19,** 2474-88.

Brummelkamp, T. R., Bernards, R., and Agami, R. (2002). A system for stable expression of short interfering RNAs in mammalian cells. *Science* **296,** 550-3.

Burgess, A. W., Cho, H. S., Eigenbrot, C., Ferguson, K. M., Garrett, T. P., Leahy, D. J., Lemmon, M. A., Sliwkowski, M. X., Ward, C. W., and Yokoyama, S. (2003). An open-and-shut case? Recent insights into the activation of EGF/ErbB receptors. [Review] [88 refs]. *Molecular Cell* **12,** 541-52.

Cairns, P., Shaw, M. E., and Knowles, M. A. (1993). Initiation of Bladder-Cancer May Involve Deletion of A Tumor-Suppressor Gene on Chromosome-9. *Oncogene* **8,** 1083-5.

Cantley, L. C. (2002). The phosphoinositide 3-kinase pathway. *Science* **296,** 1655-7.

Carter, P., Presta, L., Gorman, C. M., Ridgway, J. B. B., Henner, D., Wong, W. L. T., Rowland, A. M., Kotts, C., Carver, M. E., and Shepard, H. M. (1992). Humanization of An Anti-P185Her2 Antibody for Human Cancer-Therapy. *Proceedings of the National Academy of Sciences of the United States of America* **89,** 4285-9.

Chen, L., Mayer, J. A., Krisko, T. I., Speers, C. W., Wang, T., Hilsenbeck, S. G., and Brown, P. H. (2009). Inhibition of the p38 Kinase Suppresses the Proliferation of Human ER-Negative Breast Cancer Cells. *Cancer Research* **69,** 8853-61.

Chen, P. C. H., Yu, H. J., Chang, Y. H., and Pan, C. C. (2013). Her2 amplification distinguishes a subset of non-muscle-invasive bladder cancers with a high risk of progression. *Journal of Clinical Pathology* **66,** 113-9.

Ching, C. B., and Hansel, D. E. (2010). Expanding therapeutic targets in bladder cancer: the PI3K/Akt/mTOR pathway. [Review]. *Laboratory Investigation* **90,** 1406-14.

Chou, T. C., and Talalay, P. (1984). Quantitative-Analysis of Dose-Effect Relationships - the Combined Effects of Multiple-Drugs Or Enzyme-Inhibitors. *Advances in Enzyme Regulation* **22,** 27-55.

Chou, T. C. (2006). Theoretical basis, experimental design, and computerized simulation of synergism and antagonism in drug combination studies. *Pharmacological Reviews* **58,** 621-81.

Chou, T. C. (2010). Drug Combination Studies and Their Synergy Quantification Using the Chou-Talalay Method. *Cancer Research* **70,** 440-6.

Choudhury, A., Charo, J., Parapuram, S. K., Hunt, R. C., Hunt, D. M., Seliger, B., and Kiessling, R. (2004). Small interfering RNA (siRNA) inhibits the expression of the Her2/neu gene, upregulates HLA class I and induces apoptosis of Her2/neu positive tumor cell lines. *International Journal of Cancer* **108,** 71-7.

Chow, N. H., Chan, S. H., Tzai, T. S., Ho, C. L., and Liu, H. S. (2001). Expression profiles of ErbB family receptors and prognosis in primary transitional cell carcinoma of the urinary bladder. *Clinical Cancer Research* **7,** 1957-62.

Ciardiello, F., and Tortora, G. (2008). Drug therapy: EGFR antagonists in cancer treatment. *New England Journal of Medicine* **358,** 1160-74.

Citri, A., and Yarden, Y. (2006). EGF-ERBB signalling: towards the systems level. [Review] [142 refs]. *Nature Reviews Molecular Cell Biology* **7,** 505-16.

Cordon-Cardo, C., Wartinger, D., Petrylak, D., Dalbagni, G., Fair, W. R., Fuks, Z., and Reuter, V. E. (1992). Altered expression of the retinoblastoma gene product: prognostic indicator in bladder cancer. *Journal of the National Cancer Institute* **84,** 1251-6.

CordonCardo, C., Zhang, Z. F., Dalbagni, G., Drobnjak, M., Charytonowicz, E., Hu, S. X., Xu, H. J., Reuter, V. E., and Benedict, W. F. (1997). Cooperative effects of p53 and pRB alterations in primary superficial bladder tumors. *Cancer Research* **57,** 1217-21.

Cote, R. J., Dunn, M. D., Chatterjee, S. J., Stein, J. P., Shi, S. R., Tran, Q. C., Hu, S. X., Xu, H. J., Groshen, S., Taylor, C. R., Skinner, D. G., and Benedict, W. F. (1998). Elevated and absent pRb expression is associated with bladder cancer progression and has cooperative effects with p53. *Cancer Research* **58,** 1090-4.

Cross, D. A. E., Alessi, D. R., Cohen, P., Andjelkovich, M., and Hemmings, B. A. (1995). Inhibition of Glycogen-Synthase Kinase-3 by Insulin-Mediated by Protein-Kinase-B. *Nature* **378,** 785-9.

Cuadrado, A., and Nebreda, A. R. (2010). Mechanisms and functions of p38 MAPK signalling. *Biochemical Journal* **429,** 403-17.

Cuenda, A., Rouse, J., Doza, Y. N., Meier, R., Cohen, P., Gallagher, T. F., Young, P. R., and Lee, J. C. (1995). Sb-203580 Is A Specific Inhibitor of A Map Kinase Homolog Which Is Stimulated by Cellular Stresses and Interleukin-1. *FEBS Letters* **364,** 229-33.

Cunningham, D., Humblet, Y., Siena, S., Khayat, D., Bleiberg, H., Santoro, A., Bets, D., Mueser, M., Harstrick, A., Verslype, C., Chau, I., and Van Cutsem, E. (2004). Cetuximab monotherapy and cetuximab plus irinotecan in irinotecan-refractory metastatic colorectal cancer. *New England Journal of Medicine* **351,** 337-45.

Doble, B. W., and Woodgett, J. R. (2003). GSK-3: tricks of the trade for a multi-tasking kinase. *Journal of Cell Science* **116,** 1175-86.

Dominguez-Escrig, J. L., Kelly, J. D., Neal, D. E., King, S. M., and Davies, B. R. (2004). Evaluation of the therapeutic potential of the epidermal growth factor receptor

tyrosine kinase inhibitor gefitinib in preclinical models of bladder cancer. *Clinical Cancer Research* **10,** 4874-84.

Dovedi, S. J., and Davies, B. R. (2009). Emerging targeted therapies for bladder cancer: a disease waiting for a drug. [Review] [105 refs]. *Cancer & Metastasis Reviews* **28,** 355-67.

Elbashir, S. M., Harborth, J., Lendeckel, W., Yalcin, A., Weber, K., and Tuschl, T. (2001). Duplexes of 21-nucleotide RNAs mediate RNA interference in cultured mammalian cells. *Nature* **411,** 494-8.

Engelman, J. A., Zejnullahu, K., Mitsudomi, T., Song, Y., Hyland, C., Park, J. O., Lindeman, N., Gale, C. M., Zhao, X., Christensen, J., Kosaka, T., Holmes, A. J., Rogers, A. M., Cappuzzo, F., Mok, T., Lee, C., Johnson, B. E., Cantley, L. C., and Janne, P. A. (2007). MET amplification leads to gefitinib resistance in lung cancer by activating ERBB3 signaling. *Science* **316,** 1039-43.

Fabian, M. A., Biggs, W. H., Treiber, D. K., Atteridge, C. E., Azimioara, M. D., Benedetti, M. G., Carter, T. A., Ciceri, P., Edeen, P. T., Floyd, M., Ford, J. M., Galvin, M., Gerlach, J. L., Grotzfeld, R. M., Herrgard, S., Insko, D. E., Insko, M. A., Lai, A. G., Lelias, J. M., Mehta, S. A., Milanov, Z. V., Velasco, A. M., Wodicka, L. M., Patel, H. K., Zarrinkar, P. P., and Lockhart, D. J. (2005). A small molecule-kinase interaction map for clinical kinase inhibitors. *Nature Biotechnology* **23,** 329-36.

Faltus, T., Yuan, J., Zimmer, B., Kramer, A., Loibl, S., Kaufmann, M., and Strebhardt, K. (2004). Silencing of the HER2/neu gene by siRNA inhibits proliferation and induces apoptosis in HER2/neu-overexpressing breast cancer cells. *Neoplasia (New York)* **6,** 786-95.

Faust, D., Schmitt, C., Oesch, F., Oesch-Bartlomowicz, B., Schreck, I., Weiss, C., and Dietrich, C. (2012). Differential p38-dependent signalling in response to cellular stress and mitogenic stimulation in fibroblasts. *Cell Communication and Signaling* **10**.

Frantz, B., Klatt, T., Pang, M., Parsons, J., Rolando, A., Williams, H., Tocci, M. J., O'Keefe, S. J., and O'Neill, E. A. (1998). The activation state of p38 mitogen-activated protein kinase determines the efficiency of ATP competition for pyridinylimidazole inhibitor binding. *Biochemistry* **37,** 13846-53.

Gaborit, N., Larbouret, C., Vallaghe, J., Peyrusson, F., Bascoul-Mollevi, C., Crapez, E., Azria, D., Chardes, T., Poul, M. A., Mathis, G., Bazin, H., and Pelegrin, A. (2011). Time-resolved Fluorescence Resonance Energy Transfer (TR-FRET) to Analyze the Disruption of EGFR/HER2 Dimers A NEW METHOD TO EVALUATE THE EFFICIENCY OF TARGETED THERAPY USING MONOCLONAL ANTIBODIES. *Journal of Biological Chemistry* **286,** 11337-45.

Garrett, J. T., Sutton, C. R., Kurupi, R., Bialucha, C. U., Ettenberg, S. A., Collins, S. D., Sheng, Q., Wallweber, J., DeFazio-Eli, L., and Arteaga, C. L. (2013). Combination of Antibody That Inhibits Ligand-Independent HER3 Dimerization and a p110 alpha Inhibitor Potently Blocks PI3K Signaling and Growth of HER2+ Breast Cancers. *Cancer Research* **73,** 6013-23.

Goldstein, N. I., Prewett, M., Zuklys, K., Rockwell, P., and Mendelsohn, J. (1995). Biological efficacy of a chimeric antibody to the epidermal growth factor receptor in a human tumor xenograft model. *Clinical Cancer Research* **1,** 1311-8.

Graus-Porta, D., Beerli, R. R., Daly, J. M., and Hynes, N. E. (1997). ErbB-2, the preferred heterodimerization partner of all ErbB receptors, is a mediator of lateral signaling. *EMBO Journal* **16,** 1647-55.

Guy, P. M., Platko, J. V., Cantley, L. C., Cerione, R. A., and Carraway, K. L. (1994). Insect Cell-Expressed P180(Erbb3) Possesses An Impaired Tyrosine Kinase-Activity. *Proceedings of the National Academy of Sciences of the United States of America* **91,** 8132-6.

Han, J., and Sun, P. (2007). The pathways to tumor suppression via route p38. *Trends in Biochemical Sciences* **32,** 364-71.

Hanahan, D., and Weinberg, R. A. (2000). The hallmarks of cancer. [Review] [94 refs]. *Cell* **100,** 57-70.

Hanahan, D., and Weinberg, R. A. (2011). Hallmarks of Cancer: The Next Generation. *Cell* **144,** 646-74.

Havaleshko, D. M., Smith, S. C., Cho, H., Cheon, S., Owens, C. R., Lee, J. K., Liotta, L. A., Espina, V., Wulfkuhle, J. D., Petricoin, E. F., and Theodorescu, D. (2009). Comparison of global versus epidermal growth factor receptor pathway profiling for prediction of lapatinib sensitivity in bladder cancer. *Neoplasia (New York)* **11,** 1185-93.

Holbro, T., Civenni, G., and Hynes, N. E. (2003). The ErbB receptors and their role in cancer progression. *Experimental Cell Research* **284,** 99-110.

Hudis, C. A. (2007). Drug therapy: Trastuzumab - Mechanism of action and use in clinical practice. *New England Journal of Medicine* **357,** 39-51.

Hussain, M. H., MacVicar, G. R., Petrylak, D. P., Dunn, R. L., Vaishampayan, U., Lara, P. N., Chatta, G. S., Nanus, D. M., Glode, L., Trump, D. L., Chen, H., and Smith, D. C. (2007). Trastuzumab, paclitaxel, carboplatin, and gemcitabine in advanced human epidermal growth factor receptor-2/neu-positive urothelial carcinoma: Results of a multicenter phase II National Cancer Institute trial. *Journal of Clinical Oncology* **25,** 2218-24.

Imao, T., Koshida, K., Endo, Y., Uchibayashi, T., Sasaki, T., and Namiki, M. (1999). Dominant role of E-cadherin in the progression of bladder cancer. *Journal of Urology* **161,** 692-8.

Jacobs, M. A., Wotkowicz, C., Baumgart, E. D., Neto, B. S., Rieger-Christ, K. M., Bernier, T., Cohen, M. S., Libertino, J. A., and Summerhayes, I. C. (2007). Epidermal growth factor receptor status and the response of bladder carcinoma cells to erlotinib. *Journal of Urology* **178,** 1510-4.

Jani, J. P., Finn, R. S., Campbell, M., Coleman, K. G., Connell, R. D., Currier, N., Emerson, E. O., Floyd, E., Harriman, S., Kath, J. C., Morris, J., Moyer, J. D., Pustilnik, L. R., Rafidi, K., Ralston, S., Rossi, A. M., Steyn, S. J., Wagner, L., Winter, S. M., and

Bhattacharya, S. K. (2007). Discovery and pharmacologic characterization of CP-724,714, a selective ErbB2 tyrosine kinase inhibitor. *Cancer Research* **67,** 9887-93.

Jebar, A. H., Hurst, C. D., Tomlinson, D. C., Johnston, C., Taylor, C. F., and Knowles, M. A. (2005). FGFR3 and Ras gene mutations are mutually exclusive genetic events in urothelial cell carcinoma. *Oncogene* **24,** 5218-25.

Jimenez, R. E., Hussain, M., Bianco, F. J., Jr., Vaishampayan, U., Tabazcka, P., Sakr, W. A., Pontes, J. E., Wood, D. P., Jr., and Grignon, D. J. (2001). Her-2/neu overexpression in muscle-invasive urothelial carcinoma of the bladder: prognostic significance and comparative analysis in primary and metastatic tumors. *Clinical Cancer Research* **7,** 2440-7.

Juanpere, N., Agell, L., Lorenzo, M., de Muga, S., Lopez-Vilaro, L., Murillo, R., Mojal, S., Serrano, S., Lorente, J. A., Lloreta, J., and Hernandez, S. (2012). Mutations in FGFR3 and PIK3CA, singly or combined with RAS and AKT1, are associated with AKT but not with MAPK pathway activation in urothelial bladder cancer. *Human Pathology* **43,** 1573-82.

Kassouf, W., Black, P. C., Tuziak, T., Bondaruk, J., Lee, S., Brown, G. A., Adam, L., Wei, C., Baggerly, K., Bar-Eli, M., McConkey, D., Czerniak, B., and Dinney, C. P. Distinctive expression pattern of ErbB family receptors signifies an aggressive variant of bladder cancer. Journal of Urology 179[1], 353-358. 2008.
Ref Type: Conference Proceeding

Kassouf, W., Dinney, C. P. N., Brown, G., McConkey, D. J., Diehl, A. J., Bar-Eli, M., and Adam, L. (2005). Uncoupling between epidermal growth factor receptor and downstream signals defines resistance to the antiproliferative effect of gefitinib in bladder cancer cells. *Cancer Research* **65,** 10524-35.

Konecny, G., Venkatesan, N., Yang, G., Dering, J., Ginther, C., Finn, R., Rahmeh, M., Fejzo, M., Toft, D., Jiang, S. W., Slamon, D., and Podratz, K. (2008). Activity of lapatinib a novel HER2 and EGFR dual kinase inhibitor in human endometrial cancer cells. *British Journal of Cancer* **98,** 1076-84.

Konecny, G. E., Pegram, M. D., Venkatesan, N., Finn, R., Yang, G. R., Rahmeh, M., Untch, M., Rusnak, D. W., Spehar, G., Mullin, R. J., Keith, B. R., Gilmer, T. M., Berger, M., Podratz, K. C., and Slamon, D. J. (2006). Activity of the dual kinase inhibitor lapatinib (GW572016) against HER-2-overexpressing and trastuzumab-treated breast cancer cells. *Cancer Research* **66,** 1630-9.

Korkolopoulou, P., Christodoulou, P., Kapralos, P., Exarchakos, M., Bisbiroula, A., Hadjiyannakis, M., Georgountzos, C., and Thomas-Tsagli, E. (1997). The role of p53, MDM2 and c-erb B-2 oncoproteins, epidermal growth factor receptor and proliferation markers in the prognosis of urinary bladder cancer. *Pathology, Research & Practice* **193,** 767-75.

Korman, B. D., Kastner, D. L., Gregersen, P. K., and Remmers, E. F. (2008). STAT4: Genetics, mechanisms, and implications for autoimmunity. *Current Allergy and Asthma Reports* **8,** 398-403.

Kosaka, T., Yatabe, Y., Endoh, H., Yoshida, K., Hida, T., Tsuboi, M., Tada, H., Kuwano, H., and Mitsudomi, T. (2006). Analysis of epidermal growth factor receptor gene mutation in patients with non-small cell lung cancer and acquired resistance to gefitinib. *Clinical Cancer Research* **12,** 5764-9.

Kramer, C., Klasmeyer, K., Bojar, H., Schulz, W. A., Ackermann, R., and Grimm, M. O. (2007). Heparin-binding epidermal growth factor-like growth factor isoforms and epidermal growth factor receptor/ErbB1 expression in bladder cancer and their relation to clinical outcome. *Cancer* **109,** 2016-24.

Kruger, S., Weitsch, G., Buttner, H., Matthiensen, A., Bohmer, T., Marquardt, T., Sayk, F., Feller, A. C., and Bohle, A. (2002). HER2 overexpression in muscle-invasive urothelial carcinoma of the bladder: prognostic implications. *International Journal of Cancer* **102,** 514-8.

Kumar, B., Sinclair, J., Khandrika, L., Koul, S., Wilson, S., and Koul, H. K. (2009). Differential effects of MAPKs signaling on the growth of invasive bladder cancer cells. *International Journal of Oncology* **34,** 1557-64.

Kumar, B., Koul, S., Petersen, J., Khandrika, L., Hwa, J. S., Meacham, R. B., Wilson, S., and Koul, H. K. (2010). p38 Mitogen-Activated Protein Kinase-Driven MAPKAPK2 Regulates Invasion of Bladder Cancer by Modulation of MMP-2 and MMP-9 Activity. *Cancer Research* **70,** 832-41.

La Monica, S., Caffarra, C., Saccani, F., Galvani, E., Galetti, M., Fumarola, C., Bonelli, M., Cavazzoni, A., Cretella, D., Sirangelo, R., Gatti, R., Tiseo, M., Ardizzoni, A., Giovannetti, E., Petronini, P. G., and Alfieri, R. R. (2013). Gefitinib Inhibits Invasive Phenotype and Epithelial-Mesenchymal Transition in Drug-Resistant NSCLC Cells with MET Amplification. *Plos One* **8**.

Lae, M., Couturier, J., Oudard, S., Radvanyi, F., Beuzeboc, P., and Vieillefond, A. (2010). Assessing HER2 gene amplification as a potential target for therapy in invasive urothelial bladder cancer with a standardized methodology: results in 1005 patients. *Annals of Oncology* **21,** 815-9.

Lali, F. V., Hunt, A. E., Turner, S. J., and Foxwell, B. M. J. (2000). The pyridinyl imidazole inhibitor SB203580 blocks phosphoinositide-dependent protein kinase activity, protein kinase B phosphorylation, and retinoblastoma hyperphosphorylation in interleukin-2-stimulated T cells independently of p38 mitogen-activated protein kinase. *Journal of Biological Chemistry* **275,** 7395-402.

Leist, M., and Jaattela, M. (2001). Four deaths and a funeral: From caspases to alternative mechanisms. *Nature Reviews Molecular Cell Biology* **2,** 589-98.

Lemmon, M. A., and Schlessinger, J. (2010). Cell signaling by receptor tyrosine kinases. [Review] [142 refs]. *Cell* **141,** 1117-34.

Lievre, A., Bachet, J. B., Le Corre, D., Boige, V., Landi, B., Emile, J. F., Cote, J. F., Tomasic, G., Penna, C., Ducreux, M., Rougier, P., Penault-Llorca, F., and Laurent-Puig, P. (2006). KRAS mutation status is predictive of response to cetuximab therapy in colorectal cancer. *Cancer Research* **66,** 3992-5.

Lipponen, P., and Eskelinen, M. (1994). Expression of epidermal growth factor receptor in bladder cancer as related to established prognostic factors, oncoprotein (c-erbB-2, p53) expression and long-term prognosis. *British Journal of Cancer* **69,** 1120-5.

Lopez-Knowles, E., Hernandez, S., Malats, N., Kogevinas, M., Lloreta, J., Carrato, A., Tardon, A., Serra, C., and Real, F. X. (2006). PIK3CA mutations are an early genetic alteration associated with FGFR3 mutations in superficial papillary bladder tumors. *Cancer Research* **66,** 7401-4.

Luis, N. M., Lopez-Knowles, E., and Real, F. X. (2007). Molecular biology of bladder cancer. [Review] [69 refs]. *Clinical & Translational Oncology: Official Publication of the Federation of Spanish Oncology Societes & of the National Cancer Institute of Mexico* **9,** 5-12.

Lynch, T. J., Bell, D. W., Sordella, R., Gurubhagavatula, S., Okimoto, R. A., Brannigan, B. W., Harris, P. L., Haserlat, S. M., Supko, J. G., Haluska, F. G., Louis, D. N., Christiani, D. C., Settleman, J., and Haber, D. A. (2004). Activating mutations in the epidermal growth factor receptor underlying responsiveness of non-small-cell lung cancer to gefitinib. *New England Journal of Medicine* **350,** 2129-39.

Maddineni, S. B., Sangar, V. K., Hendry, J. H., Margison, G. P., and Clarke, N. W. (2005). Differential radiosensitisation by ZD1839 (Iressa), a highly selective epidermal growth factor receptor tyrosine kinase inhibitor in two related bladder cancer cell lines. *British Journal of Cancer* **92,** 125-30.

Manning, B. D., and Cantley, L. C. (2007). AKT/PKB signaling: Navigating downstream. *Cell* **129,** 1261-74.

Massarelli, E., Varella-Garcia, M., Tang, X., Xavier, A. C., Ozburn, N. C., Liu, D. D., Bekele, B. N., Herbst, R. S., and Wistuba, I. I. (2007). KRAS mutation is an important predictor of resistance to therapy with epidermal growth factor receptor tyrosine kinase inhibitors in non-small-cell lung cancer. *Clinical Cancer Research* **13,** 2890-6.

McHugh, L. A., Sayan, A. E., Mejlvang, J., Griffiths, T. R., Sun, Y., Manson, M. M., Tulchinsky, E., Mellon, J. K., and Kriajevska, M. (2009). Lapatinib, a dual inhibitor of ErbB-1/-2 receptors, enhances effects of combination chemotherapy in bladder cancer cells. *International Journal of Oncology* **34,** 1155-63.

McHugh, L. A., Kriajevska, M., Mellon, J. K., and Griffiths, T. R. (2007). Combined Treatment of Bladder Cancer Cell Lines with Lapatinib and Varying Chemotherapy Regimens--Evidence of Schedule-Dependent Synergy. *Urology* **69,** 390-4.

Medina, P. J., and Goodin, S. (2008). Lapatinib: A dual inhibitor of human epidermal growth factor receptor tyrosine kinases. *Clinical Therapeutics* **30,** 1426-47.

Mellinghoff, I. K., Wang, M. Y., Vivanco, I., Haas-Kogan, D. A., Zhu, S. J., Dia, E. Q., Lu, K. V., Yoshimoto, K., Huang, J. H. Y., Chute, D. J., Riggs, B. L., Horvath, S., Liau, L. M., Cavenee, W. K., Rao, P. N., Beroukhim, R., Peck, T. C., Lee, J. C., Sellers, W. R., Stokoe, D., Prados, M., Cloughesy, T. F., Sawyers, C. L., and Mischel, P. S. (2005). Molecular determinants of the response of glioblastomas to EGFR kinase inhibitors. *New England Journal of Medicine* **353,** 2012-24.

Mellon, J. K., Lunec, J., Wright, C., Horne, C. H. W., Kelly, P., and Neal, D. E. (1996). C-erbB-2 in bladder cancer: Molecular biology, correlation with epidermal growth factor receptors and prognostic value. *Journal of Urology* **155,** 321-6.

Memon, A. A., Sorensen, B. S., Meldgaard, P., Fokdal, L., Thykjaer, T., and Nexo, E. (2006). The relation between survival and expression of HER1 and HER2 depends on the expression of HER3 and HER4: a study in bladder cancer patients. *British Journal of Cancer* **94,** 1703-9.

Memon, A. A., Sorensen, B. S., Melgard, P., Fokdal, L., Thykjaer, T., and Nexo, E. (2004). Expression of HER3, HER4 and their ligand heregulin-4 is associated with better survival in bladder cancer patients. *British Journal of Cancer* **91,** 2034-41.

Mendelsohn, J., and Baselga, J. (2000). The EGF receptor family as targets for cancer therapy. *Oncogene* **19,** 6550-65.

Mitra, A. P., and Cote, R. J. (2009). Molecular pathogenesis and diagnostics of bladder cancer. [Review] [194 refs]. *Annual Review Of Pathology* **4,** 251-85.

Moasser, M. M. (2007). The oncogene HER2: its signaling and transforming functions and its role in human cancer pathogenesis. [Review] [211 refs]. *Oncogene* **26,** 6469-87.

Moasser, M. M., Basso, A., Averbuch, S. D., and Rosen, N. (2001). The tyrosine kinase inhibitor ZD1839 ("Iressa") inhibits HER2-driven signaling and suppresses the growth of HER2-overexpressing tumor cells. *Cancer Research* **61,** 7184-8.

Mostafa, M. H., Sheweita, S. A., and O'Connor, P. J. (1999). Relationship between schistosomiasis and bladder cancer. *Clinical Microbiology Reviews* **12,** 97-+.

Moyer, J. D., Barbacci, E. G., Iwata, K. K., Arnold, L., Boman, B., Cunningham, A., DiOrio, C., Doty, J., Morin, M. J., Moyer, M. P., Neveu, M., Pollack, V. A., Pustilnik, L. R., Reynolds, M. M., Sloan, D., Theleman, A., and Miller, P. (1997). Induction of apoptosis and cell cycle arrest by CP-358,774, an inhibitor of epidermal growth factor receptor tyrosine kinase. *Cancer Research* **57,** 4838-48.

Munk, M., Memon, A., Poulsen, S. S., Borre, M., Nexo, E., and Sorensen, B. S. (2013). The HER4 isoform JM-a/CYT2 relates to improved survival in bladder cancer patients but only if the estrogen receptor a is not expressed. *Scandinavian Journal of Clinical & Laboratory Investigation* **73,** 503-13.

Munk, M., Memon, A. A., Nexo, E., and Sorensen, B. S. (2007). Inhibition of the epidermal growth factor receptor in bladder cancer cells treated with the DNA-damaging drug etoposide markedly increases apoptosis. *BJU International* **99,** 196-201.

Nagasawa, J., Mizokami, A., Koshida, K., Yoshida, S., Naito, K., and Namiki, M. (2006). Novel HER2 selective tyrosine kinase inhibitor, TAK-165, inhibits bladder, kidney and androgen-independent prostate cancer in vitro and in vivo. *International Journal of Urology* **13,** 587-92.

Naito, S., Bilim, V., Yuuki, K., Ugolkov, A., Motoyama, T., Nagaoka, A., Kato, T., and Tomita, Y. (2010). Glycogen Synthase Kinase-3 beta: A Prognostic Marker and a

Potential Therapeutic Target in Human Bladder Cancer. *Clinical Cancer Research* **16,** 5124-32.

Neal, D. E., Sharples, L., Smith, K., Fennelly, J., Hall, R. R., and Harris, A. L. (1990). The Epidermal Growth-Factor Receptor and the Prognosis of Bladder-Cancer. *Cancer* **65,** 1619-25.

Ni, C. Y., Murphy, M. P., Golde, T. E., and Carpenter, G. (2001). gamma-Secretase cleavage and nuclear localization of ErbB-4 receptor tyrosine kinase. *Science* **294,** 2179-81.

Ni, Z. Y., Lou, W., Lee, S. O., Dhir, R., DeMiguel, F., Grandis, J. R., and Gao, A. C. (2002). Selective activation of members of the signal transducers and activators of transcription family in prostate carcinoma. *Journal of Urology* **167,** 1859-62.

Nicholson, R. I., Gee, J. M. W., and Harper, M. E. (2001). EGFR and cancer prognosis. *European Journal of Cancer* **37,** S9-S15.

Normanno, N., De, L. A., Bianco, C., Strizzi, L., Mancino, M., Maiello, M. R., Carotenuto, A., De, F. G., Caponigro, F., and Salomon, D. S. (2006). Epidermal growth factor receptor (EGFR) signaling in cancer. [Review] [176 refs]. *Gene* **366,** 2-16.

Okuyama, H., Yoshida, T., Endo, H., Nakayama, M., Nonomura, N., Nishimura, K., and Inoue, M. (2013). Involvement of Heregulin/HER3 in the Primary Culture of Human Urothelial Cancer. *Journal of Urology* **190,** 302-10.

Olayioye, M. A., Neve, R. M., Lane, H. A., and Hynes, N. E. (2000). The ErbB signaling network: receptor heterodimerization in development and cancer. *EMBO Journal* **19,** 3159-67.

Ono, K., and Han, J. H. (2000). The p38 signal transduction pathway - Activation and function. *Cellular Signalling* **12,** 1-13.

Ono, M., Hirata, A., Kometani, T., Miyagawa, M., Ueda, S., Kinoshita, H., Fujii, T., and Kuwano, M. (2004). Sensitivity to gefitinib (Iressa, ZD1839) in non-small cell lung cancer cell lines correlates with dependence on the epidermal growth factor (EGF) receptor/extracellular signal-regulated kinase 1/2 and EGF receptor/Akt pathway for proliferation. *Molecular Cancer Therapeutics* **3,** 465-72.

Otto, K. B., Acharya, S. S., and Robinson, V. L. (2012). Stress-activated kinase pathway alteration is a frequent event in bladder cancer. *Urologic Oncology* **30,** 415-20.

Ozbek, E., Otunctemur, A., Calik, G., Aliskan, T., Cakir, S., Dursun, M., and Somay, A. (2011). Comparison of p38MAPK (mitogene activated protein kinase), p65 NFkappaB (nuclear factor kappa b) and EMMPRIN (extracellular matrix metalloproteinase inducer) expressions with tumor grade and stage of superficial and invasive bladder tumors. *Archivio italiano di urologia, andrologia : organo ufficiale [di] Societa italiana di ecografia urologica e nefrologica / Associazione ricerche in urologia* **83,** 181-7.

Paez, J. G., Janne, P. A., Lee, J. C., Tracy, S., Greulich, H., Gabriel, S., Herman, P., Kaye, F. J., Lindeman, N., Boggon, T. J., Naoki, K., Sasaki, H., Fujii, Y., Eck, M. J.,

Sellers, W. R., Johnson, B. E., and Meyerson, M. (2004). EGFR mutations in lung cancer: correlation with clinical response to gefitinib therapy. *Science* **304,** 1497-500.

Pao, W., Miller, V., Zakowski, M., Doherty, J., Politi, K., Sarkaria, I., Singh, B., Heelan, R., Rusch, V., Fulton, L., Mardis, E., Kupfer, D., Wilson, R., Kris, M., and Varmus, H. (2004). EGF receptor gene mutations are common in lung cancers from "never smokers" and are associated with sensitivity of tumors to gefitinib and erlotinib. *Proceedings of the National Academy of Sciences of the United States of America* **101,** 13306-11.

Pao, W., Miller, V. A., Politi, K. A., Riely, G. J., Somwar, R., Zakowski, M. F., Kris, M. G., and Varmus, H. (2005). Acquired resistance of lung adenocarcinomas to gefitinib or erlotinib is associated with a second mutation in the EGFR kinase domain. *PLoS Medicine / Public Library of Science* **2,** e73.

Petrylak, D. P., Tangen, C. M., Van Veldhuizen, P. J., Goodwin, J., Twardowski, P. W., Atkins, J. N., Kakhil, S. R., Lange, M. K., Mansukhani, M., and Crawford, E. D. (2010). Results of the Southwest Oncology Group phase II evaluation (study S0031) of ZD1839 for advanced transitional cell carcinoma of the urothelium. *BJU International* **105,** 317-21.

Platt, F. M., Hurst, C. D., Taylor, C. F., Gregory, W. M., Harnden, P., and Knowles, M. A. (2009). Spectrum of phosphatidylinositol 3-kinase pathway gene alterations in bladder cancer. *Clinical Cancer Research* **15,** 6008-17.

Poot, A., Slobbe, P., Hendrikse, N., Windhorst, A., and van Dongen, G. (2013). Imaging of TKI-Target Interactions for Personalized Cancer Therapy. *Clinical Pharmacology & Therapeutics* **93,** 239-41.

Pruthi, R. S., Nielsen, M., Heathcote, S., Wallen, E. M., Rathmell, W. K., Godley, P., Whang, Y., Fielding, J., Schultz, H., Grigson, G., Smith, A., Kim, W., and O'Donnell, P. H. (2010). A phase II trial of neoadjuvant erlotinib in patients with muscle-invasive bladder cancer undergoing radical cystectomy: clinical and pathological results. *BJU International* **106,** 349-56.

Puzio-Kuter, A. M., Castillo-Martin, M., Kinkade, C. W., Wang, X., Shen, T. H., Matos, T., Shen, M. M., Cordon-Cardo, C., and Abate-Shen, C. (2009). Inactivation of p53 and Pten promotes invasive bladder cancer. *Genes & Development* **23,** 675-80.

Quesnelle, K. M., Boehm, A. L., and Grandis, J. R. (2007). STAT-mediated EGFR signaling in cancer. *Journal of Cellular Biochemistry* **102,** 311-9.

Raingeaud, J., Whitmarsh, A. J., Barrett, T., Derijard, B., and Davis, R. J. (1996). MKK3- and MKK6-regulated gene expression is mediated by the p38 mitogen-activated protein kinase signal transduction pathway. *Molecular and Cellular Biology* **16,** 1247-55.

Reddy, E. P., Reynolds, R. K., Santos, E., and Barbacid, M. (1982). A Point Mutation Is Responsible for the Acquisition of Transforming Properties by the T24 Human Bladder-Carcinoma Oncogene. *Nature* **300,** 149-52.

Rieger, K. M., Little, A. R., Swart, J. M., Kastrinakis, W. V., Fitzgerald, J. M., Hess, D. T., Libertino, J. A., and Summerhayes, I. C. (1995). Human Bladder-Carcinoma Cell-Lines As Indicators of Oncogenic Change Relevant to Urothelial Neoplastic Progression. *British Journal of Cancer* **72,** 683-90.

Rodriguezviciana, P., Warne, P. H., Dhand, R., Vanhaesebroeck, B., Gout, I., Fry, M. J., Waterfield, M. D., and Downward, J. (1994). Phosphatidylinositol-3-Oh Kinase As A Direct Target of Ras. *Nature* **370,** 527-32.

Roh, H., Pippin, J., and Drebin, J. A. (2000). Down-regulation of HER2/neu expression induces apoptosis in human cancer cells that overexpress HER2/neu. *Cancer Research* **60,** 560-5.

Roskoski, R. (2004). The ErbB/HER receptor protein-tyrosine kinases and cancer. *Biochemical and Biophysical Research Communications* **319,** 1-11.

Rotterud, R., Nesland, J. M., Berner, A., and Fossa, S. D. (2005). Expression of the epidermal growth factor receptor family in normal and malignant urothelium. *BJU International* **95,** 1344-50.

Roux, P. P., and Blenis, J. (2004). ERK and p38 MAPK-activated protein kinases: a family of protein kinases with diverse biological functions. *Microbiology and Molecular Biology Reviews* **68,** 320-+.

Rusnak, D. W., Alligood, K. J., Mullin, R. J., Spehar, G. M., Arenas-Elliott, C., Martin, A. M., Degenhardt, Y., Rudolph, S. K., Haws, T. F. J., Hudson-Curtis, B. L., and Gilmer, T. M. (2007). Assessment of epidermal growth factor receptor (EGFR, ErbB1) and HER2 (ErbB2) protein expression levels and response to lapatinib (Tykerb (R), GW572016) in an expanded panel of human normal and tumour cell lines. *Cell Proliferation* **40,** 580-94.

Rusnak, D. W., Lackey, K., Affleck, K., Wood, E. R., Alligood, K. J., Rhodes, N., Keith, B. R., Murray, D. M., Knight, W. B., Mullin, R. J., and Gilmer, T. M. (2001). The effects of the novel, reversible epidermal growth factor Receptor/ErbB-2 tyrosine kinase inhibitor, GW2016, on the growth of human normal and tumor-derived cell lines in vitro and in vivo. *Molecular Cancer Therapeutics* **1,** 85-94.

Sahin, U., Weskamp, G., Kelly, K., Zhou, H. M., Higashiyama, S., Peschon, J., Hartmann, D., Saftig, P., and Blobel, C. P. (2004). Distinct roles for ADAM10 and ADAM17 in ectodomain shedding of six EGFR ligands. *Journal of Cell Biology* **164,** 769-79.

Sanchez-Martin, M., and Pandiella, A. (2012). Differential action of small molecule HER kinase inhibitors on receptor heterodimerization: Therapeutic implications. *International Journal of Cancer* **131,** 244-52.

Sarbassov, D. D., Guertin, D. A., Ali, S. M., and Sabatini, D. M. (2005). Phosphorylation and regulation of Akt/PKB by the rictor-mTOR complex. *Science* **307,** 1098-101.

Sartor, C. I., Zhou, H., Kozlowska, E., Guttridge, K., Kawata, E., Caskey, L., Harrelson, J., Hynes, N., Ethier, S., Calvo, B., and Earp, H. S., III (2001). Her4 mediates ligand-

dependent antiproliferative and differentiation responses in human breast cancer cells. *Molecular & Cellular Biology* **21,** 4265-75.

Sassen, A., Diermeier-Daucher, S., Sieben, M., Ortmann, O., Hofstaedter, F., Schwarz, S., and Brockhoff, G. (2009). Presence of HER4 associates with increased sensitivity to Herceptin in patients with metastatic breast cancer. *Breast Cancer Research* **11,** R50.

Schulz, W. A. (2006). Understanding urothelial carcinoma through cancer pathways. *International Journal of Cancer* **119,** 1513-8.

Schulze, W. X., Deng, L., and Mann, M. (2005). Phosphotyrosine interactome of the ErbB-receptor kinase family. *Molecular Systems Biology* **1,** 2005.

Sergina, N. V., and Moasser, M. M. (2007). The HER family and cancer: emerging molecular mechanisms and therapeutic targets. [Review] [83 refs]. *Trends in Molecular Medicine* **13,** 527-34.

Sergina, N. V., Rausch, M., Wang, D., Blair, J., Hann, B., Shokat, K. M., and Moasser, M. M. (2007). Escape from HER-family tyrosine kinase inhibitor therapy by the kinase-inactive HER3. *Nature* **445,** 437-41.

She, Q. B., Solit, D., Basso, A., and Moasser, M. M. (2003). Resistance to gefitinib in PTEN-null HER-overexpressing tumor cells can be overcome through restoration of PTEN function or pharmacologic modulation of constitutive phosphatidylinositol 3 '-kinase/Akt pathway signaling. *Clinical Cancer Research* **9,** 4340-6.

Sheng, G., Guo, J., and Warner, B. W. (2007). Epidermal growth factor receptor signaling modulates apoptosis via p38 alpha MAPK-dependent activation of Bax in intestinal epithelial cells. *American Journal of Physiology-Gastrointestinal and Liver Physiology* **293,** G599-G606.

Shrader, M., Pino, M. S., Brown, G., Black, P., Adam, L., Bar-Eli, M., Dinney, C. P., and McConkey, D. J. (2007). Molecular correlates of gefitinib responsiveness in human bladder cancer cells. *Molecular Cancer Therapeutics* **6,** 277-85.

Sithanandam, G., and Anderson, L. (2008). The ERBB3 receptor in cancer and cancer gene therapy. *Cancer Gene Therapy* **15,** 413-48.

Slamon, D. J., Clark, G. M., Wong, S. G., Levin, W. J., Ullrich, A., and McGuire, W. L. (1987). Human breast cancer: correlation of relapse and survival with amplification of the HER-2/neu oncogene. *Science* **235,** 177-82.

Soltoff, S. P., Carraway, K. L., III, Prigent, S. A., Gullick, W. G., and Cantley, L. C. (1994). ErbB3 is involved in activation of phosphatidylinositol 3-kinase by epidermal growth factor. *Molecular & Cellular Biology* **14,** 3550-8.

Sos, M. L., Koker, M., Weir, B. A., Heynck, S., Rabinovsky, R., Zander, T., Seeger, J. M., Weiss, J., Fischer, F., Frommolt, P., Michel, K., Peifer, M., Mermel, C., Girard, L., Peyton, M., Gazdar, A. F., Minna, J. D., Garraway, L. A., Kashkar, H., Pao, W., Meyerson, M., and Thomas, R. K. (2009). PTEN Loss Contributes to Erlotinib Resistance in EGFR-Mutant Lung Cancer by Activation of Akt and EGFR. *Cancer Research* **69,** 3256-61.

Sridhar, S. S., Seymour, L., and Shepherd, F. A. (2003). Inhibitors of epidermal-growth-factor receptors: a review of clinical research with a focus on non-small-cell lung cancer. [Review] [73 refs]. *Lancet Oncology* **4,** 397-406.

Stambolic, V., Suzuki, A., de la Pompa, J. L., Brothers, G. M., Mirtsos, C., Sasaki, T., Ruland, J., Penninger, J. M., Siderovski, D. P., and Mak, T. W. (1998). Negative regulation of PKB/Akt-dependent cell survival by the tumor suppressor PTEN. *Cell* **95,** 29-39.

Stenzl, A., Cowan, N. C., De Santis, M., Kuczyk, M. A., Merseburger, A. S., Jose Ribal, M., Sherif, A., and Witjes, J. (2011). Treatment of Muscle-invasive and Metastatic Bladder Cancer: Update of the EAU Guidelines. *European Urology* **59,** 1009-18.

Stephens, P., Hunter, C., Bignell, G., Edkins, S., Davies, H., Teague, J., Stevens, C., O'Meara, S., Smith, R., Parker, A., Barthorpe, A., Blow, M., Brackenbury, L., Butler, A., Clarke, O., Cole, J., Dicks, E., Dike, A., Drozd, A., Edwards, K., Forbes, S., Foster, R., Gray, K., Greenman, C., Halliday, K., Hills, K., Kosmidou, V., Lugg, R., Menzies, A., Perry, J., Petty, R., Raine, K., Ratford, L., Shepherd, R., Small, A., Stephens, Y., Tofts, C., Varian, J., West, S., Widaa, S., Yates, A., Brasseur, F., Cooper, C. S., Flanagan, A. M., Knowles, M., Leung, S. Y., Louis, D. N., Looijenga, L. H. J., Malkowicz, B., Pierotti, M. A., Teh, B., Chenevix-Trench, G., Weber, B. L., Yuen, S. T., Harris, G., Goldstraw, P., Nicholson, A. G., Futreal, P. A., Wooster, R., Stratton, M. R., and Canc Genome Project Collaborat Grp (2004). Intragenic ERBB2 kinase mutations in tumours. *Nature* **431,** 525-6.

Sternberg, C. N., Donat, S. M., Bellmunt, J., Millikan, R. E., Stadler, W., De Mulder, P., Sherif, A., von der Maase, H., Tsukamoto, T., and Soloway, M. S. (2007). Chemotherapy for bladder cancer: Treatment guidelines for neoadjuvant chemotherapy, bladder preservation, adjuvant chemotherapy, and metastatic cancer. *Urology* **69,** 62-79.

Sun, C. H., Chang, Y. H., and Pan, C. C. (2011). Activation of the PI3K/Akt/mTOR pathway correlates with tumour progression and reduced survival in patients with urothelial carcinoma of the urinary bladder. *Histopathology* **58,** 1054-63.

Suzuki, T., Nakagawa, T., Endo, H., Mitsudomi, T., Masuda, A., Yatabe, Y., Sugiura, T., Takahashi, T., and Hida, T. (2003). The sensitivity of lung cancer cell lines to the EGFR-selective tyrosine kinase inhibitor ZD1839 ('Iressa") is not related to the expression of EGFR or HER-2 or to K-ras gene status. *Lung Cancer* **42,** 35-41.

Swiatkowski, S., Seifert, H. H., Steinhoff, C., Prior, A., Thievessen, I., Schliess, F., and Schulz, W. A. (2003). Activities of MAP-kinase pathways in normal uroepithelial cells and urothelial carcinoma cell lines. *Experimental Cell Research* **282,** 48-57.

Tari, A. M., and Lopez-Berestein, G. (2000). Serum predominantly activates MAPK and Akt kinases in EGFR- and ErbB2-over-expressing cells, respectively. *International Journal of Cancer* **86,** 295-7.

Thornton, T. M., Pedraza-Alva, G., Deng, B., Wood, C., Aronshtam, A., Clements, J. L., Sabio, G., Davis, R. J., Matthews, D. E., Doble, B., and Rincon, M. (2008).

Phosphorylation by p38 MAPK as an alternative pathway for GSK3 beta inactivation. *Science* **320,** 667-70.

Trempolec, N., Dave-Coll, N., and Nebreda, A. R. (2013). SnapShot: p38 MAPK Signaling. *Cell* **152,** 656.

Tsai, Y. S., Cheng, H. L., Tzai, T. S., and Chow, N. H. (2012). Clinical Significance of ErbB Receptor Family in Urothelial Carcinoma of the Bladder: A Systematic Review and Meta-Analysis. *Advances in urology* **2012,** 181964.

Tzahar, E., Waterman, H., Chen, X., Levkowitz, G., Karunagaran, D., Lavi, S., Ratzkin, B. J., and Yarden, Y. (1996). A hierarchical network of interreceptor interactions determines signal transduction by Neu differentiation factor/neuregulin and epidermal growth factor. *Molecular & Cellular Biology* **16,** 5276-87.

Van Schaeybroeck, S., Karaiskou-McCaul, A., Kelly, D., Longley, D., Galligan, L., Van Cutsem, E., and Johnston, P. (2005). Epidermal growth factor receptor activity determines response of colorectal cancer cells to gefitinib alone and in combination with chemotherapy. *Clinical Cancer Research* **11,** 7480-9.

von der Maase, H., Hansen, S. W., Roberts, J. T., Dogliotti, L., Oliver, T., Moore, M. J., Bodrogi, I., Albers, P., Knuth, A., Lippert, C. M., Kerbrat, P., Rovira, P. S., Wersall, P., Cleall, S. P., Roychowdhury, D. F., Tomlin, I., Visseren-Grul, C. M., and Conte, P. F. (2000). Gemcitabine and cisplatin versus methotrexate vinblastine, doxorubicin, and cisplatin in advanced or metastatic bladder cancer: Results of a large randomized, multinational, multicenter, phase III study. *Journal of Clinical Oncology* **18,** 3068-77.

Wainberg, Z. A., Anghel, A., Desai, A. J., Ayala, R., Luo, T., Safran, B., Fejzo, M. S., Hecht, J., Slamon, D. J., and Finn, R. S. (2010). Lapatinib, a Dual EGFR and HER2 Kinase Inhibitor, Selectively Inhibits HER2-Amplified Human Gastric Cancer Cells and is Synergistic with Trastuzumab In vitro and In vivo. *Clinical Cancer Research* **16,** 1509-19.

Walker, M. C., Povey, S., Parrington, J. M., Riddle, P. N., Knuechel, R., and Masters, J. R. W. (1990). Development and Characterization of Cisplatin-Resistant Human Testicular and Bladder-Tumor Cell-Lines. *European Journal of Cancer* **26,** 742-7.

Wang, D. S., Rieger-Christ, K., Latini, J. M., Moinzadeh, A., Stoffel, J., Pezza, J. A., Saini, K., Libertino, J. A., and Summerhayes, I. C. (2000). Molecular analysis of PTEN and MXI1 in primary bladder carcinoma. *International Journal of Cancer* **88,** 620-5.

Wang, L., Liu, Q., Zhao, H., Cui, K., Yao, L., Nie, F., Jin, G., Hao, A., and Wong, S. T. (2013). Differential effects of low- and high-dose GW2974, a dual epidermal growth factor receptor and HER2 kinase inhibitor, on glioblastoma multiforme invasion. *Journal of Neuroscience Research* **91,** 128-37.

Waterhouse, B. R., Gijsen, M., Barber, P. R., Tullis, I. D., Vojnovic, B., and Kong, A. (2011). Assessment of EGFR/HER2 dimerization by FRET-FLIM utilizing Alexa-conjugated secondary antibodies in relation to targeted therapies in cancers. *Oncotarget* **2,** 728-36.

Weinberg, R. A. (1995). The Retinoblastoma Protein and Cell-Cycle Control. *Cell* **81,** 323-30.

Wieduwilt, M. J., and Moasser, M. M. (2008). The epidermal growth factor receptor family: biology driving targeted therapeutics. [Review] [196 refs]. *Cellular & Molecular Life Sciences* **65,** 1566-84.

Williams, S. G., and Stein, J. P. (2004). Molecular pathways in bladder cancer. [Review] [126 refs]. *Urological Research* **32,** 373-85.

Wong, Y. N., Litwin, S., Vaughn, D., Cohen, S., Plimack, E. R., Lee, J., Song, W., Dabrow, M., Brody, M., Tuttle, H., and Hudes, G. (2012). Phase II Trial of Cetuximab With or Without Paclitaxel in Patients With Advanced Urothelial Tract Carcinoma. *Journal of Clinical Oncology* **30,** 3545-51.

Wood, E. R., Truesdale, A. T., McDonald, O. B., Yuan, D., Hassell, A., Dickerson, S. H., Ellis, B., Pennisi, C., Horne, E., Lackey, K., Alligood, K. J., Rusnak, D. W., Gilmer, T. M., and Shewchuk, L. (2004). A unique structure for epidermal growth factor receptor bound to GW572016 (Lapatinib): Relationships among protein conformation, inhibitor off-rate, and receptor activity in tumor cells. *Cancer Research* **64,** 6652-9.

Wright, C., Mellon, K., Johnston, P., Lane, D. P., Harris, A. L., Horne, C. H., and Neal, D. E. (1991). Expression of mutant p53, c-erbB-2 and the epidermal growth factor receptor in transitional cell carcinoma of the human urinary bladder. *British Journal of Cancer* **63,** 967-70.

Wu, X., Obata, T., Khan, Q., Highshaw, R. A., De Vere, W. R., and Sweeney, C. (2004). The phosphatidylinositol-3 kinase pathway regulates bladder cancer cell invasion. *BJU International* **93,** 143-50.

Wu, X. R. (2005). Urothelial tumorigenesis: a tale of divergent pathways. [Review] [145 refs]. *Nature Reviews* **Cancer.,** 713-25.

Wulfing, C., Machiels, J. P., Richel, D. J., Grimm, M. O., Treiber, U., De Groot, M. R., Beuzeboc, P., Parikh, R., Petavy, F., and El-Hariry, I. A. (2009). A single-arm, multicenter, open-label phase 2 study of lapatinib as the second-line treatment of patients with locally advanced or metastatic transitional cell carcinoma. *Cancer* **115,** 2881-90.

Xia, W. L., Mullin, R. J., Keith, B. R., Liu, L. H., Ma, H., Rusnak, D. W., Owens, G., Alligood, K. J., and Spector, N. L. (2002). Anti-tumor activity of GW572016: a dual tyrosine kinase inhibitor blocks EGF activation of EGFR/erbB2 and downstream Erk1/2 and AKT pathways. *Oncogene* **21,** 6255-63.

Xia, Z. G., Dickens, M., Raingeaud, J., Davis, R. J., and Greenberg, M. E. (1995). Opposing Effects of Erk and Jnk-P38 Map Kinases on Apoptosis. *Science* **270,** 1326-31.

Yamasaki, F., Johansen, M. J., Zhang, D., Krishnamurthy, S., Felix, E., Bartholomeusz, C., Aguilar, R. J., Kurisu, K., Mills, G. B., Hortobagyi, G. N., and Ueno, N. T. (2007). Acquired resistance to erlotinib in A-431 epidermoid cancer cells requires down-regulation of MMAC1/PTEN and up-regulation of phosphorylated Akt. *Cancer Research* **67,** 5779-88.

Yarden, Y., and Sliwkowski, M. X. (2001). Untangling the ErbB signalling network. [Review] [112 refs]. *Nature Reviews Molecular Cell Biology* **2,** 127-37.

Yong, H. Y., Koh, M. S., and Moon, A. (2009). The p38 MAPK inhibitors for the treatment of inflammatory diseases and cancer. *Expert Opinion on Investigational Drugs* **18,** 1893-905.

Youssef, R. F., Mitra, A. P., Bartsch, G., Jr., Jones, P. A., Skinner, D. G., and Cote, R. J. (2009). Molecular targets and targeted therapies in bladder cancer management. [Review] [107 refs]. *World Journal of Urology* **27,** 9-20.

Zhang, D., Pal, A., Bornmann, W. G., Yamasaki, F., Esteva, F. J., Hortobagyi, G. N., Bartholomeusz, C., and Ueno, N. T. (2008). Activity of lapatinib is independent of EGFR expression level in HER2-overexpressing breast cancer cells. *Molecular Cancer Therapeutics* **7,** 1846-50.

Zhong, Z., Wen, Z. L., and Darnell, J. E. (1994). Stat3 and Stat4 - Members of the Family of Signal Transducers and Activators of Transcription. *Proceedings of the National Academy of Sciences of the United States of America* **91,** 4806-10.